

UNCLASSIFIED

AD

434352

DEFENSE DOCUMENTATION CENTER

FOR

SCIENTIFIC AND TECHNICAL INFORMATION

CAMERON STATION, ALEXANDRIA, VIRGINIA



UNCLASSIFIED

NOTICE: When government or other drawings, specifications or other data are used for any purpose other than in connection with a definitely related government procurement operation, the U. S. Government thereby incurs no responsibility, nor any obligation whatsoever; and the fact that the Government may have formulated, furnished, or in any way supplied the said drawings, specifications, or other data is not to be regarded by implication or otherwise as in any manner licensing the holder or any other person or corporation, or conveying any rights or permission to manufacture, use or sell any patented invention that may in any way be related thereto.

5 818 600

64-11



434352

AD No. 434352

DDC FILE COPY

USE OF THE BEVERAGE ANTENNA IN WIDE APERTURE HIGH FREQUENCY DIRECTION FINDING

[PART IV: THEORY]

Douglas N. Travers
Paul E. Martin
W. M. Sherrill

APR 9 1964

Part IV of IV parts of a cumulative reporting on Beverage antenna D/F research for the U. S. Navy. (Part I published 7 Feb 1962 as Fifth Interim Report on Contract Nr. NObsr-85364.) This report is submitted as an Interim Report, covering the period 4 Dec 1963 to 3 March 1964, prepared for the Navy Department, Bureau of Ships, Electronics Division, Contract Nr. NObsr-89345, Project Serial Nr. SF 0010805, Task 9094, Date of Report 23 March 1964.

SOUTHWEST RESEARCH INSTITUTE
SAN ANTONIO HOUSTON

1710 \$12.50

⑤ 818 600

⑥ USE OF THE BEVERAGE ANTENNA IN WIDE APERTURE HIGH FREQUENCY DIRECTION FINDING.

[PART IV: THEORY].

⑩ by Douglas N. Travers,
Paul E. Martin and
W. M. Sherrill.

⑨ Interim rept. 4 Dec 63 - 3 Mar 64,

Part IV of IV parts of a cumulative reporting on Beverage antenna D/F research for the U. S. Navy. (Part I published 7 Feb 1962 as Fifth Interim Report on Contract Nr. NObsr-85364.) This report is submitted as an Interim Report, covering the period 4 Dec 1963 to 3 March 1964, prepared for the Navy Department, Bureau of Ships, Electronics Division, Contract ~~Nr.~~ NObsr-89345 Project Serial Nr. ~~CF 0018805, Task 9094~~, Date of Report 23 March 1964.

⑮

APPROVED:

W. Lyle Donaldson
W. Lyle Donaldson, Director
Electronics and Electrical
Engineering

SOUTHWEST RESEARCH INSTITUTE
SAN ANTONIO HOUSTON

ABSTRACT

A detailed analysis is presented for a circular array of Beverage antennas over a conducting earth. Equations are derived for azimuth and elevation patterns for any number of similar antennas in the array taken any number at a time, spaced in any manner, and summed in any arbitrary manner with or without phasing. Of particular interest for HF direction finding applications are sector arrays of 10 to 20 antennas located 2° apart and operated between 1 and 40 mc. Simple summing ~~(nonphased)~~ of typical sector arrays produces patterns which have greatly reduced beamwidth compared to single element patterns. At 10 mc, a 25 meter long single element, one meter high, has a 3 db beamwidth of about 78° , while a circular sector array of 21 similar elements 2° apart has a beamwidth of about 18° without phasing. Elevation patterns for short element, large sector arrays show similarly narrow azimuth patterns up to elevation angles of 70° at 10 mc for an array diameter of less than 900 feet.

The analysis provides both ground wave and sky wave patterns. For sky wave patterns the polarization of the incident field may be linear or elliptical ~~(any condition between vertical and horizontal polarization)~~. Calculations show the sector arrays considered so far to have low polarization error. Polarization error is further reduced as beamwidth is reduced.

The analysis also provides antenna impedance, antenna line constants, effective height, wave tilt angle and various other parameters. Calculated performance shows the antennas to have impedances and patterns normally associated with frequency independent antennas. The results show that D/F performance over a 100 to 1 frequency range extending as low as 1.5 mc, should be obtained in a single array including good azimuth patterns at high elevation angles. Furthermore, the simplicity of the antenna element design permits what is probably the lowest cost wide aperture direction finder antenna array yet designed for the MF, HF, and VHF frequency ranges.

Calculated ~~(and also as reported in Part II, measured)~~ effective heights indicate that the summed sector arrays provide an adequate sensitivity with resulting effective heights ranging from a few meters to the vicinity of 100 meters. Bearing sensitivity is probably as good as present day instrumentation can utilize either in a scanning or fixed beam mode.

It is also apparent from the analysis that the performance of the antenna array is not highly dependent on a specific earth conductivity as in the case of some D/F antennas. Reception is improved by an increased wave tilt angle usually associated with poorly conducting earth. Thus the system is probably more adaptable to varying site terrain than is the usual D/F system.

This is Part IV of a four-part report and is concerned primarily with theory. Part II is concerned with system design and performance for long range HF D/F while Part III is a detailed report on measured accuracy of a 900-ft diameter array of 180 antennas. Part I was submitted in 1962. All theoretical background material necessary to the analysis has been reproduced in the Appendix.

TABLE OF CONTENTS

	<u>Page</u>
LIST OF ILLUSTRATIONS	vi
LIST OF TABLES	viii
A. Analysis of a Circular Array of Beverage Antennas	1
1. Outline of the Derivation of Array Equations	1
2. Symbol Definitions and Some Assumptions	2
3. Derivation of the Total Electric Field at a Point P_k on the k th Antenna	10
4. Derivation of the Array Pattern	15
B. Specification of the Beverage Antenna Elements	21
1. Antenna Constants and the Wave Tilt Angle	21
2. Theoretical Calculation of Characteristic Impedance, Input Impedance and Propaga- tion Constant	23
3. Estimate of the Radiation Resistance	34
C. Effective Height, Sensitivity and Signal-to-Noise Ratio	35
D. Beverage Antenna Array Calculations with a Digital Computer	41
E. Theoretical Antenna Patterns	56
F. Comments and Conclusions	131
1. Accuracy Expected Based on Theory	131
2. Bandwidth	132
3. Effective Height and Sensitivity	132
4. Computer Analysis	133
5. Continued Investigation	133
G. Recommendations	134
H. Bibliography	135

TABLE OF CONTENTS (Cont'd)

	<u>Page</u>
APPENDICES	
I. Reprint of "Wave Propagation in Overhead Wires with Ground Return" by John R. Carson	138
II. Reprint of "Propagation of High-Frequency Currents in Ground Return Circuits" by W. H. Wise	148
III. Letter from W. H. Wise Correcting Previous Papers	153
IV. Reprint of "Potential Coefficients for Ground Return Circuits" by W. H. Wise	155

LIST OF ILLUSTRATIONS

<u>Figure</u>		<u>Page</u>
1	Circular Array of Beverage Antennas	3
2	Detail of the Ground Wave Near the k^{th} Antenna	4
3	Detail of the Earth Reflection Near the k^{th} Antenna	5
4	Wave Tilt Angle vs Frequency	24
5	r_c/h vs. Conductivity and Frequency	26
6	The Magnitude of the Correction Fraction S for Typical Conditions	28
7	P vs. r_c (taken from Carson's paper Figure 2, $\theta = 0$)	30
8	Q vs. r_c (taken from Carson's paper Figure 3, $\theta = 0$)	31
9	Sketch of Beverage Array Calculation Geometry	43
10	Beverage Array IIC Simplified Input-Output-Sense Switch Block Diagram	49
11	Beverage Array Pattern Calculation, Program for Digital Computation (Start)	50
12	Beverage Array Pattern Calculation, Program for Digital Computation (A)	50
13	Beverage Array Pattern Calculation, Program for Digital Computation (B)	51
14	Beverage Array Pattern Calculation, Program for Digital Computation (C)	51
15	Beverage Array Pattern Calculation, Program for Digital Computation (D)	52

LIST OF ILLUSTRATIONS (Cont'd)

<u>Figure</u>		<u>Page</u>
16	Beverage Array Pattern Calculation, Program for Digital Computation (E)	52
17	Beverage Array Pattern Calculation, Program for Digital Computation (F)	53
18	Beverage Array Pattern Calculation, Program for Digital Computation (G)	53
Antenna Pattern Figures (See list commencing on page 63)		

LIST OF TABLES

<u>Table</u>		<u>Page</u>
1	Symbol Definitions	6
2	Earth Conductivity Conversion Table (with Typical Dielectric Constants)	24
3	Analysis and Machine Symbols Input Parameters	44
4	List of Input Cards for Beverage Array II _C Run on GE-225 with WIZ Language	45
5	Sense Switch Options-Beverage Array II _C	46
6	List of Program Output Quantities	47

A. Analysis of a Circular Array of Beverage Antennas

1. Outline of the Derivation of Array Equations

It was required that a procedure be developed for deriving optimum circular arrays of Beverage antennas for high frequency direction finding. Criteria for an optimum array are bearing accuracy, a narrow beam azimuth pattern and a favorable elevation pattern for sky waves. Although bearing accuracies will not be calculated directly in the analysis which follows, it will be assumed that if the azimuth pattern, formed by a wide aperture distribution of antenna elements, can be made more directive, then the resulting bearing information will move in the direction of improved accuracy. The conditions for favorable elevation patterns and maximum effective height will also be determined. The analysis will also permit estimates of polarization error.

The principal variables to be optimized are the number of antennas, the manner of summing, antenna spacing geometry, antenna location or overall array size, antenna length and height above ground. Other variables such as the termination geometry and antenna conductor geometry will usually be determined more on the basis of practical requirements rather than on optimization of electrical characteristics. Certain other variables will not be considered in this analysis, such as the mutual coupling between antennas, it being assumed that acceptable conditions can be specified from experience. (The reference of Appendix I is sufficiently general to treat mutual impedance theoretically if this should be of interest at any future time.)

The procedure followed in the derivations given below was to assume the geometry shown in Figures 1, 2 and 3 and to assume independent ground and sky wave components arriving at the same azimuth. The sky wave component includes both vertical and horizontal polarization components which may be specified independently.

The total field strength for direct and reflected rays is calculated at a point on the antenna wire, with phase referred to the origin. The exact reflection coefficients of the earth for both polarizations are retained in the calculation for the sky waves, and the earth constants as they determine the wave tilt for the ground wave.

The analysis is applied to the k th antenna of a circular array as shown in Figure 1, all antennas being arranged in symmetrical pairs about the x axis. All antennas are assumed to have similar geometry and electrical characteristics. The earth under the antennas is assumed to be constant in the x and y directions.

The receiving end current of the kth antenna is found by integration along the conductor. The currents for all antennas are then summed and assigned arbitrary amplitude and phase constants such as would correspond to insertion of a goniometer or special phasing networks for fixed beams.

Analytical methods of summing antenna element currents to determine the complete array patterns are various, such as the use of Fourier transforms. Most of these methods are useful on linear arrays particularly with omnidirectional elements. In the case of radially oriented end fire elements in a circular array, no significantly useful short-cut methods have been found which allow clear-cut trading between beamwidth and side lobe level (for instance). It has, therefore, been decided to use a digital computer to sum the antenna currents derived. For the present, "trial and error" pattern calculations are being used; that is, most calculations are based on assumed antenna arrays, with substitution of measured electrical characteristics which are appropriate to the local site. The resulting patterns are then evaluated for quality. This method has been found to be quite satisfactory.

A large number of calculated patterns are presented in this report (Part IV). *At some later date it may be advantageous to use more advanced programming methods to design arrays for specific optimum conditions, i. e., specified side lobe level, bandwidth, etc. At the present time, however, the problem to be solved does not require this degree of sophistication. Some of the more interesting patterns calculated have been experimentally checked by field measurements. A few examples of these checks have been included in Part II of this report.

2. Symbol Definitions and Some Assumptions

The following symbols and definitions will be adopted in addition to those of Figures 1, 2, 3 and 9. All parameters are in MKS units except where noted. (The use of emu units has been retained in certain parts of the calculation which are based on early references).

*Although detailed analysis and interpretation of the patterns has been placed in Part II.

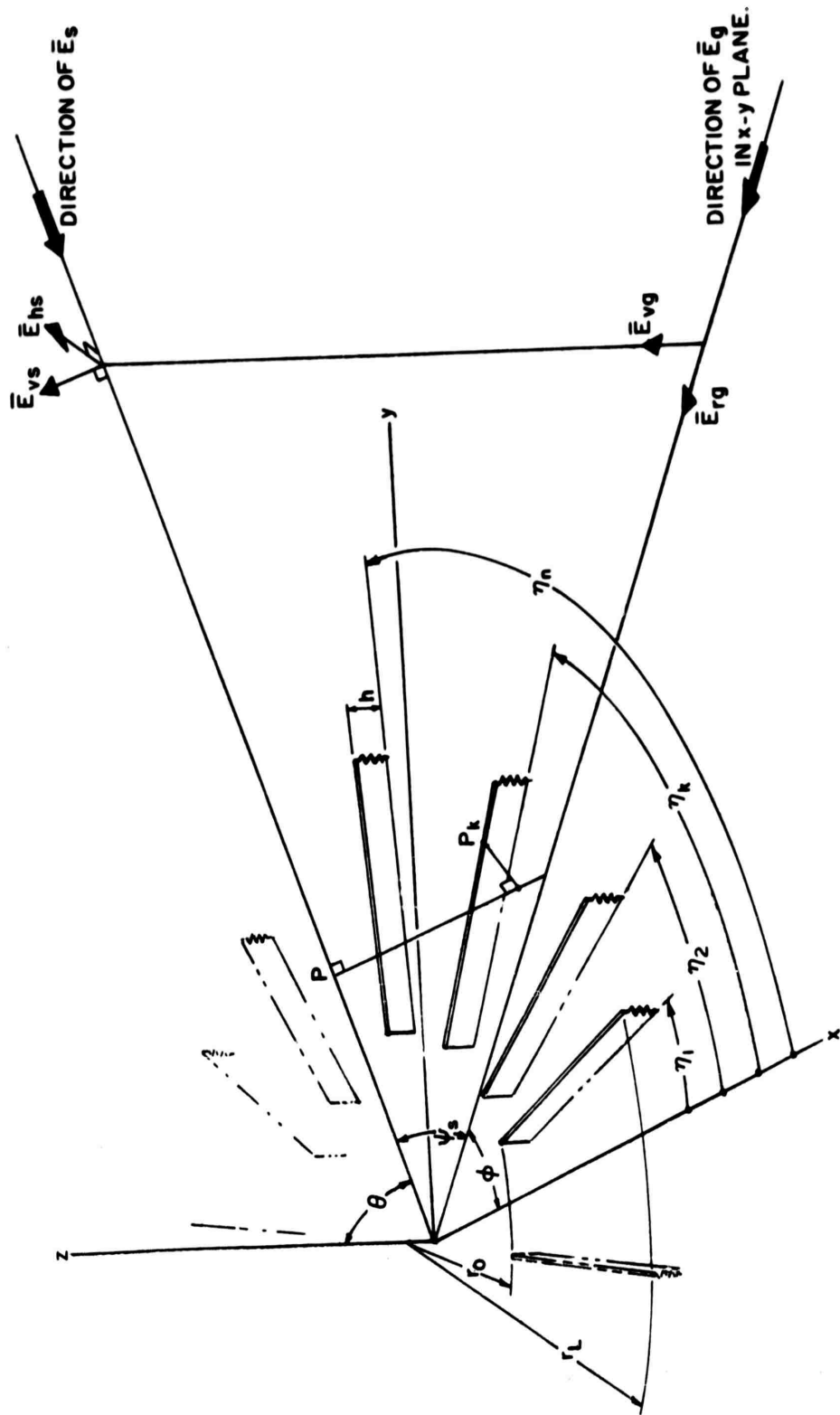


FIGURE 1
CIRCULAR ARRAY OF BEVERAGE ANTENNAS.

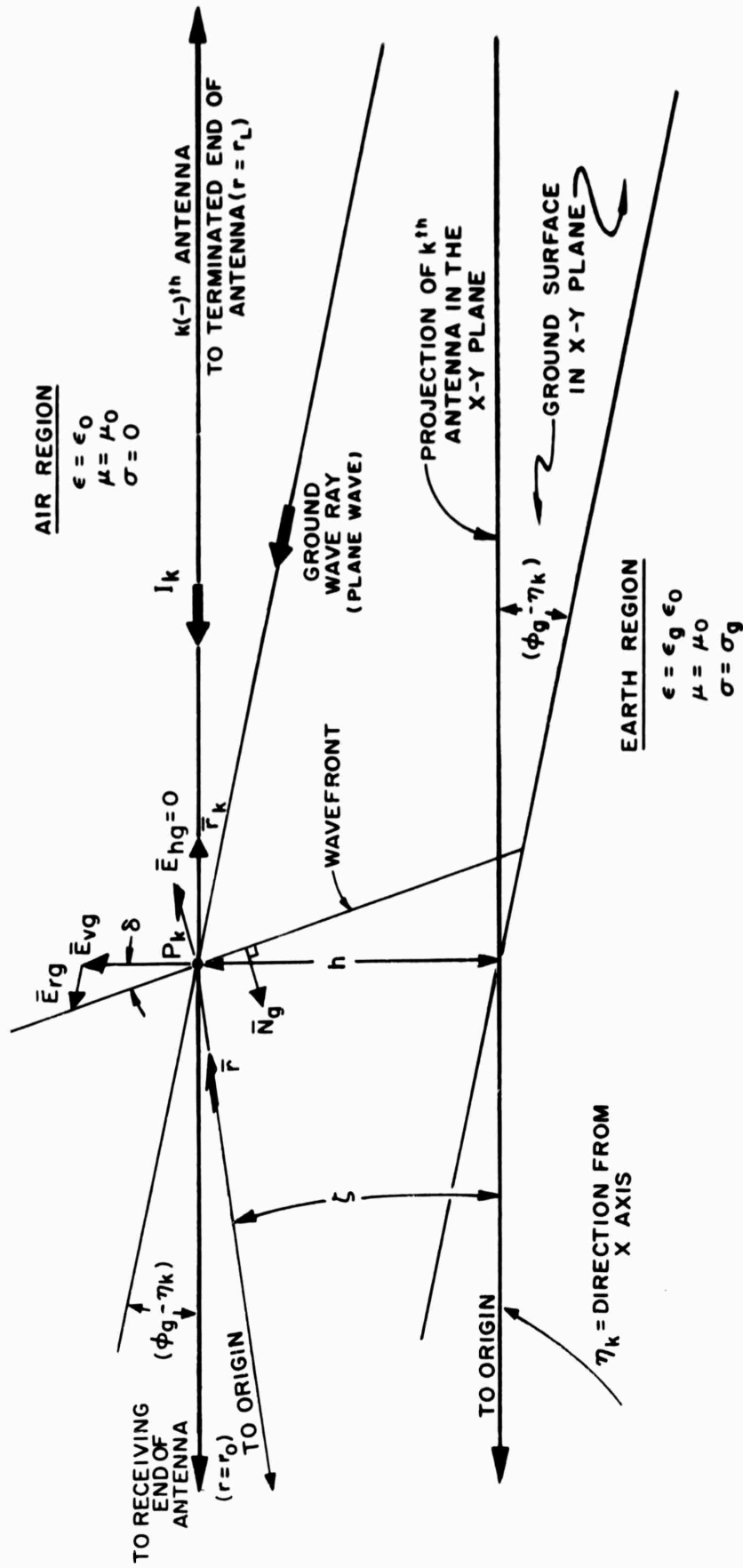


FIGURE 2
 DETAIL OF THE GROUND WAVE NEAR THE k th ANTENNA.

TABLE 1. SYMBOL DEFINITIONS

α	= Attenuation constant (nepers per meter)
β	= Phase constant = $2\pi/\lambda$ (radians per meter)
β_0	= Free space phase constant
Γ_k	= Parameter designating an arbitrary antenna
γ	= Propagation constant = $\alpha + j\beta$
δ	= Wave tilt angle
ϵ	= Permittivity
ϵ_g	= Relative dielectric constant of the earth
ϵ_0	= Permittivity of free space
ζ	= Angle defined in Figure 3
ζ_w	= Amplitude of Wise's correction factor
η	= Phase of Wise's correction factor
η_k	= Plus or minus azimuth of kth antenna
θ	= Angle of incidence
λ	= Wavelength, or wavelength on the antenna
λ_0	= Free space wavelength
μ	= Permeability, also an integration parameter in equation (44)
μ_g	= Permeability of the earth
μ_0	= Permeability of free space
ξ	= Phase angle representing path length difference between direct ray and reflected ray at Point P_k
$\rho_{k(-)}$	= Arbitrary phase constant for k(-)th antenna
$\rho_{k(+)}$	= Arbitrary phase constant for k(+)th antenna
$\sigma^{k(+)}$	= Conductivity
σ_g	= Conductivity of the earth
Φ_{hs}	= Arbitrary phase constant for horizontally polarized sky wave
Φ_{rg}	= Arbitrary phase constant for ground wave
Φ_{vs}	= Arbitrary phase constant for vertically polarized sky wave
ϕ	= - Azimuth of signal arrival
ϕ_g	= - Azimuth of arrival of \bar{E}_g
ϕ_s	= - Azimuth of arrival of \bar{E}_s
ψ_s	= Angle of elevation above xy plane of direction of arrival of \bar{E}_s
ω	= $2\pi f$
A	= Parameter in Wise's analysis
a_1	= Arbitrary constant
a_2	= Arbitrary constant
B	= Parameter in Wise's analysis
b	= Radius of the antenna conductor

TABLE 1. SYMBOL DEFINITIONS (Cont'd)

C	= Capacitance per unit length
c	= Velocity of light = 3×10^8 meters/second
\bar{E}_{gp}	= Component of ground wave electric field parallel to kth antenna at P_k
\bar{E}_{hg}	= Horizontally polarized part of ground wave electric field (perpendicular to direction of travel)
\bar{E}_{hgp}	= Component of horizontally polarized ground wave electric field parallel to kth antenna at P_k
\bar{E}_{hs}	= Horizontally polarized part of sky wave electric field (perpendicular to plane of incidence and direction of travel)
\bar{E}_p	= Total electric field parallel to kth antenna at P_k
\bar{E}_{rg}	= Horizontally polarized part of ground wave which is also in direction of propagation, sometimes called the wave tilt component or the radial component (lies parallel to the xy plane)
\bar{E}_{rgp}	= Component of radial ground wave electric field parallel to kth antenna at P_k
\bar{E}_{sp}	= Component of sky wave electric field parallel to the kth antenna at P_k
\bar{E}_{vg}	= Vertically polarized part of ground wave
\bar{E}_{vs}	= Vertically polarized part of sky wave (in plane of incidence and perpendicular to direction of travel)
f	= Frequency
G	= Conductance per unit length
$G_{k(-)}$	= Arbitrary amplitude constant for k(-)th antenna
$G_{k(+)}$	= Arbitrary amplitude constant for k(+)th antenna
h	= Height of antenna above ground
h_e	= Effective height
h'	= Parameter in equation (44)
I	= Current
I_k	= Current of kth pair modified by summing networks
I_{ko}	= Current from the kth pair
$I_{k(-)}$	= Current on k(-)th antenna at P_k
$I_{k(-)o}$	= Current from k(-)th antenna
$I_{k(+)}$	= Current on k(+)th antenna at P_k
$I_{k(+)o}$	= Current from k(+)th antenna
j	= Imaginary unit
K	= A constant proportional to square root of resistivity as in equation (67)
$k(-)$	= Denoting the k(-)th antenna
$k(+)$	= Denoting the k(+)th antenna
L	= Length of the Beverage antenna in meters, also inductance per unit length in henries per meter

TABLE 1. SYMBOL DEFINITIONS (Cont'd)

l	= First direction cosine
l_g	= First direction cosine for \bar{N}_g
l_s	= First direction cosine for \bar{N}_s
l_1	= First direction cosine for \bar{r}_1
l_2	= First direction cosine for \bar{r}_2
m	= Second direction cosine, also a constant integer
m_g	= Second direction cosine for \bar{N}_g
m_s	= Second direction cosine for \bar{N}_s
m_1	= Second direction cosine for \bar{r}_1
m_2	= Second direction cosine for \bar{r}_2
\bar{N}_g	= Unit vector in direction of propagation of ground wave
\bar{N}_s	= Unit vector in direction of propagation of sky wave
N	= Summing index in computer program
n	= Velocity ratio or subscript denoting the n th antenna, also the third direction cosine
n_g	= Third direction cosine for \bar{N}_g
n_s	= Third direction cosine for \bar{N}_s
n_1	= Third direction cosine for \bar{r}_1
n_2	= Third direction cosine for \bar{r}_2
P	= Parameter used in Carson's analysis as in equation (43), emu units
P'	= $P \times 10^{-7}$ (P' is in MKS units)
Q	= Parameter used in Carson's analysis as in equation (43), emu units
Q'	= $Q \times 10^{-7}$ (Q' is in MKS units)
R	= Resistance per unit length
R_o	= Real part of Z_o
R_r	= Radiation resistance
R_h	= Complex reflection coefficient of the earth for horizontal polarization
R_v	= Complex reflection coefficient of the earth for vertical polarization
r	= Distance from origin to P_k
r_c	= Carson's parameter defined by equation (49) in emu
r_{cw}	= Wise's modification of Carson's parameter r_c in emu
r_k	= Distance to P_k from point ($Z = h, y = 0, x = 0$)
r_o	= Inner radius of the array circle
r_L	= Outer radius of the array circle
r_s	= Distributed loss resistance in Carson's analysis
\bar{r}	= Vector in radial direction from origin to P_k
\bar{r}_1	= Arbitrary vector
\bar{r}_2	= Arbitrary vector

TABLE 1. SYMBOL DEFINITIONS (Cont'd)

s	= Wise's correction factor
t	= Time
V	= Voltage
V_p	= Voltage induced by \bar{E}_p
v	= Signal velocity on the antenna
X_o	= Imaginary part of Z_o
Z_o	= Characteristic impedance
Z_L	= Load impedance, terminating impedance of the line
Z_{in}	= Impedance looking into the line at the point P_k
Z_r	= Sending end (receiver end) impedance of the line

Certain other symbols and equivalents to the above symbols are given in Section D of this report where the digital computer program is described.

A previous analysis by A. D. Bailey¹ considered the problem of a single Beverage antenna. The analysis which follows is similar and extends results to the case of the array described in Figure 1.

We first wish to establish the total electric field intensity at an arbitrary point on the kth antenna; the induced current will then be summed over the length of the antenna. Proceeding with the ground wave \bar{E}_g arriving at the azimuth direction $-\phi_g$, for the components parallel to the antenna at P_k we have

$$\bar{E}_{rgp} = \bar{E}_{rg} \cos(\phi_g - \eta_k) \quad (1)$$

$$\bar{E}_{hgp} = 0 \quad (2)$$

In extreme circumstances such as a very close target transmitter, or very unusual values for the earth constants σ_g and ϵ_g , it might occur that the horizontally polarized ground wave \bar{E}_{hg} is not equal to zero, hence equation (2) is an approximation. Nevertheless, it is valid under almost all circumstances of practical interest, especially when a vertically polarized far zone transmitter is used. The case of the antenna considered as a source yields a solution which bears this out as the \bar{E}_{hg} component

1. Bailey, A. D., Dyson, J. D., and Hayden, E. C., "Studies and Investigations Leading to the Design of a Radio Direction Finder System for the MF-HF-VHF Range," Fourth Quarterly Report, 30 June 1962, Contract No. DA 36-093-SC-87264, EERL, University of Illinois, Urbana, Illinois.

tangential to the ground "varies as the inverse square of the distance and is of no significance at radio frequencies²."

Proceeding with the sky wave there are four components, two direct and two reflected (or two vertical and two horizontal), all arriving from -azimuth ϕ_s

$$\begin{aligned} \bar{E}_{sp} = & \bar{E}_{vs} \cos(\phi_s - \eta_k) \sin \psi_s + \bar{E}_{hs} \sin(\phi_s - \eta_k) \\ & + \bar{E}_{vs} R_{ve}^{j\xi} \cos(\phi_s - \eta_k) \sin \psi_s + \bar{E}_{hs} R_{he}^{j\xi} \sin(\phi_s - \eta_k) \end{aligned} \quad (3)$$

There is no radial component of the sky wave since the medium above the earth is nonconducting. The total parallel electric field at the point P_k is therefore

$$\bar{E}_p = \bar{E}_{gp} + \bar{E}_{sp} \quad (4)$$

where \bar{E}_{gp} is the sum of equations (1) and (2).

A plane earth is assumed with electromagnetic constants which range within reasonable values such as

$$\mu_g = \mu_0$$

$$1 \leq \epsilon_g \leq 100$$

$$10^{-5} \leq \sigma_g \leq 5 \text{ mks}$$

It has also been assumed that the transmission efficiency of the line is reasonable, that is, the attenuation constant of the line is not excessively large, and the phase velocity on the line is somewhere in the vicinity of the velocity of light (at least .3c).

3. Derivation of the Total Electric Field at a Point P_k on the k th Antenna

From inspection of Figure 1, which is based on a conventional spherical coordinate system, the direction cosines of any radial direction from the origin, defined by the vector \bar{r} , are by definition:

2. Wait, James R., "Radiation from a Ground Antenna," Canadian Journal of Technology, Vol. 32, No. 1, January 1954, pp. 1-9.

$$\begin{aligned}
 l &= \sin \theta \sin \phi \\
 m &= \sin \theta \cos \phi \\
 n &= \cos \theta
 \end{aligned} \tag{5}$$

The cosine of the angle between any two directions defined by unit vectors \bar{r}_1 and \bar{r}_2 is therefore

$$\bar{r}_1 \cdot \bar{r}_2 = l_1 l_2 + m_1 m_2 + n_1 n_2 \tag{6}$$

Now consider the ground wave component at the point P_k on the k (-)-th antenna as indicated in Figures 1 and 2. Note that the planes of constant phase are tilted forward by an angle δ . The coordinates of the point P_k are

$$\begin{aligned}
 x &= |\bar{r}| \cos \zeta \cos \eta_k \\
 y &= |\bar{r}| \cos \zeta \sin \eta_k \\
 z &= |\bar{r}| \sin \zeta
 \end{aligned} \tag{7}$$

The direction cosines of the unit vector \bar{N}_g normal to the plane of constant phase (wavefront) of the ground wave³ are

$$\begin{aligned}
 l_g &= -\cos \delta \cos \phi_g \\
 m_g &= -\cos \delta \sin \phi_g \\
 n_g &= \sin \delta
 \end{aligned} \tag{8}$$

Note that the ground wave is assumed to arrive from a direction above the x-y plane by the amount of the wave tilt angle δ . The details of the wave tilt phenomena are covered briefly in a later section and are

3. In general \bar{E}_{rg} and \bar{E}_{vg} are not in phase, in which case what is meant is the direction of the minor axis of the ellipse formed.

thoroughly reported in the literature⁴⁻⁶. The wave tilt angle normally ranges from zero (or near zero) over highly conducting surfaces to something less than 25° over most dry soil surfaces. Wait⁷ has shown that this may be increased over a stratified ground. Typical values are given in a later section of this report.

The equation of the plane of constant phase which passes through the point P_k is therefore $\bar{N}_g \cdot \bar{r} = \text{a constant}$ ⁸. Therefore

$$\begin{aligned} \bar{N}_g \cdot \bar{r} = l_g x + m_g y + n_g z = - |\bar{r}| (\cos \zeta \cos \delta \cos \eta_k \cos \phi_g \\ + \cos \zeta \cos \delta \sin \eta_k \sin \phi_g - \sin \zeta \sin \delta) \end{aligned} \quad (9)$$

Now since $r = |\bar{r}|$, the phase distance from the origin, of the point P_k along the direction \bar{N}_g , is by simplification of (9)

$$\beta_o (\bar{N}_g \cdot \bar{r}) = - \beta_o r [\cos \delta \cos \zeta \cos (\phi_g - \eta_k) - \sin \delta \sin \zeta] \quad (10)$$

Hence the ground wave component of the electric field parallel to the k th antenna at P_k is

$$\bar{E}_{rgp} = |\bar{E}_{rg}| \cos (\phi_g - \eta_k) e^{j\omega \left(t - \frac{\bar{N}_g \cdot \bar{r}}{c} - \frac{\Phi_{rg}}{\omega} \right)} \quad (11)$$

4. Zenneck, J., "The Propagation of Plane Electromagnetic Waves over a Flat Earth and Its Application to Wireless Telegraphy," *Annalen der Physik*, Vol. 23, 1907, p. 846.

5. Feldman, C. B., "The Optical Behavior of the Ground for Short Radio Waves," *Proceedings of the I.R.E.*, Vol. 21, No. 6, June 1933, pp. 764-801.

6. Piggott, W. R., "A Method of Determining the Polar Diagrams of Long Wire and Horizontal Rhombic Aerials," Dept. of Scientific and Industrial Research, Radio Research Special Report No. 16, London, H. M. Stationery Office, 1948.

7. Wait, James R., "Propagation of Radio Waves over a Stratified Ground," *Geophysics*, Vol. 18, 1953, pp. 416-422.

8. Jordan, Edward C., Electromagnetic Waves and Radiating Systems, New York, Prentice-Hall, Inc., 1950.

where $\omega = \beta_0 c$ and Φ_{rg} is an arbitrary phase constant used only to relate \bar{E}_{rg} to the other electric field components. Substituting equation (10) into (11), the complete expression for the ground wave component parallel to the k th antenna at P_k is

$$|\bar{E}_{rgp}| = |\bar{E}_{rg}| \cos(\phi_g - \eta_k) e^{j\omega \left\{ t + \frac{r}{c} [\cos \delta \cos \zeta \cos(\phi_g - \eta_k) - \sin \delta \sin \zeta] - \frac{\Phi_{rg}}{\omega} \right\}} \quad (12)$$

When only the ground wave is present, equation (12) is sufficient to complete the analysis; however, when sky waves are present, the component \bar{E}_{sp} is also required. Referring to Figure 3 the sky wave ray which is reflected at R is delayed in phase by an amount ξ at P_k where

$$\xi = \vec{RP}_k - \vec{QP}_k \quad (13)$$

This simplifies to

$$\xi = \frac{\beta_0 h}{\sin \psi_s} - \frac{\beta_0 h \cos 2\psi_s}{\sin \psi_s} = \frac{4\pi h \sin \psi_s}{\lambda_0} = 2\beta_0 h \sin \psi_s \quad (14)$$

Therefore, the total sky wave at P_k may be written

$$\bar{E}_s = \bar{E}_{vs} \left(1 - R_v e^{-j2\beta_0 h \sin \psi_s} \right) e^{-j\Phi_{vs}} + \bar{E}_{hs} \left(1 + R_h e^{-j2\beta_0 h \sin \psi_s} \right) e^{-j\Phi_{hs}} \quad (15)$$

The phase of \bar{E}_s at P_k relative to the origin is $\beta_0(\bar{N}_s \cdot \bar{r})$ similar to the manner in which equations (9), (10) and (11) derived the ground wave phase $\beta_0(\bar{N}_g \cdot \bar{r})$. The direction cosines of \bar{N}_s are

$$\left. \begin{aligned} \ell_s &= -\cos \psi_s \cos \phi_s \\ m_s &= -\cos \psi_s \sin \phi_s \end{aligned} \right\} \begin{array}{l} \text{both direct} \\ \text{and reflected} \end{array} \quad (16)$$

$$n_s = +\sin \psi_s \quad (\text{direct})$$

$$n_s = -\sin \psi_s \quad (\text{reflected})$$

Now equation (15) has been written entirely in terms of the incident field, hence the third direction cosine with the minus sign is not used. [If equation (15) were written in terms of the incident and reflected components, the difference in the third direction cosine would contribute the term $2\beta_0 r \sin \zeta \sin \psi_s$, however, this term was derived by another method as shown by equation (14).] The coordinates of P_k are given by equation (7), hence

$$\beta_0(\bar{N}_s \cdot \bar{r}) = -\beta_0 r [\cos \zeta \cos \psi_s \cos \phi_s \cos \eta_k + \cos \zeta \cos \psi_s \sin \phi_s \sin \eta_k - \sin \zeta \sin \psi_s] \quad (17)$$

Therefore, the total sky wave parallel to the antenna at P_k is

$$\begin{aligned} \bar{E}_{sp} = & \left\{ |\bar{E}_{vs}| \sin \psi_s \cos(\phi_s - \eta_k) \left[1 - R_v e^{-j2\beta_0 h \sin \psi_s} \right] e^{-j\Phi_{vs}} \right. \\ & \left. + |\bar{E}_{hs}| \sin(\phi_s - \eta_k) \left[1 + R_h e^{-j2\beta_0 h \sin \psi_s} \right] e^{-j\Phi_{hs}} \right\} e^{j\omega \left(t - \frac{\bar{N}_s \cdot \bar{r}}{c} \right)} \end{aligned} \quad (18)$$

where

$$\bar{N}_s \cdot \bar{r} = -r [\cos \zeta \cos \psi_s \cos(\phi_s - \eta_k) - \sin \zeta \sin \psi_s] \quad (19)$$

When the ground wave and the sky wave arrive at the same azimuth, then $\phi = \phi_s = \phi_g$. The total electric field parallel to the antenna at P_k is therefore the sum of equations (11) and (18)

$$\begin{aligned} \bar{E}_p = & \left\{ |\bar{E}_{rg}| \cos(\phi - \eta_k) e^{-j(\beta_0 \bar{N}_g \cdot \bar{r} + \Phi_{rg})} \right. \\ & + |\bar{E}_{vs}| \sin \psi_s \cos(\phi - \eta_k) \left[1 - R_v e^{-j2\beta_0 h \sin \psi_s} \right] e^{-j(\beta_0 \bar{N}_s \cdot \bar{r} + \Phi_{vs})} \\ & \left. + |\bar{E}_{hs}| \sin(\phi - \eta_k) \left[1 + R_h e^{-j2\beta_0 h \sin \psi_s} \right] e^{-j(\beta_0 \bar{N}_s \cdot \bar{r} + \Phi_{hs})} \right\} e^{j\omega t} \end{aligned} \quad (20)$$

where

$$\bar{N}_g \cdot \bar{r} = -r [\cos \delta \cos \zeta \cos (\phi - \eta_k) - \sin \delta \sin \zeta]$$

$$\bar{N}_s \cdot \bar{r} = -r [\cos \psi_s \cos \zeta \cos (\phi - \eta_k) - \sin \psi_s \sin \zeta]$$

$$R_v = \frac{\left(\epsilon_g - j \frac{\sigma_g}{\omega \epsilon_0} \right) \sin \psi_s - \sqrt{\left(\epsilon_g - j \frac{\sigma_g}{\omega \epsilon_0} \right) - \cos^2 \psi_s}}{\left(\epsilon_g - j \frac{\sigma_g}{\omega \epsilon_0} \right) \sin \psi_s + \sqrt{\left(\epsilon_g - j \frac{\sigma_g}{\omega \epsilon_0} \right) - \cos^2 \psi_s}} \quad (21)$$

$$R_h = \frac{\sin \psi_s - \sqrt{\left(\epsilon_g - j \frac{\sigma_g}{\omega \epsilon_0} \right) - \cos^2 \psi_s}}{\sin \psi_s + \sqrt{\left(\epsilon_g - j \frac{\sigma_g}{\omega \epsilon_0} \right) - \cos^2 \psi_s}}$$

4. Derivation of the Array Pattern

It may be assumed that in an elemental length dr_k of the k th antenna, at the point P_k , the parallel electric field \bar{E}_p will induce a voltage such that

$$dV_p = \bar{E}_p dr_k \quad (22)$$

Thus the potential gradient is

$$\frac{dV_p}{dr_k} = \bar{E}_p \quad (23)$$

The current and voltage distribution on the Beverage antenna may be expressed by transmission line equations⁹. If the transmission line (or Beverage antenna) is immersed in a field \bar{E}_p , parallel to the line, the usual transmission line equation for the potential gradient must include a term such as given by equation (23). Therefore, the transmission line equations when written for a Beverage antenna are:

9. Beverage. Harold H., Rice, Chester W., and Kellogg, Edward W., "The Wave Antenna, a New Type of Highly Directive Antenna," Transactions of the American Institute of Electrical Engineers, Volume 42, February 1923, pp. 215-266.

$$\frac{dV}{dr_k} = - (R + j\omega L) I + \frac{dV_p}{dr_k} \quad (24)$$

$$\frac{dI}{dr_k} = - (G + j\omega C) V$$

These equations may be solved in the usual manner for the receiving end current as was done by Herlitz¹⁰, or the line may be assumed to be terminated in the characteristic impedance $Z_0 = R_0 + jX_0$, at the far end (the point where $r_k = r_L$ for the k th antenna), and also at the sending end ($r_k = r_0$), and the current at the sending end found by integration as was done by Kellogg¹¹. Either method will yield the same result. Following Kellogg's procedure, the elemental current at P_k due to \bar{E}_p is

$$dI_{k(\cdot)} = \frac{dV_p}{Z_{in1} + Z_{in2}} \quad (25)$$

where the denominator ($Z_{in1} + Z_{in2}$) is the complete series impedance of the circuit. (Z_{in1} and Z_{in2} are the impedances seen looking into the line in each direction; with respect to the current in the antenna conductor, these impedances are in series through the ground.) Z_{in1} and Z_{in2} are in general given by the usual equations

$$Z_{in1} = Z_0 \left[\frac{Z_L \cosh \gamma (r_L - r) + jZ_0 \sinh \gamma (r_L - r)}{Z_0 \cosh \gamma (r_L - r) + jZ_L \sinh \gamma (r_L - r)} \right] \quad (25a)$$

$$Z_{in2} = Z_0 \left[\frac{Z_r \cosh \gamma (r - r_0) + jZ_0 \sinh \gamma (r - r_0)}{Z_0 \cosh \gamma (r - r_0) + jZ_r \sinh \gamma (r - r_0)} \right] \quad (25b)$$

10. Herlitz, Ivar, "Appendix B, Analysis of Action of Wave Antenna," (An Appendix to the paper by Beverage, Rice and Kellogg, "The Wave Antenna, a New Type of Highly Directive Antenna"), Transactions of the American Institute of Electrical Engineers, Volume 42, February 1923, pp. 260-266.

11. Beverage, Harold H., Rice, Chester W., and Kellogg, Edward W., "The Wave Antenna, a New Type of Highly Directive Antenna," Transactions of the American Institute of Electrical Engineers, Volume 42, February 1923, p. 224, footnote 10.

The elemental current $dI_{k(-)0}$ at the receiving end is retarded in phase and changed in amplitude by the propagation constant of the line, hence

$$dI_{k(-)0} = dI_{k(-)} e^{-\gamma(r_k - r_0)} \quad (26)$$

[Note again that r_k is the distance measured from the point ($z = h$, $y = 0$, $x = 0$) to P_k whereas r is the distance from the origin to P_k , or $r_k = r \cos \zeta$.] The total current at the receiving end is

$$I_{k(-)0} = \int_{r_L}^{r_0} dI_{k(-)0} = \int_{r_0}^{r_L} dI_{k(-)} e^{-\gamma(r_k - r_0)} \quad (27)$$

Substituting (25) into (27) yields the current at the receiving end

$$I_{k(-)0} = \int_{r_0}^{r_L} \bar{E}_p e^{-\gamma(r - r_0)} \frac{1}{Z_{in1} + Z_{in2}} dr_k \quad (28a)$$

where \bar{E}_p may in general be given by equation (20).

The integration of equation (28a) is greatly simplified if it is assumed that

$$Z_{in1} = Z_{in2} = Z_0 \quad (28b)$$

This assumption is in accord with the usual manner of terminating the antenna, although in practice it is never possible to achieve a termination exactly equal to Z_0 for two reasons. First, the ground resistance of the ground rod cannot be made zero, and second, Z_0 has a small reactive component which cannot be matched over a wide range of frequencies. Nevertheless, it is a good approximation in practice, and, when equation (28b) is closely approximated, equation (28a) becomes

$$I_{k(-)0} = \frac{1}{2Z_0} \int_{r_0}^{r_L} \bar{E}_p e^{-\gamma(r_k - r_0)} dr_k \quad (28c)$$

In most instances it will be true that $h \ll r_0$ so that $\cos \zeta \approx 1$ and $\sin \zeta \approx 0$. Hence equation (28c) may be rewritten replacing r_k by r

$$I_{k(-)0} = \frac{1}{2Z_0} \int_{r_0}^{r_L} \bar{E}_p e^{-\gamma(r - r_0)} dr \quad (29)$$

and the phase terms for equation (20) may be rewritten as

$$\begin{aligned} (\bar{N}_g \cdot \bar{r})' &= -r \cos \delta \cos (\phi - \eta_k) \\ (\bar{N}_s \cdot \bar{r})' &= -r \cos \psi_s \cos (\phi - \eta_k) \end{aligned} \quad (30)$$

Substituting equations (30) into (20) yields

$$\begin{aligned} \bar{E}_p &= \left\{ |\bar{E}_{rg}| \cos (\phi - \eta_k) e^{j[\beta_0 r \cos \delta \cos (\phi - \eta_k) - \Phi_{rg}]} \right. \\ &\quad + |\bar{E}_{vs}| \sin \psi_s \cos (\phi - \eta_k) \left[1 - R_v e^{-j2\beta_0 h \sin \psi_s} \right] e^{j[\beta_0 r \cos \psi_s \cos (\phi - \eta_k) - \Phi_{vs}]} \\ &\quad \left. + |\bar{E}_{hs}| \sin (\phi - \eta_k) \left[1 + R_h e^{-j2\beta_0 h \sin \psi_s} \right] e^{j[\beta_0 r \cos \psi_s \cos (\phi - \eta_k) - \Phi_{hs}]} \right\} e^{j\omega t} \end{aligned} \quad (31)$$

Hence the receiving end current for this case is given by equation (29) with (31) substituted for \bar{E}_p . This yields

$$\begin{aligned} I_{k(-)0} &= \frac{e^{j\omega t}}{2Z_0} \left\{ |\bar{E}_{rg}| \cos (\phi - \eta_k) e^{-j\Phi_{rg}} \int_{r_0}^{r_L} e^{j[\beta_0 r \cos \delta \cos (\phi - \eta_k)] - \gamma(r - r_0)} dr \right. \\ &\quad + \left[|\bar{E}_{vs}| \sin \psi_s \cos (\phi - \eta_k) (1 - R_v e^{-j2\beta_0 h \sin \psi_s}) e^{-j\Phi_{vs}} + |\bar{E}_{hs}| \sin (\phi - \eta_k) (1 + \right. \\ &\quad \left. + R_h e^{-j2\beta_0 h \sin \psi_s}) e^{-j\Phi_{hs}} \right] \cdot \int_{r_0}^{r_L} e^{j[\beta_0 r \cos \psi_s \cos (\phi - \eta_k)] - \gamma(r - r_0)} dr \left. \right\} \end{aligned} \quad (32)$$

The integrals are all of the form

$$\int_{r_0}^{r_L} e^{a_1 r + a_2} dr$$

where

$$a_1 = j\beta_0 \cos (\delta, \psi_s) \cos (\phi - \eta_k) - \gamma$$

$$a_2 = \gamma r_0$$

Therefore

$$\int_{r_0}^{rL} e^{a_1 r + a_2 dr} = \frac{e^{j\beta_0 rL \cos(\delta, \psi_s) \cos(\phi - \eta_k) - \gamma(rL - r_0)} - e^{j\beta_0 r_0 \cos(\delta, \psi_s) \cos(\phi - \eta_k)}}{j\beta_0 \cos(\delta, \psi_s) \cos(\phi - \eta_k) - \gamma}$$

Substituting the above solution into equation (32) and factoring the common terms of the sky wave component yields for the receiving end current of the $k(-)$ th antenna

$$\begin{aligned} I_{k(-)0} = \frac{e^{j\omega t}}{2Z_0} & \left\{ |\bar{E}_{rg}| \cos(\phi - \eta_k) e^{-j\Phi_{rg}} \left(\frac{1 - e^{j\beta_0 L \cos \delta \cos(\phi - \eta_k) - \gamma L}}{\gamma - j\beta_0 \cos \delta \cos(\phi - \eta_k)} \right) e^{j\beta_0 r_0 \cos \delta \cos(\phi - \eta_k)} \right. \\ & + \left[|\bar{E}_{vs}| \sin \psi_s \cos(\phi - \eta_k) \left(1 - R_{ve}^{-j2\beta_0 h \sin \psi_s} \right) e^{-j\Phi_{vs}} + |\bar{E}_{hs}| \sin(\phi - \eta_k) \left(1 + \right. \right. \\ & \left. \left. + R_{he}^{-j2\beta_0 h \sin \psi_s} \right) e^{-j\Phi_{hs}} \right] \cdot \left(\frac{1 - e^{j\beta_0 L \cos \psi_s \cos(\phi - \eta_k) - \gamma L}}{\gamma - j\beta_0 \cos \psi_s \cos(\phi - \eta_k)} \right) \\ & \left. \cdot e^{j\beta_0 r_0 \cos \psi_s \cos(\phi - \eta_k)} \right\} \end{aligned} \quad (33)$$

The current from the k th pair will be

$$I_{k0} = I_{k(-)0} + I_{k(+)0} \quad (34)$$

where $I_{k(-)0}$ is given by equation (33) and $I_{k(+)0}$ is given by equation (33) with $\cos(\phi + \eta_k)$ substituted for each $\cos(\phi - \eta_k)$ term, and $\sin(\phi + \eta_k)$ for each $\sin(\phi - \eta_k)$ term.

Introducing arbitrary amplitude and phase parameters $G_{k(\bar{\tau})}$ and $\rho_{k(\bar{\tau})}$ for each antenna to correspond to an arbitrary combining network equation (34) becomes

$$I_k = G_{k(-)} I_{k(-)0} e^{j\rho_{k(-)}} + G_{k(+)} I_{k(+)0} e^{j\rho_{k(+)}} \quad (35)$$

In general $G_{k(-)} \neq G_{k(+)}$ and $\rho_{k(+)} = \rho_{k(-)}$. For instance, to investigate a single antenna at $\eta_k = 0$, let $G_{k(-)} = 1$, $G_{k(+)} = 0$ and $\rho_{k(+)} = 0$. To investigate a difference pattern of two equal antennas let $G_{k(-)} = G_{k(+)}$ and $\rho_{k(-)} = 0$, $\rho_{k(+)} = \pi$, etc.

The sum of a circular array is therefore

$$I_{\text{total array}} = \sum_{k=1}^n I_k \quad (36)$$

Equation (36) is the complete three-dimensional pattern of the array.

B. Specification of the Beverage Antenna Elements

1. Antenna Constants and the Wave Tilt Angle

In order to use equation (36), it is necessary to specify the electric fields incident on the array, the array geometry, the propagation constant γ of the antenna, and the earth constants. It may also be preferable in some cases to specify the wave tilt angle determined by the earth constants. In the case of complex summing with phasing, it is also necessary to specify the goniometer amplitude and phase functions G_k and ρ_k . In order to simplify these steps in preparation for numerical calculations, formulas for the propagation constant and the wave tilt angle are required.

The propagation constant of a transmission line is defined to be

$$\gamma = \alpha + j\beta \quad (37)$$

where the symbols are defined in Table 1 and are:

α = attenuation constant in nepers/unit length

β = phase constant = $2\pi/\lambda$ where λ is the wavelength of the antenna

The attenuation constant of the Beverage antenna may be determined experimentally and found to vary with the earth constants and height above ground as well as other factors. For most purposes where the Beverage antenna is one or two meters above ground, the attenuation constant in the range of 3 to 30 mcs will be found to be in the range of .01 to .1 db per meter respectively for a reasonably good conductor such as number 12 or 14 copper conductor. To convert db/meter to nepers/meter, divide the db/meter figures by 8.686. This yields for the attenuation constant range mentioned the following very approximate but typical values:

$$\alpha = 10^{-3} \text{ neper/meter at 3 mc}$$

$$\alpha = 10^{-2} \text{ neper/meter at 30 mc}$$

These figures are a good rule of thumb for heights of about one meter. At lower heights the attenuation may increase considerably.

The phase constant may be conveniently expressed in terms of a "velocity ratio" n where:

$$n = \frac{\lambda}{\lambda_0} = \frac{v}{c} = \frac{\beta_0}{\beta} \quad (38)$$

An approximate value for n may be experimentally determined by exciting the antenna as an open circuited line, noting the wavelength on the antenna and dividing by the free space wavelength. Then it is possible to write the propagation constant in terms of measured data as:

$$\gamma = \frac{\alpha(\text{db/unit length})}{8.686} + j \frac{\beta_0(\text{radians/unit length})}{n} \quad (39)$$

Nearly exact values of n or β may also be calculated from Carson¹² and Wise¹³ as was stated previously for the attenuation constant¹⁴.

The wave tilt angle δ may be calculated from formulas given by various authors⁵⁻⁷ or it may be measured experimentally.¹⁵ Since the measurements are usually dependent on special equipment, calculation of the tilt from the earth constants and the frequency is the easier procedure when a nonstratified earth is approximated. Piggot⁷ gives the formula

$$\delta = \tan^{-1} \left[\frac{(\epsilon_g - 1)^2 + \left(\frac{2\sigma_g}{f}\right)^2}{\left[\epsilon_g + \left(\frac{2\sigma_g}{f}\right)^2\right]^2} \right]^{1/4} \quad (\text{esu units}) \quad (40)$$

which may be rewritten in MKS units as follows:

12. Carson, John R., "Wave Propagation in Overhead Wires with Ground Return," The Bell System Technical Journal, Volume V, 1926, pp. 539-554 (paper uses emu units).

13. Wise, W. H., "Propagation of High-Frequency Currents in Ground Return Circuits," Proceedings of the IRE, Vol. 22, No. 4, April 1934, pp. 522-527 (paper uses emu units).

14. Values of α and n which were obtained in a number of experimental cases are given in the Fifth Interim Report of this contract dated 7 February 1962, "Use of the Beverage Antenna in Wide Aperture High Frequency Direction Finding."

15. Gill, E. W. B., "A Simple Method of Measuring Earth Constants," Proc. of the Inst. of Electrical Engineers (London), Vol. 96, March 1949, pp. 141-145.

$$\delta = \tan^{-1} \left[\frac{(\epsilon_g - 1)^2 + \left(\frac{\sigma_g}{\epsilon_0 \omega}\right)^2}{\left[\epsilon_g^2 + \left(\frac{\sigma_g}{\epsilon_0 \omega}\right)^2\right]^2} \right]^{1/4} \quad (41)$$

In MKS units $\epsilon_0 = 8.854 \times 10^{-12}$. As a matter of interest equation (41) is plotted in Figure 4 for a variety of typical conditions. Typical values of σ_g may be inferred from these curves; other typical values for the earth constants are given in Table 2. It is evident that wave tilt angles are in general less than 20° with perhaps 10° a rough rule of thumb. Note that equation (41) gives the magnitude of the angle and does not include information relating the phase of the tilted component to the vertical component. Such data are available in the literature^{6, 8}.

Equations (39) and (41) may now be used to determine numerical values for substitution into the pattern equations.

2. Theoretical Calculation of Characteristic Impedance, Input Impedance and Propagation Constant

Nearly exact values of the characteristic impedance Z_0 and the propagation constant γ may be calculated from the antenna geometry and the earth constants by a method devised by Carson¹² and modified by Wise.¹³

The exact values of Z_0 and γ for a uniform transmission line are usually defined as¹⁶

$$Z_0 = \sqrt{\frac{R + j\omega L}{G + j\omega C}} \quad (42)$$

$$\gamma = \sqrt{(R + j\omega L)(G + j\omega C)} \quad (43)$$

Carson¹² provides the following expression for $(R + j\omega L)$ in electromagnetic cgs units (abohms/centimeter)

$$R + j\omega L = r_s + j2\omega l n \left(\frac{2h}{b} \right) + 4\omega \int_0^\infty (\sqrt{\mu^2 + j - \mu}) e^{-2h'\mu} d\mu \quad (44)$$

16. Skilling, Hugh Hildreth, Transient Electric Currents, McGraw-Hill Book Company, Inc., New York, 1952.

TABLE 2 EARTH CONDUCTIVITY CONVERSION TABLE
(With Typical Dielectric Constants)

Type of Earth	Conductivity (σ)			Resistivity $\left(\frac{1}{\sigma}\right)$ MKS (ohm-meter)	Dielectric Constant (Typical) (Relative Units)
	emu (abmho cm)	esu (statmho cm)	MKS (mho-meter)		
Sea Water	5×10^{-11}	4.5×10^{10}	5	.2	81
Sea Water	3×10^{-11}	2.7×10^{10}	3	.33	81
Wet Rich Soil	3×10^{-13}	2.7×10^8	.03	33	15 - 36
Average Soil (Wet)	1×10^{-13}	9×10^7	.01	100	10 - 25
Average Soil (Dry)	3×10^{-14}	2.7×10^7	3×10^{-3}	333	10 - 15
Poor Soil	1×10^{-14}	9×10^6	1×10^{-3}	10^3	10
Poor Soil (Dry)	3×10^{-15}	2.7×10^6	3×10^{-4}	3.3×10	8
Dry Sand	1×10^{-15}	9×10^5	1×10^{-4}	10^4	5
Dry Granite (Subsurface)	1×10^{-18}	900	10^{-7}	10^7	Probably <5

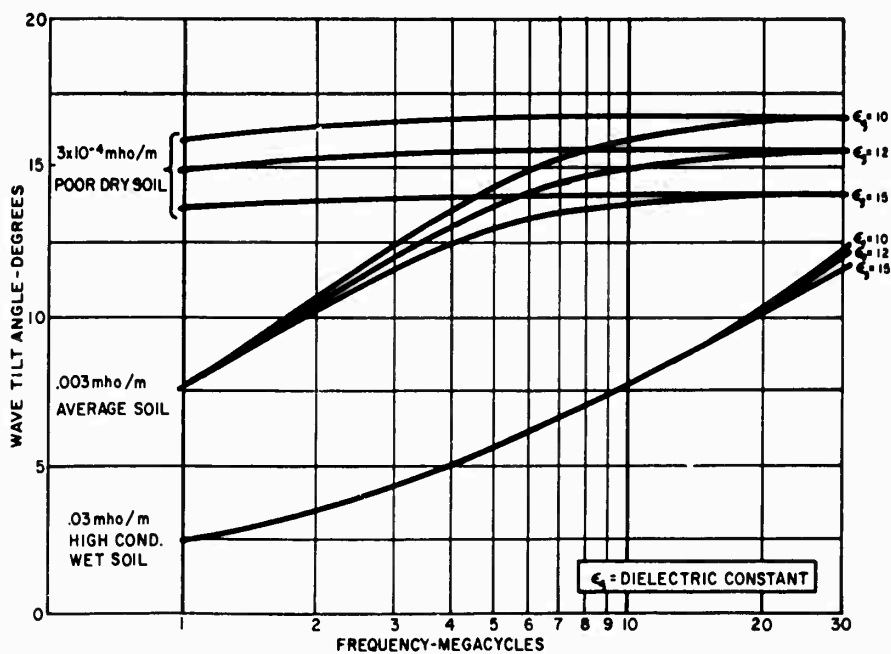


FIGURE 4
WAVE TILT ANGLE VS. FREQUENCY.

where μ is an integration parameter and has nothing to do with permeability.

The term r_s represents the distributed loss resistance of the antenna conductor, and the second term the distributed inductive reactance of the antenna conductor alone over a perfectly conducting ground plane. The integral term formulates the effect of the finite conductivity of the earth. Carson provides the solution to the integral neglecting displacement current (neglecting the dielectric constant of the earth) as

$$R + j\omega L = r_s + j2\omega \ln \left[\frac{2h}{b} \right] + 4\omega(P + jQ) \text{ emu} \quad (45)$$

This equation may be rewritten in MKS units throughout as follows

$$R + j\omega L = r_s + j2\omega 10^{-7} \ln \left(\frac{2h}{b} \right) + 4\omega(P' + jQ') \frac{\text{ohms}}{\text{meter}} \quad (46)$$

where

$$P' + jQ' = (P + jQ)10^{-7} \quad (47)$$

P and Q as derived by Carson are complicated functions (to be considered below) of r_c where

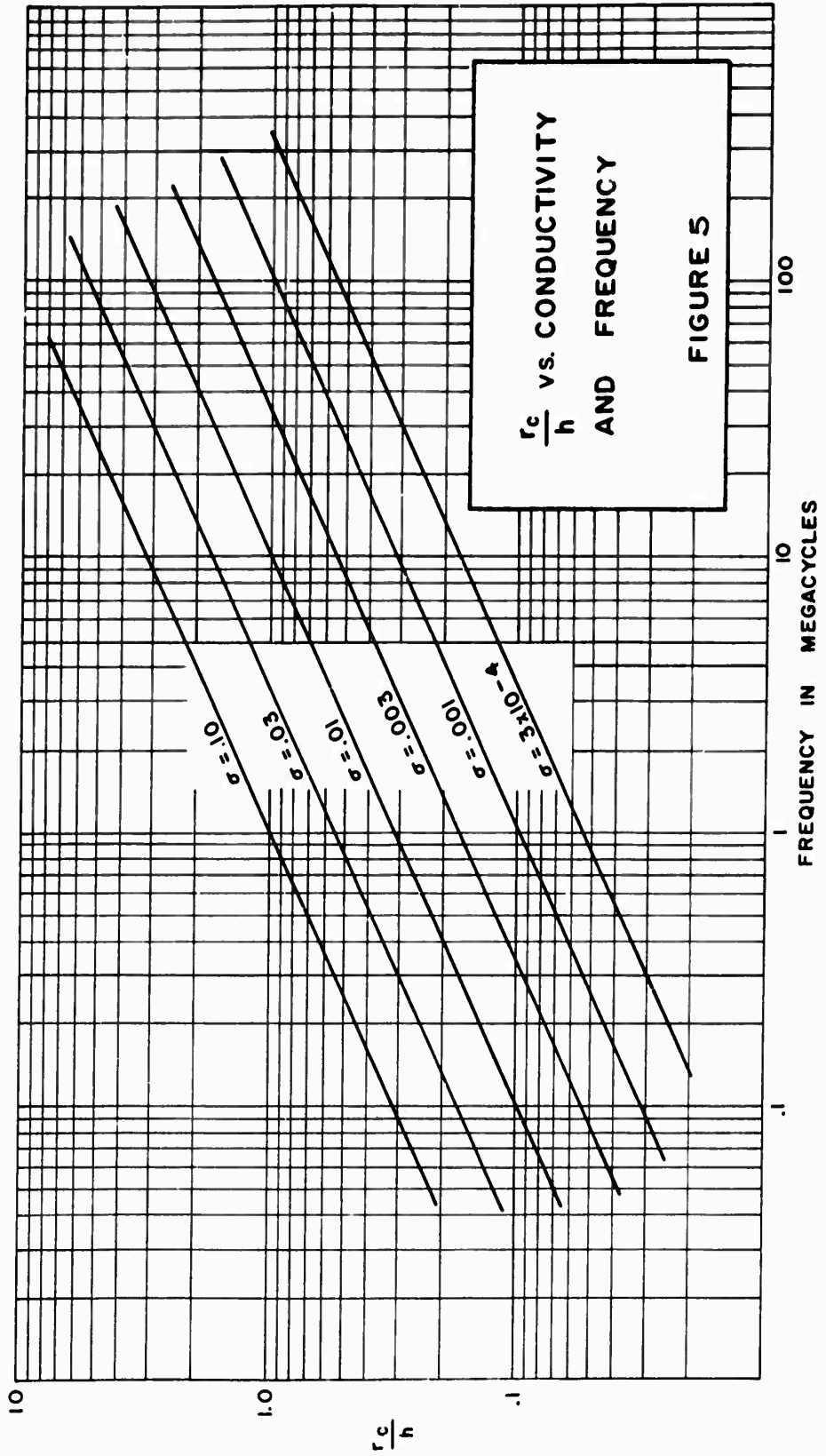
$$r_c = 2h\sqrt{4\pi\sigma_g\omega} (\sqrt{10} \times 10^{-4}) \quad (48)$$

In equation (48), when h and σ_g are in MKS units, r_c is in emu so that reference to Carson's original equations for P and Q may be made without conversion. Equation (48) may be simplified by writing

$$r_c = .00317 h \sqrt{\sigma_g f} \quad (49)$$

This function is plotted in Figure 5 for various conductivities in order to illustrate that practical HF values for r_c will be in the vicinity of $.5 < r_c < 6.0$.

Wise¹³ states that above 60 kc the dielectric constant cannot be neglected. For earth constants corresponding to a "highly conducting earth," the error does not appear to be serious below 10 mc. Above this frequency the correction may become significant. The effect of Wise's correction is to multiply Carson's parameter r_c by a complex correction factor s where:



$$s = \zeta_w e^{j\eta} = \left[1 + j \frac{(\epsilon_g - 1)}{2c\lambda\sigma_g} \right]^{1/2} \text{ emu} \quad (50)$$

The function s is plotted in Figure 6 for typical conditions of $\sigma_g = .03$, $\epsilon_r = 12$. It seems evident that the correction should be made at higher frequencies or lower conductivities. Wise's correction obtains a new parameter $r_{cw} = r_c s$, which is to be used in Carson's original equations in place of r_c . The new parameter is therefore

$$r_{cw} = r_c \left[1 + j \frac{(\epsilon_g - 1)}{2c\lambda\sigma_g} \right]^{1/2} \text{ emu} \quad (51)$$

This may be rewritten with the term on the right-hand side in MKS units as follows

$$r_{cw} = r_c \left[1 + j \frac{(\epsilon_g - 1)}{2c\lambda\sigma_g 10^{-7}} \right]^{1/2} \text{ emu} \quad (52)$$

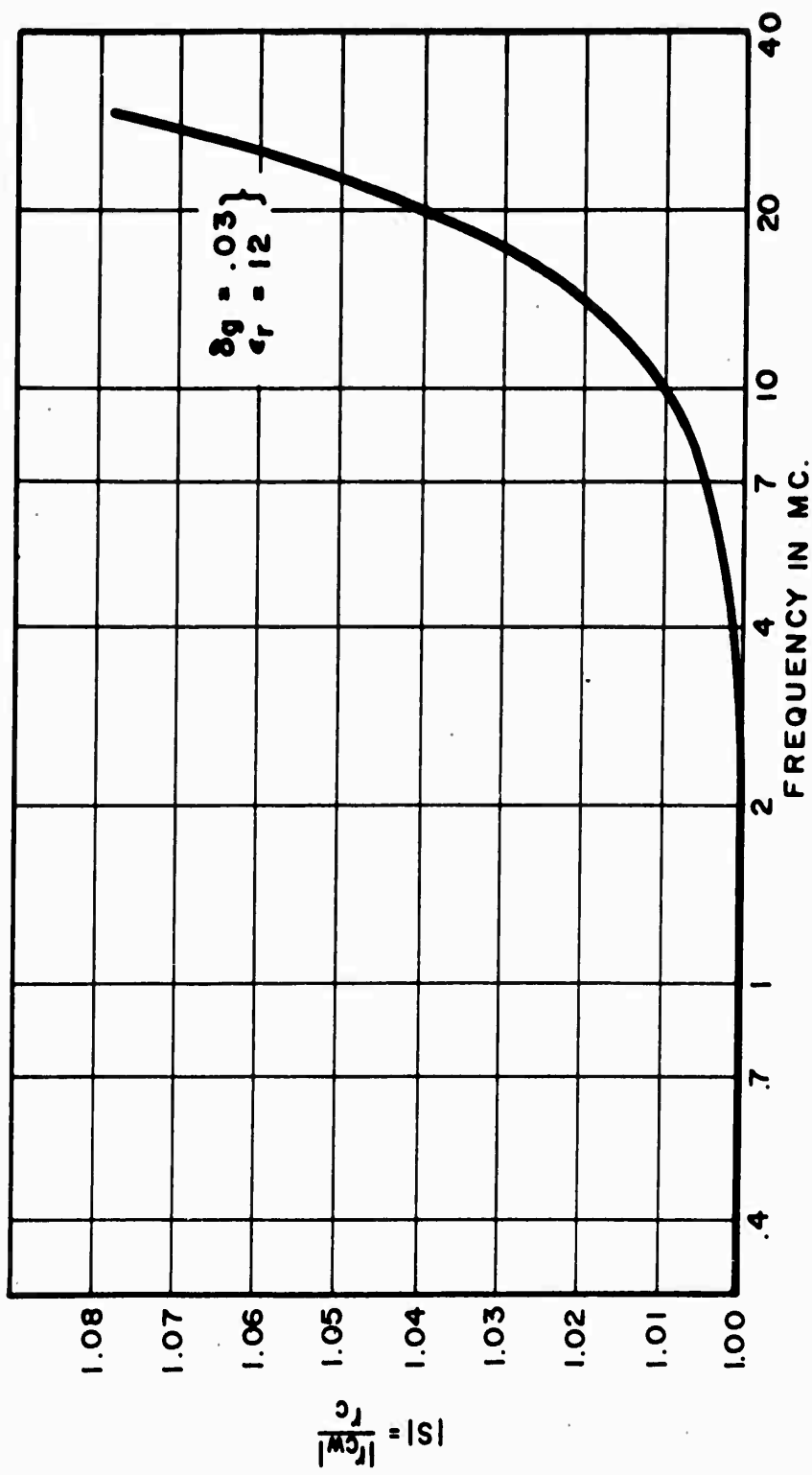
Equation (52) provides the same numerical value for r_{cw} as equation (51), if MKS input data for λ and σ_g are used. This allows the direct use of Carson's original curves or equations without further concern over conversion of units (the papers by Carson and Wise are in emu units). The corrected formula for $P + jQ$ is therefore given by the following.¹⁷

$$\begin{aligned} P + jQ = & \frac{\pi}{8} (1 - S_4) + \frac{1}{2} \left(\ln \frac{2}{(1.7811)(r_{cw})} \right) S_2 + \frac{1}{\sqrt{2}} (\sigma_3 - \sigma_1) \\ & + \frac{1}{2} \sigma_2 + j \left\{ \frac{1}{4} + \frac{1}{2} \left(\ln \frac{2}{1.7811 r_{cw}} \right) (1 - S_4) \right. \\ & \left. + \frac{1}{\sqrt{2}} (\sigma_3 + \sigma_1) - \frac{\pi}{8} S_2 - \frac{1}{2} \sigma_4 \right\} \end{aligned} \quad (53)$$

where

$$S_2 = \frac{1}{1!2!} \left(\frac{r_{cw}}{2} \right)^2 - \frac{1}{3!4!} \left(\frac{r_{cw}}{2} \right)^6 + \dots \quad (54)$$

17. Equation (53) is suitable for self-impedance calculations since Carson's parameters θ , S_2' and S_4' are zero and hence have been omitted. As Carson¹² shows, it is possible to make mutual impedance calculations in which case these parameters are not zero. The complete formulas are given in the Appendix reprint of Carson's paper. In general it will be found that mutual coupling as it affects input impedance may be ignored when the spacing between elements is greater than the height above ground.



THE MAGNITUDE OF THE CORRECTION FACTOR S FOR TYPICAL CONDITIONS
FIGURE 6

$$S_4 = \frac{1}{2!3!} \left(\frac{r_{cw}}{2}\right)^4 - \frac{1}{4!5!} \left(\frac{r_{cw}}{2}\right)^8 + \dots \quad (55)$$

$$\sigma_1 = \frac{r_{cw}}{3} - \frac{r_{cw}^5}{3^2 \cdot 5^2 \cdot 7} + \frac{r_{cw}^9}{3^2 \cdot 5^2 \cdot 7^2 \cdot 9^2 \cdot 11} - \dots \quad (56)$$

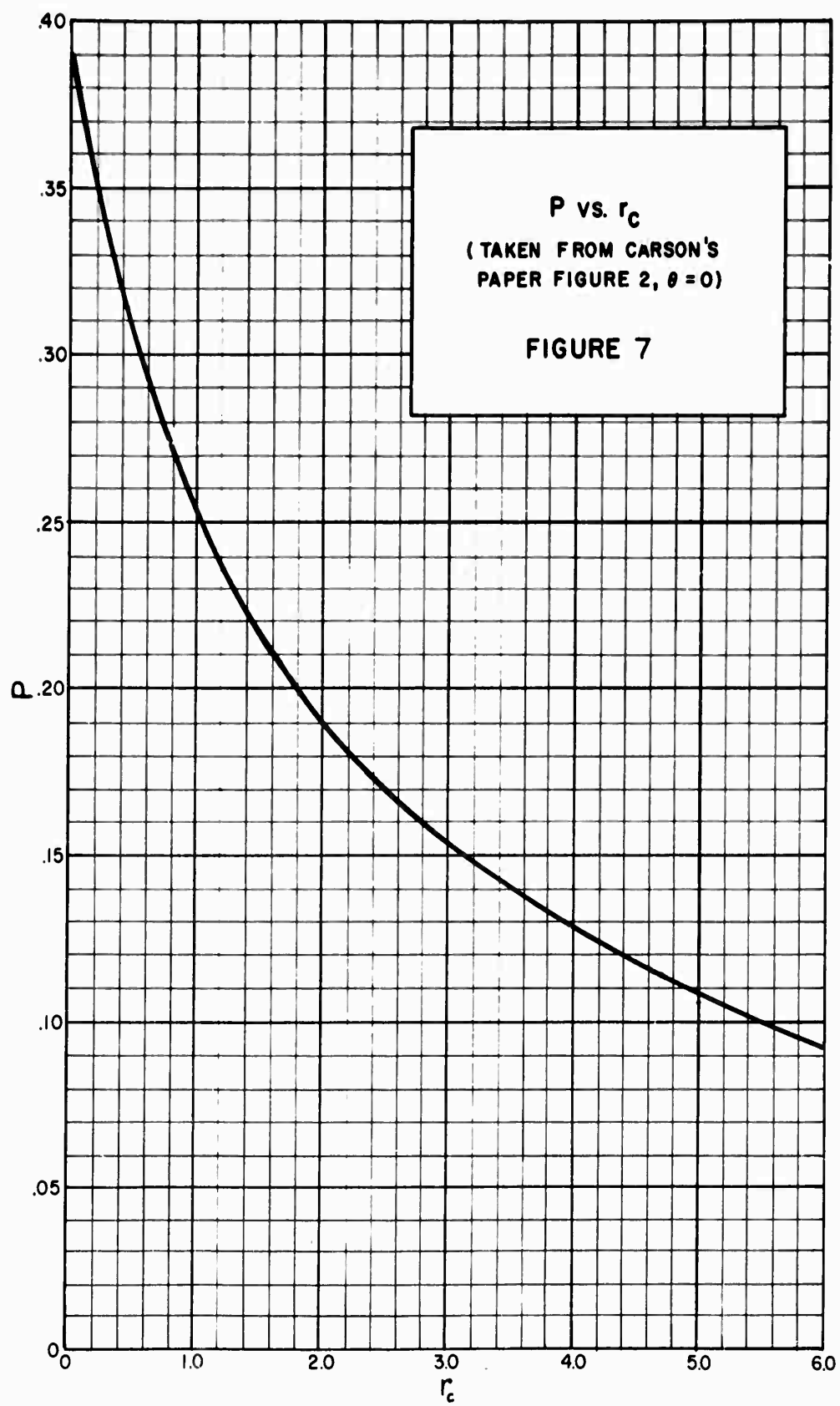
$$\sigma_2 = \left[1 + \frac{1}{2} - \frac{1}{4}\right] \frac{1}{1!2!} \left(\frac{r_{cw}}{2}\right)^2 - \left[1 + \frac{1}{2} + \frac{1}{3} + \frac{1}{4} - \frac{1}{8}\right] \frac{1}{3!4!} \left(\frac{r_{cw}}{2}\right)^6 + \dots \quad (57)$$

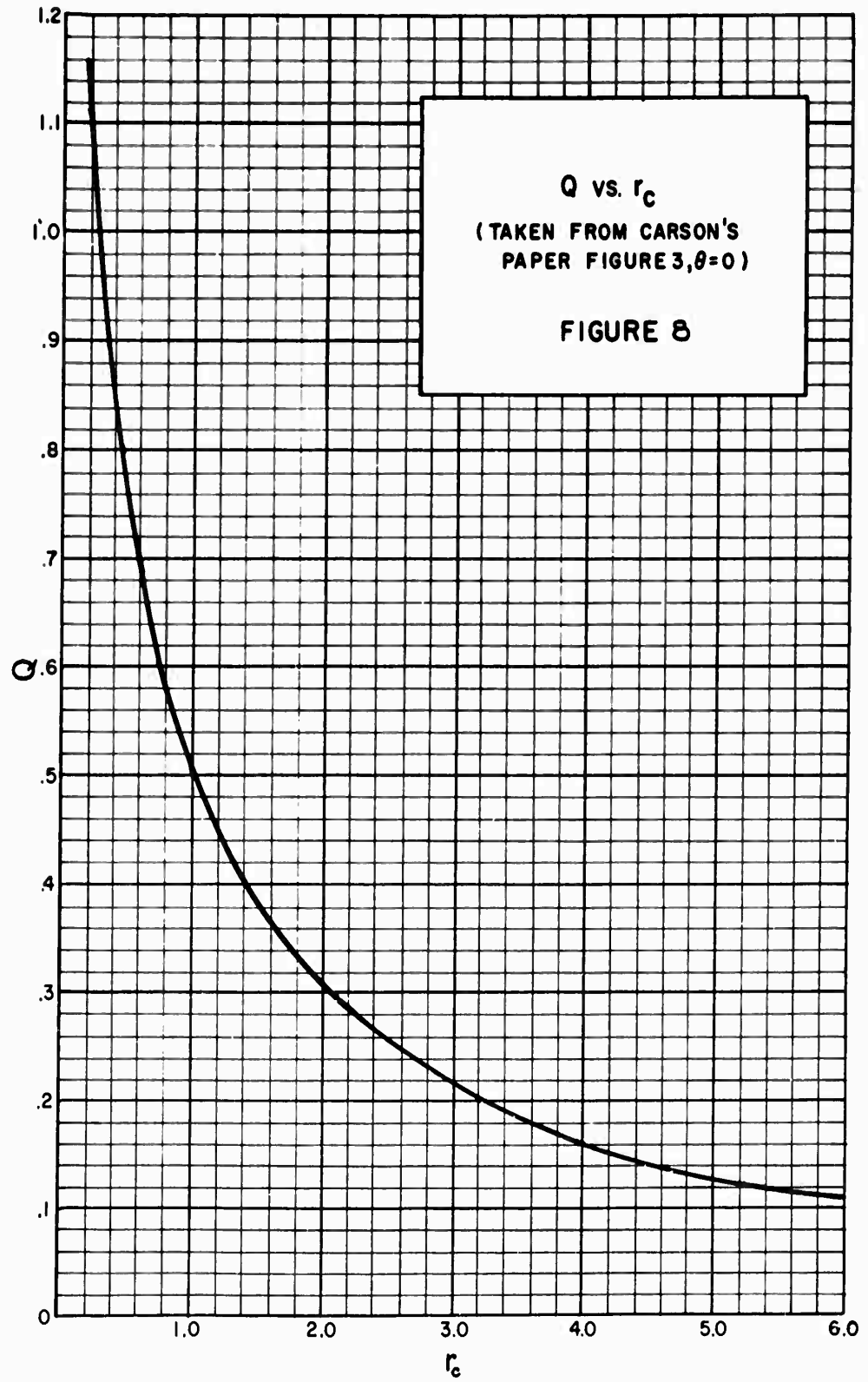
$$\sigma_3 = \frac{r_{cw}^3}{3^2 \cdot 5} - \frac{r_{cw}^7}{3^2 \cdot 5^2 \cdot 7^2 \cdot 9} + \frac{r_{cw}^{11}}{3^2 \cdot 5^2 \cdot 7^2 \cdot 9^2 \cdot 11^2 \cdot 13} - \dots \quad (58)$$

$$\begin{aligned} \sigma_4 &= \left[1 + \frac{1}{2} + \frac{1}{3} - \frac{1}{6}\right] \frac{1}{2!3!} \left(\frac{r_{cw}}{2}\right)^4 - \left[1 + \frac{1}{2} + \frac{1}{3} + \frac{1}{4} + \frac{1}{5} - \frac{1}{10}\right] \frac{1}{4!5!} \left(\frac{r_{cw}}{2}\right)^8 + \dots \\ &= \frac{5}{3} S_4 \text{ approximately} \end{aligned} \quad (59)$$

When the dielectric constant is neglected ($\epsilon_g = 1$), the above series and equation (53) reduce to Carson's original solution. Plots of P and Q taken from Carson's original paper (in terms of r_c , not r_{cw}) are given in Figures 7 and 8.

Unfortunately, Wise did not provide either curves of P and Q versus r_{cw} or simple approximations valid in the range of greatest interest particularly $r_c < 5$. He does provide formulas for $r_c < .25$ and $r_c > 5$. Thus, in the important range of $.25 < r_c < 5$ it is necessary to use equation (53), or if the correction by Wise can be considered negligible, then the curves of Figures 7 and 8 may be used. In the latter case (negligible dielectric) approximate formulas may be derived empirically for the range of $.25 < r_c < 5$. It is then possible to write a set of simple equations for all values of r_c as follows: (Note the range limits imposed by Carson have been relaxed somewhat since it appears that his limits were quite conservative.)





$$P = \frac{1}{2.54 + 1.34 r_c} \quad 0 < r_c < 6.0 \quad (\text{empirical}) \quad (60)$$

$$P = \frac{.707 r_c - 1}{r_c^2} \quad 6.0 < r_c < \infty \quad (\text{Carson}) \quad (61)$$

$$Q = -.0368 + \frac{1}{2} \ln \left(\frac{2}{r_c} \right) + \frac{r_c}{4.24} \quad 0 < r_c < .5 \quad (\text{Carson}) \quad (62)$$

$$Q = \frac{1}{.560 + 1.42 r_c} \quad .5 < r_c < 6.0 \quad (\text{empirical}) \quad (63)$$

$$Q = \frac{.707}{r_c} \quad 6.0 < r_c < \infty \quad (\text{Carson}) \quad (64)$$

where $r_c > 15$, a simple formula results which may be used with either r_c or r_{cw}

$$P + jQ = \frac{.707}{r_c} (1 + j) \quad 15 < r_c < \infty \quad (65)$$

Up to this point we have been evaluating the term $R + j\omega L$ in equation (43). The term $G + j\omega C$ in equation (43) may be evaluated by noting that in all practical cases $G \approx 0$ (nonconducting support posts) so that

$$G + j\omega C = j\omega \frac{2\pi\epsilon_0}{\ln \left(\frac{2h}{b} \right)} \frac{\text{farads}}{\text{meter}} \quad (66)$$

Equation (66) is also an approximation as was shown by Wise in 1948.¹⁸ To see that it is just an approximation, one has only to imagine the earth turning into air in which case the height h ceases to have significance. Nevertheless, the approximation is a good one for typical conductivities, and no analysis of a more exact solution will be provided. Wise's paper is reproduced in Appendix IV, should further reference be required.

18. Wise, W. H., "Potential Coefficients for Ground Return Circuits," The Bell System Technical Journal, Vol. 27, April 1948, pp. 365-371.

The quantity r_s in equation (46) may be determined from any suitable text. For instance

$$r_s = \frac{2K\sqrt{f}}{b} \frac{\text{ohms}}{\text{unit length}} \quad (67)$$

where $K = 41.6 \times 10^{-9}$ for copper¹⁹.

Combining the solutions found thus far in equations (46), (66) and (67) the characteristic impedance is given by equation (42) as

$$Z_o = \sqrt{10^{-7}} \left[\frac{.832 \frac{\sqrt{f}}{b} + j2\omega l n\left(\frac{2h}{b}\right) + 4\omega(P + jQ)}{\frac{j\omega 2\pi\epsilon_o}{\ln\left(\frac{2h}{b}\right)}} \right]^{1/2} \quad (68)$$

(MKS)

The propagation constant is given by equation (43) as

$$\gamma = \left[\left(.832 \frac{\sqrt{f}}{b} + j2\omega l n\left(\frac{2h}{b}\right) + 4\omega(P + jQ) \right) \frac{j\omega 2\pi\epsilon_o 10^{-7}}{\ln\left(\frac{2h}{b}\right)} \right]^{1/2} \quad (69)$$

(MKS)

The input impedance of the Beverage antenna may also be calculated from the above relations for Z_o and γ using the familiar transmission line equation

$$Z_{in} = Z_o \left[\frac{Z_L \cosh \gamma L + jZ_o \sinh \gamma L}{Z_o \cosh \gamma L + jZ_L \sinh \gamma L} \right] \quad (70)$$

Note that to obtain an ideal (reflectionless) termination, the terminating impedance must have a reactive component. This probably partially accounts for the fact that, in practice, it has been impossible to find a value for the terminating resistance which eliminates oscillatory variations in the input impedance with frequency.

19. Skilling, Hugh H., Electric Transmission Lines, McGraw-Hill Book Co., New York, 1951. Equations (12-15) through (12-17). $K = 40.2 \times 10^{-9}$ for silver, 83×10^{-9} for brass, etc.

3. Estimate of the Radiation Resistance

The question is sometimes raised as to the radiation resistance of the Beverage antenna. An approximate value may be found by reference to formulas²⁰ for the radiation resistance of a matched two-wire transmission line section. The following formula may be used for the latter

$$R_r = 60(2\beta_0 h)^2 \left[\cosh aL - \frac{\sin(2\beta_0 L)}{2\beta_0 L} \right] e^{-aL} \quad (71)$$

For a single wire over a good ground plane, the radiation resistance will be one-half the above value. Simplifying yields

$$R_r = 4730 \left(\frac{h}{\lambda_0} \right)^2 \left[\cosh aL - \frac{\sin(2\beta_0 L)}{2\beta_0 L} \right] e^{-aL} \quad (72)$$

It is evident that even the best line ($a = 0$) will have a maximum radiation resistance when

$$\frac{4\pi L}{\lambda_0} = m\pi$$

where m is any integer.

This reduces equation (72) to

$$R_r = 4730 \left(\frac{h}{\lambda_0} \right)^2 \text{ ohms} \quad (73)$$

For $h = 1$ meter and λ_0 ranging from 100 to 10 meters (the high frequency range, 3 to 30 mcs) the radiation resistance ranges between .47 and 47 ohms. Thus the radiation resistance never exceeds 10 percent of the characteristic impedance, and is therefore probably not an important factor in determining the input impedance of low Beverage antennas. It is also apparent that the efficiency of the Beverage antenna will be low since R_r is low compared to Z_0 .

20. Storer, James E., and King, Ronold, "Radiation Resistance of a Two-Wire Line," Proceedings of the IRE, Vol. 39, No. 6, 1951, pp. 1408-1412. Equation (5), Case I, first unnumbered equation.

C. Effective Height, Sensitivity and Signal-to-Noise Ratio

The effective height of the Beverage array may be defined as²¹:

$$h_e = \frac{\left| \left(\begin{array}{c} I_{\text{total}} \\ \text{array} \end{array} \right) Z_0 \right|}{|\bar{E}_{vg}|} \quad (74)$$

where $\phi = 0$, $|\bar{E}_{vs}| = 0$, $|\bar{E}_{hs}| = 0$, and all $G_k = 1$, all $\rho_k = 0$. Substituting equations (33) and (36) into (74) yields for the above special case

$$h_e = \frac{|\bar{E}_{rg}|}{2|\bar{E}_{vg}|} \sum_{k=1}^n \cos \eta_k \frac{1 - e^{(j\beta_0 \cos \delta \cos \eta_k - \gamma)L}}{\gamma - \beta_0 \cos \delta \cos \eta_k} \quad (75)$$

It is evident from Figure 2 that

$$|\bar{E}_{rg}| = |\bar{E}_{vg}| \tan \delta \quad (76)$$

Hence the effective height is

$$h_e = \frac{\tan \delta}{2} \sum_{k=1}^n \cos \eta_k \frac{1 - e^{(j\beta_0 \cos \delta \cos \eta_k - \gamma)L}}{\gamma - \beta_0 \cos \delta \cos \eta_k} \quad (77)$$

This may be rearranged as follows

$$h_e = \frac{L \tan \delta}{2} \sum_{k=1}^n \cos \eta_k \cdot \frac{\sinh\left(\frac{\Gamma_k L}{2}\right)}{\left(\frac{\Gamma_k L}{2}\right)} \cdot e^{(j\beta_0 \cos \delta \cos \eta_k - \gamma)L/2} \quad (78)$$

where

$$\Gamma_k = \gamma - j\beta_0 \cos \delta \cos \eta_k \quad (79)$$

Since the term $|e^{j\beta_0 \cos \delta \cos \eta_k (L/2)}| = \text{unity}$, equation (78) simplifies to:

21. Schelkunoff, Sergei A., and Friis, Harald T., Antennas Theory and Practice, New York, John Wiley & Sons, Inc., 1952, p. 301, problem 9.13. It is true that E_{vg} is not parallel to the antenna conductors; however, it is more convenient to refer the effective height to a vertically polarized field normal to the earth's surface.

$$h_e = \frac{L}{2} \tan \delta \sum_{k=1}^n \cos \eta_k \cdot \frac{\sinh \left(\frac{\Gamma_k L}{2} \right)}{\left(\frac{\Gamma_k L}{2} \right)} \cdot e^{-\gamma L/2} \quad (80)$$

Since $\gamma = \alpha + j\beta$, equation (80) simplifies to

$$h_e = \frac{L}{2} \tan \delta e^{-\alpha L/2} \sum_{k=1}^n \cos \eta_k \frac{\sinh \left(\frac{\Gamma_k L}{2} \right)}{\left(\frac{\Gamma_k L}{2} \right)} \quad (81)$$

If equations (37) and (38) are substituted into equation (79) and the result simplified and substituted in equation (81), and also $\alpha = 0$, the effective height becomes

$$h_e = \frac{L}{2} \tan \delta \sum_{k=1}^n \cos \eta_k \frac{\sin \left[\frac{L\pi}{\lambda_0} \left(\frac{1}{n} - \cos \delta \cos \eta_k \right) \right]}{\left[\frac{L\pi}{\lambda_0} \left(\frac{1}{n} - \cos \delta \cos \eta_k \right) \right]} \quad (82)$$

For a single antenna at $\eta_k = 0$, this becomes

$$h_e = \frac{L}{2} \tan \delta \frac{\sin \left[\frac{L\pi}{\lambda_0} \left(\frac{1}{n} - \cos \delta \right) \right]}{\left[\frac{L\pi}{\lambda_0} \left(\frac{1}{n} - \cos \delta \right) \right]} \quad (83)$$

single
antenna

When the velocity ratio $n = 1$ and $\cos \delta$ approaches unity, then $(\sin X)/X \approx 1$ and

$$h_e = \frac{L}{2} \tan \delta \quad (84)$$

This may be taken as a rule of thumb for the effective height of an ideal Beverage antenna.

It will be noted however that when $\cos \delta$ approaches unity δ approaches zero, hence $\tan \delta$ approaches zero. Hence equation (84) is only valid for small wave tilt angles, and since $\tan \delta \approx \delta$ when δ is small equation (84) may be written as:

$$h_e = \frac{\delta L}{2} \quad (85)$$

where δ is in radians.

Equation (83) implies a minimum effective height at some frequency. When (81) is simplified to a single antenna then

$$h_e = \frac{L}{2} \tan \delta e^{-\alpha L/2} \left[\frac{\sinh\left[\left(\gamma - j\beta_0 \cos \delta\right) \frac{L}{2}\right]}{\left(\gamma - j\beta_0 \cos \delta\right) \frac{L}{2}} \right] \quad (86)$$

single
antenna

According to equation (83) a minimum effective height for $\alpha = 0$ occurs when

$$\frac{L\pi}{\lambda_0} \left(\frac{1}{n} - \cos \delta \right) = m\pi$$

where m may be any integer. Thus the frequency of the first minimum h_e is approximately

$$f = \frac{c}{L \left(\frac{1}{n} - \cos \delta \right)} = \frac{nc}{L(1 - n \cos \delta)} \quad (87)$$

or

$$f = \frac{300n}{L(1 - n \cos \delta)} \text{ megacycles} \quad (88)$$

This may be thought of as a cutoff frequency for the antenna, for only below this frequency can relatively large effective heights be obtained. In order to design to maintain this frequency above 30 mcs, it is necessary that $f > 30$ and hence

$$10n = L(1 - n \cos \delta) = L - nL \cos \delta$$

$$n(10 + L \cos \delta) = L$$

or

$$n = \frac{L}{10 + L \cos \delta} \quad (89)$$

but $n > 1$ cannot be obtained without modifying the antenna so the length is limited to

$$L = (10 + L \cos \delta) n$$

$$L(1 - n \cos \delta) = 10n$$

$$L = \frac{10n}{1 - n \cos \delta} \text{ for } n < 1$$

To successfully use 300-meter antennas, then

$$30 = \frac{n}{1 - n \cos \delta}$$

or

$$30 - 30n \cos \delta = n$$

$$\cos \delta = \frac{30 - n}{30n}$$

which means for $\delta \approx 0$, $30n = 30 - n$, $n = \frac{30}{31}$ (min n) or for $n = 1$ $\cos \delta = \frac{29}{30}$.
Therefore

$$\delta_{\max} = 15^\circ \text{ max for } n = 1$$

$$n = .965 \text{ min}$$

(90)

Experience has shown for $h = 1$ meter these criteria can be met for $L = 300$ at $f = 30$ mcs.

The sensitivity of the Beverage antenna may be estimated from the minimum field strength which may be received, determined by noise limitations. For this estimate we will make the simple assumption that the antenna equivalent circuit consists of the radiation resistance in series with a loss resistance equal to the characteristic impedance of the antenna. The noise arising in the antenna may be calculated by Nyquist's theorem which states that the mean square fluctuation e. m. f. in the frequency band ν to $\nu + d\nu$ appearing in an impedance $Z = R + jX$ is given by:²²

22. Nyquist, H., "Thermal Agitation of Electric Charge in Conductors," Physical Review, Vol. 32, July 1928, p. 110.

$$\overline{de} = \sqrt{4kTRd\nu} \quad (91)$$

where k = Boltzmann's constant = 1.374×10^{-23} joules per degree Kelvin, and T is the absolute temperature in degrees Kelvin. The value R is assumed to be constant over the bandwidth $d\nu$; if R is a function of frequency, a more general form of equation (91) is required.²³ However, for the present analysis we will be concerned with bandwidths which are less than one-half of one percent of the center frequency, so that while the previously calculated radiation resistances are rapidly changing with frequency, the changes are small over the bandwidths considered and equation (91) is closely approximated.

Burgess²⁴ shows that the radiation resistance of an antenna can apparently be the source of thermal noise and that it obeys Nyquist's theorem when the aerial is in radiative equilibrium with its surroundings.²⁵ Thus

$$\overline{de_r} = \sqrt{4kTR_r d\nu} \quad (92)$$

The equivalent noise temperature T_r of the radiation resistance R_r is defined as that temperature which must be ascribed to R_r so as to give the value of the received noise electromotive force when substituted in Nyquist's equation, so that

$$\overline{de_r} = \sqrt{4kT_r R_r d\nu} \quad (93)$$

Thus an antenna in an enclosure at a uniform temperature, T , is in effect the source of a thermal e. m. f. whose value corresponds to the condition $T_r = T$. If the antenna temperature T_a is not equal to T of the enclosure, radiative equilibrium does not exist and there will be an unbalanced energy flow between the antenna and its surroundings in the sense which tends to equalize T_a and T . It is concluded that the radiation resistance of an antenna in free space has an equivalent noise temperature of zero; expressed otherwise, there is no other source of radiation present to return energy to the antenna and thus to induce a fluctuation e. m. f.

23. For instance see Terman, F., "Radio Engineers Handbook," p. 476.

24. Burgess, R. E., "Noise in Receiving Aerial Systems," Proceedings of Physical Society, Vol. 53, May 1941, p. 293.

25. Burgess points out that this statement is in disagreement with other authors in papers published prior to his 1941 paper. The validity of Burgess' paper now seems well established however.

T_r will in general be independent of the bandwidth, but it will not be independent of antenna gain or effective height if the noise source is not uniformly distributed in all directions. Burgess points out therefore that T_r will, in general, exceed T , and, in fact, high frequency measurements by Jansky have shown that T_r is always greater than T and can exceed $1000T$ in unfavorable circumstances.

Assuming that the proper T_r is attributed to the radiation resistance, then the noise e. m. f. of the lossless antenna is

$$e_r = \sqrt{4kT_r R_r B} \quad (94)$$

where B is the bandwidth. The noise e. m. f. of the assumed Beverage antenna is therefore

$$e_r = \sqrt{4kT_r B (R_r + R_o)} \quad (95)$$

Now the voltage output of an antenna is related to an incident signal field E by

$$V = E h_e \quad (96)$$

Hence for unity signal-to-noise ratio at the output terminals, the incident signal field strength must be

$$E = \frac{\sqrt{4kT_r (R_r + R_o)}}{h_e} \quad (97)$$

Thus for typical values of $R_r = 10\Omega$, $R_o = 400\Omega$, $h_e = 10$ meters, $B = 3 \times 10^3$ cycles and $T = 300$ degrees Kelvin, one could expect the unity signal-to-noise ratio to occur at

$$E = \frac{\sqrt{(4)(1.374 \times 10^{-23})(300)(410)(3 \times 10^3)}}{10} \frac{\mu v}{\text{meter}} \quad (98)$$

or $E = .014$ microvolt per meter. Of course, the "signal" in this case could be atmospheric noise, or any other external source.

D. Beverage Antenna Array Calculations with a Digital Computer

To differentiate the present calculation from past calculations of a similar nature on this and previous projects, the present computer program is referred to as the "Beverage Array II_c Program." The program is written for a GE-225 using IBM cards and the GE "WIZ" program language. (Note: Much of the information which follows in this section is of interest only to personnel at this laboratory. It is provided herein in order to maintain a permanent record and for the future convenience of project personnel. Those readers not interested in the computer programming details may skip to Section E for plotted patterns.)

The Beverage Array II_c Program calculates the response of a Beverage antenna or a circular array of radial Beverage antennas to the following incident waves:

- | | |
|--------------------------------------|--|
| (1) Vertically polarized ground wave | } At the same azimuth
if more than one is
specified at one time. |
| (2) Vertical polarized sky wave | |
| (3) Horizontally polarized sky wave | |

The equation calculated gives the current at the receiver end of a Beverage antenna or the array under excitation by any or all of the above waves. The equation calculated is equivalent to equation (36) and is written

$$\begin{aligned} N &= 10 \\ K &= 4N + 1 \\ \vec{I}_T &= \sum_{\substack{K=0 \\ N=0}} G_K e^{j\rho(K+1)} \left[\vec{T}_1 + (\vec{T}_2 + \vec{T}_3)\vec{T}_4 \right] \cdot \frac{1}{2Z_0} \end{aligned} \quad (99)$$

where

$$\begin{aligned} \vec{T}_1 &= E_{rg} \cos[\phi - \eta(N)] e^{j\Phi_{rg}} \left(\frac{1 - e^{j\beta_0 L \cos \delta \cos[\phi - \eta(N)] - \gamma L}}{\gamma - j\beta_0 \cos \delta \cos[\phi - \eta(N)]} \right) \\ &\quad \cdot e^{j\beta_0 R_0 \cos \delta \cos[\phi - \eta(N)]} \end{aligned}$$

$$\vec{T}_2 = E_{vs} \sin \psi \cos[\phi - \eta(N)] e^{j\Phi_{vs}} [1 - R_v e^{j2\beta_0 h \sin \psi}]$$

$$\bar{T}_3 = E_{hs} \sin \psi [e^{j\Phi_{hs}}] [1 + \bar{R}_h e^{j2\beta_0 h \sin \psi}]$$

$$\bar{T}_4 = \left(\frac{1 - e^{j\beta_0 L \cos \psi \cos [\phi - \eta(N)] - \gamma L}}{\gamma - j\beta_0 \cos \psi \cos [\phi - \eta(N)]} \right) e^{j\beta_0 R_0 \cos \psi \cos [\phi - \eta(N)]} \quad (100)$$

Auxiliary calculations in order to obtain the antenna current given above include the Carson impedance parameters P and Q, and the propagation constant for the Beverage antenna, see equations (53) and (69).

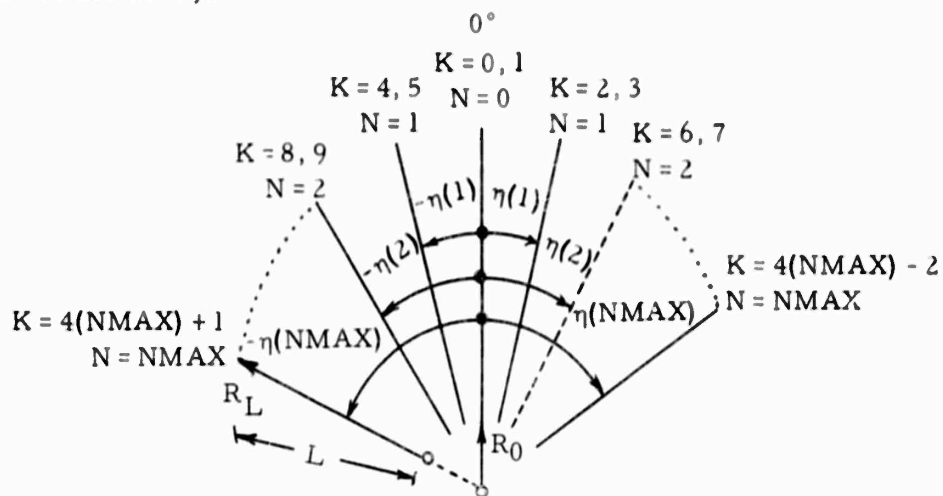
The array of Beverage antennas is assumed to be circular with prescribed inner and outer radii (R_o , R_L) specifying antennas of desired lengths (L). If a phased array is required, provision is made for the multiplication of each antenna output by a magnitude and phase number which has the effect of modifying the effective array geometry as desired (as for instance, the insertion of delay lines). This array of multipliers is referred to as the goniometer function [see equation (35)].

The calculation proceeds by summing antennas by pairs, symmetric about 0° azimuth. A center antenna at 0 degrees may also be specified and calculated. The antennas do not need to be equally spaced.

The array consists of (2N + 1) antennas, or less, divided into (N) pairs either with or without the degenerate pair N = 0, which is a single antenna located at 0 degrees. The specification of the number of pairs is carried out by specifying the variable NIM (either 0 or 1) naming the minimum number of the N array. Thus when NIM = 0, the single 0° antenna is included; when NIM = 1, the calculation begins with the first true pair and the center antenna is omitted. The total number of pairs computed is, therefore, NMAX - NIM including the degenerate center antenna. (This means it is possible to use NIM values greater than one, however, there seems to be no advantage to this.) The variable NMAX specifies the number of antenna pairs. The azimuth of each pair is specified by the variable ETA(N) symmetric about the 0 degree axis. Therefore, ETA(N) where N = 0 specifies the 0 degree antenna.

Although the antennas are specified in pairs, a suitable goniometer function with 0 magnitude for the appropriate Kth antenna will specify an array of irregular antenna spacings as desired.

The Beverage array calculated by the program is diagrammed schematically below. One antenna, $N = 2$, on one side has been eliminated by specifying a zero goniometer function at that position on the right side of the array.



Example Goniometer Function $G_{(K)}e^{jG_{(K+1)}}$

<u>N</u>	<u>$G_{(K)}e^{jG_{(K+1)}}$</u>	<u>K</u>
0	$1e^{j0}$	0
		1
1	$1e^{j0}$	2
		3
		4
		5
2	$0e^{j0}$	6
		7
		8
		9

FIGURE 9. SKETCH OF BEVERAGE ARRAY CALCULATION GEOMETRY

Table 3 summarizes the computer input parameters and their definitions. Table 4 gives the order of input cards to the program. Table 5 gives the description of sense switch options available to the program operator. Table 6 gives the available output quantities.

The printed output from the computer consists of:

TABLE 3
ANALYSIS AND MACHINE SYMBOLS
INPUT PARAMETERS

<u>Analysis</u>	<u>Machine</u>	<u>Remark</u>
b	B	Conductor radius
h	H	Height above ground
σ_g	SIG	Ground conductivity
ϵ_g	EPC	Ground dielectric constant
R_o	RO	Array inner radius
R	RL	Array outer radius
λ	LAMBDA	Wavelength
η	ETA	Location of antenna
$G_k(\pm)$	G(K) Coniometer	Amplitude of Antenna
$\rho_k(\pm)$	G(K + 1) Coniometer	Phase of Antenna
E_{rg}	ERG	Amplitude ground wave
Φ_{rg}	FRG	Phase ground wave
E_{vs}	EVS	Amplitude vertical sky wave
Φ_{vs}	FVS	Phase vertical sky wave
E_{hs}	EHS	Amplitude horizontal sky wave
Φ_{hs}	FHS	Phase horizontal sky wave
ϕ	PHI	Azimuth variable
ψ	PSI	Polar variable
$\Delta\phi$	DELPHI	Azimuth increment
ϕ_{max}	PHIMAX	Maximum azimuth
$\Delta\psi$	DELPSI	Polar angle increment
ψ_{max}	PSIMAX	Polar angle maximum
ϕ_o	PHIO	Initial ϕ
ψ_o	PSIO	Initial ψ
N	N	No. antenna pairs in array
P	P	Antenna parameters real part
Q	Q	Antenna parameters imaginary part
α	ALPHA	Attenuation constant
β	BETA	Phase constant
B	BMWTH	Beamwidth criterion
A	Amprcrit	Amplitude criterion for
Z_o	ZO	Characteristic impedance
	NOF	Number of frequencies to be run in parameter study

All input numbers in MKS units

TABLE 4. LIST OF INPUT CARDS FOR BEVERAGE ARRAY II_C
RUN ON GE-225 WITH WIZ LANGUAGE

Card No.	Data on Each Card	Quantity of Numbers on Each Card	Description of Card
1	T, NOF	2	Mode of calculation, T = 0 or T = 5 (see options below). Number of frequencies to be run in parameter study when T = 5, when T = 0 set NOF = 0.
1a	α, VR, R_0, X_0	4	Not required unless sense switch 5 is down. When required put α in nepers per meter, velocity ratio (dimensionless), R_0 in ohms and X_0 in ohms where $R_0 + jX_0 = Z_0 =$ characteristic impedance.
2	B, H, F	3	Wire radius in meters, wire height in meters and frequency in mcs.
3	σ_g, ϵ_g	2	Ground constants. Conductivity σ_g in MKS units, and ϵ_g the dielectric constant (dimensionless).
4	$E_{vg}, \theta_{vg},$ $E_{vh}, \theta_{vh},$ E_{hs}, θ_{hs}	6	Wave parameters. Vertical ground wave, vertical sky wave and horizontal sky wave in arbitrary amplitude units (E) and degrees (θ).
5	NIM, NMAX R_0, R_L, ϕ_n, ψ_n	6	Array parameters. When center antenna (the degenerate pair) is present set NIM = 0, when center antenna is absent set NIM = 1, NMAX is number of symmetrical pairs, R_0 is the inner radius in meters, R_L is the outer radius in meters, ϕ_n is the normalized azimuth in degrees and ψ_n is the normalized elevation angle in degrees. (When calculating azimuth patterns at different elevation angles specify the elevation angle with ψ_n .)
6	$\eta(N)$	(NMAX + 1) when NIM = 0 and (NMAX) when NIM = 1	Locations of pairs of antennas in azimuth in degrees. (For a pair of antennas at $\pm 4^\circ$ put only a single 4 on card, for two pairs at $\pm 2^\circ$ and $\pm 4^\circ$ put only a 2 and a 4 on card, etc. When NIM = 0 first number on card will be zero.) Maximum of 10 pairs plus the center antenna (or 21 antennas).
6a	G(K)	(4NMAX + 2)	Not required unless sense switch 1 is down. When sense switch 1 is down specify an amplitude and phase constant for the center antenna and all other pairs used. There should be two numbers (which are the first numbers on the card) to specify the amplitude and phase (in that order) for the center antenna. Thereafter there should be four numbers for each antenna pair. In the first group of four numbers the first two numbers correspond to the right-hand element (as seen from the array center) of the pair closest to the center. The second two numbers correspond to the left-hand element of the same pair. The first number in each group is an arbitrary amplitude constant and the second number is a phase constant in degrees. The next closest pair of antennas is specified by another group of four numbers and so on. Note that two numbers must be used to specify the center antenna even when it is omitted by setting NIM = 1 on card 6. In this case, the first two numbers on card 6a will always be 00.
7		6	Calculation parameters. Initial azimuth point, azimuth increment, maximum azimuth point, initial elevation point, elevation increment, maximum elevation point (up to 180°). All units in degrees.
7a	BMWTH, AMPCTR	2	Not required unless sense switch 3 is down. When required put beamwidth (degrees) and amplitude criterion (normalized amplitude) on this card. For instance, for 20° beamwidth at the 3 db points the 2 numbers would be: (20, .707).

T	Description of Option
0	Random data changes for successive cases (when T = 0, set NOF = 0).
1	Not used.
2	Not used.
3	Not used.
4	Not used.
5	Only the frequency is changed in successive cases and/or ϕ_n, ψ_n . Provide seven cards as usual for the first case, then the eighth card will have f, ϕ_n, ψ_n for next case only, etc., and thereafter only one card per case.

TABLE 5

SENSE SWITCH OPTIONS-BEVERAGE ARRAY II_c

Sense Switch	Resulting Output																														
None	<p>Pattern calculation giving the following output arranged as shown:</p> <table style="margin-left: auto; margin-right: auto;"> <tr><td>SIG</td><td>EPG</td></tr> <tr><td>EVC</td><td>FRG</td></tr> <tr><td>EVS</td><td>FVS</td></tr> <tr><td>EHS</td><td>FHS</td></tr> </table> <p>Antenna Parameters</p> <table style="margin-left: auto; margin-right: auto;"> <tr><td>NIM</td><td>NMAX</td></tr> <tr><td>R_o</td><td>R_L</td></tr> <tr><td>B</td><td>H</td></tr> </table> <p>ETA(N) ETA(N + 1)</p> <table style="margin-left: auto; margin-right: auto;"> <tr><td>ϕ_o</td><td>ψ_o</td></tr> <tr><td>ϕ_{max}</td><td>ψ_{max}</td></tr> <tr><td>ϕ_N</td><td>ψ_N</td></tr> </table> <p>Normalized Point</p> <table style="margin-left: auto; margin-right: auto;"> <tr><td>ψ_N</td><td>ϕ_N</td><td>IMAG</td><td>HE</td></tr> <tr><td>PHI</td><td>IMAG</td><td>IPHASE</td><td>INORM</td><td>-Ndb</td><td>HE</td></tr> </table> <ol style="list-style-type: none"> 1. Goniometer function incorporated. (See Fig. 11) Note the G(K) array is printed in an array above all the other output data only when and always when switch 1 is down. (Requires card 6a.) 2. Print α, β, VR, R_o, X_o in addition to usual data. 3. Beamwidth option. (Requires card 7a.) 4. Print R_v, R_v Phase, R_H, R_H Phase. 5. Rd α, VR, R_o, X_o, input data. (Requires card 1a.) 6. Self-normalization. (Requires no additional cards.) Computer searches in azimuth or elevation until first maximum is found, pattern is normalized to this maximum. When function is decreasing at zero the pattern is normalized at zero. 7. Exit to next case after calculating normalized point. 8. Not used. 9. Unconditional exit to next case. 10. Diagnostic print. 	SIG	EPG	EVC	FRG	EVS	FVS	EHS	FHS	NIM	NMAX	R _o	R _L	B	H	ϕ_o	ψ_o	ϕ_{max}	ψ_{max}	ϕ_N	ψ_N	ψ_N	ϕ_N	IMAG	HE	PHI	IMAG	IPHASE	INORM	-Ndb	HE
SIG	EPG																														
EVC	FRG																														
EVS	FVS																														
EHS	FHS																														
NIM	NMAX																														
R _o	R _L																														
B	H																														
ϕ_o	ψ_o																														
ϕ_{max}	ψ_{max}																														
ϕ_N	ψ_N																														
ψ_N	ϕ_N	IMAG	HE																												
PHI	IMAG	IPHASE	INORM	-Ndb	HE																										

TABLE 6
LIST OF PROGRAM OUTPUT QUANTITIES

<u>Analysis</u>	<u>Machine</u>	<u>Remark</u>
α	ALPHA	Attenuation constant
β	BETA	Phase constant
η	VR	Velocity ratio v/c
R	R	Antenna resistance
X	X	Antenna reactance
δ	DELTA	Wave tilt angle
$ I_T $	IMAG	Magnitude of antenna current
Φ_T	IPHASE	Phase of antenna current
	INORM	Normalized magnitude
	-Ndb	Normalized magnitude (db)
h_e	HE(M)	Effective height (meters)
R_v	RV(0)	Magnitude vertical Fresnel reflection coefficient
ρ_v	RV(1)	Phase vertical Fresnel reflection coefficient
R_h	RH(0)	Magnitude horizontal reflection coefficient
ρ_h	RH(1)	Phase horizontal reflection coefficient

- (1) The specified input parameters.
- (2) The calculated characteristic impedance, propagation constant and wave tilt angle, if desired, by placing sense switch 2 down.
- (3) The Fresnel reflection coefficients, if desired, by placing sense switch 4 down.
- (4) The initial current value at the normalized point on the pattern (both azimuth and elevation) and the effective height.
- (5) The antenna pattern.

The output numbers associated with each azimuth or angle of inclination obtained for the antenna pattern include the magnitude of the current, the phase of the current, the current normalized to the initial normalizing point, the normalized current in terms of db down with respect to the normalized point, and the effective height of the antenna or antenna array (calculated only for the ground wave case). Both azimuth plane and polar plane plots are available. An input-output block diagram of the calculation is included in Figure 10. A detailed block diagram of the program is given in Figures 11 thru 18.

One option (sense switch 3) enables a series of cases to be calculated in terms of beamwidth and an amplitude criterion. With switch (3) down and the desired half beamwidth for a given normalized amplitude specified, successive array patterns will be calculated but not printed until the amplitude and beamwidth criteria are met. Then with switch (3) reset to zero, the desired pattern will be calculated and printed. For the rejected cases the description of the array and the beamwidth at the prescribed amplitude criterion is printed before exit to the next case.

With switch (6) down, the program performs a self-normalizing calculation as follows:

- (1) Calculate the antenna response at ϕ_N, ψ_N .
- (2) Increment the appropriate variable (ϕ for azimuth, ψ for polar plane or elevation).
- (3) Compare this contribution with the previously calculated point until $I(\phi + \Delta\phi) - I(\phi)$ is negative.

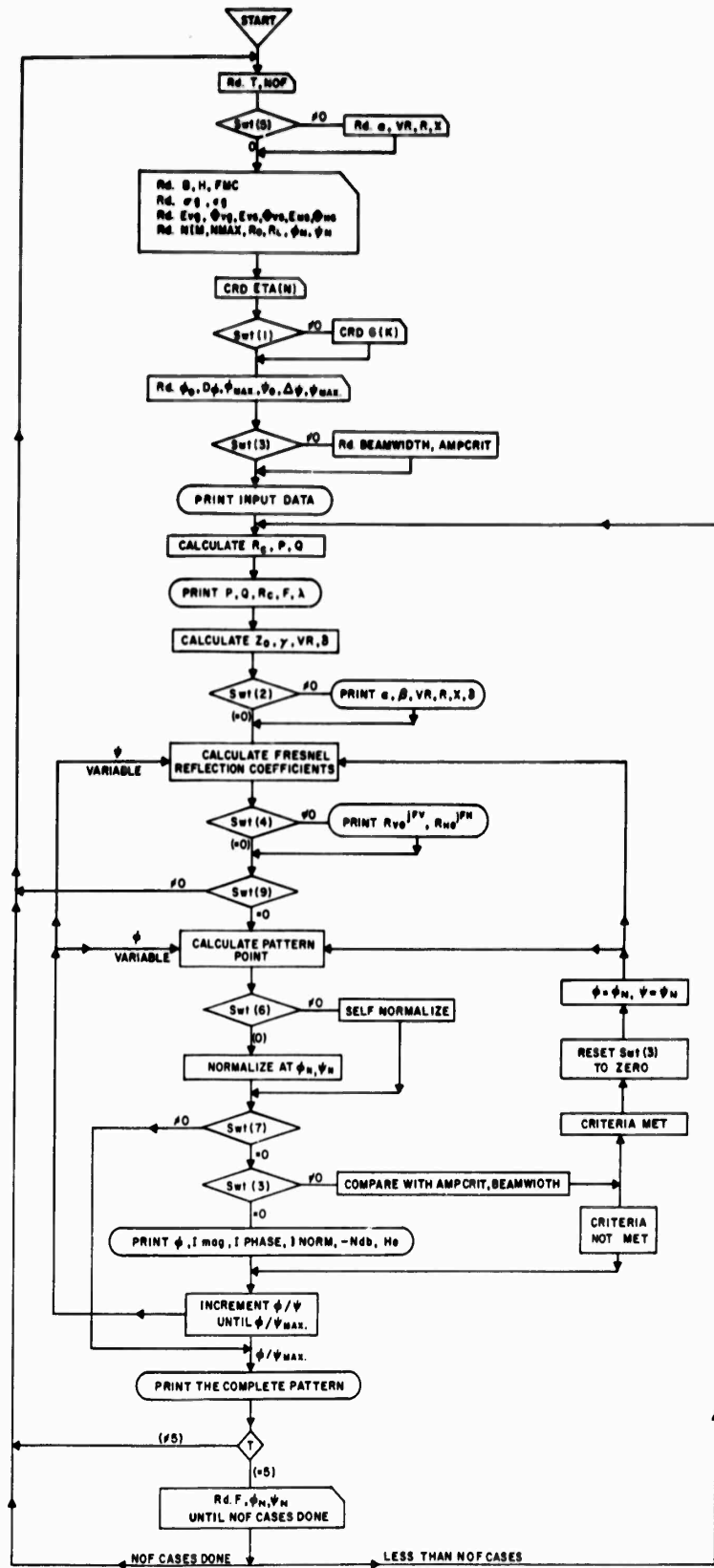


FIGURE 10.
BEVERAGE ARRAY IC SIMPLIFIED INPUT-OUTPUT-SENSE SWITCH BLOCK DIAGRAM.

BEVERAGE ARRAY PATTERN CALCULATION PROGRAM FOR DIGITAL COMPUTATION

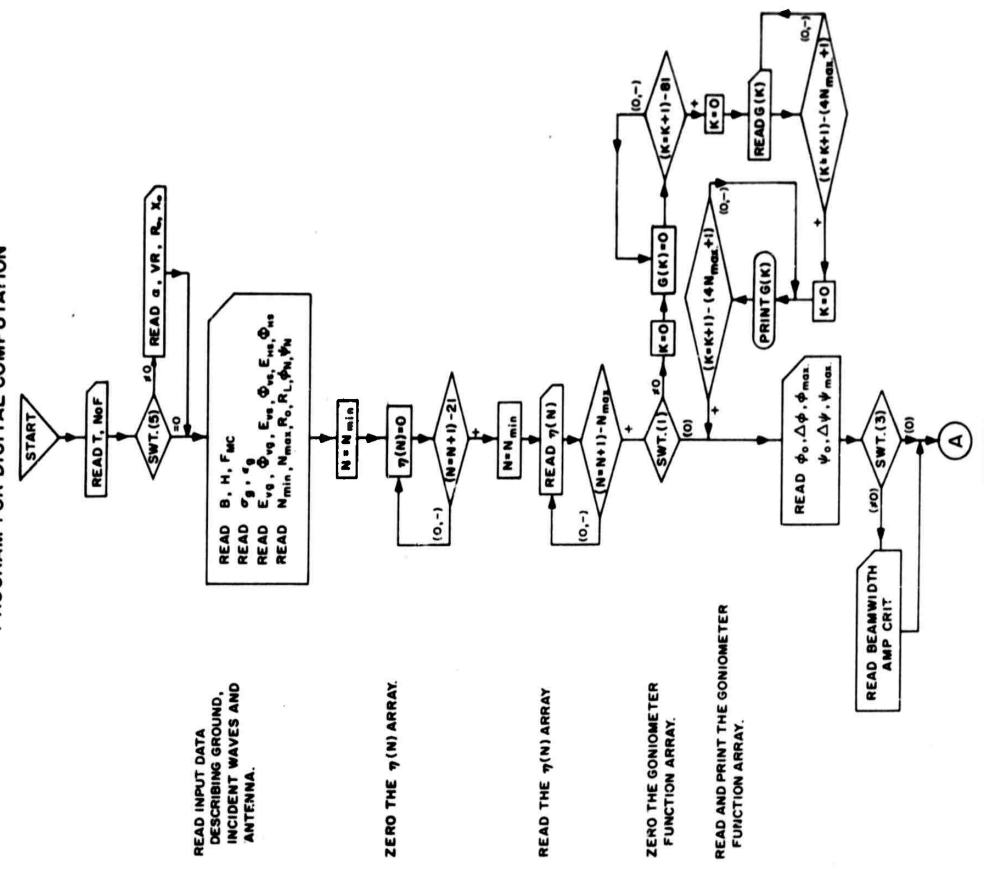
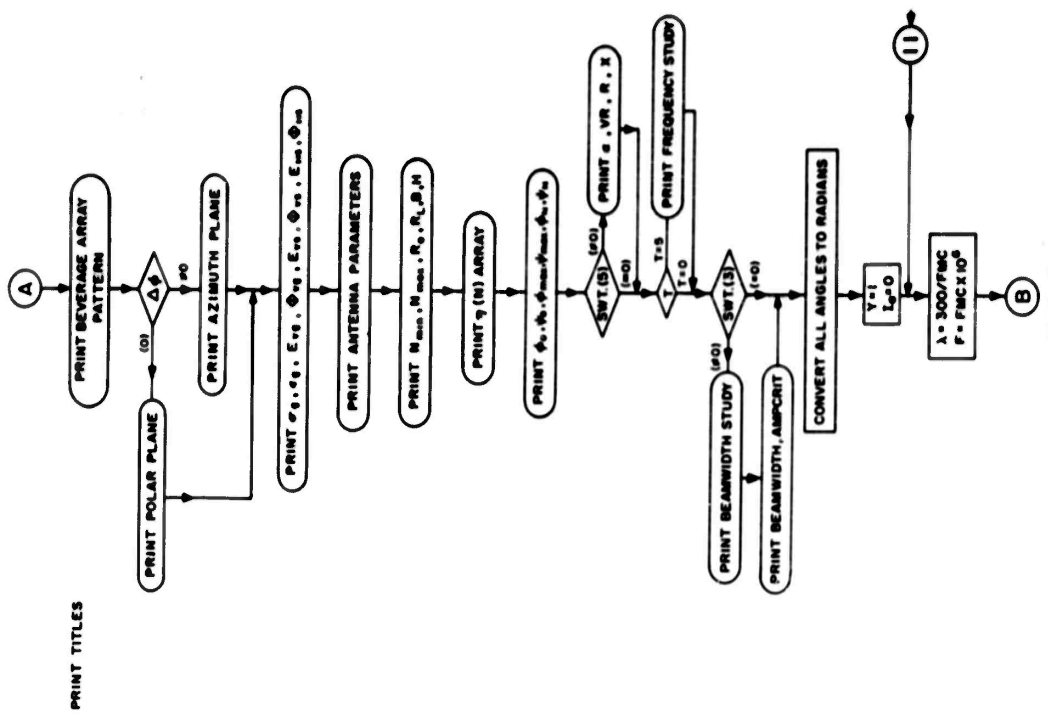


FIGURE 11



PRINT TITLES

FIGURE 12

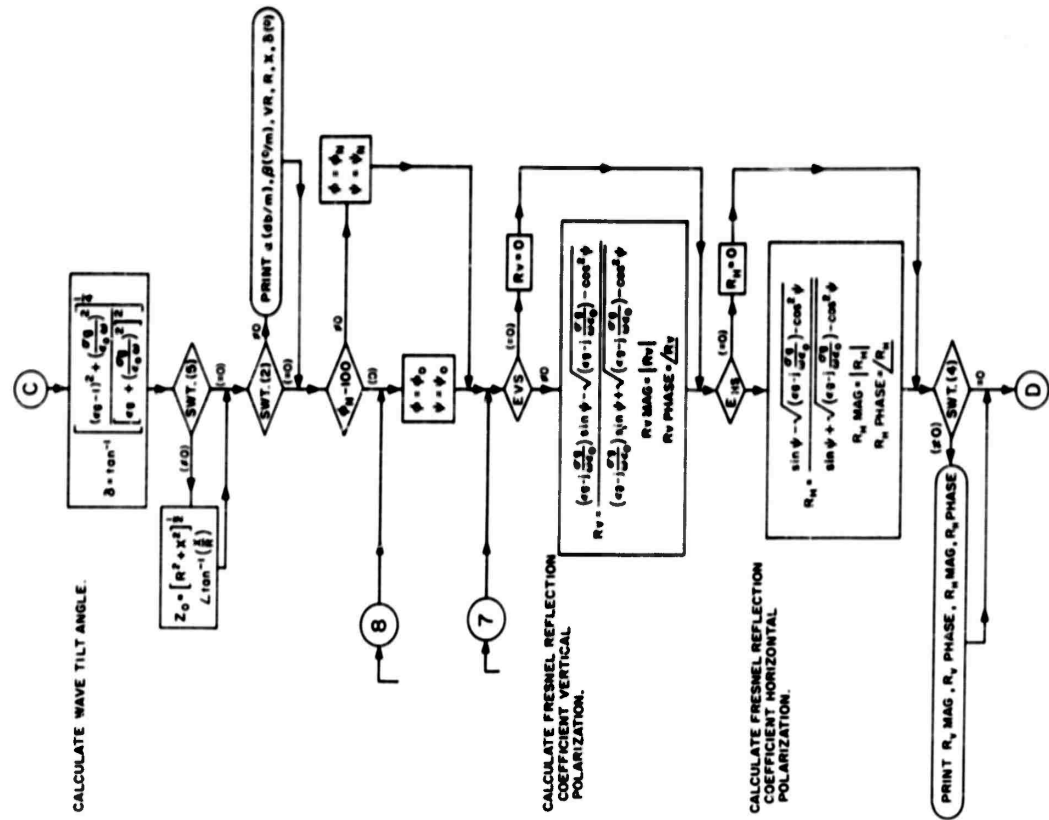


FIGURE 14

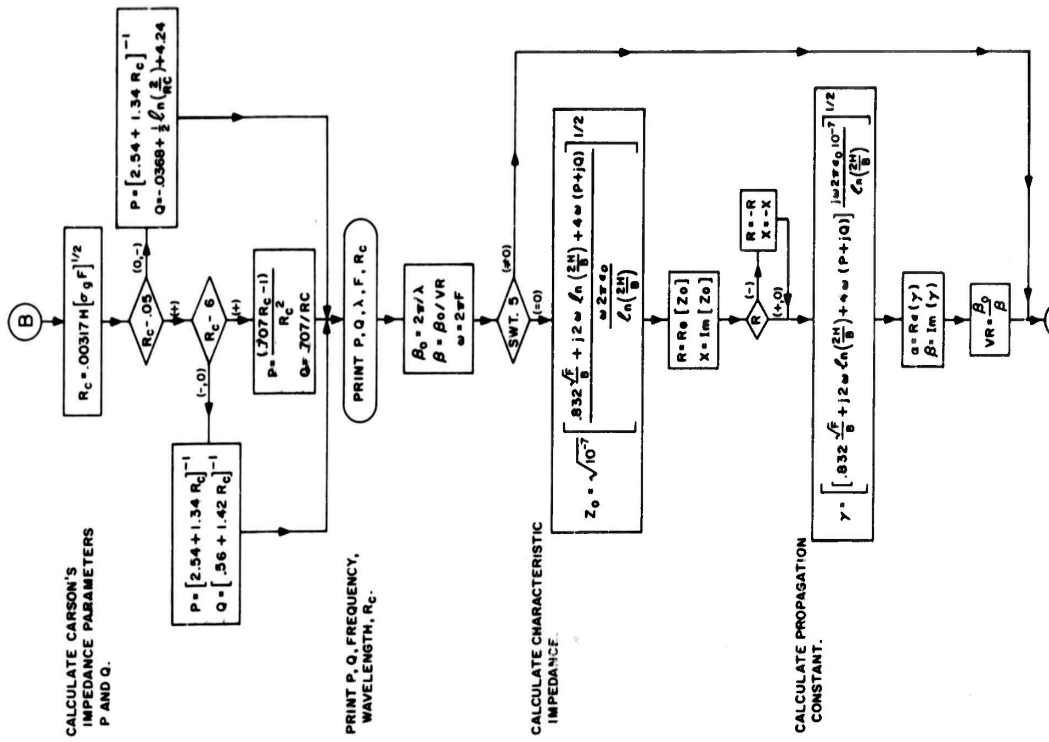


FIGURE 13

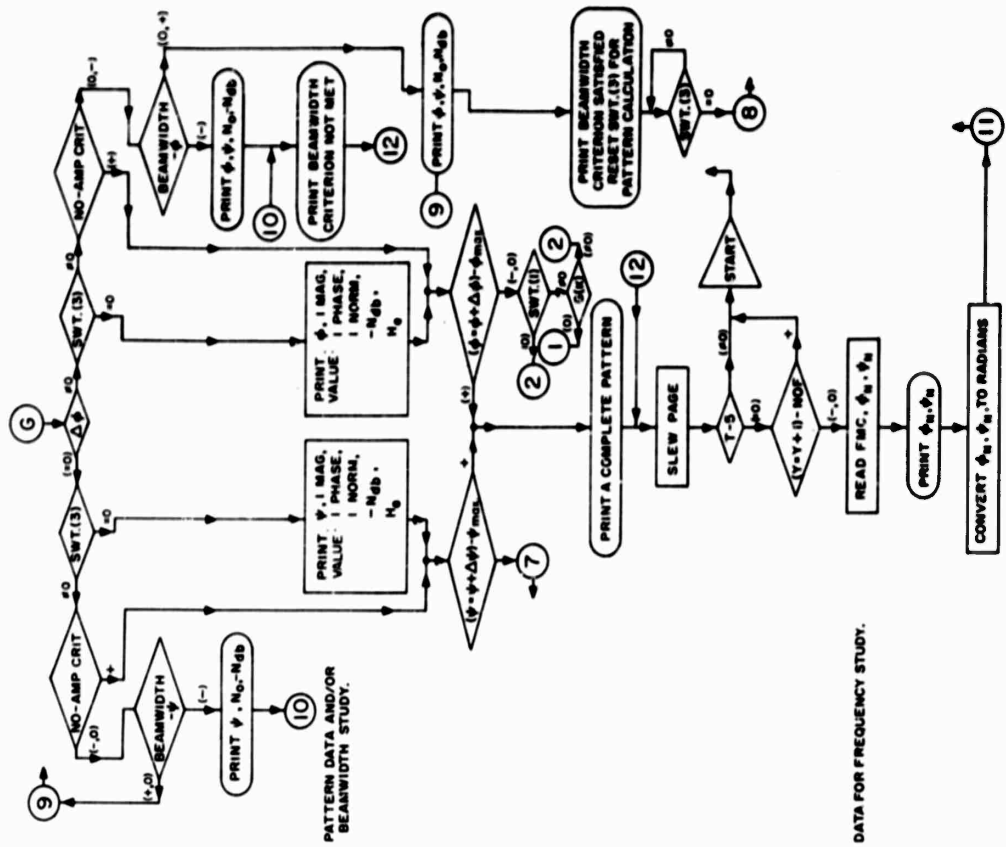


FIGURE 14
END

DATA FOR FREQUENCY STUDY.

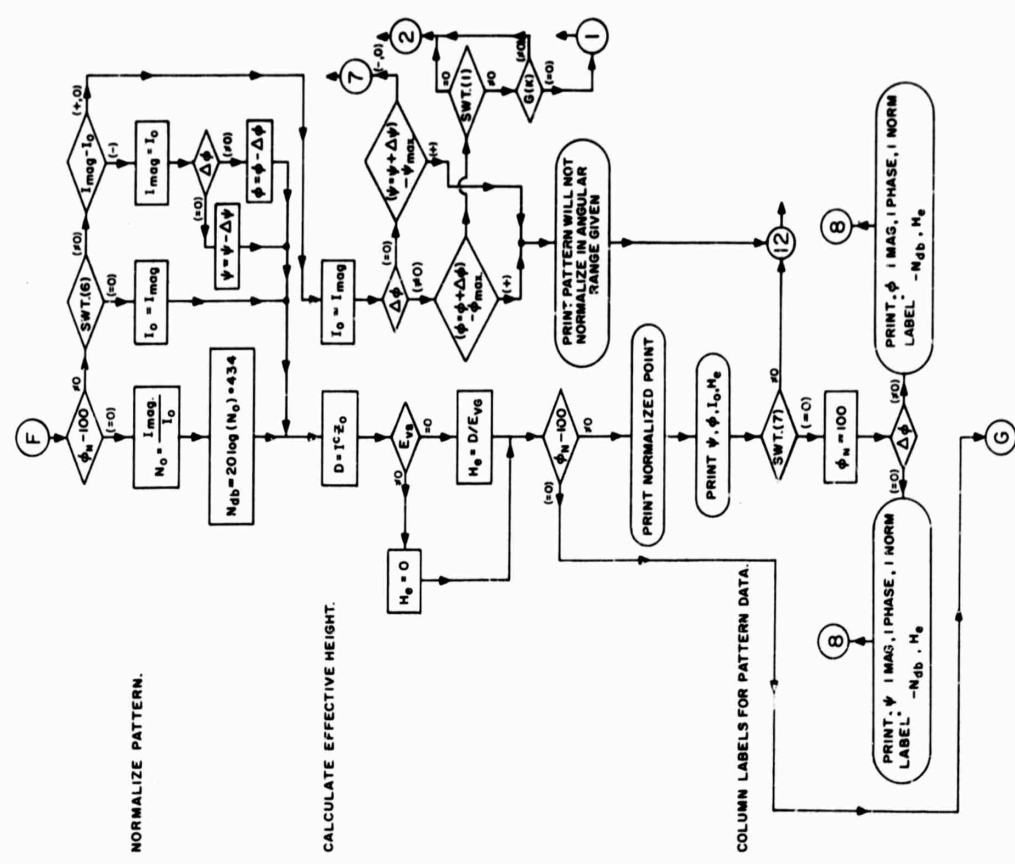


FIGURE 17

NORMALIZE PATTERN.

CALCULATE EFFECTIVE HEIGHT.

COLUMN LABELS FOR PATTERN DATA.

The normalized point is $I(\phi)$. This is a satisfactory method of normalization when there is a single main lobe adjacent or coincident with the initial ϕ_N, ψ_N .

With switch (7) down, the normalized point is obtained only, in addition to the initial parameters as desired which are available from switch (2) and switch (4). This provides the effective height and location of the main lobe, but exit to the next case is obtained automatically so that the complete pattern is not calculated. This option is useful for instance in computing polarization error vs frequency.

Further notes on program operation include the following:

- (1) For goniometer function operation the complete array beginning with the 0° antenna is called for, even though $G(o)$ may be zero. Therefore, $NIM = 0$ for all goniometer cases and $\eta(o) = 0$ must begin the $ETA(N)$ array.
- (2) For operation without the goniometer function and without the center antenna, it is necessary to begin with the first pair in specifying antenna locations.
- (3) For parameter studies with the frequency as the only variable, the input for successive cases consists only of the desired (mc) frequencies and the desired normalized point ϕ_N, ψ_N . For these cases $T = 5$, $NOF =$ total number of frequencies to be run including the first case. After NOF cases are run, the program reads in the next complete set of data.
- (4) The following equations were used for P and Q in the appropriate ranges:

$$P + jQ = \frac{1}{2.54 + 1.34 r_c} + j \left[-.0368 + \frac{1}{2} \ln \left(\frac{2}{r_c} \right) + \frac{r_c}{4.24} \right]$$

for $0 \leq r \leq .5$ (101)

$$= \frac{1}{2.54 + 1.34 r_c} + j \frac{1}{.56 + 1.42 r_c}$$

for $.5 \leq r_c \leq 6$ (102)

$$= \frac{.707 r_c - 1}{r_c^2} + j \frac{.707}{r_c}$$

$$\text{for } 6 \leq r_c \leq \infty \quad (103)$$

where

$$r_c = 0.00317h\sqrt{\sigma_g f_{\text{cps}}} \quad (104)$$

E. Theoretical Antenna Patterns

Ground wave azimuth patterns were calculated and reported in Figure 3 of Part I of this report. These earlier patterns were displayed as a function of antenna length and velocity ratio, and were calculated by specifying the velocity ratio and other parameters in addition to antenna geometry. Thus these earlier patterns while quite valid for the values chosen did not relate directly to the earth constants. The theory has since been improved, and the data are obtained without assuming velocity ratio values or attenuation constants. It is now only necessary to specify the antenna geometry and the earth constants (conductivity and dielectric constants). The computer program (see Section IV) will determine all the intermediate parameters previously assumed and calculate the proper pattern, either azimuth or elevation, in addition to the effective height.

In the patterns which follow, the data have been grouped according to certain fixed conditions and the frequency (or some other characteristic) varied. For instance, in group I the patterns are for antennas 111.9 meters long or shorter with the same outer radius. The earth conductivity has been assumed to be .03 mho/meter and the dielectric constant equal to 12 though any other reasonable values could have been chosen. The chosen values correspond to the D/F array which was described in Part I, page 67, and which has been the subject of extensive experimental investigation as described elsewhere in this report.

The analysis and associated computer program also permits calculation of theoretical values for the attenuation constant, velocity ratio, characteristic impedance and wave tilt angle. These calculated values are also given for most of the patterns which follow.

The computer patterns are divided into four groups.

Group I consists of single and multiple element arrays, most 111.9 meters long, and all applicable to the present Navy D/F array at the Southwest Research Institute D/F tower (outer radius 136.65 meters). This group also includes some patterns for antennas and arrays which could be formed by increasing the inner radius so as to shorten the antennas but keep the outer radius fixed.

Group II consists of similar patterns for antennas 300 meters long with a fixed outer array radius of 325 meters. This group includes some patterns for arrays which could be formed by increasing the inner radius and/or decreasing the outer radius of the array. These patterns are primarily applicable to the Signal Corps D/F site.

Group III consists of patterns for pure horizontal polarization and for mixture of vertical and horizontal polarization usually equal amplitudes and in phase (linear polarization at 45°). These are for various lengths.

Group IV consists of a number of miscellaneous patterns plotted to show certain special conditions, such as the elevation angle at which a maximum occurs as a function of velocity ratio.

The patterns which appear in the four groups are listed at the end of this section.

Data Group I first shows in Figure I-1a through I-12b both the azimuth and elevation patterns from 1 to 40 mcs for a single antenna 1 meter above ground. The "a" figure is the azimuth pattern, the "b" figure the elevation pattern. The source field is assumed to be a vertically polarized ground wave for the azimuth patterns, and a vertically polarized sky wave for the elevation patterns. Many of the elevation patterns have been plotted from 0° to 180° elevation angle at zero azimuth, thus these also show the elevation pattern of the back lobe at 180° azimuth. Both rectangular log plots and polar plots are shown.

It is characteristic of the sky wave elevation pattern to return to zero amplitude at zero elevation. This is not a mathematical limitation; for a smooth earth it is quite correct for the sky wave component alone (no ground wave) and always results when the ground wave or surface wave component is ignored. The relationship between the sky wave and ground wave for a real transmitter depends on the distance to the transmitter, and yet there seems to be no reason to pick a particular transmitter distance as representative of the manner in which the sky wave blends into the ground wave. However, it is evident that if a transmitter were to be varied in elevation from some height down to zero degrees, and simultaneously was adjusted to maintain the incident field strength constant at the Beverage receiving antenna, as zero elevation was approached, the elevation response pattern would not return to zero at zero elevation. At zero elevation, in such a case, the response would be that typical of the ground wave. This amplitude value (at zero elevation or the ground wave case) has been indicated on each polar plot of the elevation pattern as a short line at the appropriate amplitude, connecting the zero elevation axis with the sky wave pattern.

For instance, this value is shown at the normalized amplitude of .44 in the polar plot of Figure I-1b. It will be noted that the transition region from sky wave to ground wave in all cases is near or, at the higher frequencies, less than the wave tilt angle. Thus the exact details of the transition

at these low angles of elevation is not of great importance because no arriving wave, either ground wave or sky wave, ever appears to arrive at a lower elevation angle than the wave tilt angle.²⁶

The azimuth and elevation patterns show a decrease in both beamwidth and angle of elevation for maximum response, as the frequency is increased. In general the back lobe of the azimuth pattern is also decreased with increasing frequency. Azimuth patterns at higher angles of elevation are given later in data Group I.

Note that the elevation patterns show the main lobe to be down to approximately 10° elevation at 30 mcs. Since most long range sky waves arrive at angles below 15° or 20° elevation, it is evident that good azimuth response patterns should be obtained at all frequencies up to 30 mcs for distant transmitters, say greater than 500 miles. This was found to be the case during the bearing accuracy tests reported in Section III. The beamwidth and beam elevation data for many of these patterns are summarized in Part II in greater detail.

Figures I-13 through I-18 show the change in the azimuth pattern as a function of the number of antennas summed for 112-meter antennas 2° apart at 10 mcs. It is evident that the beamwidth is significantly reduced even though no phasing is used. Figures I-18 through I-28 show azimuth patterns for the same 21-antenna array, as the elevation angle is increased. It can be seen that a good azimuth pattern is obtained only for elevations below approximately the 3-db point on the upper side of the main beam. Above this elevation the azimuth pattern is split. This result is the first of several calculations which suggest that optimum patterns for higher angles of elevation will be obtained with short elements at a large array radius. Figure I-28 is the elevation pattern for this example and shows that the poor azimuth patterns obtained around 38° to 40° elevation are associated with a minimum in the elevation pattern. It is apparent that

26. This is because the resultant field, which is the sum of the incident and reflected rays, is tilted forward at an angle which approaches the wave tilt angle, at low angles of elevation, but never achieves a value less than the ground wave tilt angle. For further reference on this point, see Jordan, E. C., Electromagnetic Waves and Radiating Systems, Prentice-Hall, New York, 1950, Chapter 16; Piggott, W. R., "A Method of Determining the Polar Diagrams of Long Wire and Horizontal Rhombic Aerials," Department of Science and Industrial Research, Radio Research Special Report No. 16, London, His Majesty's Stationery Office, 1948, page 5. See also Feldman, C. B., "The Optical Behavior of the Ground for Short Radio Waves," particularly page 789, Proceedings of the IRE, Vol. 21, No. 6, June 1933.

if the antenna length is decreased this minimum will go up in elevation improving the azimuth pattern at higher angles.

Figures I-29 thru I-32 show that for nonequally spaced arrays narrow azimuth patterns may be obtained at the cost of high side lobe levels.

Figures I-33 through I-44 are largely a repeat of Figures I-1 through I-12 at a slightly lower height above ground. The selected value of .85 meter is the average height of the 112 meter long antennas in the experimental arrays described in Part II of this report. The results are similar to those of the previous figures except that attenuation is slightly greater, and the patterns are slightly modified in shape.

Figures I-45 through I-55 show reduction in beamwidth with an increased inner radius as a function of the number of antennas summed. Note that both a more favorable elevation pattern and a narrower azimuth pattern are obtained. Figures I-56 through I-66 show the same result for a still shorter element. Figures I-57 through I-82 then explore azimuth patterns vs elevation angle at a number of antennas which produce minimum azimuth beamwidth at zero elevation.

These patterns with larger inner radii and the same as previous outer radius show much improved elevation patterns and in addition reduced polarization error as will be shown in Group III. Twenty-five meter long antennas show good azimuth patterns at all angles of elevation of a summed group of 19 antennas each 2° apart with an outer radius of 136.65 meters.

The figures in Group II are concerned with antennas 300 meters long or shorter but on a site capable of holding 300 meter long antennas. Figures II-1 through II-12 show single element patterns vs frequency for both azimuth and elevation planes. These patterns are for antennas one meter high. It is evident that the longer element has produced a more favorable azimuth pattern and a less favorable elevation pattern compared to the 112 meter long antennas (unless only low angles of arrival are of interest). Figures II-13 thru II-24 show the elevation patterns for the same antenna at a height of two meters.

Figures II-25 thru II-32 show azimuth patterns vs elevation at 6.0 mcs for a single element 2 meters high and 300 meters long. Again, as with the 112-meter antennas, split azimuth patterns are obtained at elevations above the main lobe. Figures II-33 thru II-36 show variation with frequency between 2.0 and 6.0 mcs at an elevation of 20° .

Figures II-37 thru II-42 show beamwidth reduction with increased number of summed antennas. Figures II-43 thru II-52 show an increased beamwidth reduction for a greater inner radius and less outer radius.

Figures II-53 thru II-64 show patterns for the same length previously shown with an outer radius of 325 meters. Minimum beamwidth of approximately 12° is obtained with 15 antennas at 10 mcs.

Figures II-65 to II-70 show azimuth patterns vs number of antennas for a shorter element length than the previous set, but the same outer radius. Figures II-71 thru 74 show a single element pattern variation with height above ground.

Figures II-75 thru II-78 show split sector arrays of antennas all 2° apart and illustrate how still narrower azimuth patterns may be obtained at the cost of higher side lobe level. A pattern designated 7 on 1 off 7 on means 14 antennas in two sectors of seven each. The two sectors are separated by a gap of 4 degrees (one missing antenna). Similarly the 6 on 3 off 6 on array means two 6 element sectors separated by an 8° gap (three missing antennas). These type arrays can be obtained with the present commutator.

Further details and discussions of the various data obtained from the patterns are given in Part II of this report.

Patterns in Group III are concerned with the effects of horizontally polarized fields, or elliptically polarized fields. The first 20 patterns shown in Figures III-1 thru III-20 show the response of one and two meter high single elements to pure horizontal polarization. These patterns are symmetrical and have a null in the direction of the antenna line.

Patterns like those in the first 20 figures of this group have rarely been observed experimentally because the horizontally polarized components almost always occur in the presence of vertically polarized components. In general the response of the antenna is greater to vertically polarized than horizontally polarized fields of equal amplitude. This is because only the vertically polarized field occurs in a manner favorable to a traveling wave buildup on the antenna. Figures III-21 thru III-24 illustrate this for low angles of elevation on longer elements.

Figures III-21 thru III-24 show that polarization error is small at low angles of elevation but may increase above the main beam. It can also be seen that the patterns are increasingly asymmetrical as the elevation angle increases (or the effect of the horizontally polarized component increases). This asymmetry also appears in practice when signals are observed which are changing in polarization. From the calculations it would be expected that a sky wave signal would appear to fade and slightly move in azimuth for low angles and long antennas. If the polarization error is slight, the pattern would appear to fade on the bearing indicated

when good symmetry occurred. This effect has been observed in practice and generally the fading drops the amplitude of the displayed pattern well below the maximum before a noticeable polarization shift occurs. One would expect then on occasion to observe pure horizontally polarized patterns at the lowest part of some fades; that is, patterns such as those in Figures III-1 thru III-20. This effect has also been observed as expected although not frequently. The fact that these expected patterns have been observed however, lends support to the general method of analysis given in this report.

If the analysis given is correct, then for long antennas at low angles, polarization error will not be appreciable for two reasons: (1) its measured value will be low, and (2) the appearance of the pattern will be such that it can be recognized that at a given instant some polarization error exists, i. e., asymmetry and slight back and forth swinging as the polarization shifts, so that bearings can be read at an optimum time. In Part III of this report results are presented for operators with no experience at pattern interpretation vs those using symmetry as criteria. Results bear out what has been stated above.

Further consideration suggests that at high angles of elevation the polarization error should increase if the antenna element is long (Figure III-23). This leads to the same design direction indicated earlier, that of using shorter elements to improve the elevation pattern.

This is explored in Figures III-30 thru III-33 where the azimuth patterns for an array of 19 antennas each 25 meters long are shown as a function of angle of elevation. It is evident that an improvement has been obtained in that the polarization error is small up to 30° . The previous remarks concerning asymmetry or a criterion for error detection are equally applicable in this case. Further and more detailed consideration of response to horizontal polarization is given in Part II of this report.

Patterns shown by Figures IV-1 thru IV-5 are a miscellaneous group included to illustrate two methods of pattern improvement which have not yet been attempted experimentally. Figures IV-1 thru IV-4 show the variation in a typical long element elevation pattern with artificial variation of the velocity ratio on the antenna. As the velocity ratio is increased to values greater than one, the angle of elevation of the main beam is increased. Thus this could be a method for controlling response for short range signal arriving at high angles. (A velocity ratio greater than one implies a phase velocity faster than the velocity of light. This may be achieved for instance by inserting series capacitance in the antenna as was done by Beverage.⁹)

Figure IV-5 shows a method whereby a very sharp azimuth beam may be obtained without using a phased array. The patterns were obtained by reversing the phase of a pair of antennas in the array before summing. The null between the main beam and the first side lobe occurs in the vicinity of the direction where the phase reversal occurs in azimuth. An array of 180 antennas could be used to produce such patterns without a phasing goniometer by using multicouplers (or other devices with both 0° and 180° phase outputs) and a 360-input commutator (2 inputs per antenna).

GROUP I - 112-METER ANTENNAS

<u>Figure No.</u>	<u>Pattern Plane</u>	<u>Freq. in Mcs</u>		
I-1a	Azimuth	1.0	} All single antennas one meter high. Azimuth patterns ground wave vertical polarization, elevation patterns sky wave vertical polarization at zero azimuth.	
I-1b	Elevation	1.0		
I-2a	Azimuth	1.5		
I-2b	Elevation	1.5		
I-3a	Azimuth	2.0		
I-3b	Elevation	2.0		
I-4a	Azimuth	3.0		
I-4b	Elevation	3.0		
I-5a	Azimuth	4.0		
I-5b	Elevation	4.0		
I-6a	Azimuth	6.0		
I-6b	Elevation	6.0		
I-7a	Azimuth	8.0		
I-7b	Elevation	8.0		
I-8a	Azimuth	10.0		
I-8b	Elevation	10.0		
I-9a	Azimuth	15.0		
I-9b	Elevation	15.0		
I-10a	Azimuth	20.0		
I-10b	Elevation	20.0		
I-11a	Azimuth	30.0		
I-11b	Elevation	30.0		
I-12a	Azimuth	40.0		
I-12b	Elevation	40.0		
I-13	Azimuth	10.0	} Single Antenna	
I-14	Azimuth	10.0		} 3 Antennas } All antennas 2° apart, 5 Antennas } 1 meter high, zero 9 Antennas } elevation 15 Antennas }
I-15	Azimuth	10.0		
I-16	Azimuth	10.0		
I-17	Azimuth	10.0		
I-18	Azimuth	10.0		} Zero Elevation } 10° Elevation } 20° Elevation } 30° Elevation } All patterns 32° Elevation } 21 antennas all 34° Elevation } 2° apart, 1 meter 36° Elevation } high, vertical 38° Elevation } polarization 40° Elevation } 42° Elevation } Zero Azimuth }
I-19	Azimuth	10.0		
I-20	Azimuth	10.0		
I-21	Azimuth	10.0		
I-22	Azimuth	10.0		
I-23	Azimuth	10.0		
I-24	Azimuth	10.0		
I-25	Azimuth	10.0		
I-26	Azimuth	10.0		
I-27	Azimuth	10.0		
I-28	Elevation	10.0		

GROUP I - 112-METER ANTENNAS (Cont'd)

<u>Figure No.</u>	<u>Pattern Plane</u>	<u>Freq. in Mcs</u>	
I-29	Azimuth	10.0	2 Antennas, $\pm 20^\circ$ azimuth
I-30	Azimuth	10.0	6 Antennas, $\pm 18^\circ, \pm 20^\circ, \pm 22^\circ$ azimuth
I-31	Azimuth	10.0	6 Antennas, $\pm 16^\circ, \pm 20^\circ, \pm 24^\circ$ azimuth
I-32	Azimuth	10.0	6 Antennas, $\pm 16^\circ, \pm 18^\circ, \pm 20^\circ$ azimuth
I-33	Azimuth	1.0	All single antennas .85 meter high. Azimuth patterns have vertically polarized ground wave.
I-34	Azimuth	1.5	
I-35	Azimuth	2.0	
I-36	Azimuth	3.0	
I-37	Azimuth	4.0	
I-38	Azimuth	6.0	
I-39	Azimuth	8.0	
I-40	Azimuth	10.0	
I-41	Azimuth	15.0	
I-42	Azimuth	20.0	
I-43	Azimuth	30.0	
I-44	Azimuth	40.0	
I-45	Azimuth	Single Antenna	All antennas 2° apart, one meter high, zero elevation. Antennas 50 meters long, inner radius 86.65 meters, outer radius 136.65 meters. All patterns at 10 mc.
I-45	Azimuth	3 Antennas	
I-47	Azimuth	5 Antennas	
I-48	Azimuth	7 Antennas	
I-49	Azimuth	9 Antennas	
I-50	Azimuth	11 Antennas	
I-51	Azimuth	15 Antennas	
I-52	Azimuth	19 Antennas	
I-53	Azimuth	21 Antennas	
I-54	Elevation	Single Antenna	
I-55	Elevation	21 Antennas	
I-56	Azimuth	Single Antenna	
I-57	Azimuth	3 Antennas	
I-58	Azimuth	5 Antennas	
I-59	Azimuth	7 Antennas	
I-60	Azimuth	9 Antennas	
I-61	Azimuth	11 Antennas	
I-62	Azimuth	15 Antennas	
I-63	Azimuth	17 Antennas	
I-64	Azimuth	21 Antennas	
I-65	Elevation	Single Antenna	
I-66	Elevation	21 Antennas	

GROUP I - 112-METER ANTENNAS (Cont'd)

<u>Figure No.</u>	<u>Pattern Plane</u>	<u>Freq. in Mcs</u>	
I-67	Azimuth	5° Elevation	} All antennas 2° apart, one meter high. Antennas 25 meters long, inner radius 111.6 meters, outer radius 136.6 meters, 10 mc. Vertically polarized sky wave. Azimuth plane patterns for sum of 19 antennas.
I-68	Azimuth	10° Elevation	
I-69	Azimuth	20° Elevation	
I-70	Azimuth	25° Elevation	
I-71	Azimuth	30° Elevation	
I-72	Azimuth	35° Elevation	
I-73	Azimuth	40° Elevation	
I-74	Azimuth	45° Elevation	
I-75	Azimuth	50° Elevation	
I-76	Azimuth	55° Elevation	
I-77	Azimuth	60° Elevation	
I-78	Azimuth	65° Elevation	
I-79	Azimuth	70° Elevation	
I-80	Azimuth	75° Elevation	
I-81	Azimuth	80° Elevation	
I-82	Azimuth	85° Elevation	

GROUP II - 300-METER ANTENNAS

<u>Figure No.</u>	<u>Pattern Plane</u>	<u>Freq. in Mcs</u>	
II-1a	Azimuth	1.0	} All single antennas one meter high. Azimuth patterns ground wave vertical polarization, elevation patterns sky wave vertical polarization at zero azimuth.
II-1b	Elevation	1.0	
II-2a	Azimuth	1.5	
II-2b	Elevation	1.5	
II-3a	Azimuth	2.0	
II-3b	Elevation	2.0	
II-4a	Azimuth	3.0	
II-4b	Elevation	3.0	
II-5a	Azimuth	4.0	
II-5b	Elevation	4.0	
II-6a	Azimuth	6.0	
II-6b	Elevation	6.0	
II-7a	Azimuth	8.0	} All single antennas two meters high. Sky wave, vertical polarization, at zero azimuth.
II-7b	Elevation	8.0	
II-8a	Azimuth	10.0	
II-8b	Elevation	10.0	
II-9a	Azimuth	15.0	
II-9b	Elevation	15.0	
II-10a	Azimuth	20.0	
II-10b	Elevation	20.0	
II-11a	Azimuth	30.0	
II-11b	Elevation	30.0	
II-12a	Azimuth	40.0	
II-12b	Elevation	40.0	
II-13	Elevation	1.0	} All single antennas two meters high. Sky wave, vertical polarization, at zero azimuth.
II-14	Elevation	1.5	
II-15	Elevation	2.0	
II-16	Elevation	3.0	
II-17	Elevation	4.0	
II-18	Elevation	6.0	
II-19	Elevation	8.0	
II-20	Elevation	10.0	
II-21	Elevation	15.0	
II-22	Elevation	20.0	
II-23	Elevation	30.0	
II-24	Elevation	40.0	

GROUP II - 300-METER ANTENNAS (Cont'd)

<u>Figure No.</u>	<u>Pattern Plane</u>	<u>Freq. in Mcs.</u>		
II-25	Azimuth	6.0	Zero Elevation	All single antennas, two meters high, sky wave vertical polarization. Antennas 300 meters long.
II-26	Azimuth	6.0	10° Elevation	
II-27	Azimuth	6.0	20° Elevation	
II-28	Azimuth	6.0	30° Elevation	
II-29	Azimuth	6.0	40° Elevation	
II-30	Azimuth	6.0	50° Elevation	
II-31	Azimuth	6.0	60° Elevation	
II-32	Elevation	6.0	Zero Azimuth	
II-33	Azimuth	2.0	All single antennas, two meters high, elevation angle 20°, sky wave vertical polarization. Antenna length 300 meters.	
II-34	Azimuth	3.0		
II-35	Azimuth	4.0		
II-36	Azimuth	6.0		
II-37	Azimuth		Single Antenna	All antennas 2° apart, two meters high, sky wave vertical polarization. Antennas 300 meters long, inner radius 25 meters, outer radius 325 meters, frequency 10 mc.
II-38	Azimuth		3 Antennas	
II-39	Azimuth		5 Antennas	
II-40	Azimuth		9 Antennas	
II-41	Azimuth		15 Antennas	
II-42	Azimuth		21 Antennas	
II-43	Azimuth		Single Antenna	All antennas 2° apart, one meter high, sky wave vertical polarization. Antennas 100 meters long, inner radius 125 meters, outer radius 225 meters, frequency 10 mc.
II-44	Azimuth		3 Antennas	
II-45	Azimuth		5 Antennas	
II-46	Azimuth		7 Antennas	
II-47	Azimuth		9 Antennas	
II-48	Azimuth		11 Antennas	
II-49	Azimuth		13 Antennas	
II-50	Azimuth		15 Antennas	
II-51	Azimuth		21 Antennas	
II-52	Elevation		Single Antenna	

GROUP II - 300-METER ANTENNAS (Cont'd)

<u>Figure No.</u>	<u>Pattern Plane</u>	<u>Freq. in Mcs</u>	
II-53	Azimuth	Single Antenna	All antennas 2° apart, one meter high, vertical polarization. Antennas 100 meters long, inner radius 225 meters, outer radius 325 meters frequency 10 mcs.
II-54	Azimuth	3 Antennas	
II-55	Azimuth	5 Antennas	
II-46	Azimuth	7 Antennas	
II-57	Azimuth	9 Antennas	
II-58	Azimuth	11 Antennas	
II-59	Azimuth	13 Antennas	
II-60	Azimuth	15 Antennas	
II-61	Azimuth	19 Antennas	
II-62	Azimuth	21 Antennas	
II-63	Elevation	Single Antenna	
II-64	Elevation	15 Antennas	
II-65	Azimuth	3 Antennas	All antennas 2° apart, one meter high, vertical polarization. Antennas 50 meters long, inner radius 275 meters, outer radius 325 meters, frequency 10 mcs.
II-66	Azimuth	5 Antennas	
II-67	Azimuth	7 Antennas	
II-68	Azimuth	9 Antennas	
II-69	Azimuth	11 Antennas	
II-70	Azimuth	15 Antennas	
II-71	Azimuth	15 Meters high	Single antenna, vertical polarization, antenna 300 meters long, frequency 10 mcs, elevation angle 20°.
II-72	Azimuth	1 Meter high	
II-73	Azimuth	2 Meters high	
II-74	Azimuth	4 Meters high	
II-75	Azimuth	"7 on, 1 off, 7 on"	15 antennas in a split sector array, all 2° apart whether on or off. Seven on, 1 off, 7 on means 7 antennas 2° apart (a 12° sector) then a 4° sector with no antennas, then 7 antennas 2° apart again to complete symmetry.
II-76	Azimuth	"6 on, 3 off, 6 on"	
II-77	Azimuth	"5 on, 5 off, 5 on"	
II-78	Azimuth	"4 on, 7 off, 4 on"	

GROUP III - HORIZONTAL POLARIZATION

<u>Figure No.</u>	<u>Pattern Plane</u>	<u>Freq. in Mcs</u>		
III-1	Azimuth	1.0	max	All single antennas, pure horizontal polarization, one meter high. Maximum and minimum refers to elevation angle chosen. Maximum is elevation angle of a maximum on elevation plane for sky wave vertical polarization. Minimum is elevation angle of a minimum on elevation plane pattern for sky wave vertical polarization.
III-2	Azimuth	1.5	max	
III-3	Azimuth	2.0	max	
III-4	Azimuth	2.0	min	
III-5	Azimuth	3.0	max	
III-6	Azimuth	3.0	min	
III-7	Azimuth	4.0	max	
III-8	Azimuth	4.0	min	
III-9	Azimuth	6.0	max	
III-10	Azimuth	6.0	min	
III-11	Azimuth	1.0	max	All single antennas, pure horizontal polarization, two meters high. Maximum and minimum refers to elevation angle chosen. Maximum is elevation angle of a maximum on elevation plane for sky wave vertical polarization. Minimum is elevation angle of a minimum on elevation plane pattern for sky wave vertical polarization.
III-12	Azimuth	1.5	min	
III-13	Azimuth	2.0	max	
III-14	Azimuth	2.0	min	
III-15	Azimuth	3.0	max	
III-16	Azimuth	3.0	min	
III-17	Azimuth	4.0	max	
III-18	Azimuth	4.0	min	
III-19	Azimuth	6.0	max	
III-20	Azimuth	6.0	min	
III-21	Azimuth	6.0	Single Antenna, 10° Elevation	Mixed polarization, vertical plus horizontal
III-22	Azimuth	6.0	Single Antenna, 20° Elevation	
III-23	Azimuth	6.0	Single Antenna, 30° Elevation	
III-24	Azimuth	6.0	Single Antenna, 40° Elevation	
III-25	Azimuth	6.0	.5 meter high	Single antennas, 20° elevation, shows both vertical and mixed polarization patterns.
III-26	Azimuth	6.0	1.0 meter high	
III-27	Azimuth	6.0	2.0 meters high	
III-28	Azimuth	6.0	4.0 meters high	
III-29	Azimuth	10.0	shows polarization error vs number of antennas	
III-30	Azimuth			All azimuth plane patterns at 10 mc. Sum of 19 antennas, 2° apart, one meter high. Antennas 25 meters long, inner radius 111.6 meters, outer radius 136.6 meters. Linear polarization at 45° in phase (equal in phase components of vertical and horizontal polarization). 10 mcs.
III-31	Azimuth			
III-32	Azimuth			
III-33	Azimuth			
III-34	Azimuth			

GROUP IV

<u>Figure No.</u>	<u>Pattern Plane</u>	<u>Freq. in Mcs</u>			
IV-1	Elevation	10.0	}	Velocity Ratio = 1.00	Single antennas 111.9 meters long, one meter high.
IV-2	Elevation	10.0		Velocity Ratio = 1.10	
IV-3	Elevation	10.0		Velocity Ratio = 1.20	
IV-4	Elevation	10.0		Velocity Ratio = 1.30	
IV-5	Azimuth	10.0		Various patterns for group of four antennas, 2 pairs 180° out of phase.	

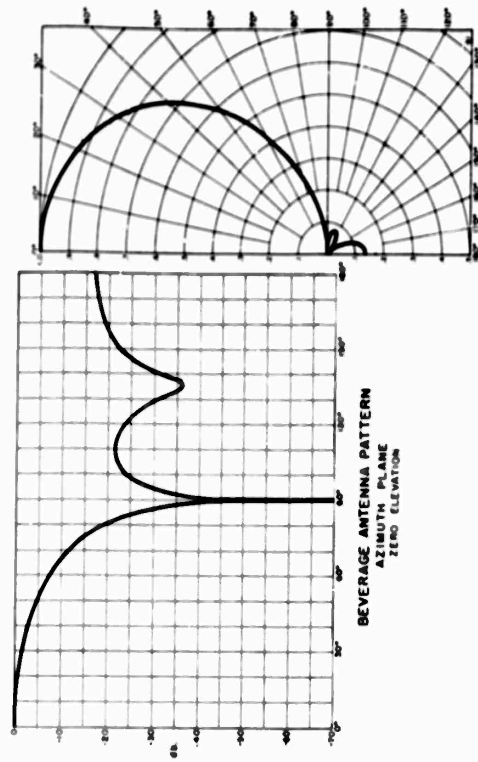


FIGURE 1-20

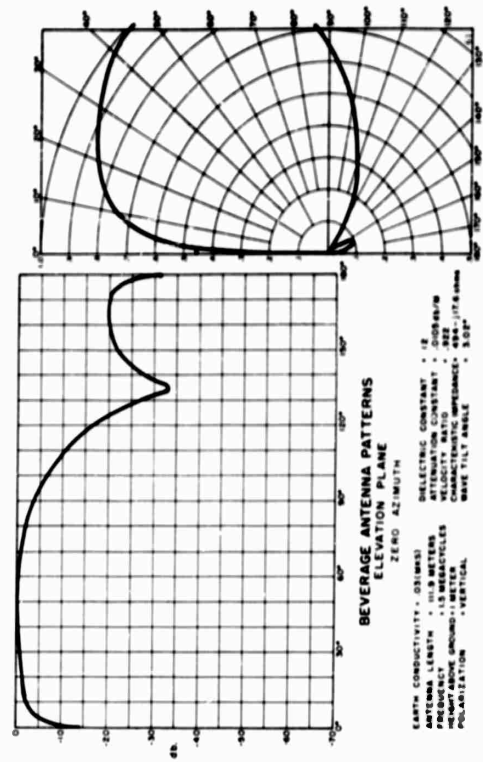


FIGURE 1-20

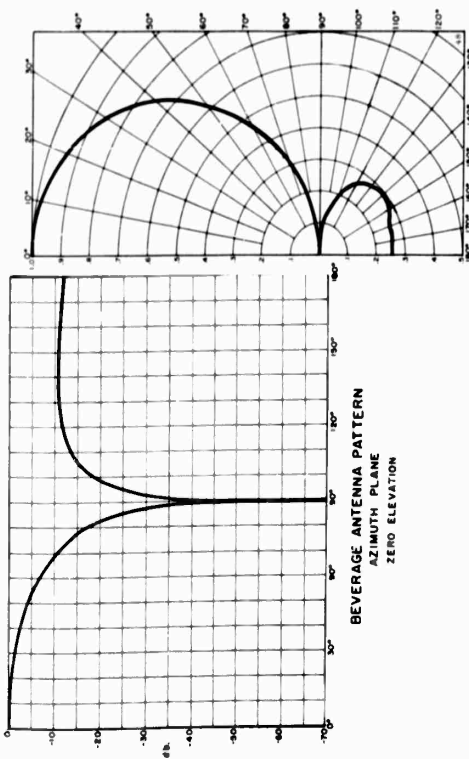


FIGURE 1-16

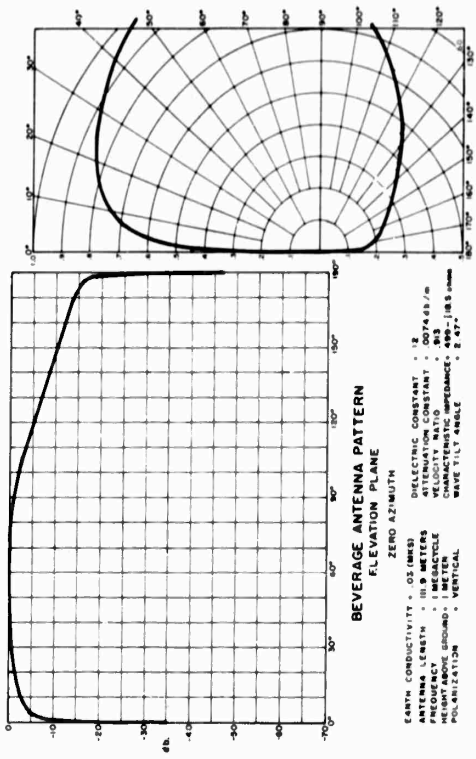


FIGURE 1-16

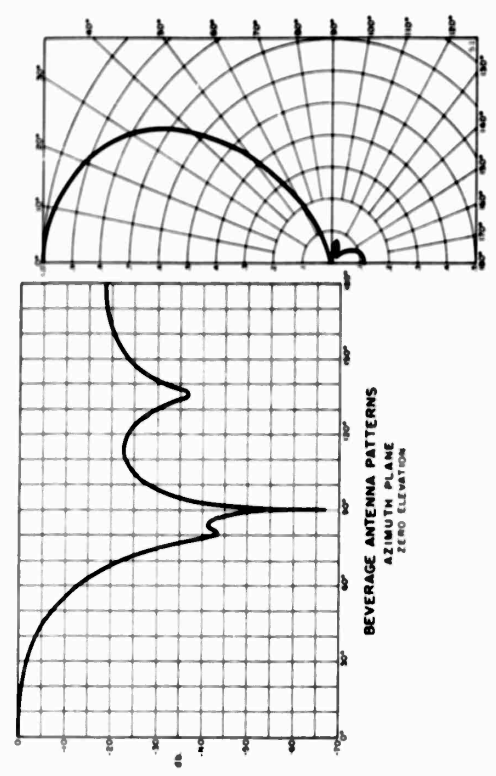


FIGURE I-38

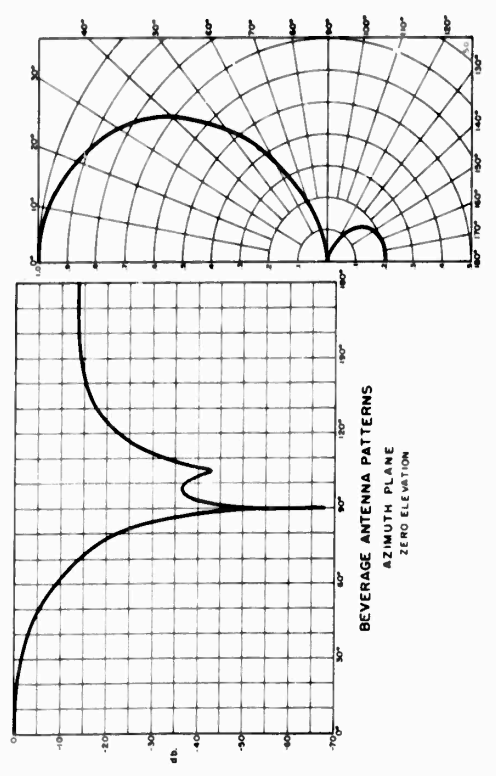


FIGURE I-39

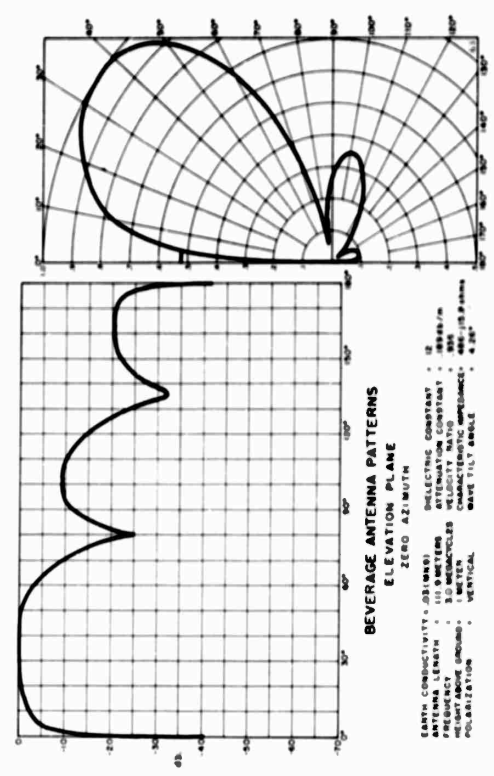


FIGURE I-40

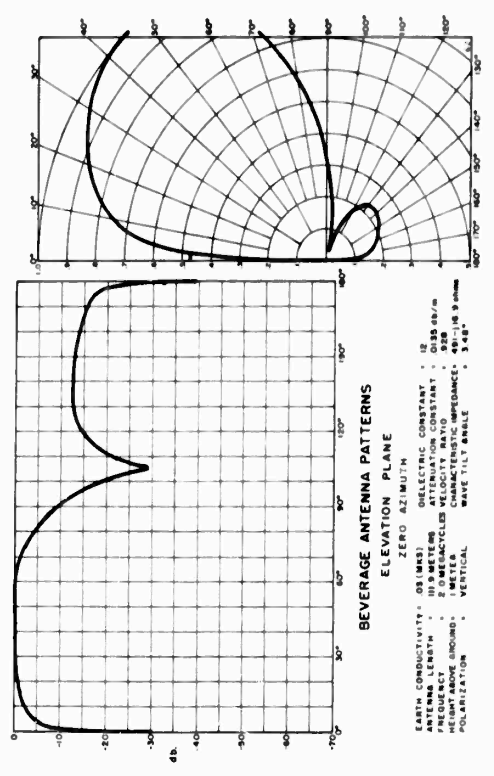


FIGURE I-41

EARTH CONDUCTIVITY: 0.01 MKS) DIELECTRIC CONSTANT: 12
 ANTENNA LENGTH: 111.9 METERS ATTENUATION CONSTANT: 0.000001
 FREQUENCY: 3.0 MEGACYCLES CHARACTERISTIC IMPEDANCE: 300 OHMS
 HEIGHT ABOVE GROUND: 1 METERS WAVELENGTHS: 100.0
 POLARIZATION: VERTICAL WAVE TILT ANGLE: 0.000

EARTH CONDUCTIVITY: 0.01 MKS) DIELECTRIC CONSTANT: 12
 ANTENNA LENGTH: 111.9 METERS ATTENUATION CONSTANT: 0.000001
 FREQUENCY: 3.0 MEGACYCLES CHARACTERISTIC IMPEDANCE: 300 OHMS
 HEIGHT ABOVE GROUND: 1 METERS WAVELENGTHS: 100.0
 POLARIZATION: VERTICAL WAVE TILT ANGLE: 0.000

EARTH CONDUCTIVITY: 0.01 MKS) DIELECTRIC CONSTANT: 12
 ANTENNA LENGTH: 111.9 METERS ATTENUATION CONSTANT: 0.000001
 FREQUENCY: 3.0 MEGACYCLES CHARACTERISTIC IMPEDANCE: 300 OHMS
 HEIGHT ABOVE GROUND: 1 METERS WAVELENGTHS: 100.0
 POLARIZATION: VERTICAL WAVE TILT ANGLE: 0.000

EARTH CONDUCTIVITY: 0.01 MKS) DIELECTRIC CONSTANT: 12
 ANTENNA LENGTH: 111.9 METERS ATTENUATION CONSTANT: 0.000001
 FREQUENCY: 3.0 MEGACYCLES CHARACTERISTIC IMPEDANCE: 300 OHMS
 HEIGHT ABOVE GROUND: 1 METERS WAVELENGTHS: 100.0
 POLARIZATION: VERTICAL WAVE TILT ANGLE: 0.000

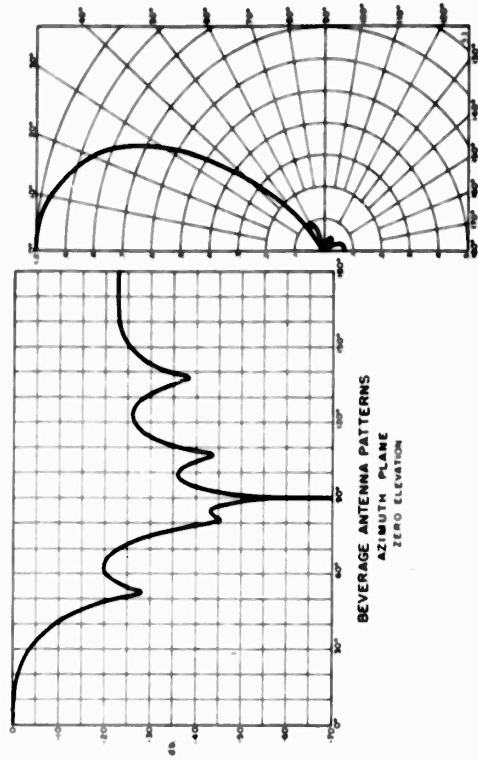


FIGURE 1-5a

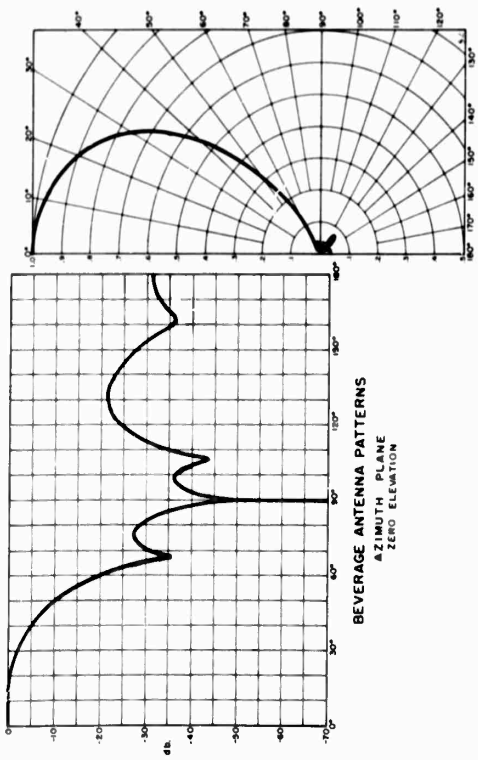


FIGURE 1-5b

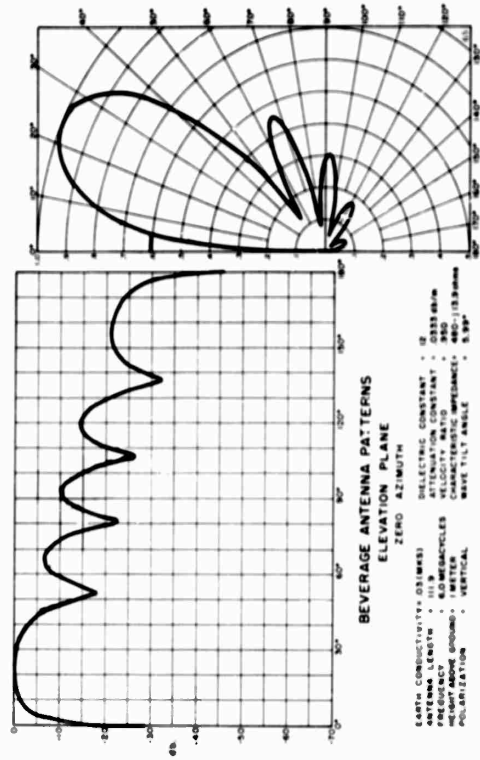


FIGURE 1-6a

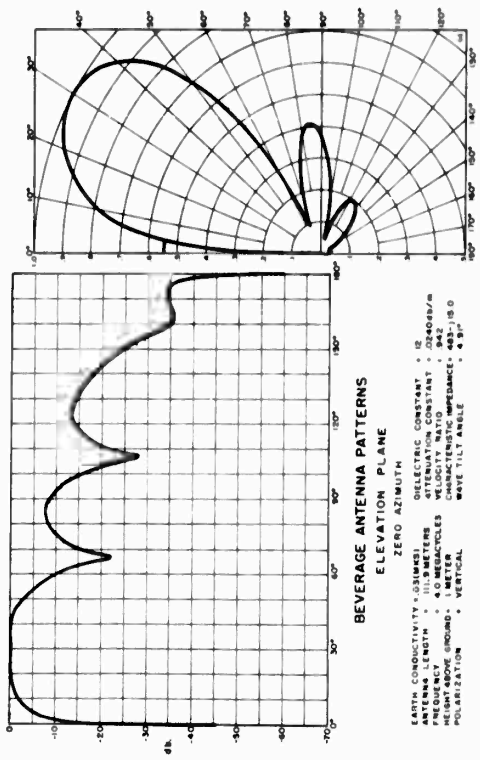


FIGURE 1-6b

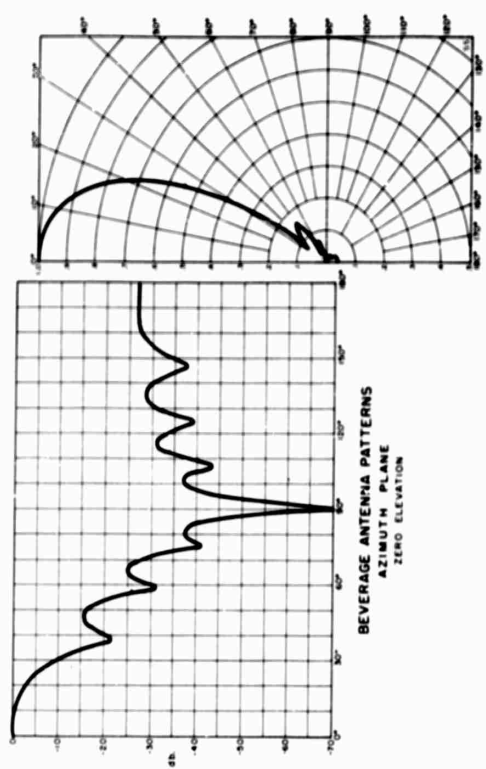


FIGURE 1-6a

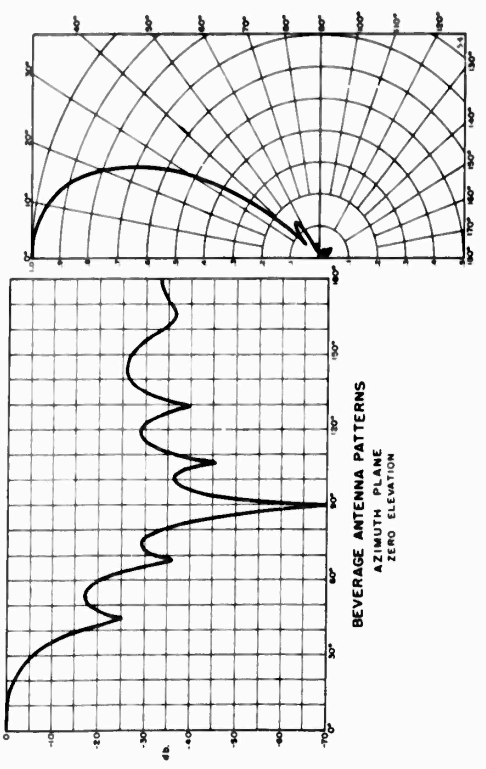


FIGURE 1-7a

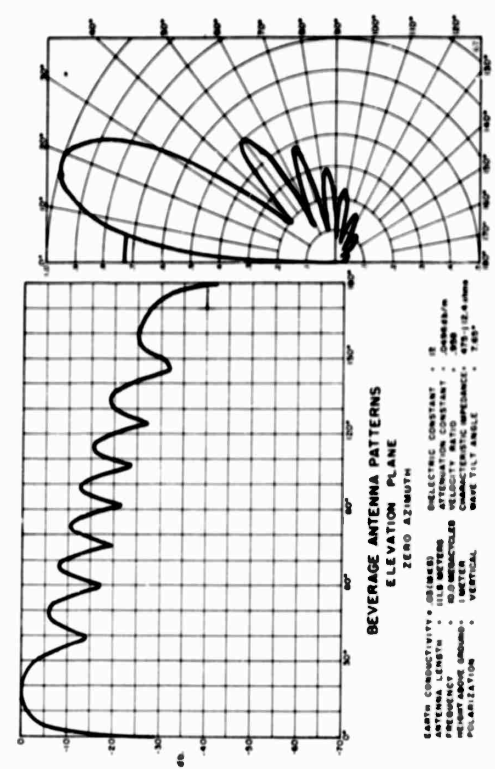


FIGURE 1-6b

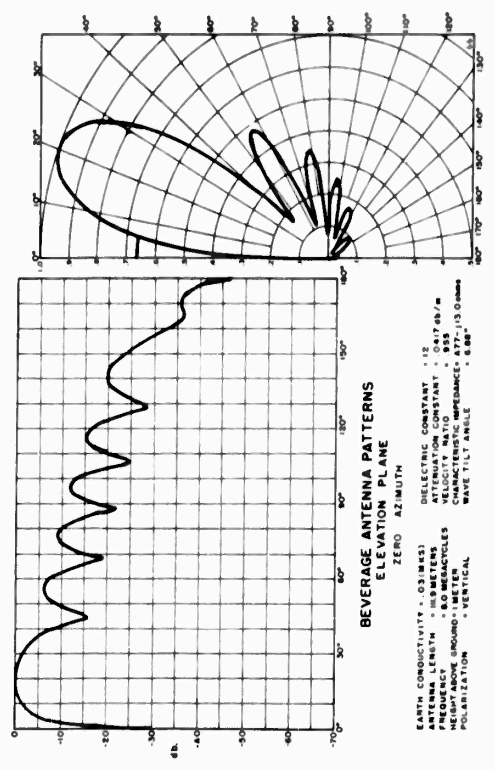


FIGURE 1-7b

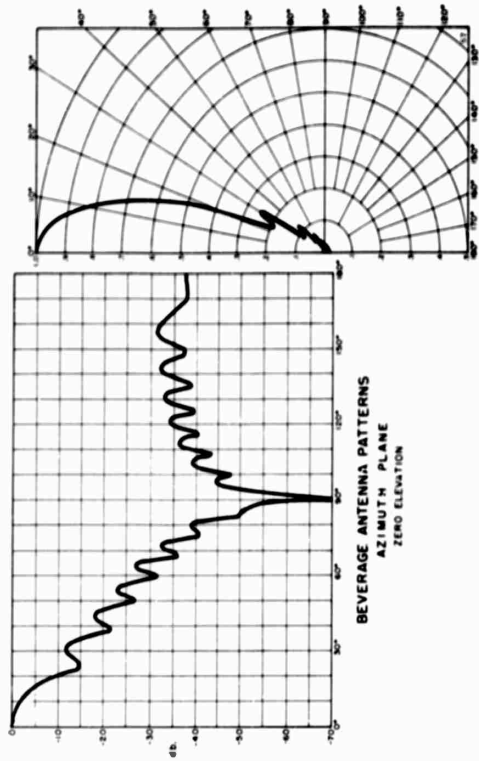


FIGURE 1-10a

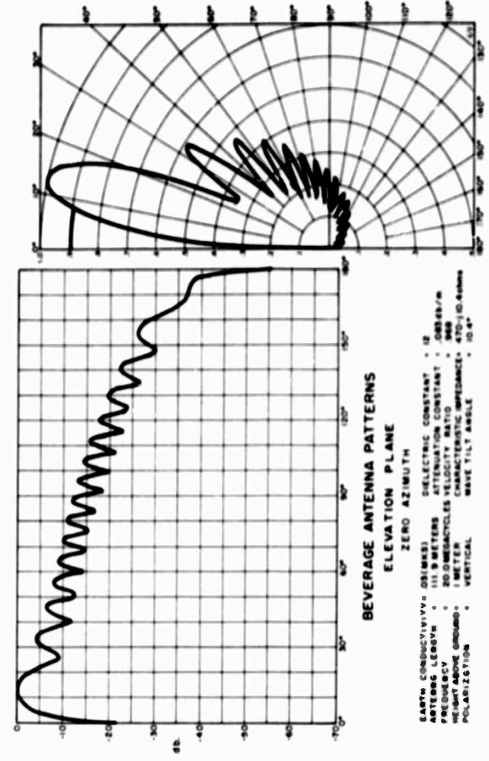


FIGURE 1-10b

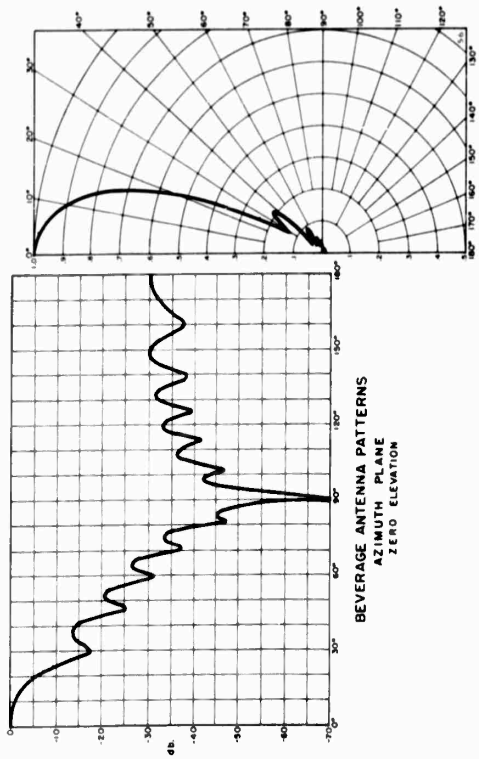


FIGURE 1-9a

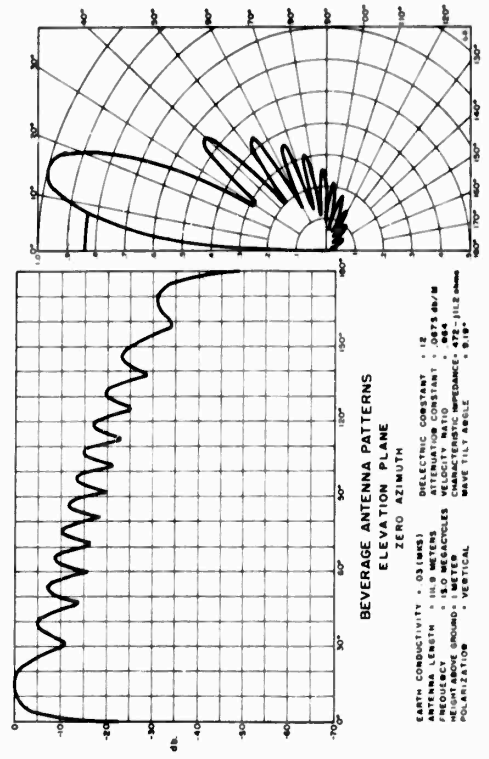


FIGURE 1-9b

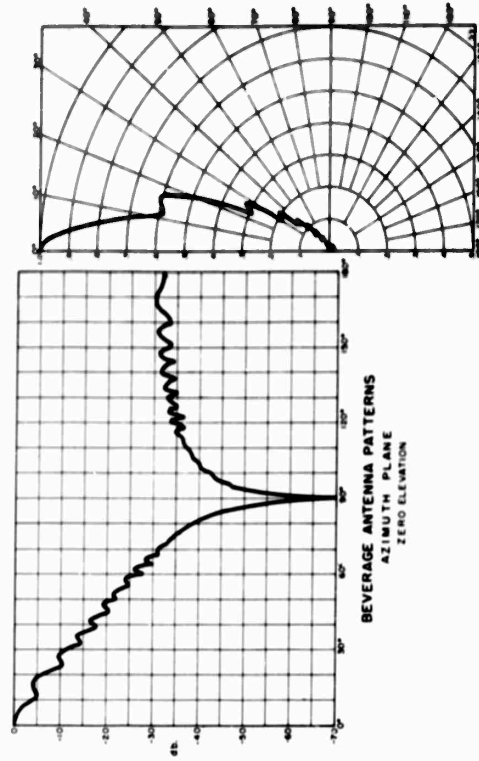


FIGURE I-114

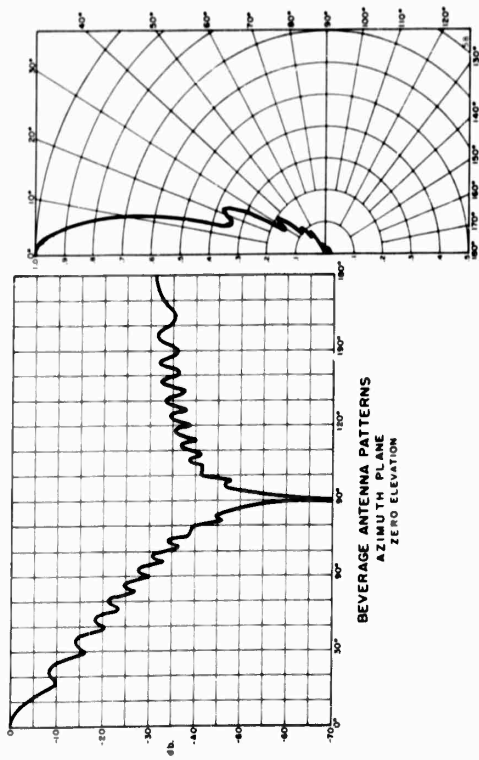


FIGURE I-115

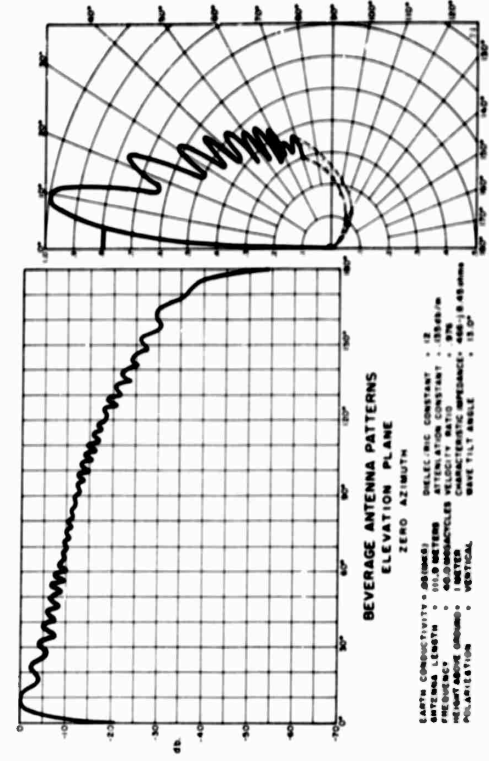


FIGURE I-116

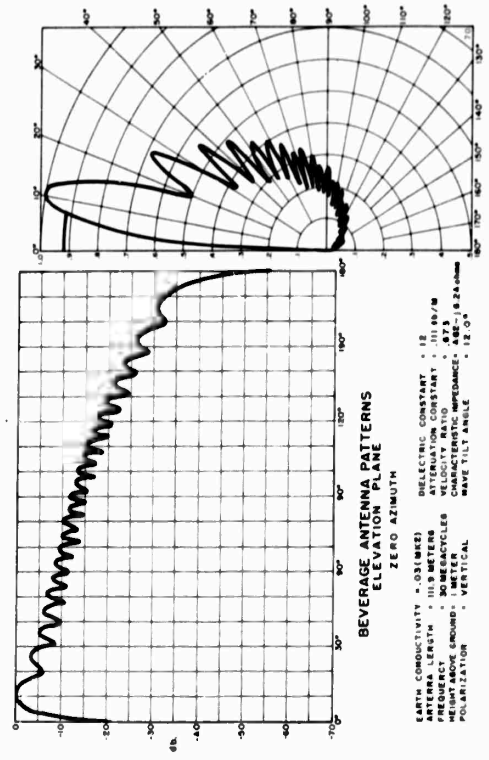


FIGURE I-117

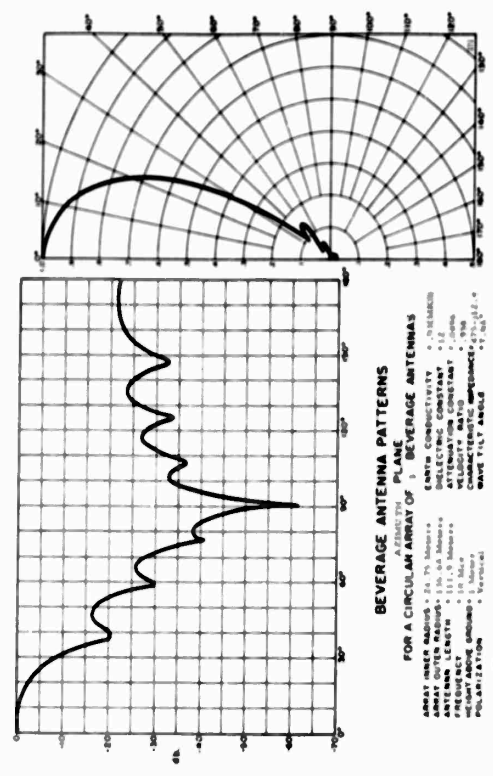


FIGURE 1-13

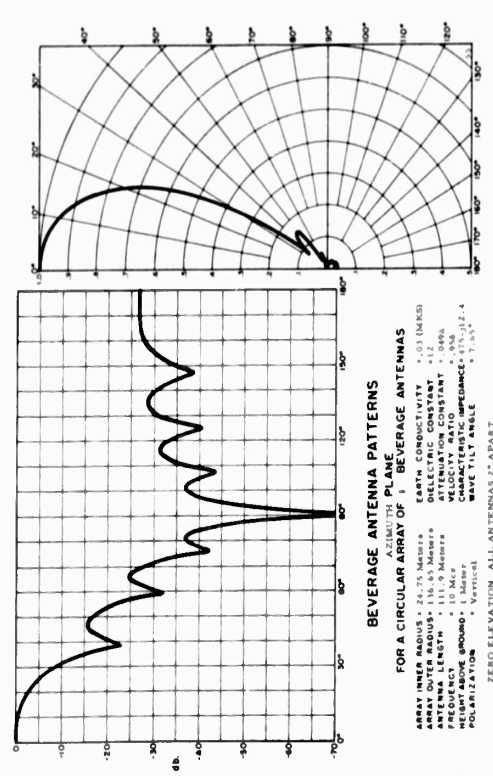


FIGURE 1-14

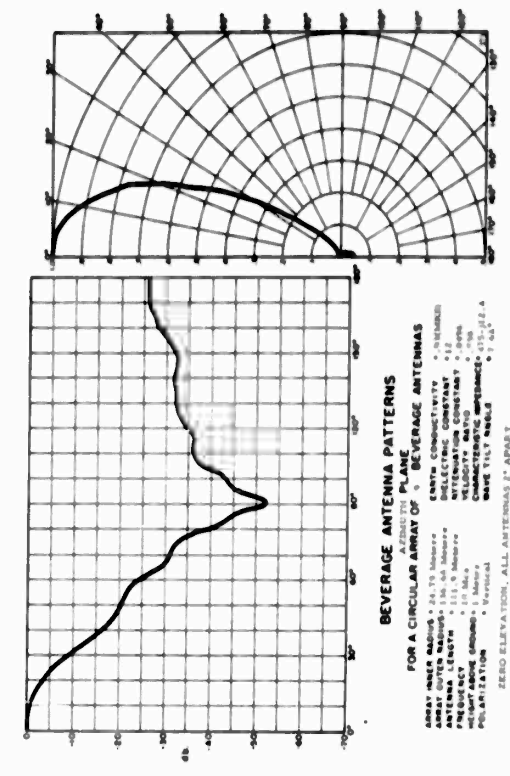


FIGURE 1-15

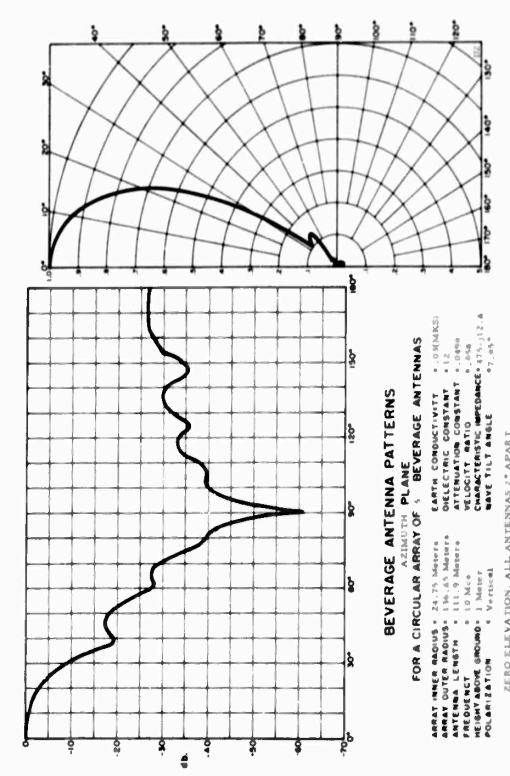


FIGURE 1-16

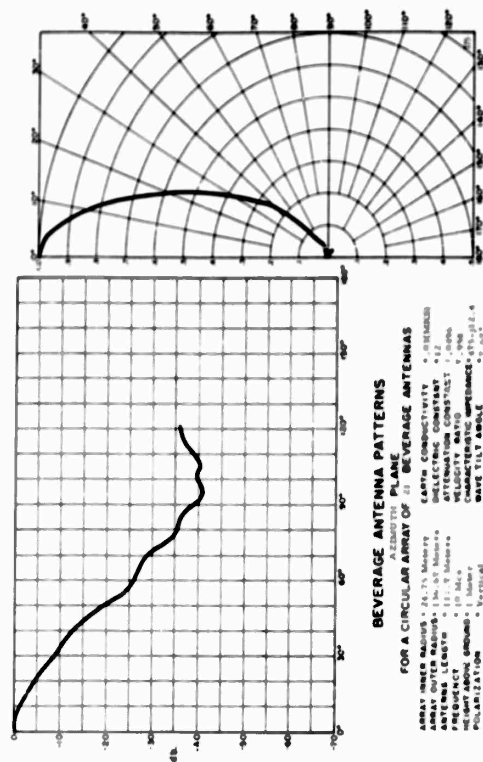


FIGURE 1-17

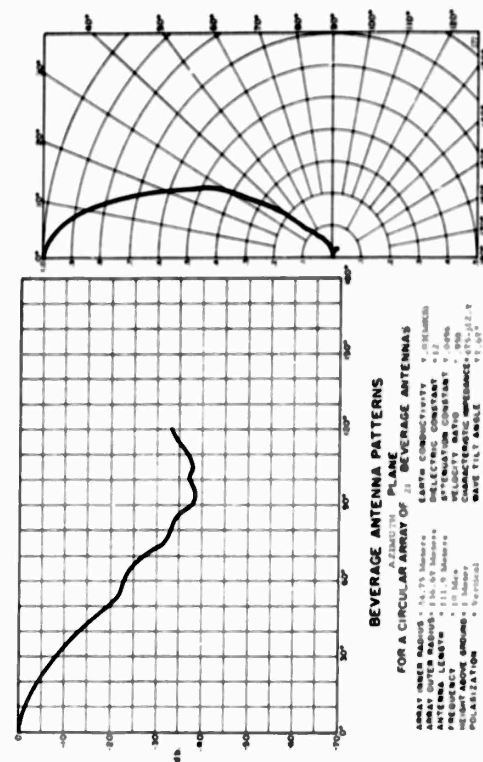


FIGURE 1-18

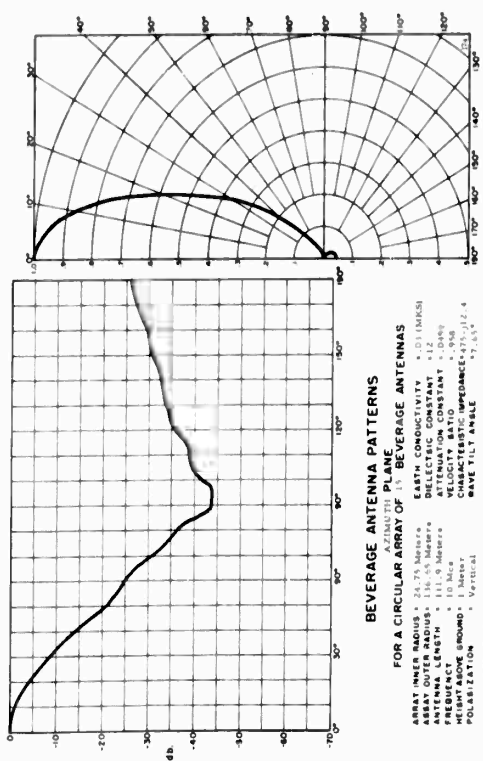


FIGURE 1-19

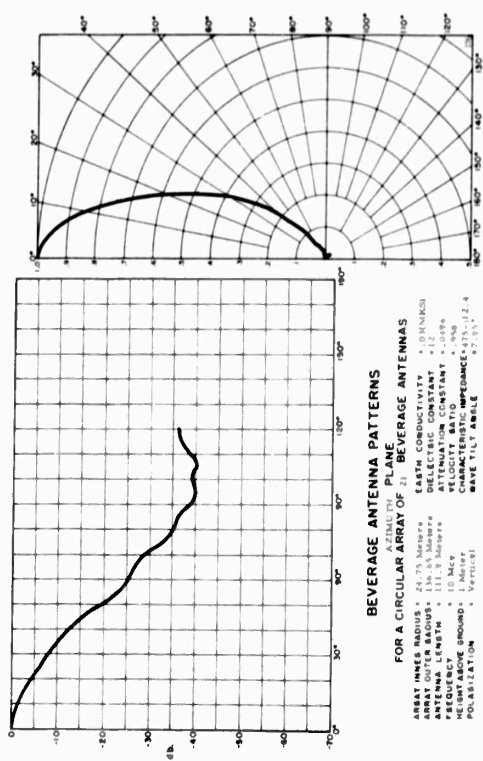


FIGURE 1-20

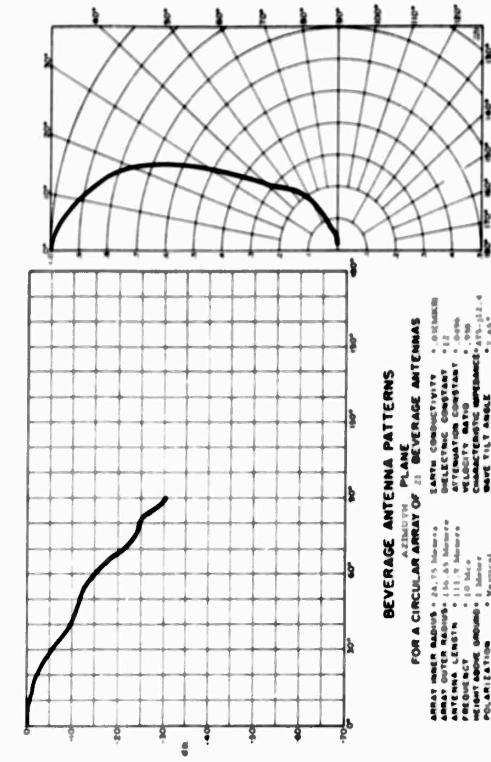


FIGURE 1-21

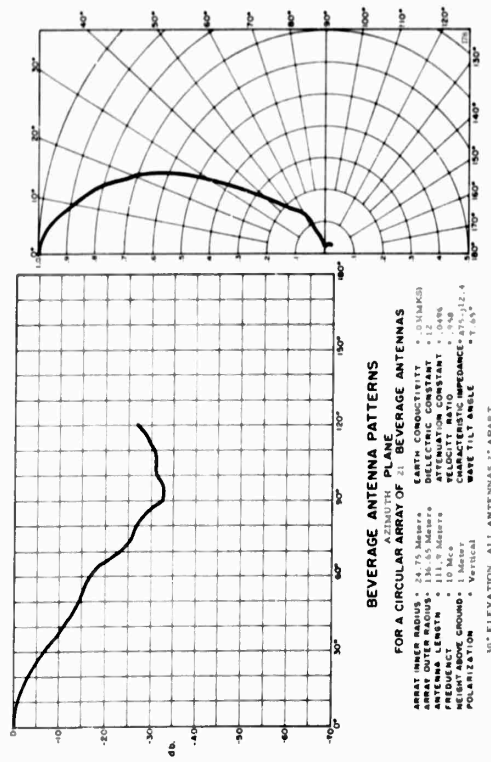


FIGURE 1-22

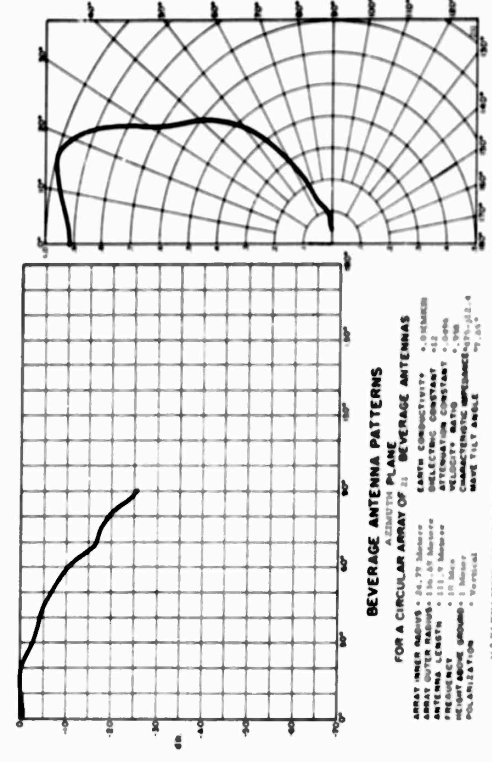


FIGURE 1-23

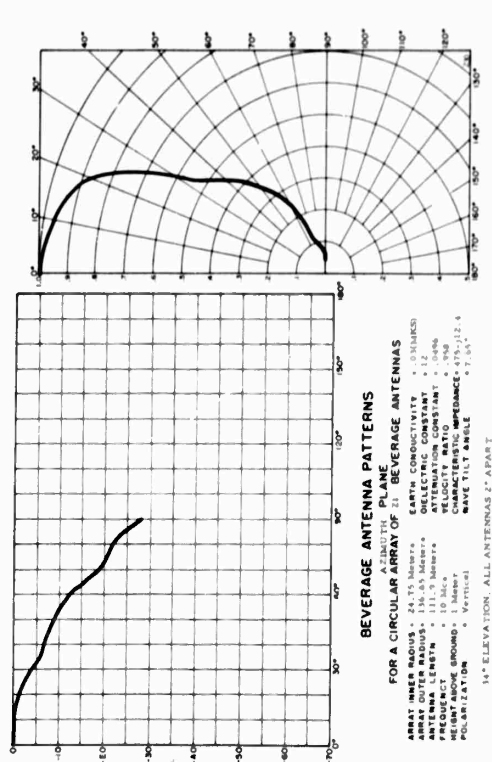


FIGURE 1-24

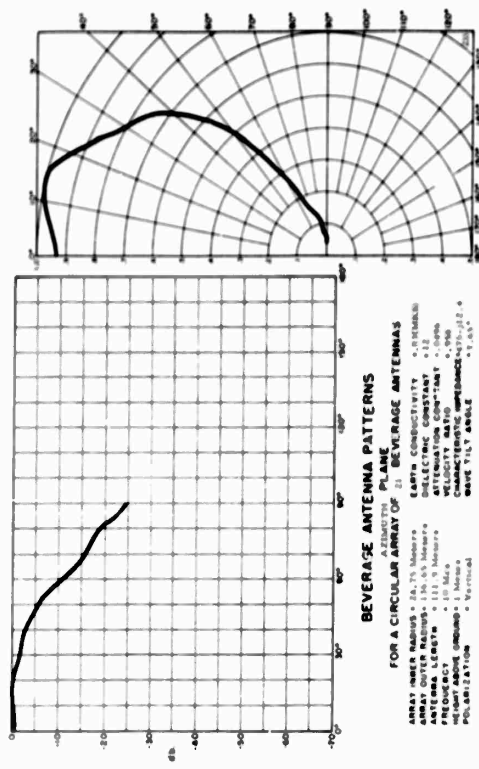


FIGURE 1-26

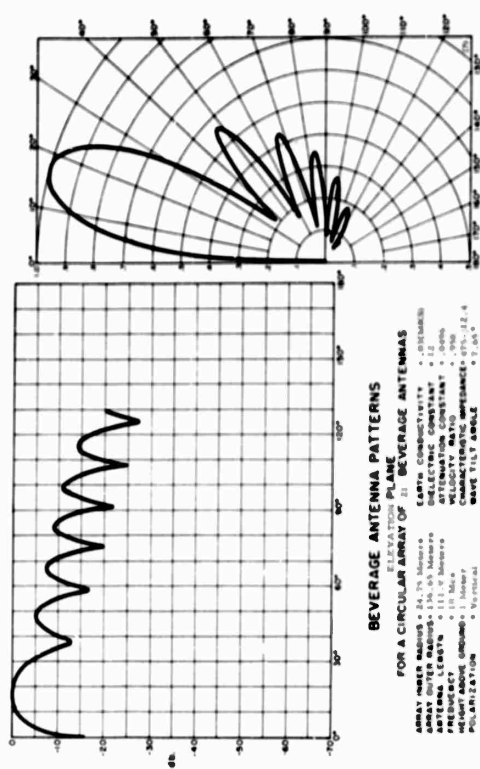


FIGURE 1-28

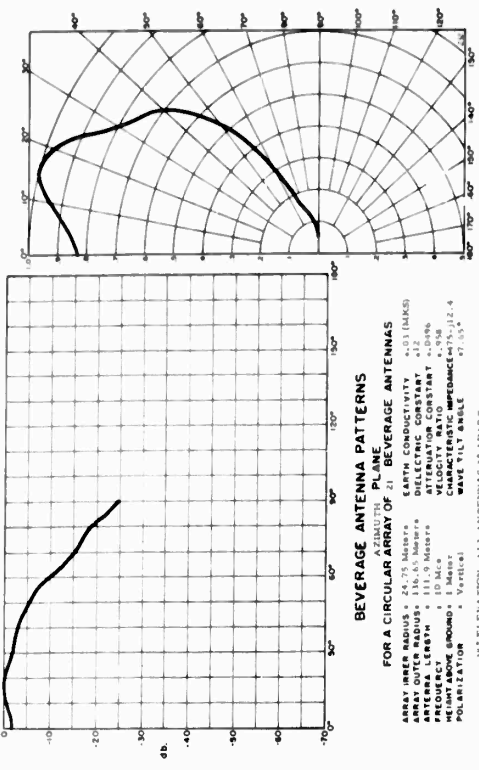


FIGURE 1-25

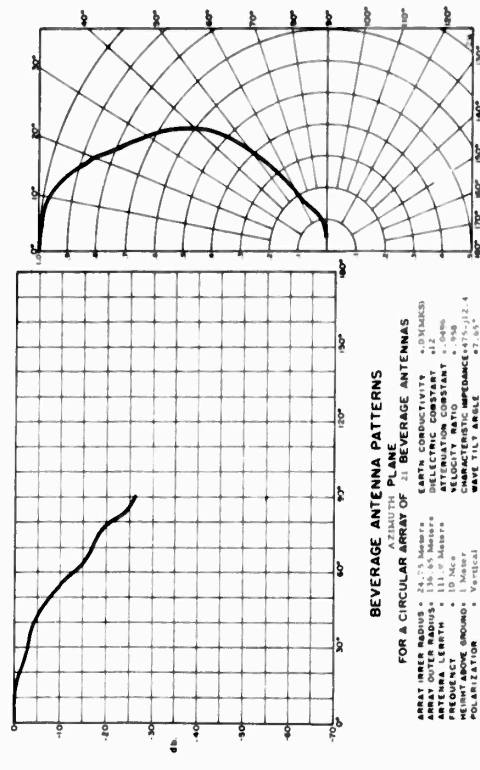
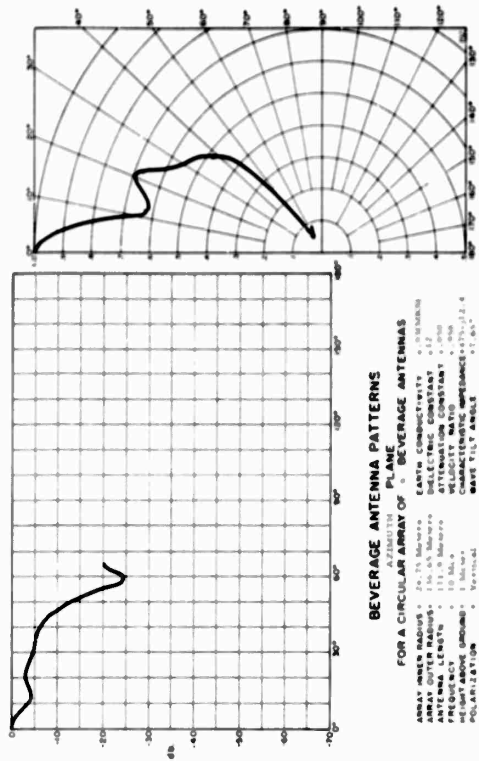


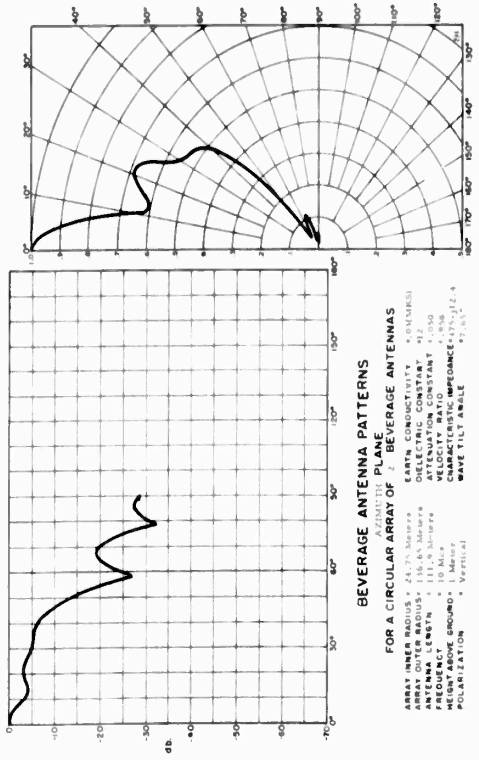
FIGURE 1-27



BEVERAGE ANTENNA PATTERNS
FOR A CIRCULAR ARRAY OF 5 BEVERAGE ANTENNAS

ARRAY INNER RADIUS = 24.75 Meters
ARRAY OUTER RADIUS = 136.45 Meters
ANTENNA LENGTH = 111.0 Meters
HEIGHT ABOVE GROUND = 1 Meter
POLARIZATION = Vertical
EARTH CONDUCTIVITY = 0.001 Mhos/m
ELECTRIC CONSTANT = 1.2
ATTENUATION CONSTANT = 0.00
VELOCITY RATIO = 0.999
CHARACTERISTIC IMPEDANCE = 473.12 Ω
WAVE TILT ANGLE = 0.85°
ELEVATION ANGLE = 10°
ANTENNAS LOCATED 115°, 120°, 122°, 127° AZIMUTH

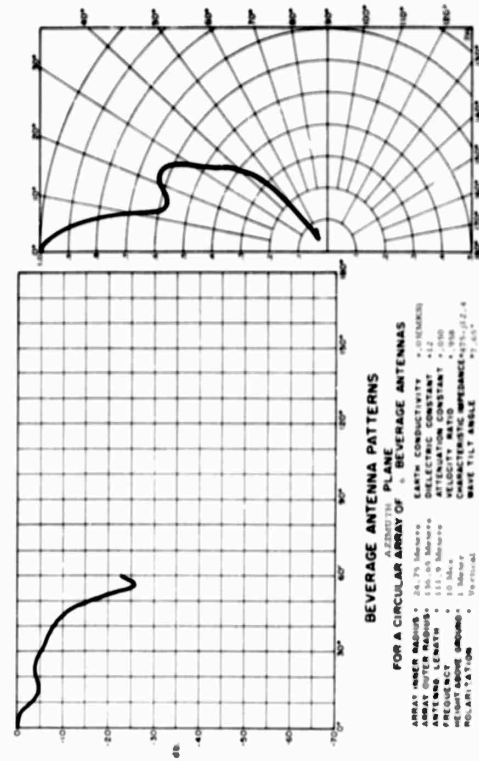
FIGURE 1-10



BEVERAGE ANTENNA PATTERNS
FOR A CIRCULAR ARRAY OF 2 BEVERAGE ANTENNAS

ARRAY INNER RADIUS = 24.75 Meters
ARRAY OUTER RADIUS = 136.45 Meters
ANTENNA LENGTH = 111.0 Meters
HEIGHT ABOVE GROUND = 1 Meter
POLARIZATION = Vertical
EARTH CONDUCTIVITY = 0.001 Mhos/m
ELECTRIC CONSTANT = 1.2
ATTENUATION CONSTANT = 0.00
VELOCITY RATIO = 0.999
CHARACTERISTIC IMPEDANCE = 473.12 Ω
WAVE TILT ANGLE = 0.85°
ELEVATION ANGLE = 10°
ANTENNAS LOCATED 115°, 120° AZIMUTH

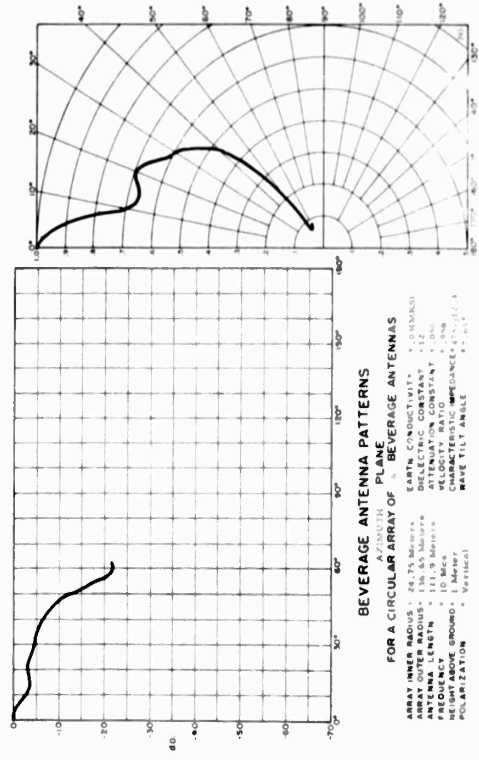
FIGURE 1-11



BEVERAGE ANTENNA PATTERNS
FOR A CIRCULAR ARRAY OF 5 BEVERAGE ANTENNAS

ARRAY INNER RADIUS = 24.75 Meters
ARRAY OUTER RADIUS = 136.45 Meters
ANTENNA LENGTH = 111.0 Meters
HEIGHT ABOVE GROUND = 1 Meter
POLARIZATION = Vertical
EARTH CONDUCTIVITY = 0.001 Mhos/m
ELECTRIC CONSTANT = 1.2
ATTENUATION CONSTANT = 0.00
VELOCITY RATIO = 0.999
CHARACTERISTIC IMPEDANCE = 473.12 Ω
WAVE TILT ANGLE = 0.85°
ELEVATION ANGLE = 10°
ANTENNAS LOCATED 115°, 118°, 120°, 127° AZIMUTH

FIGURE 1-12



BEVERAGE ANTENNA PATTERNS
FOR A CIRCULAR ARRAY OF 2 BEVERAGE ANTENNAS

ARRAY INNER RADIUS = 24.75 Meters
ARRAY OUTER RADIUS = 136.45 Meters
ANTENNA LENGTH = 111.0 Meters
HEIGHT ABOVE GROUND = 1 Meter
POLARIZATION = Vertical
EARTH CONDUCTIVITY = 0.001 Mhos/m
ELECTRIC CONSTANT = 1.2
ATTENUATION CONSTANT = 0.00
VELOCITY RATIO = 0.999
CHARACTERISTIC IMPEDANCE = 473.12 Ω
WAVE TILT ANGLE = 0.85°
ELEVATION ANGLE = 10°
ANTENNAS LOCATED 115°, 118°, 120°, 127° AZIMUTH

FIGURE 1-13

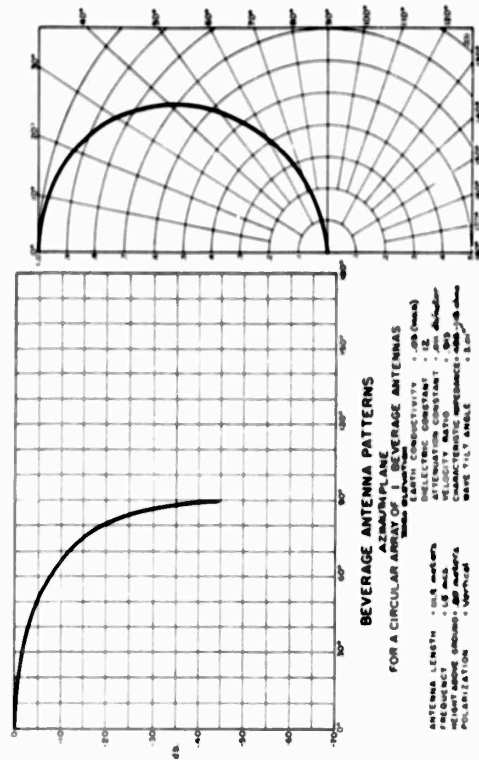


FIGURE 1-11

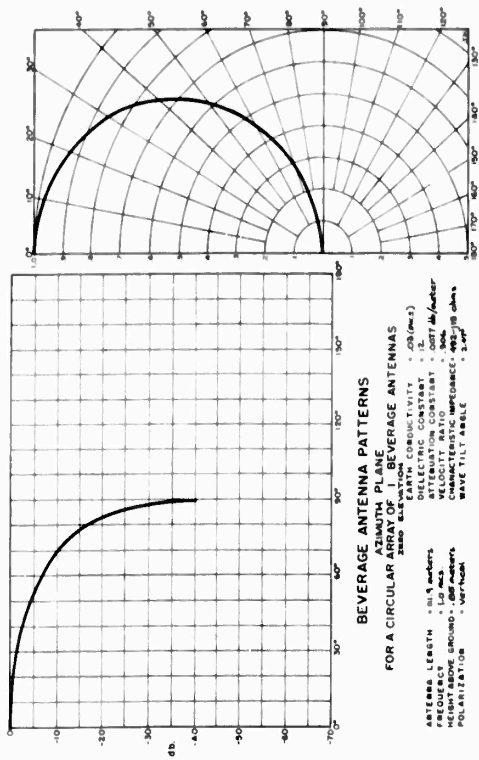


FIGURE 1-12

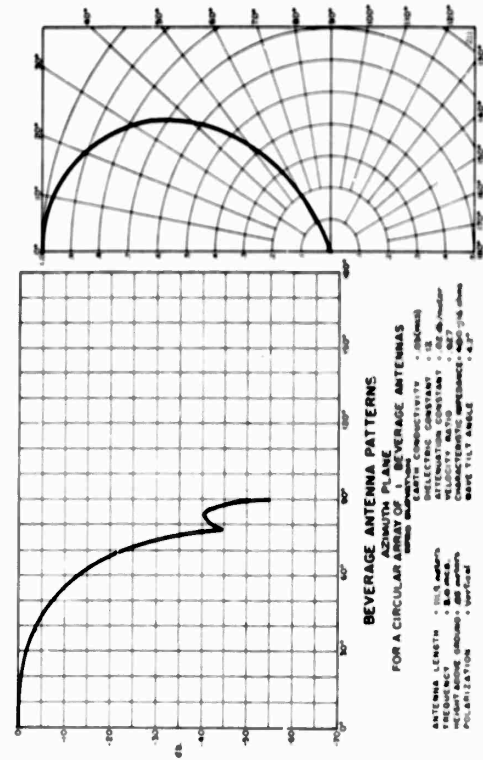


FIGURE 1-13

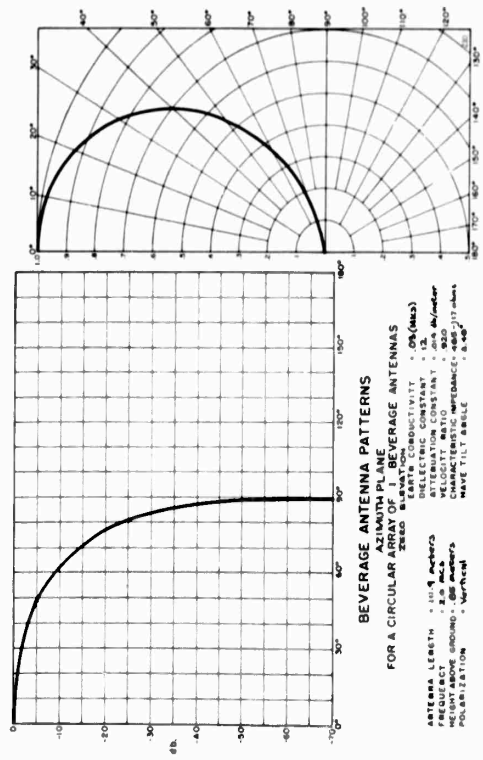


FIGURE 1-14

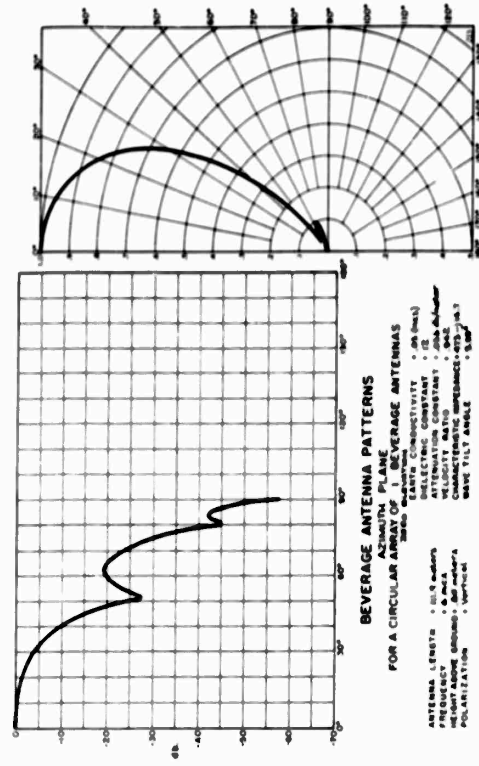


FIGURE 1-37

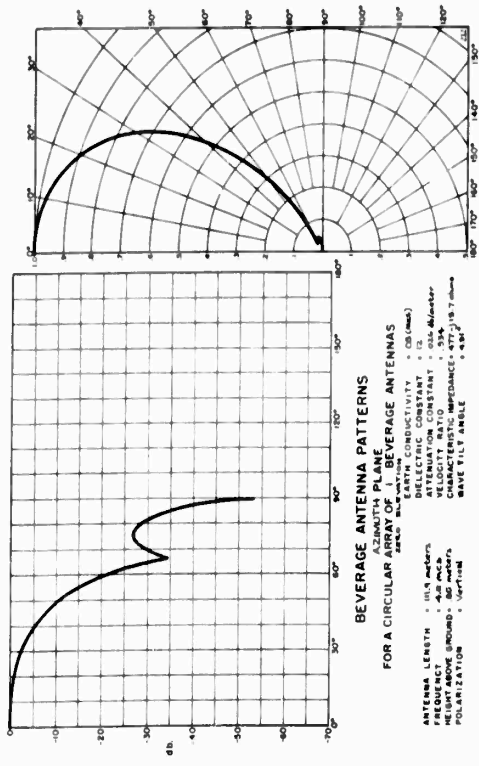


FIGURE 1-38

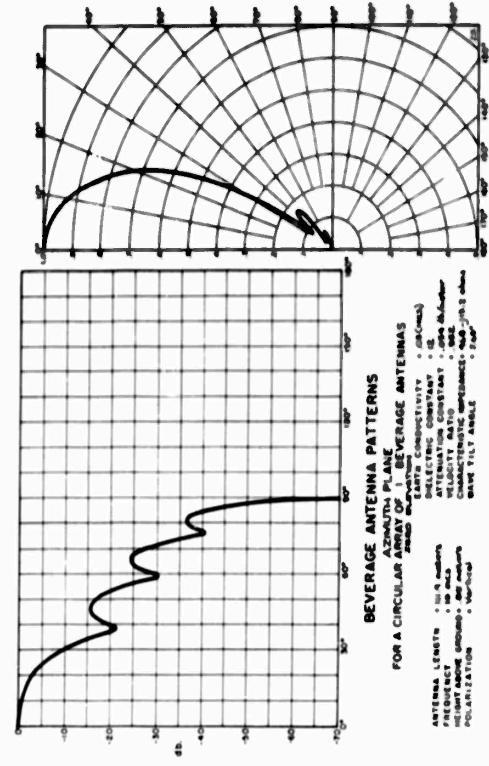


FIGURE 1-39

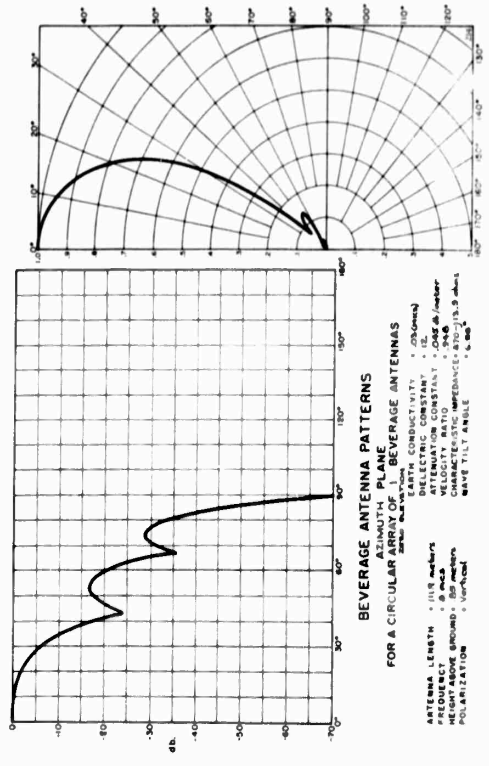


FIGURE 1-40

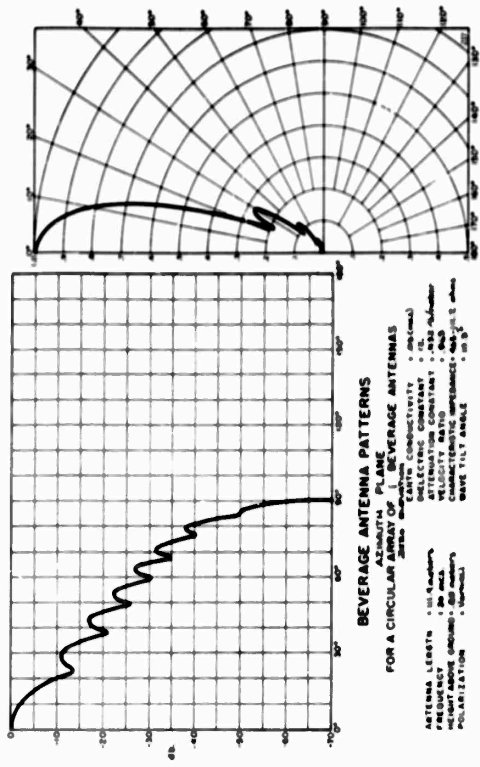


FIGURE 1-41

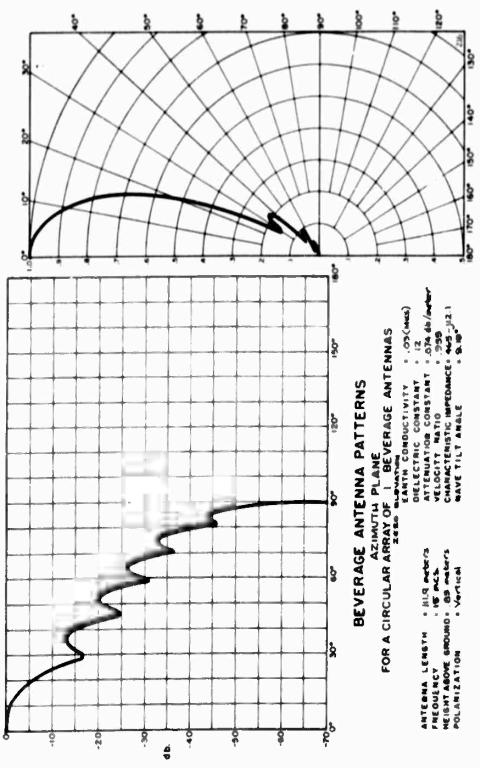


FIGURE 1-42

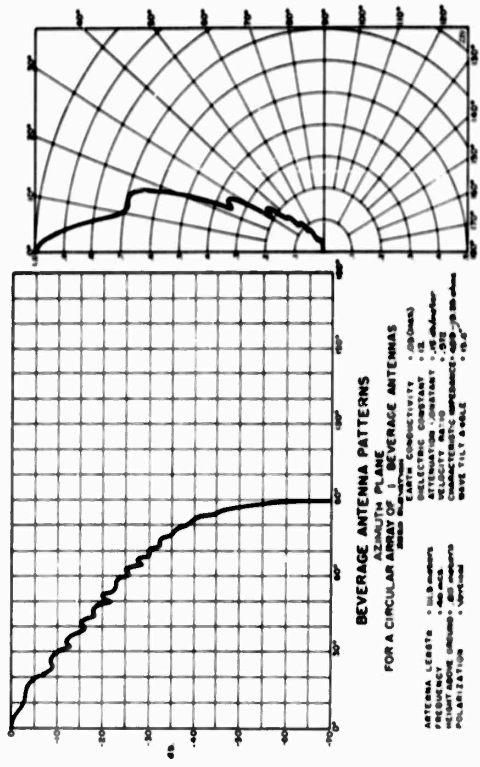


FIGURE 1-43

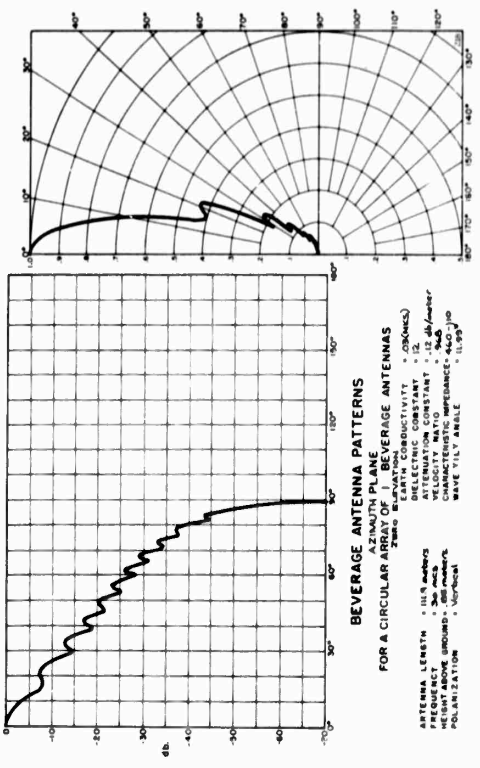


FIGURE 1-44

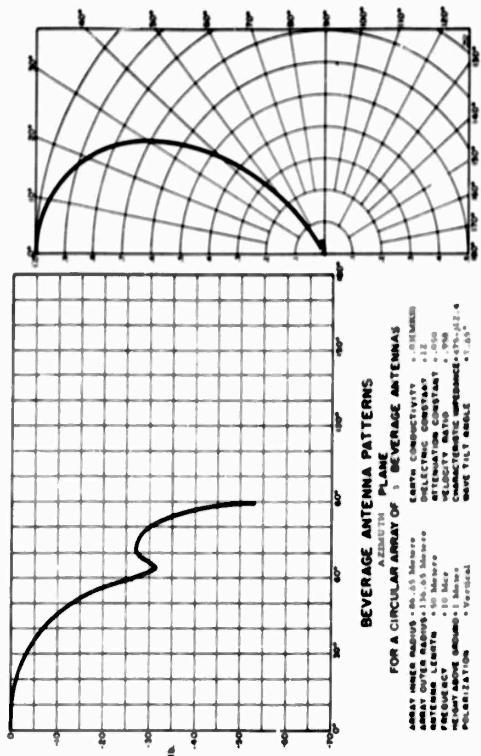


FIGURE 1-46

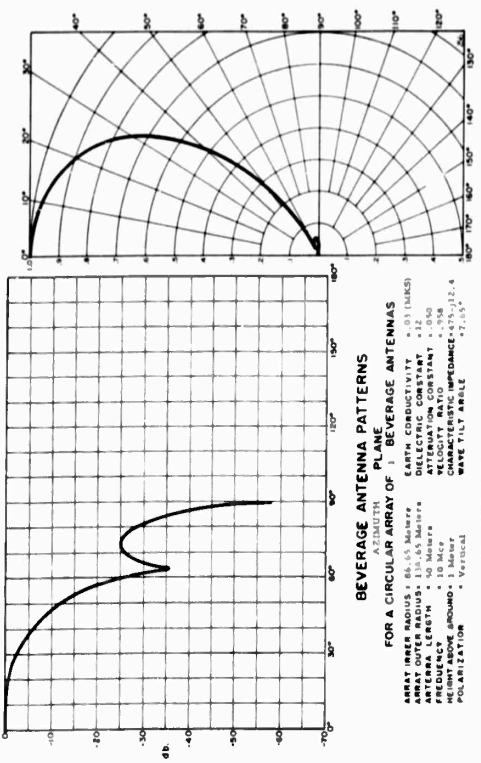


FIGURE 1-45

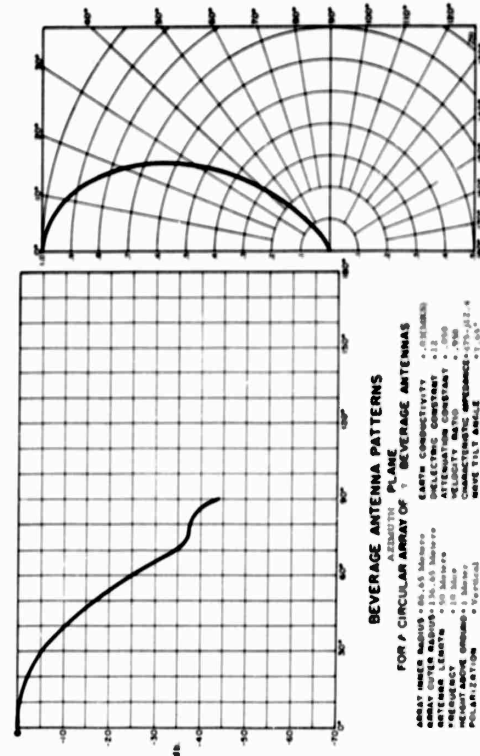


FIGURE 1-48

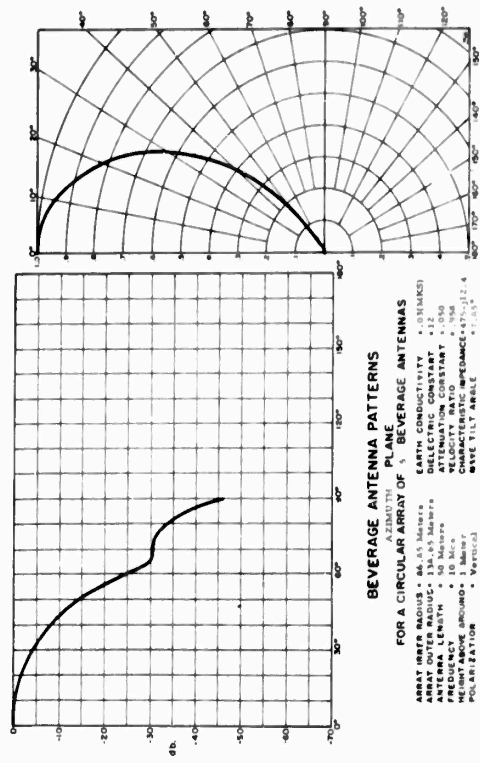


FIGURE 1-47

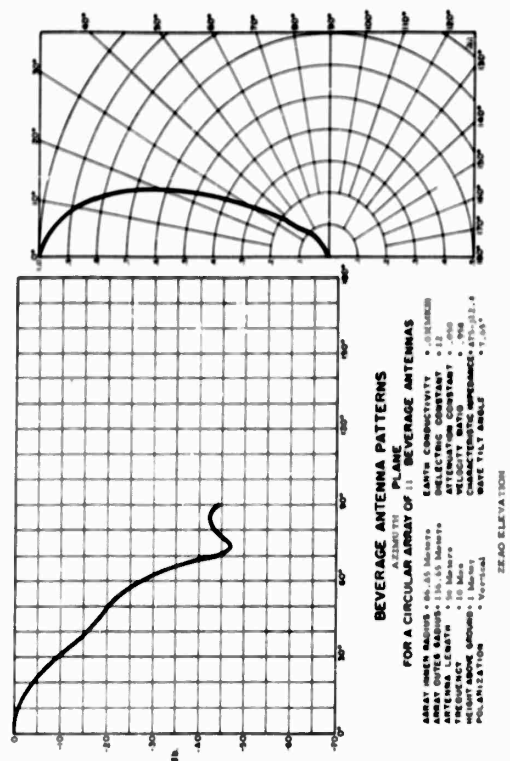


FIGURE 1-49

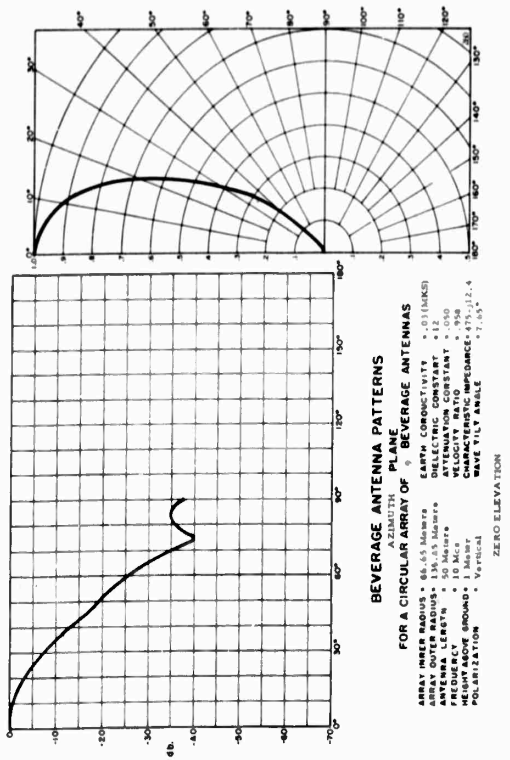


FIGURE 1-50

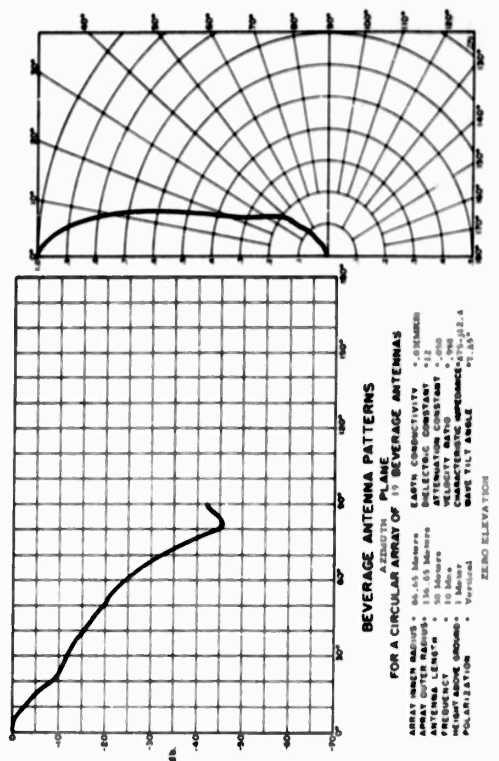


FIGURE 1-51

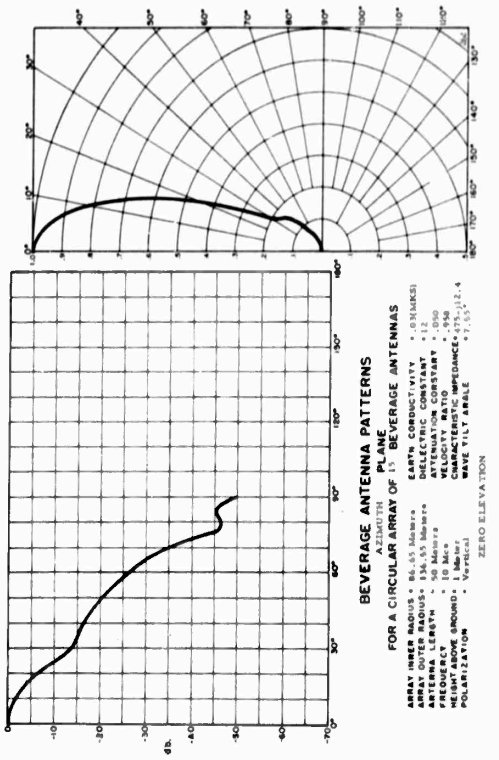


FIGURE 1-52

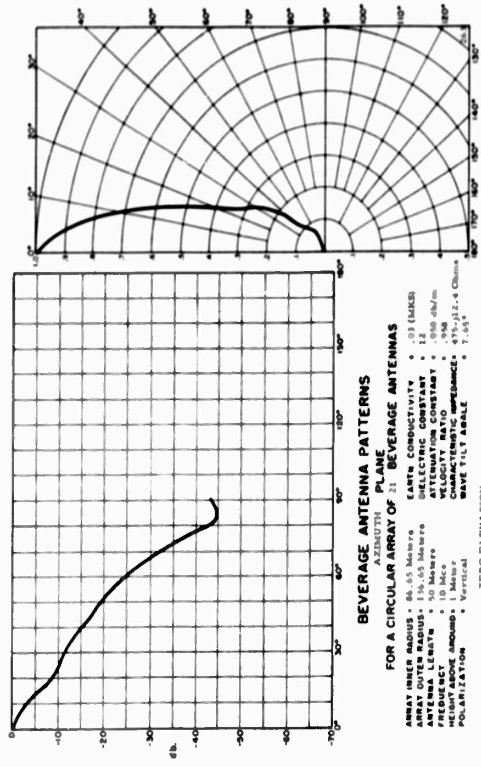


FIGURE 1-53

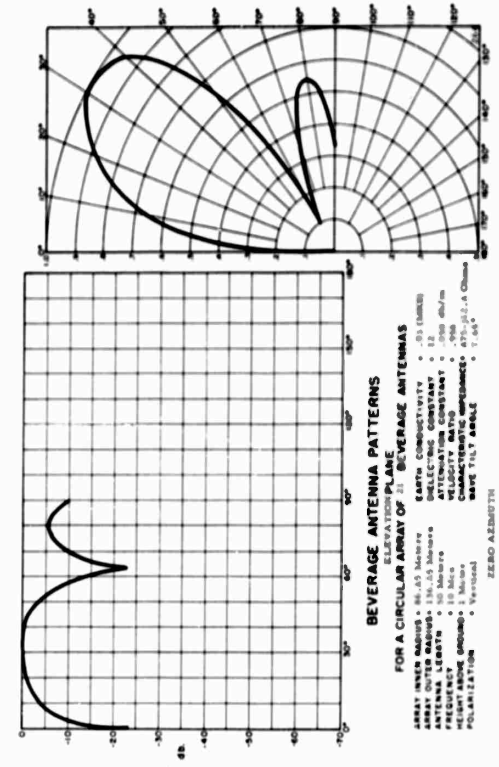


FIGURE 1-54

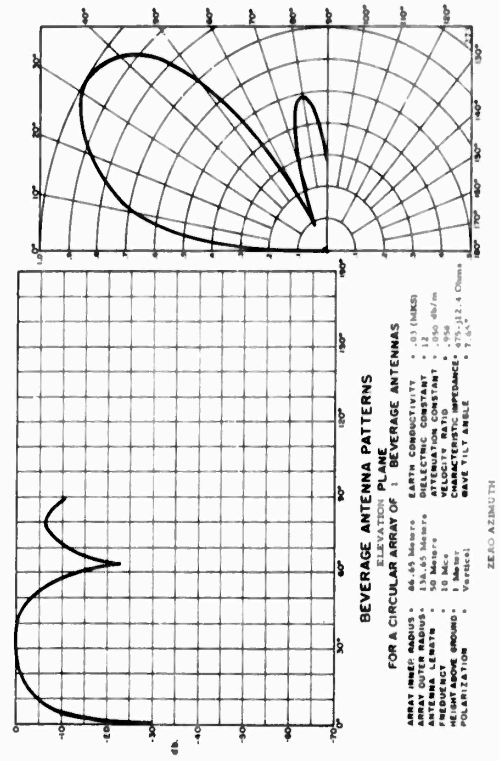


FIGURE 1-55

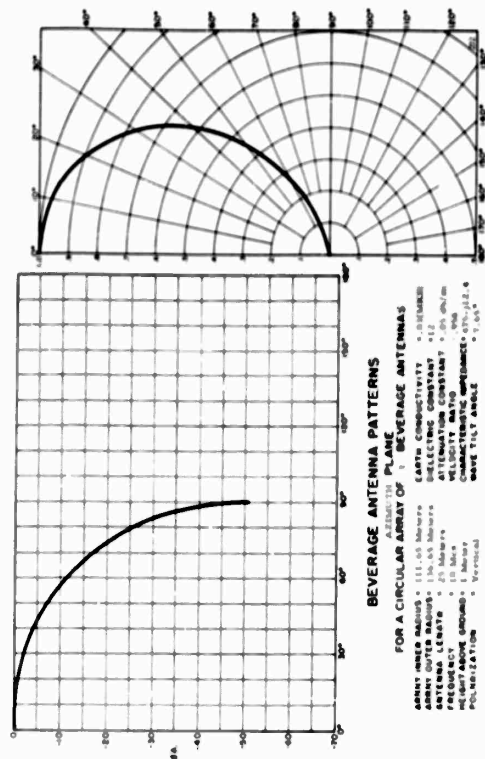


FIGURE 1-87

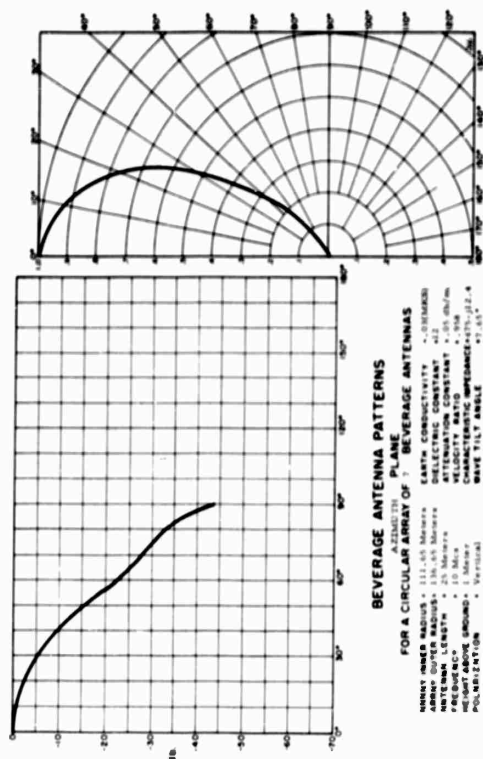


FIGURE 1-88

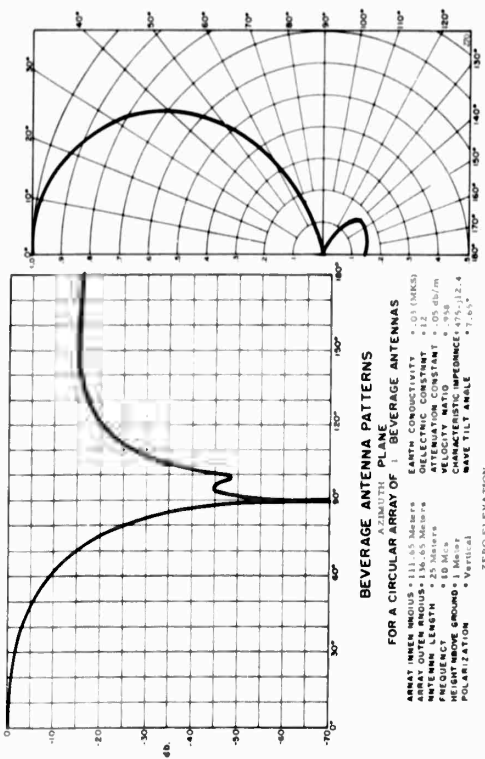


FIGURE 1-89

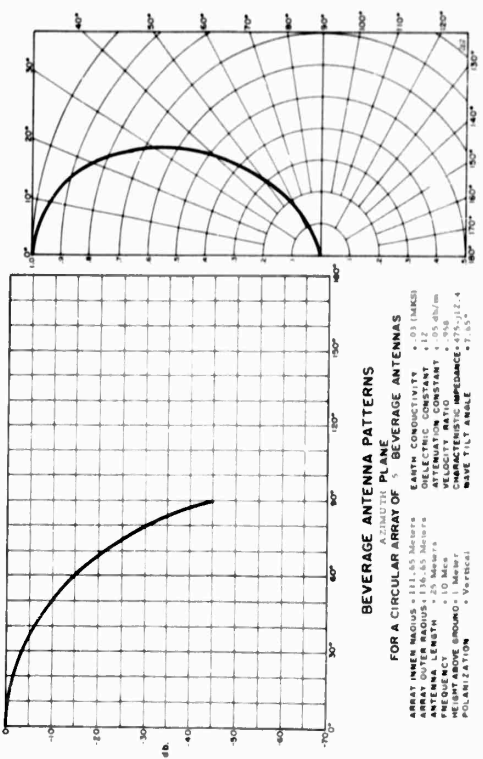


FIGURE 1-90

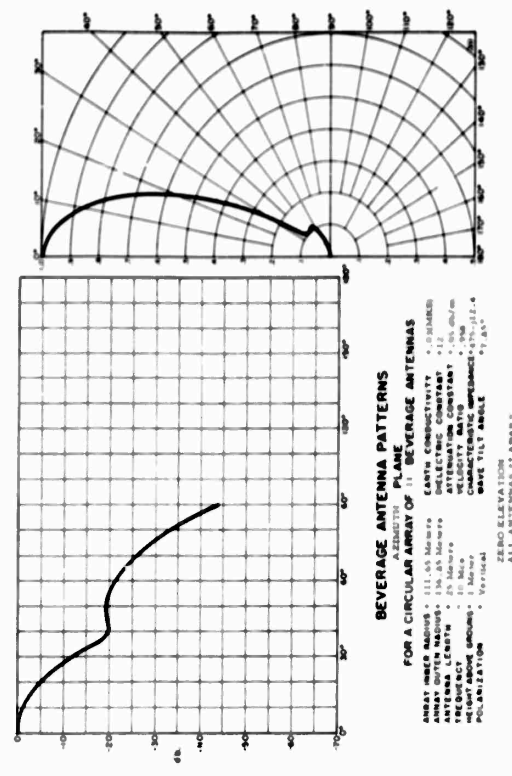


FIGURE 1-40

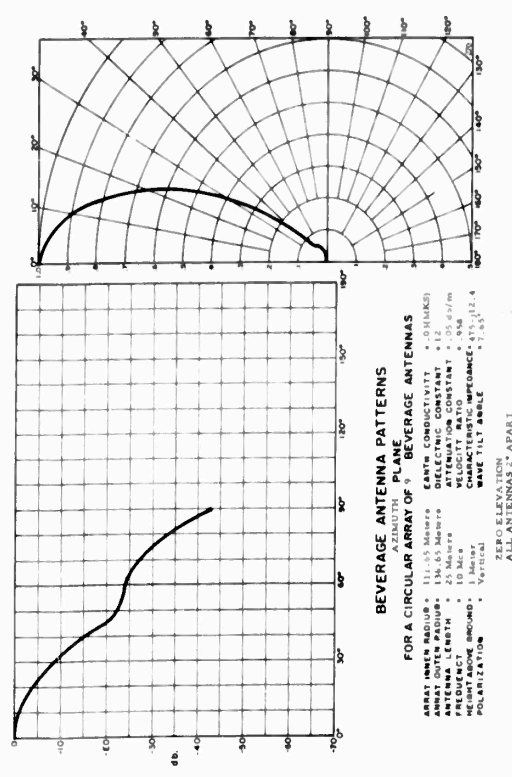


FIGURE 1-41

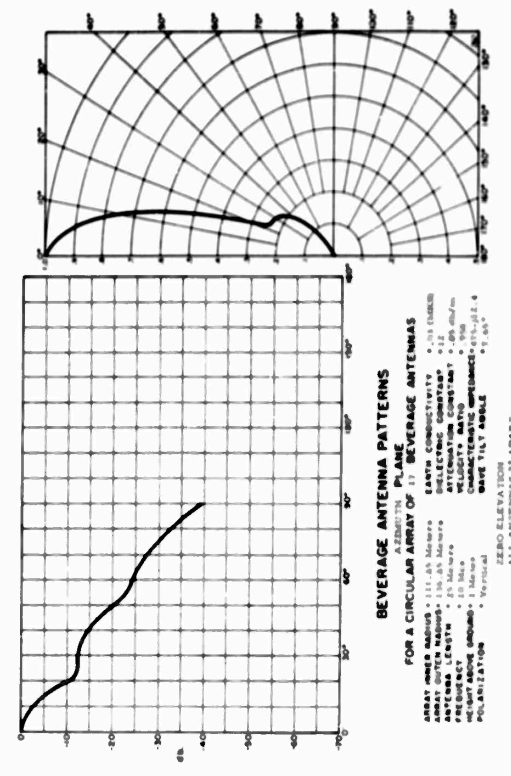


FIGURE 1-42

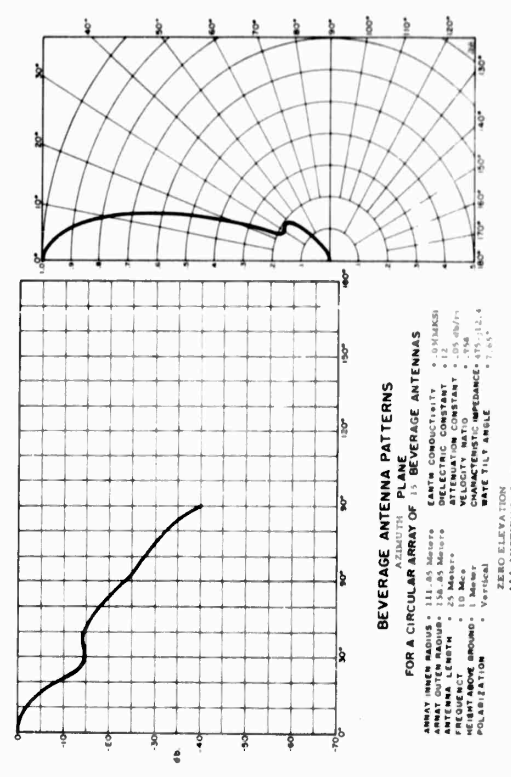


FIGURE 1-43

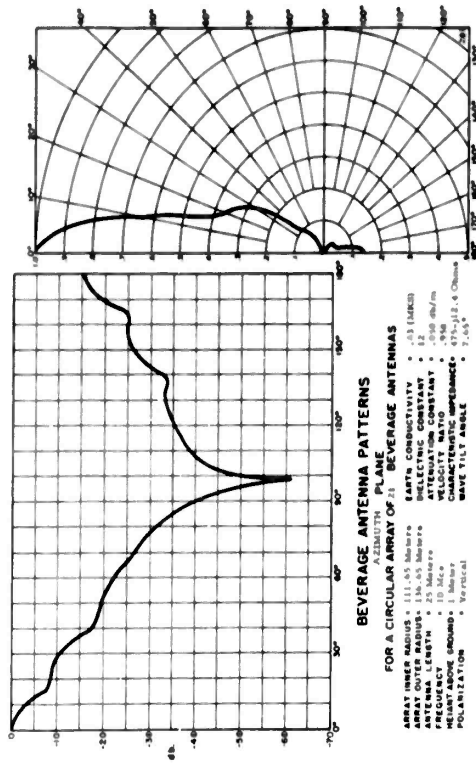


FIGURE 1-44

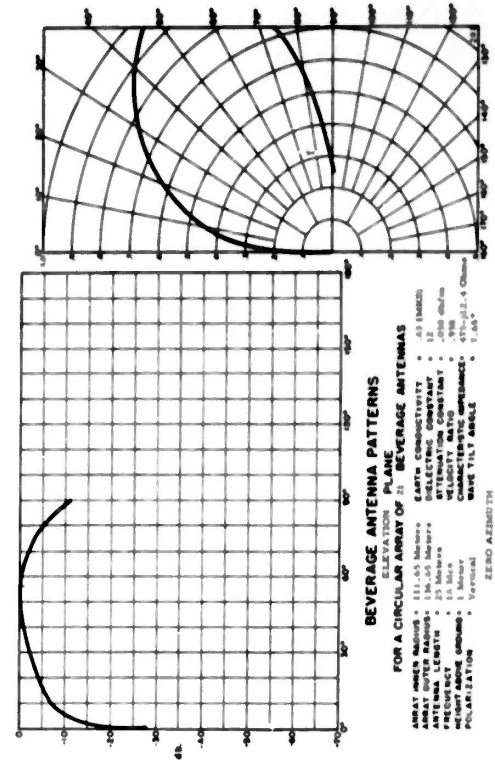


FIGURE 1-45

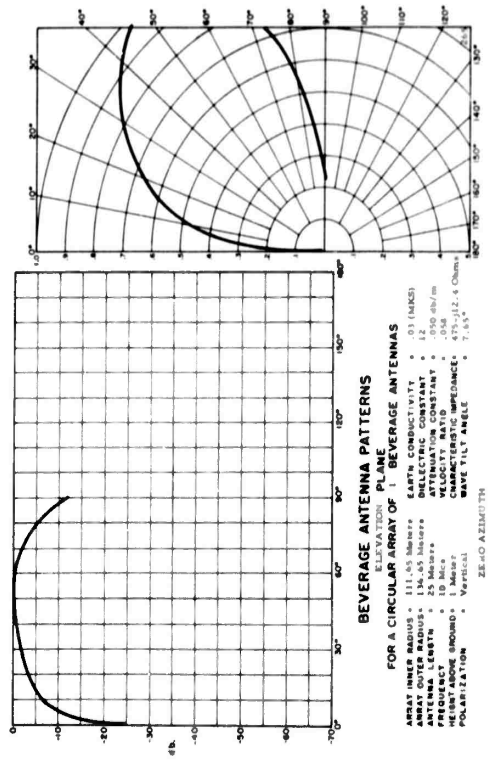


FIGURE 1-46

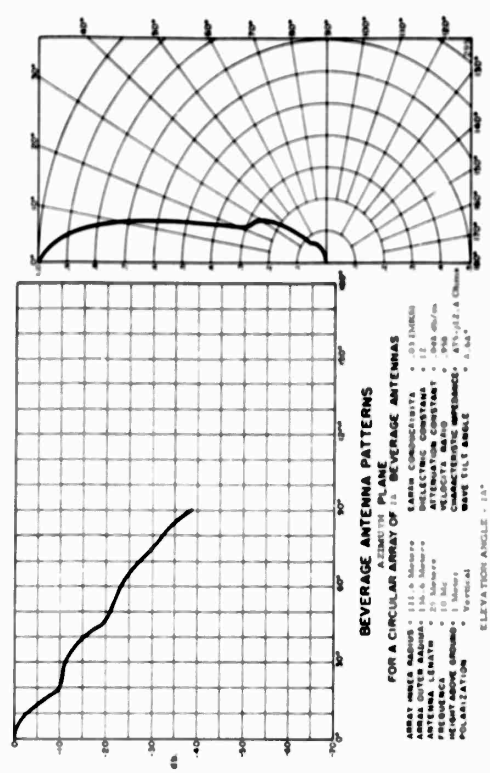


FIGURE 1-16

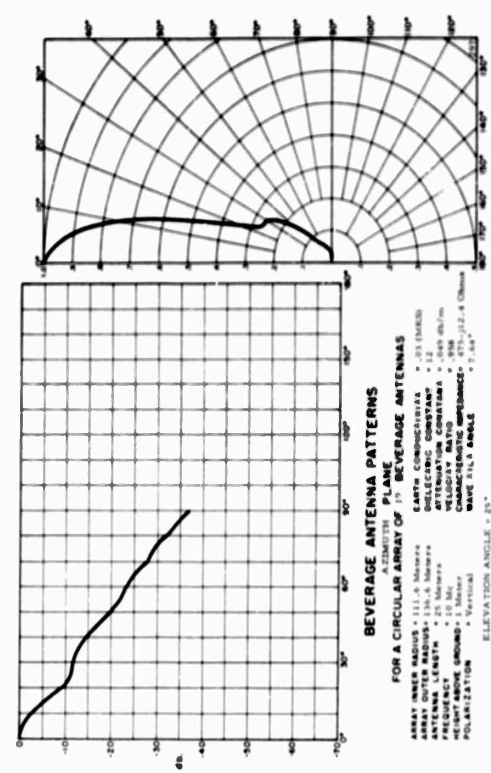


FIGURE 1-17

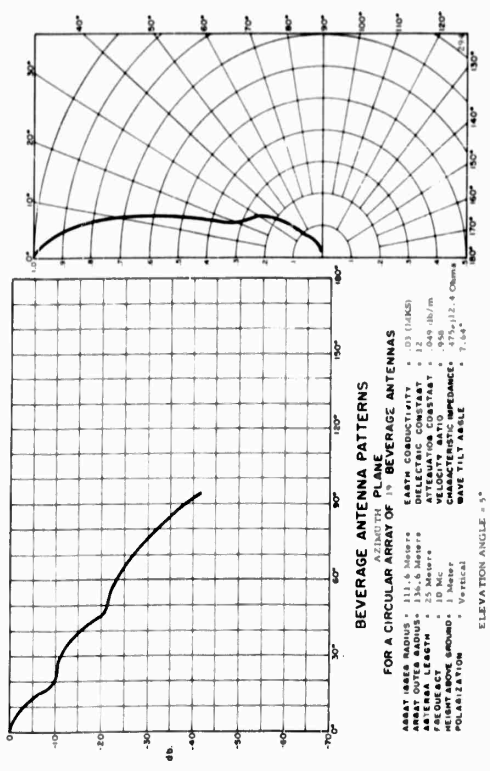


FIGURE 1-18

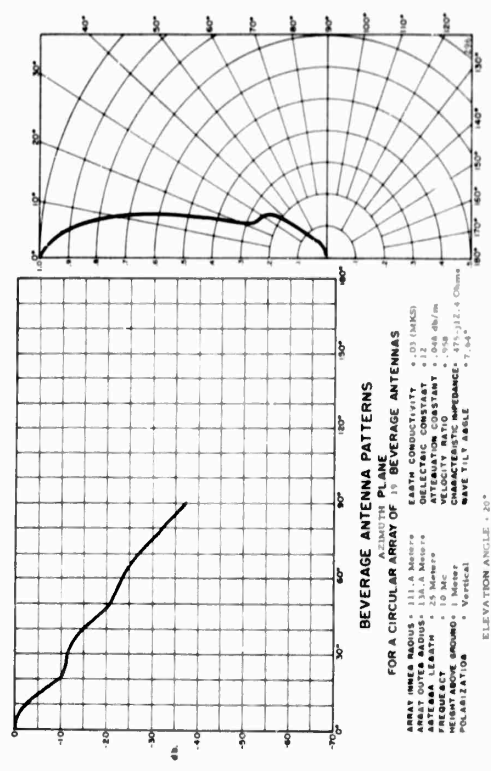


FIGURE 1-19

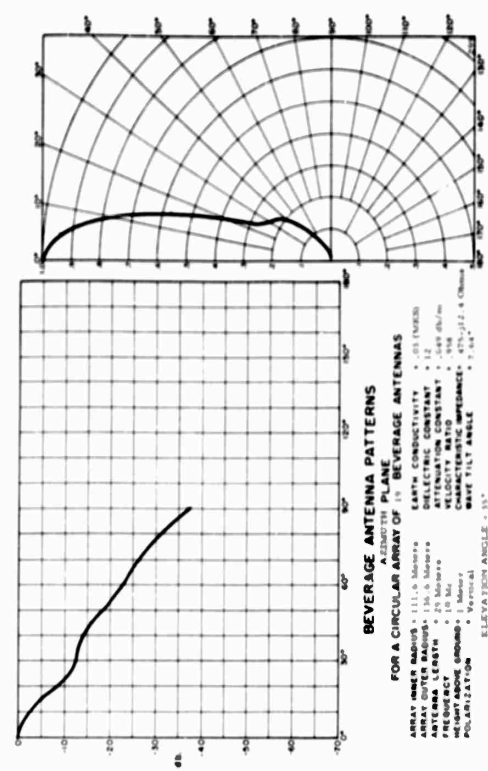


FIGURE 1-72

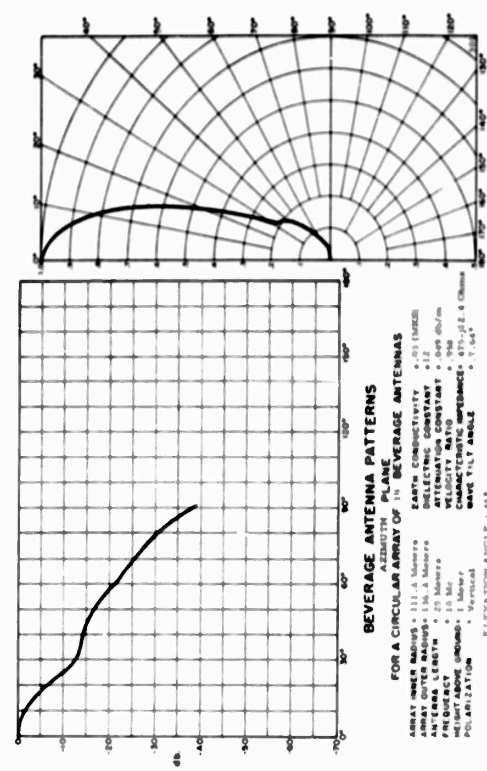


FIGURE 1-74

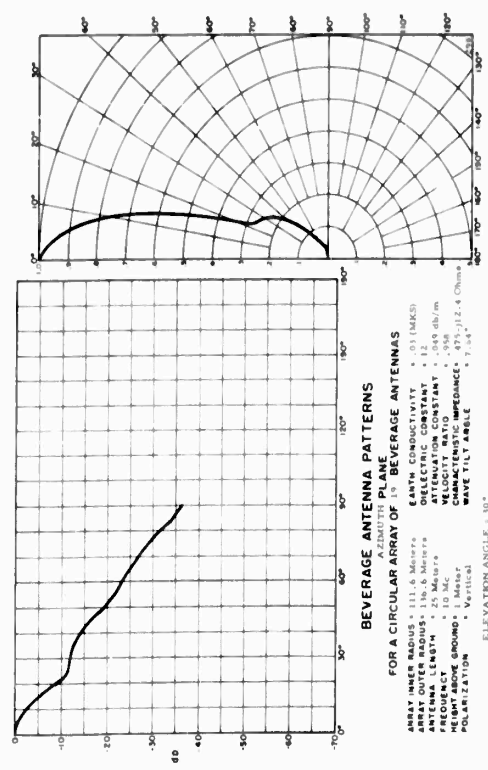


FIGURE 1-73

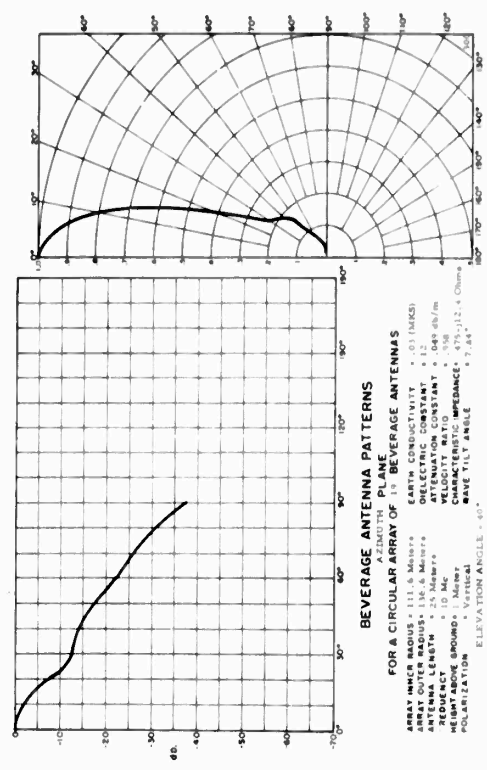


FIGURE 1-71

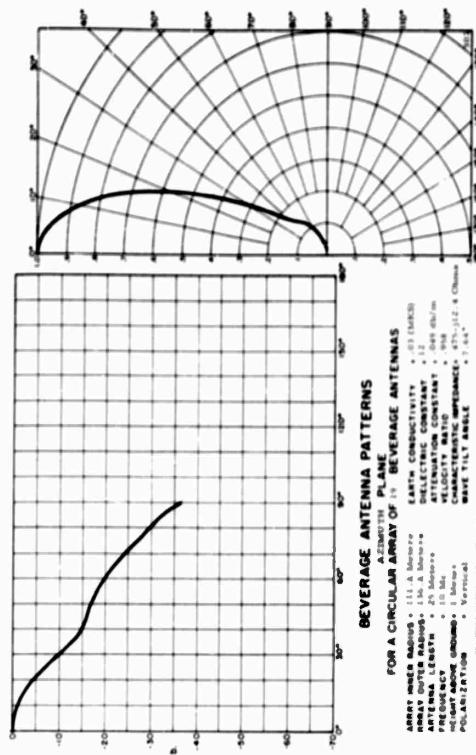


FIGURE 1-75

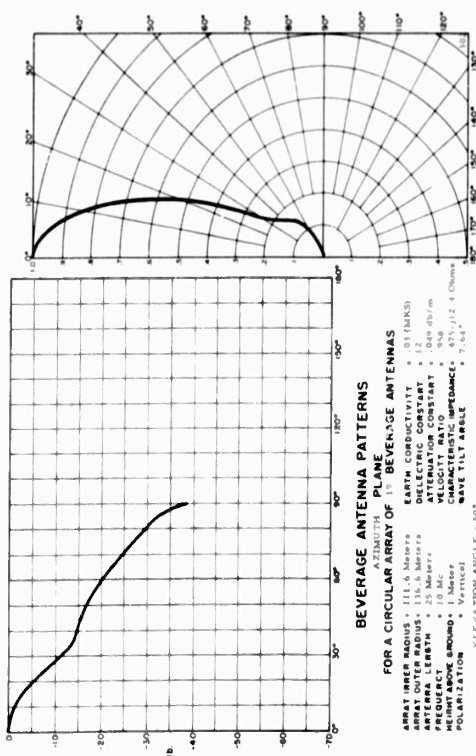


FIGURE 1-76

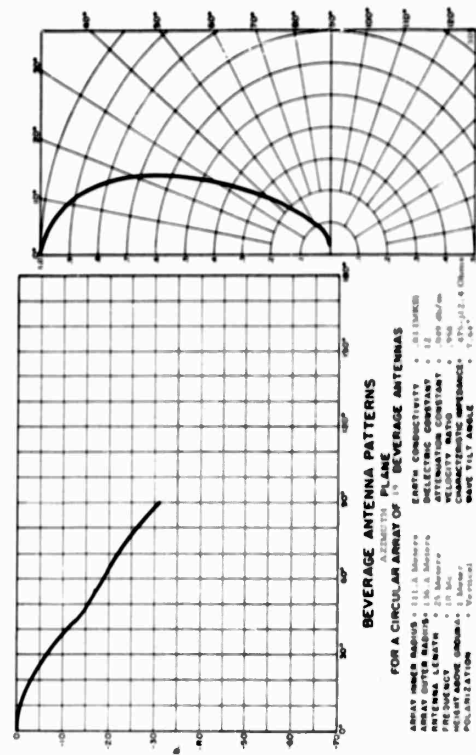


FIGURE 1-77

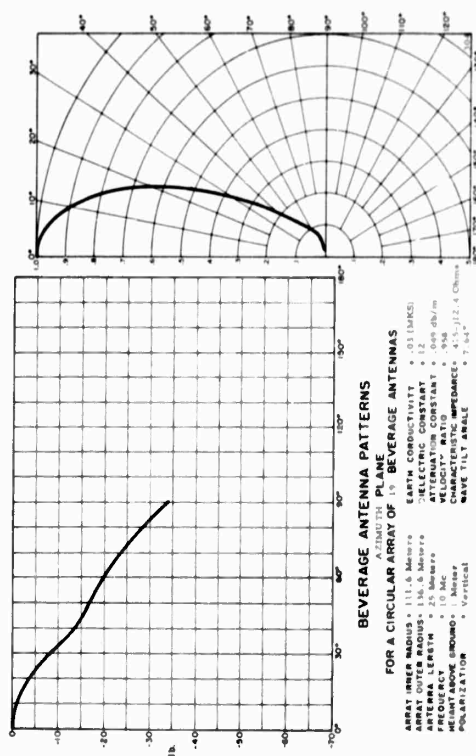


FIGURE 1-78

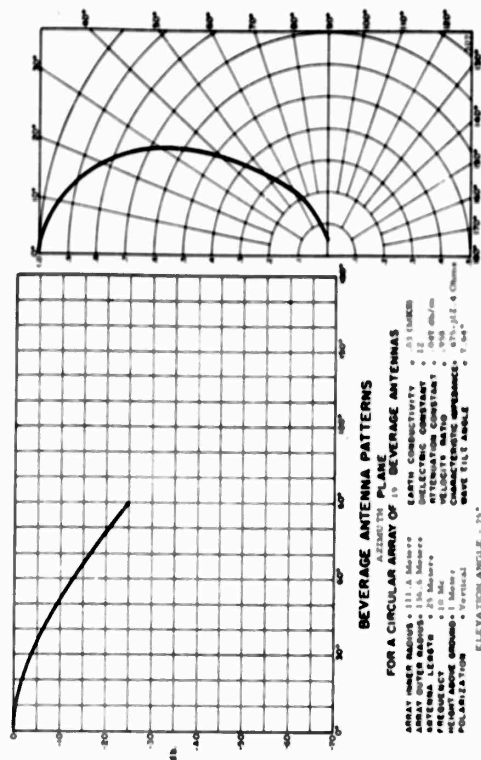


FIGURE 1-79

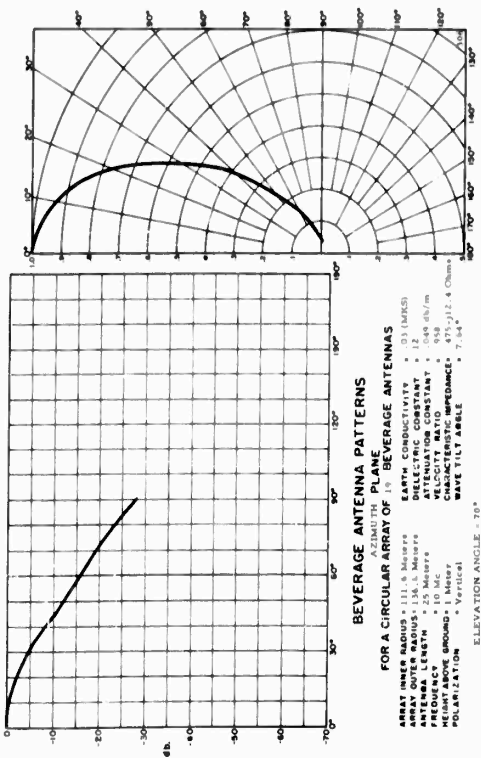


FIGURE 1-80

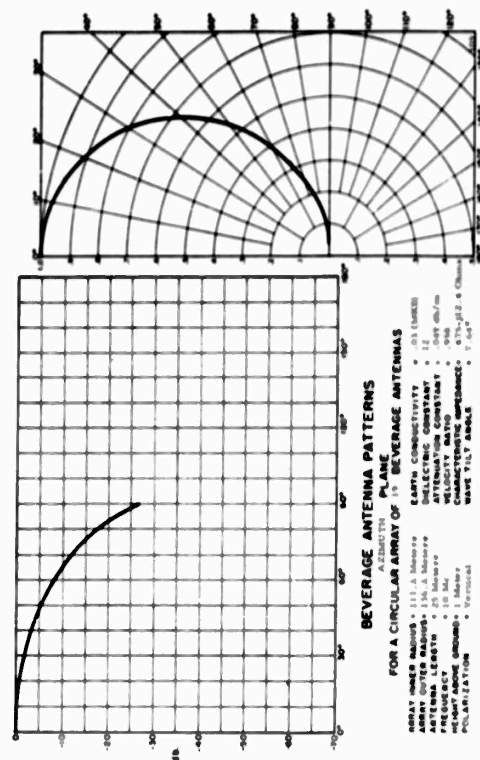


FIGURE 1-81

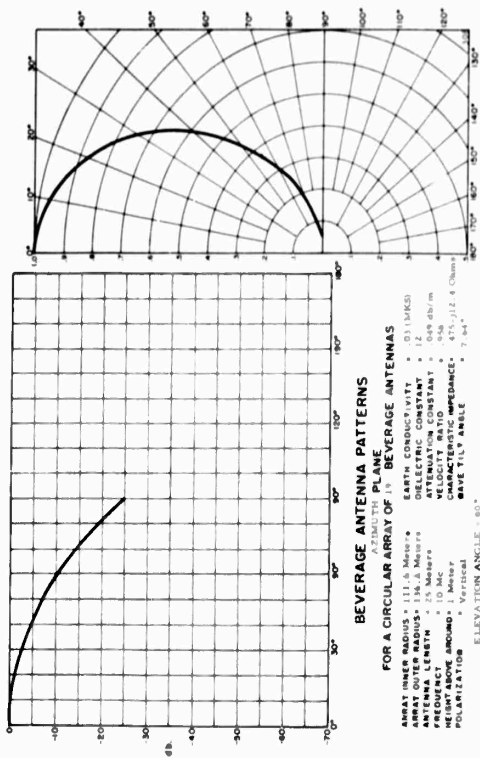


FIGURE 1-82

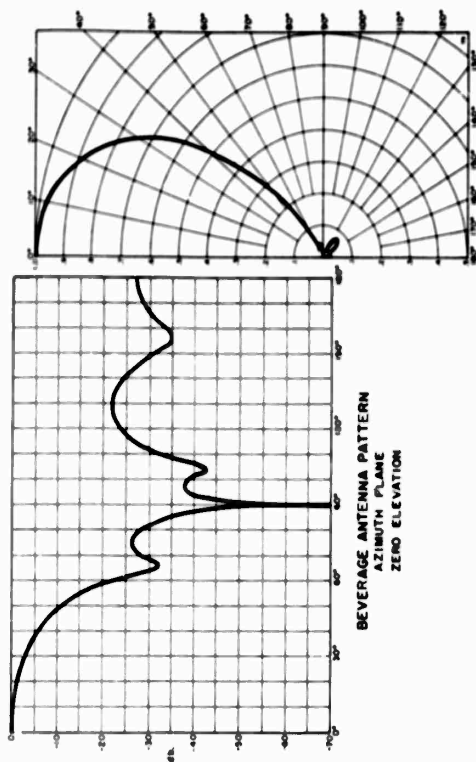


FIGURE 11-2a

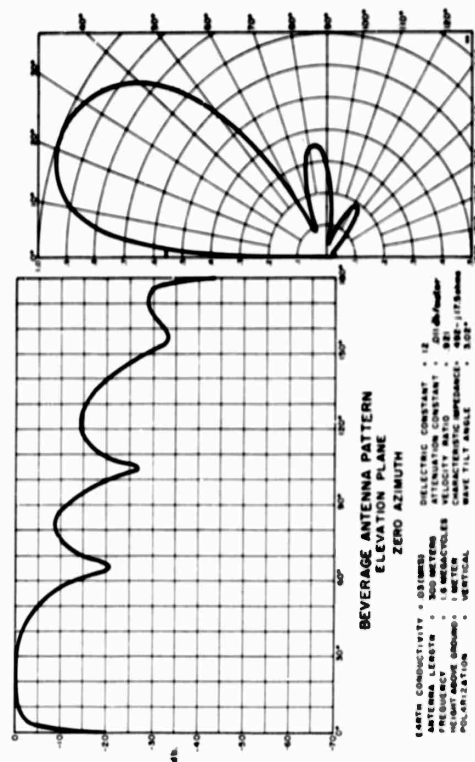


FIGURE 11-2b

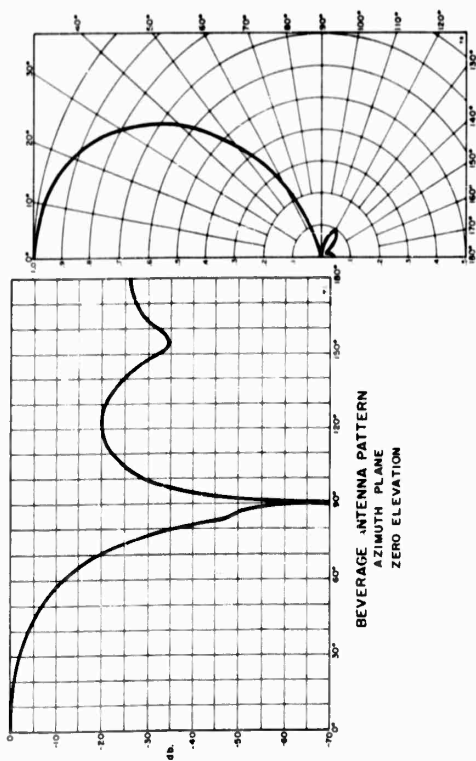


FIGURE 11-1a

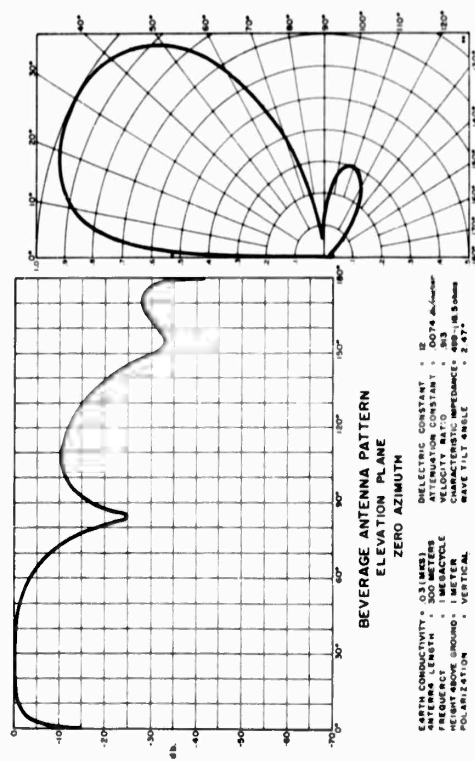


FIGURE 11-1b

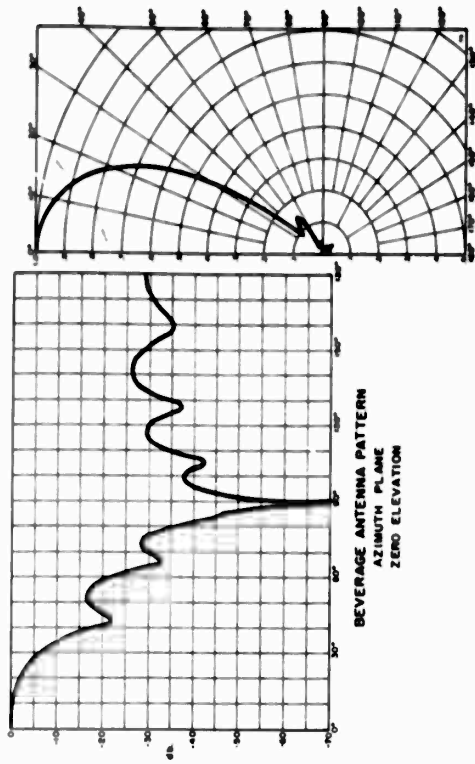


FIGURE 11-14

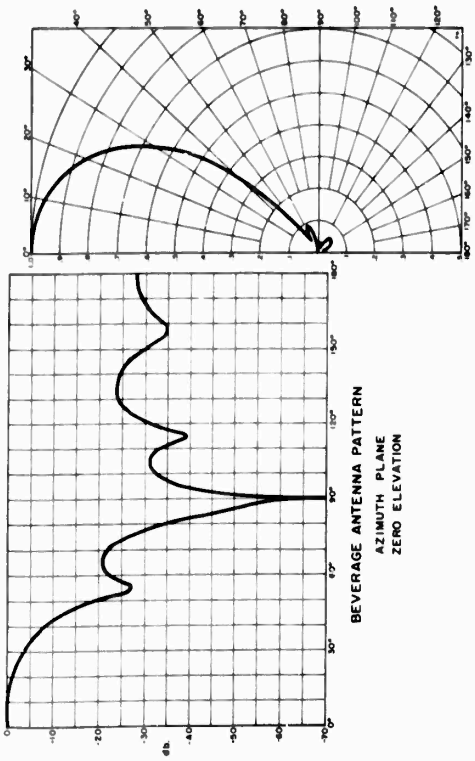


FIGURE 11-15a

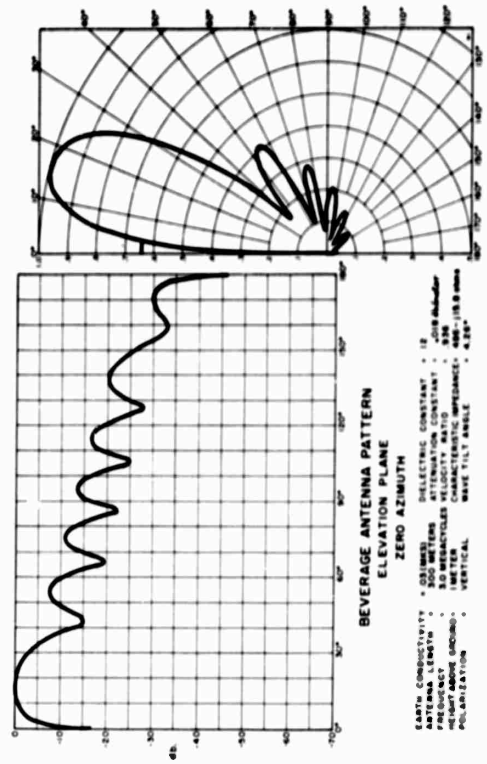


FIGURE 11-15b

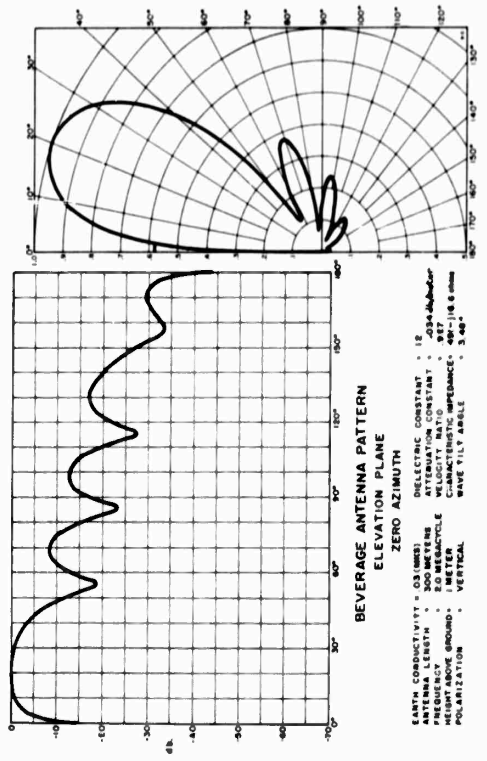


FIGURE 11-15c

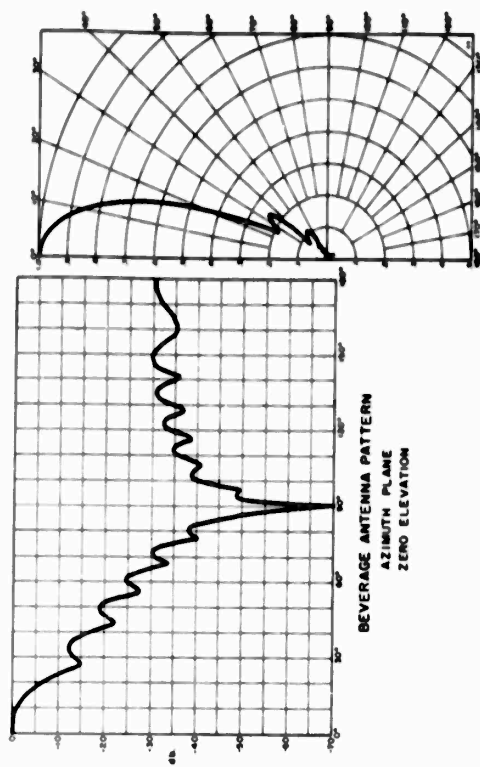


FIGURE 11-5a

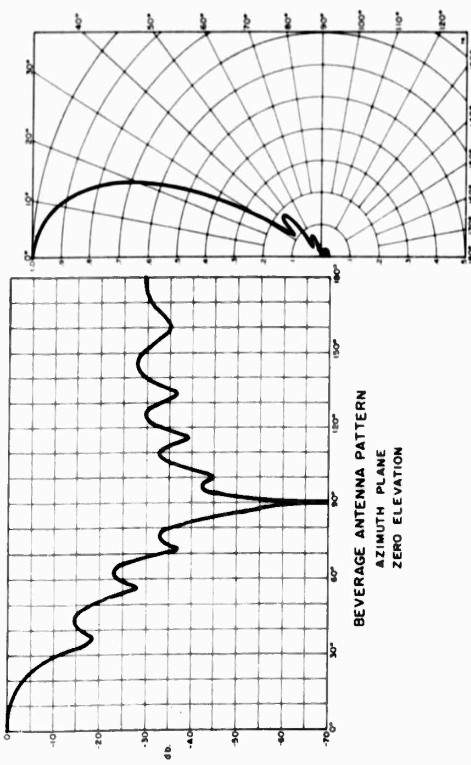


FIGURE 11-5b

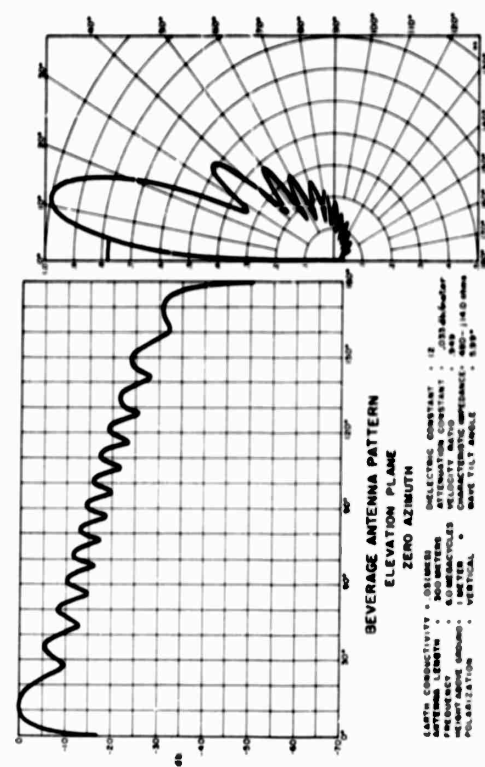


FIGURE 11-6a

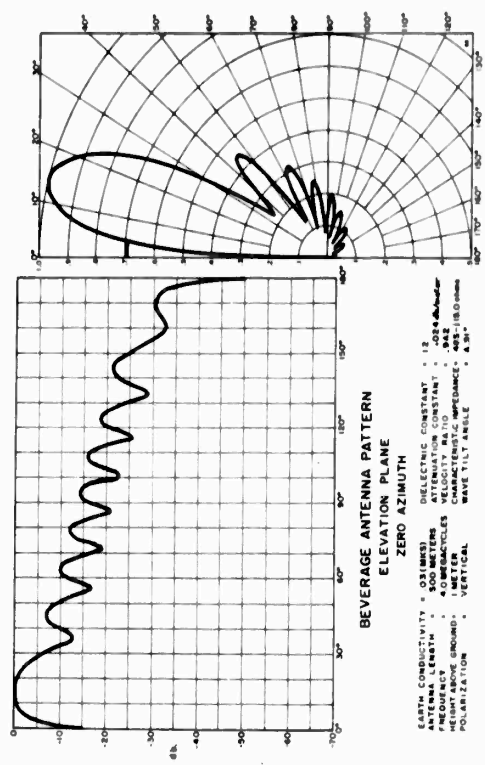


FIGURE 11-6b

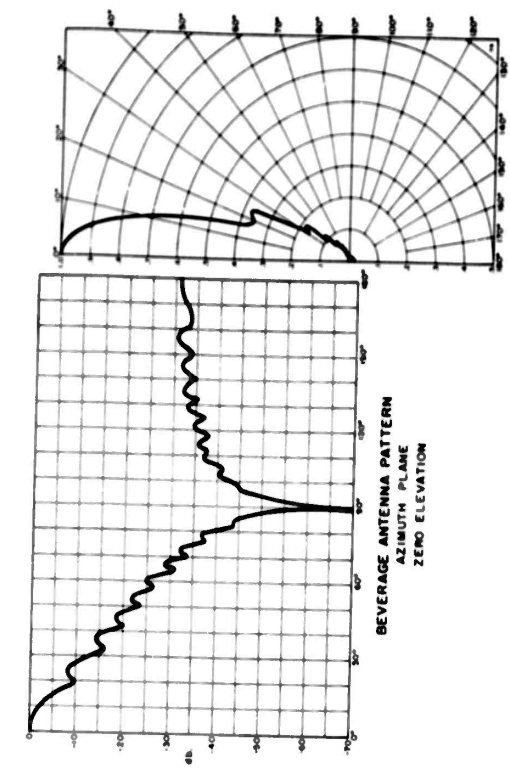


FIGURE 11-6a

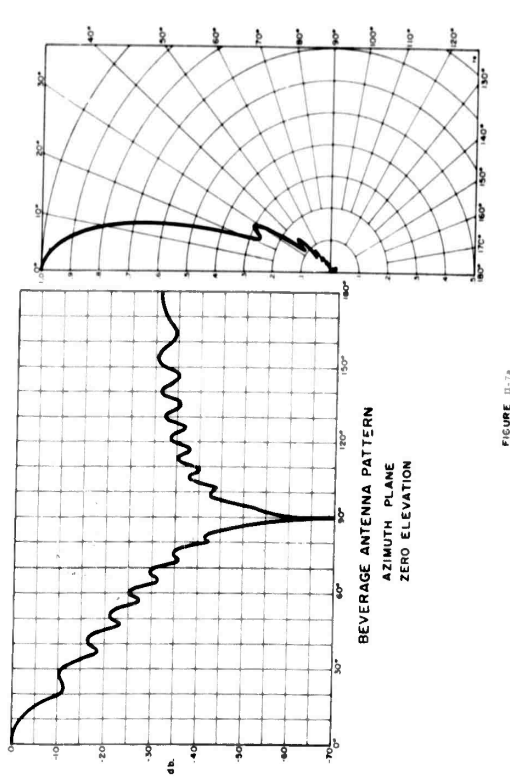


FIGURE 11-7a

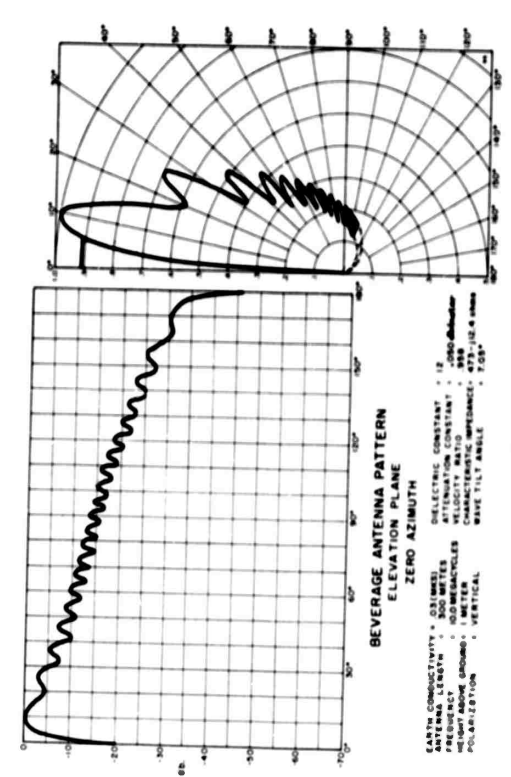


FIGURE 11-6b

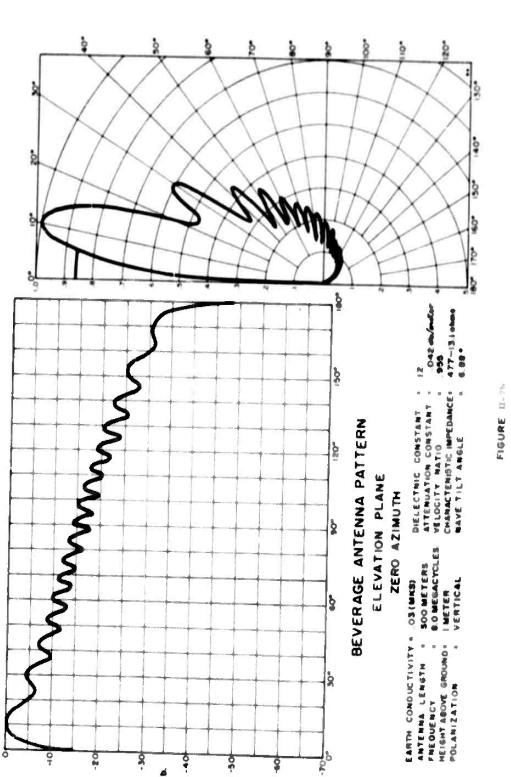


FIGURE 11-7b

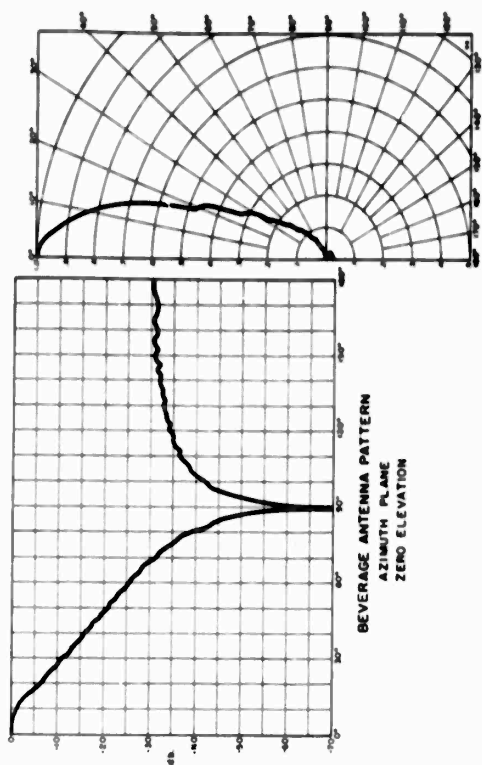


FIGURE 11-10a

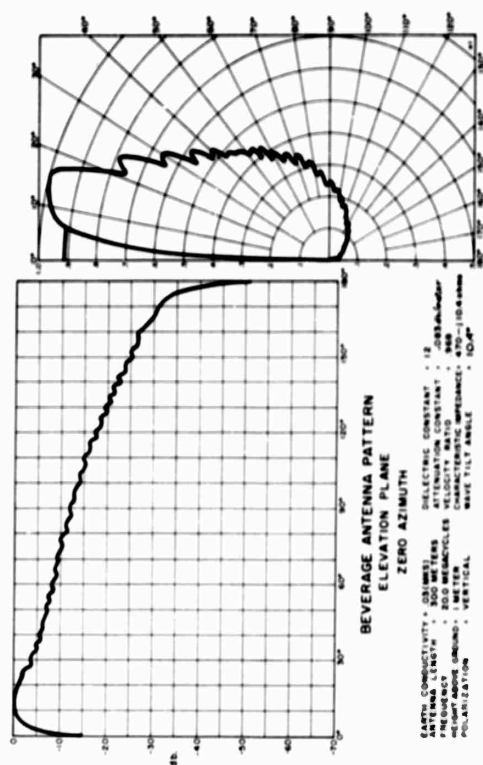


FIGURE 11-10b

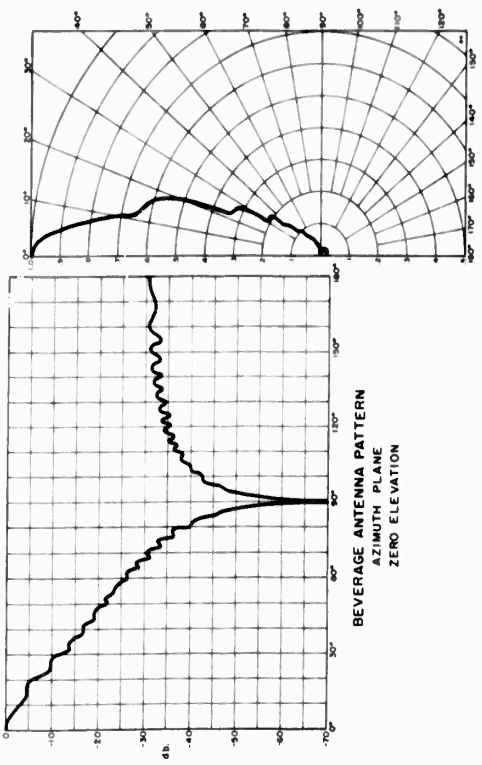


FIGURE 11-9a

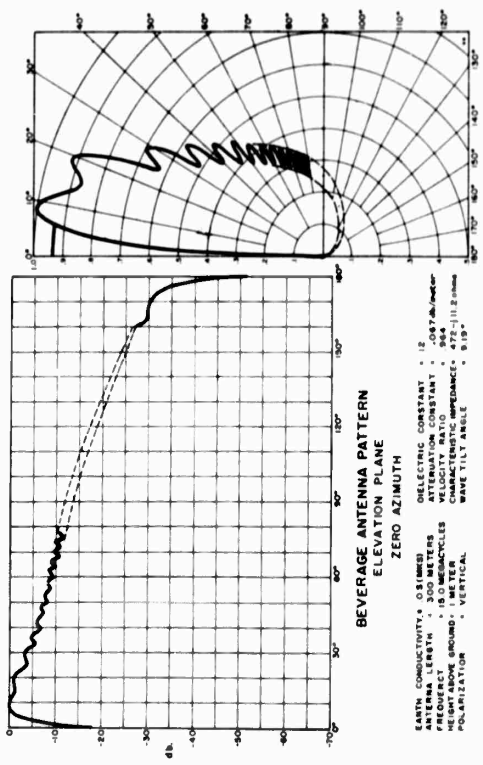


FIGURE 11-9b

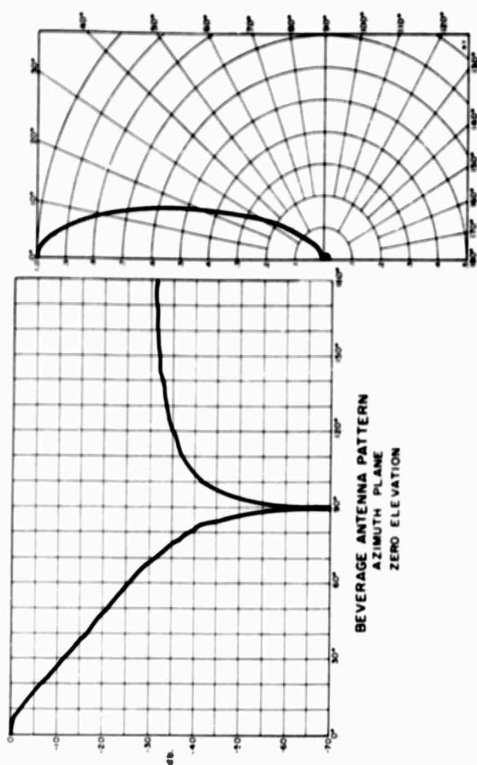


FIGURE 8-11a

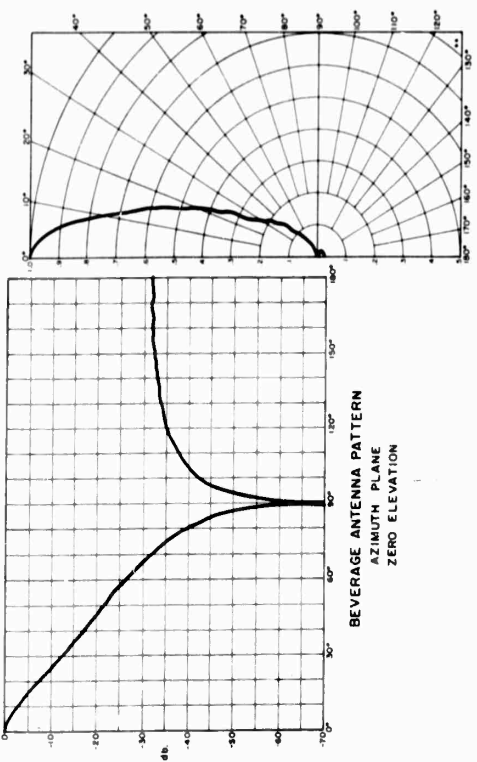


FIGURE 8-11b

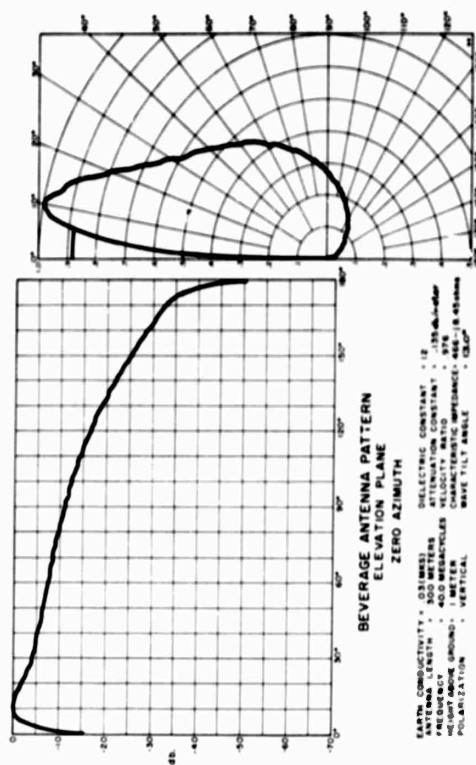


FIGURE 8-11c

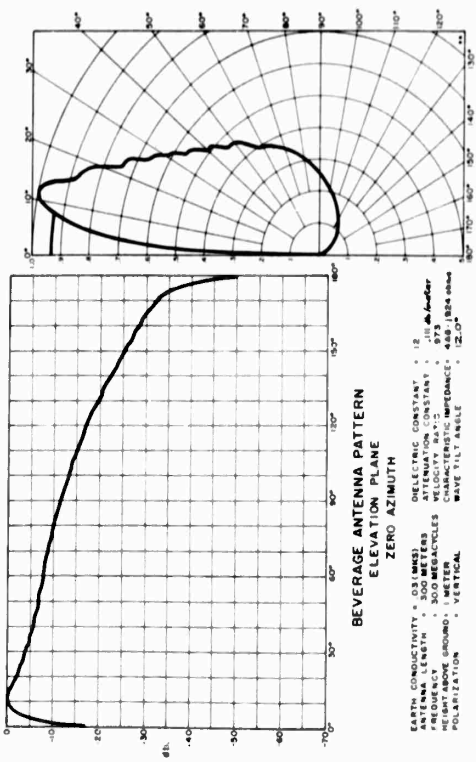


FIGURE 8-11d

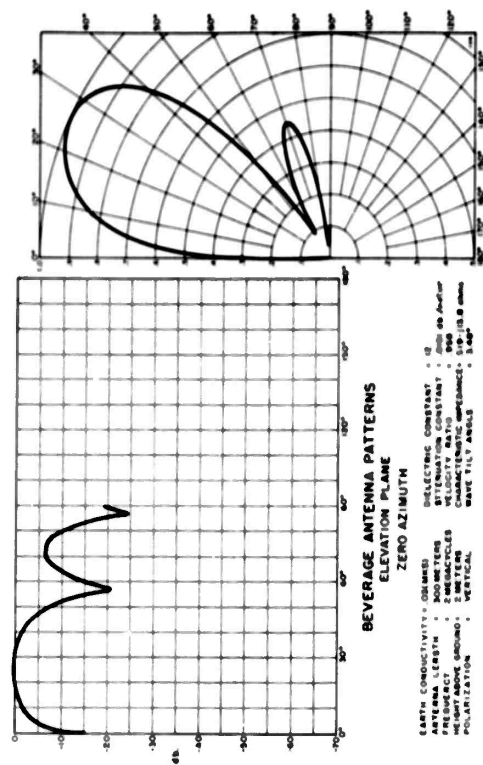


FIGURE 11-13

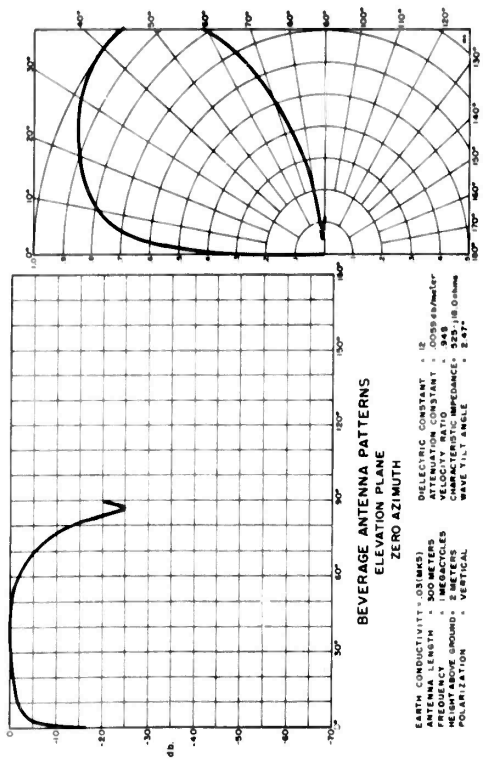


FIGURE 11-14

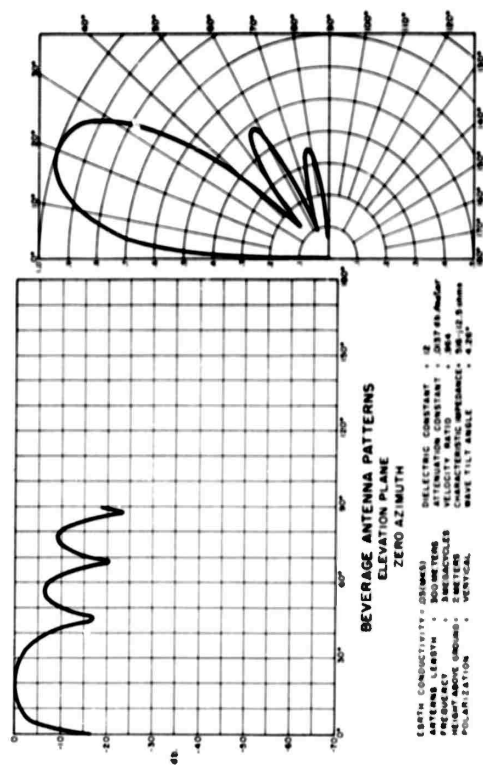


FIGURE 11-15

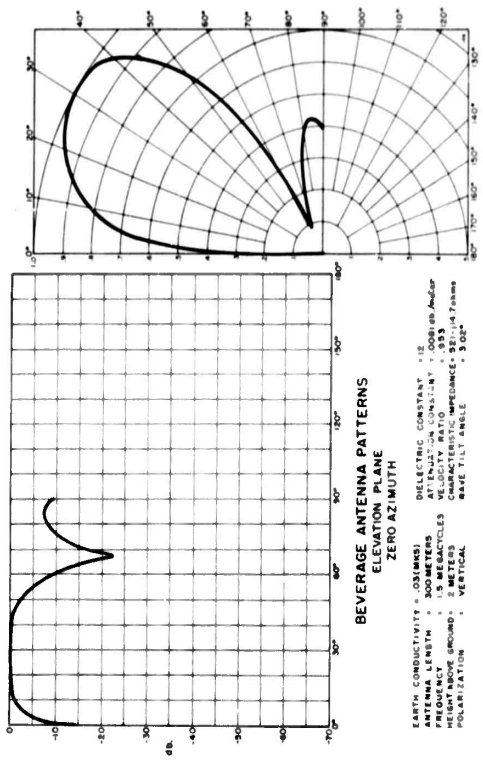


FIGURE 11-16

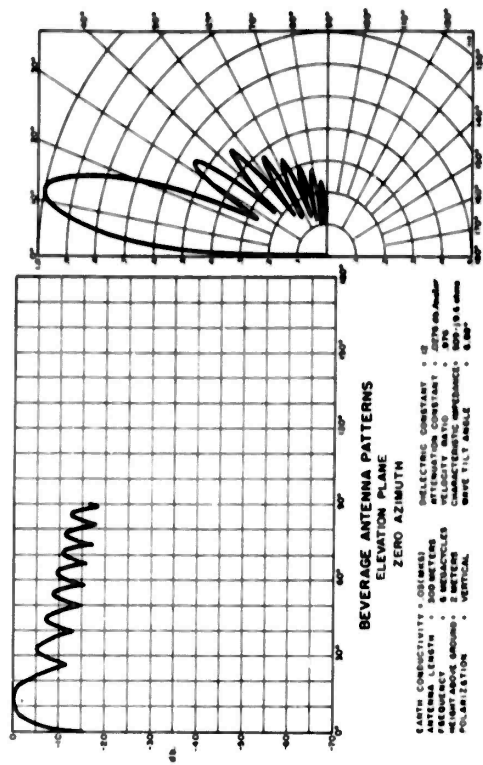


FIGURE 11-16

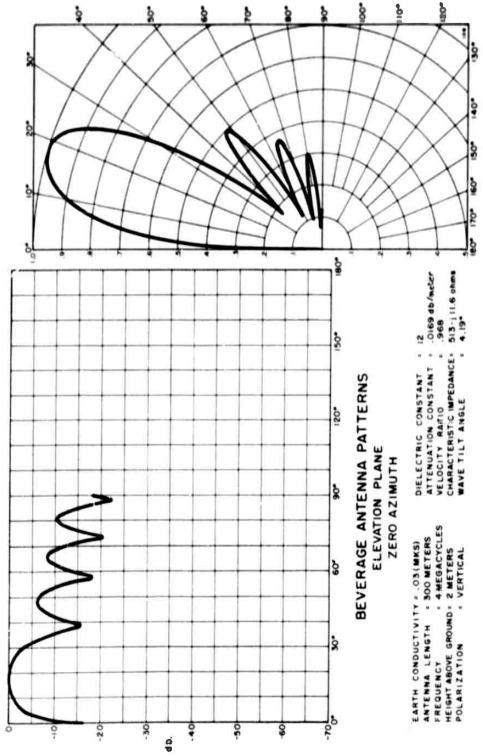


FIGURE 11-17

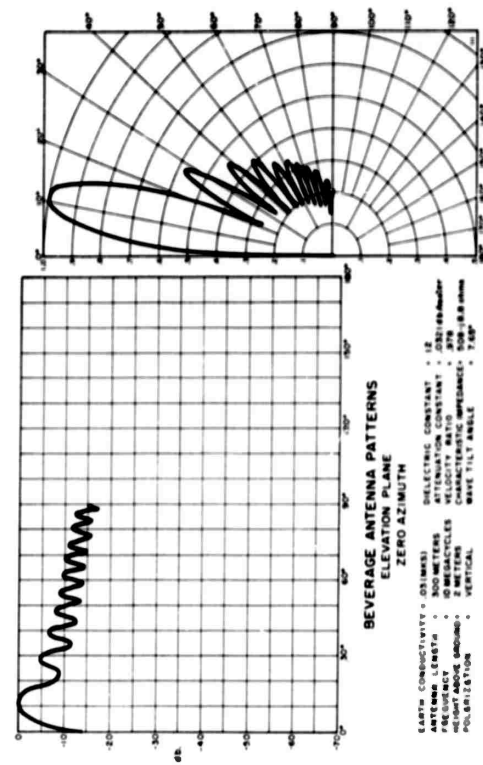


FIGURE 11-18

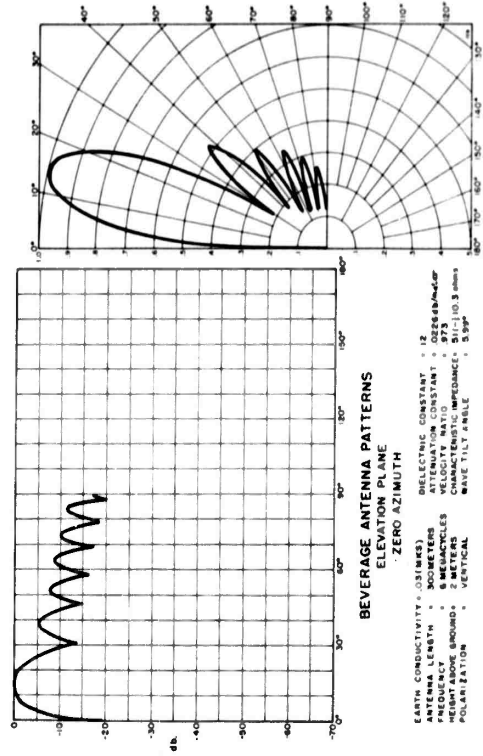


FIGURE 11-19

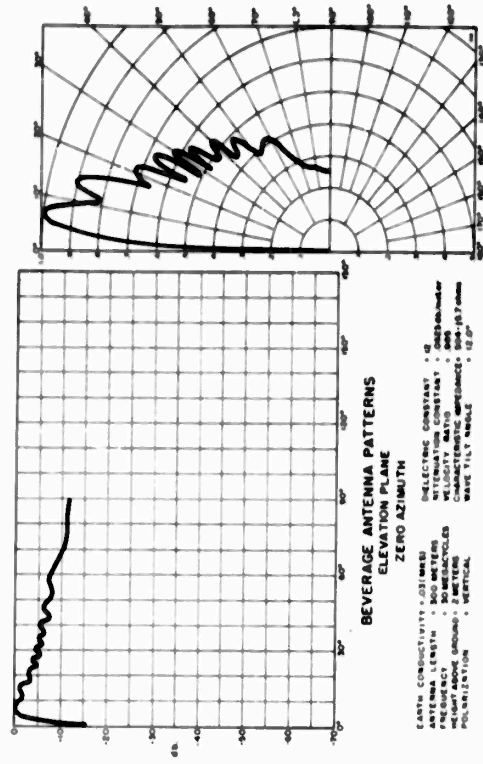


FIGURE 11-21

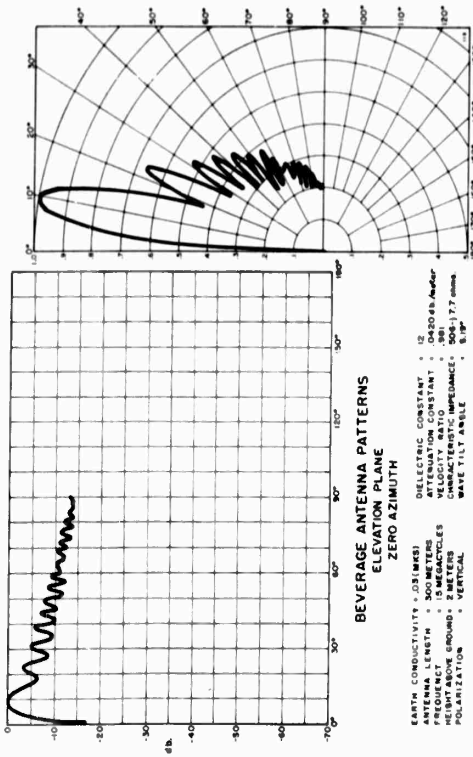


FIGURE 11-22

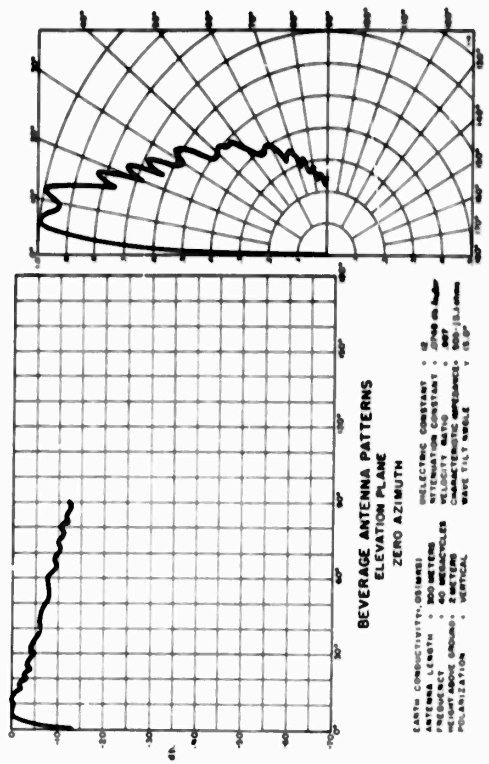


FIGURE 11-23

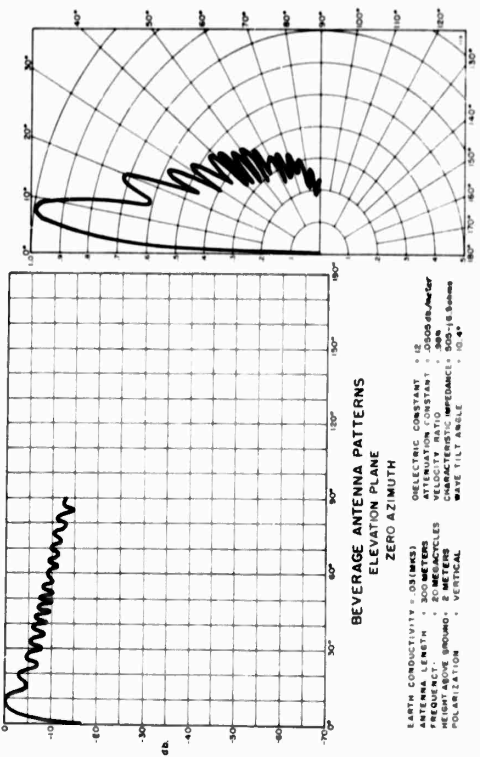


FIGURE 11-24

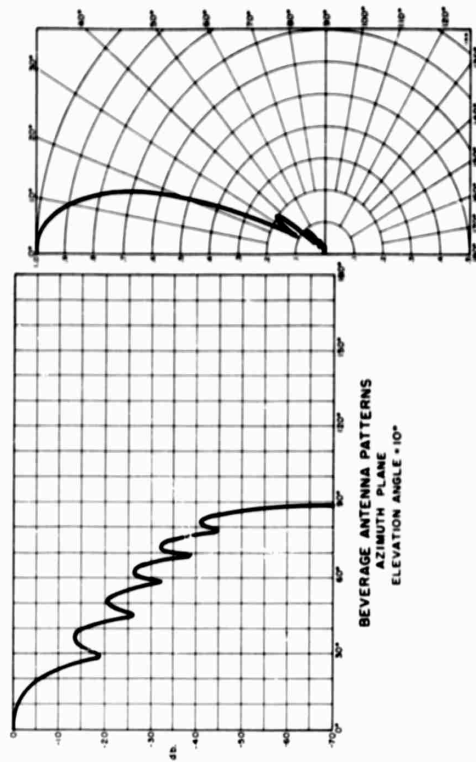


FIGURE 11-28

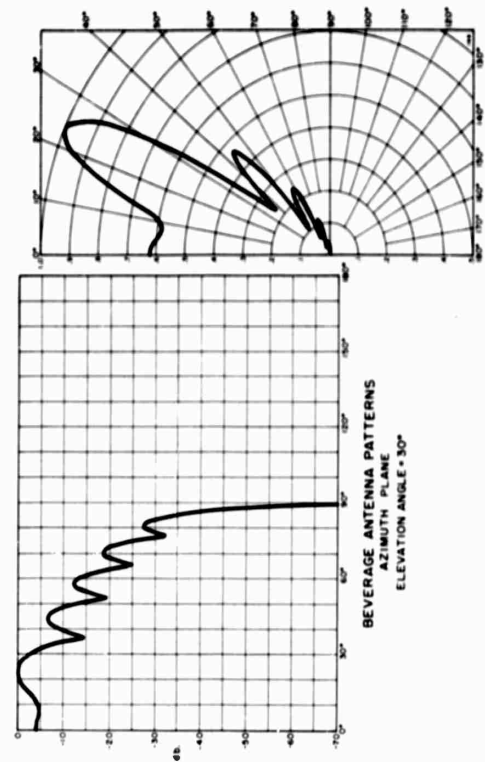


FIGURE 11-29

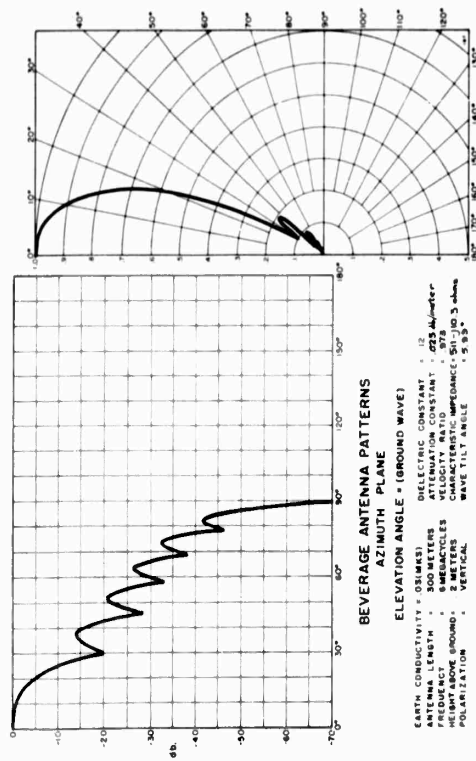


FIGURE 11-27

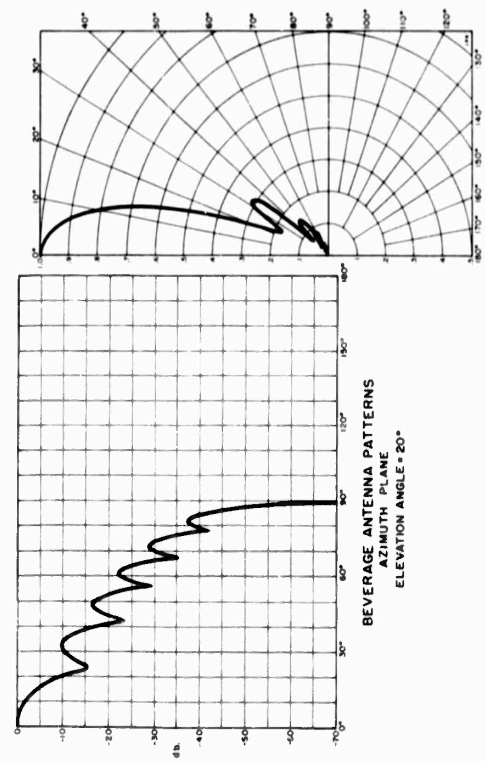


FIGURE 11-26

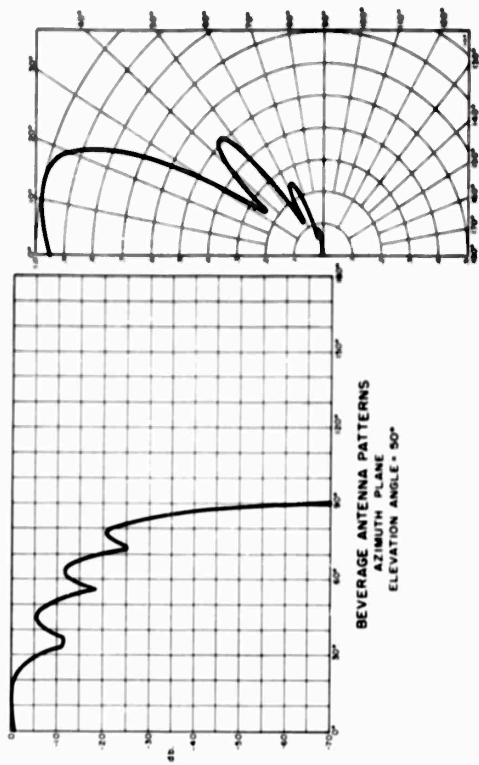


FIGURE 11-16

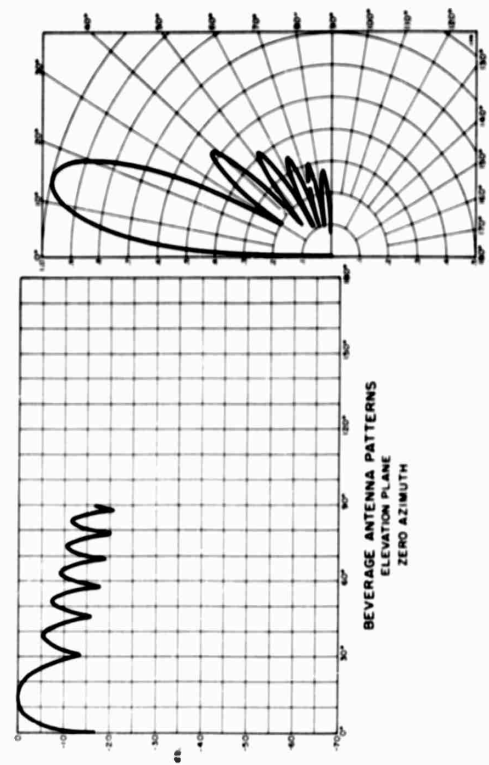


FIGURE 11-17

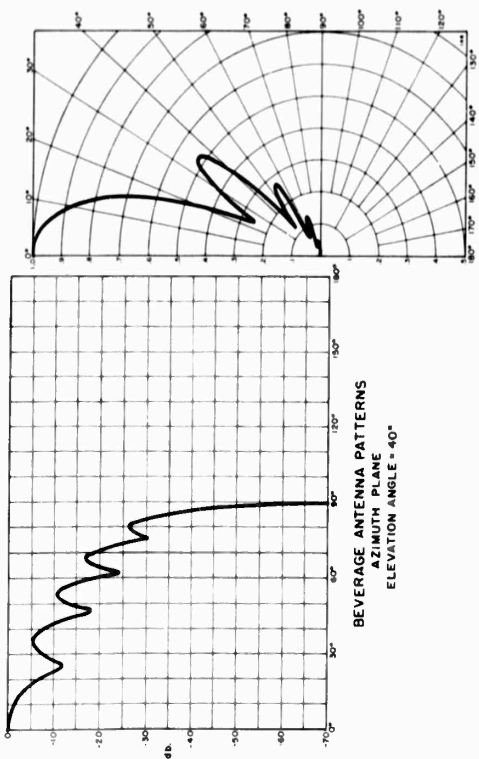


FIGURE 11-18

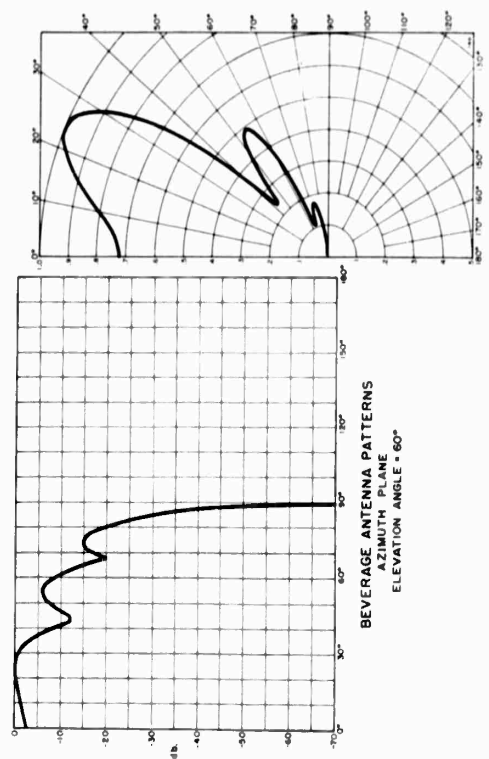


FIGURE 11-19

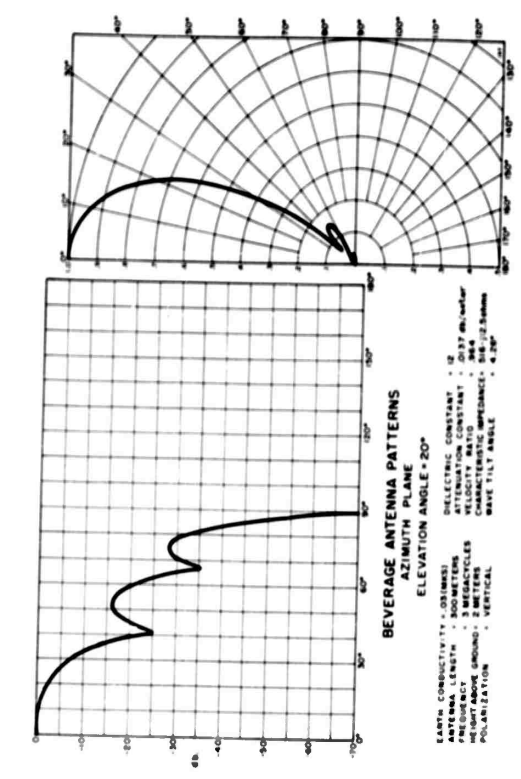


FIGURE II-14

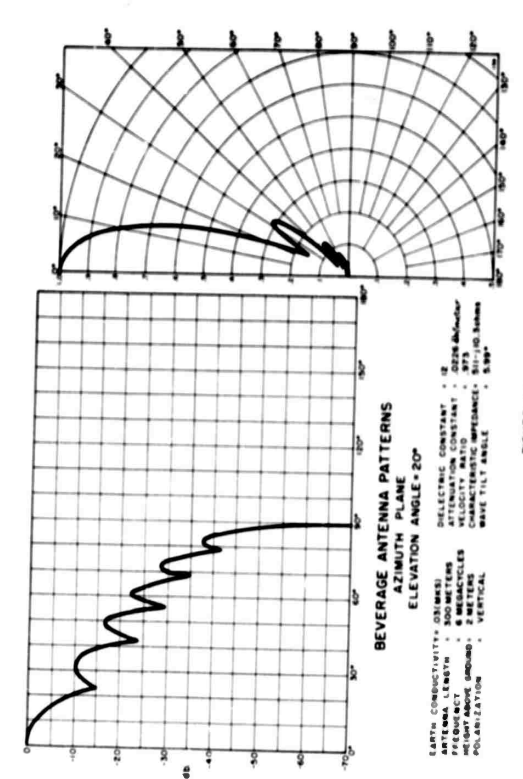


FIGURE II-15

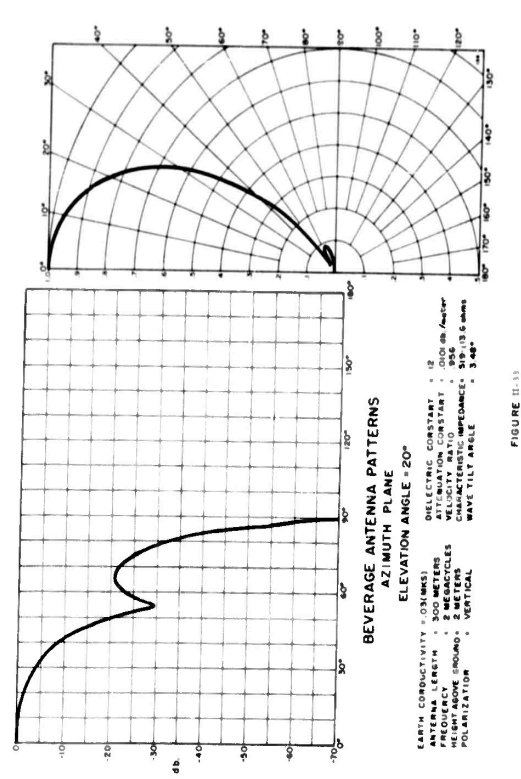


FIGURE II-33

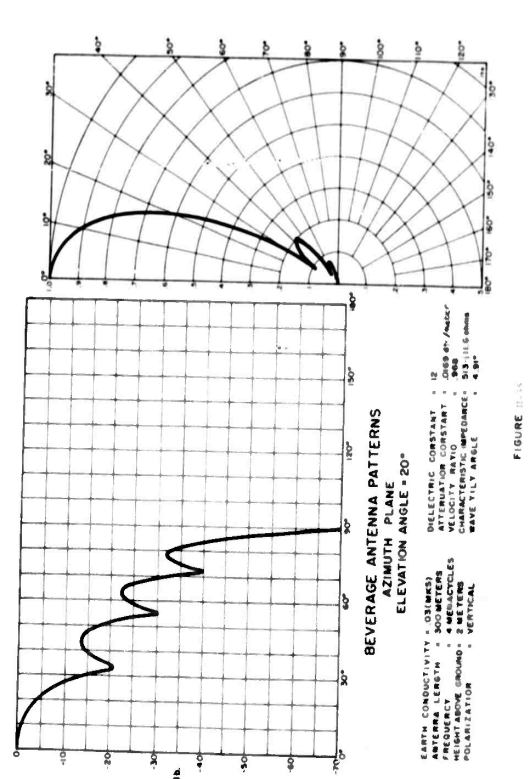


FIGURE II-34

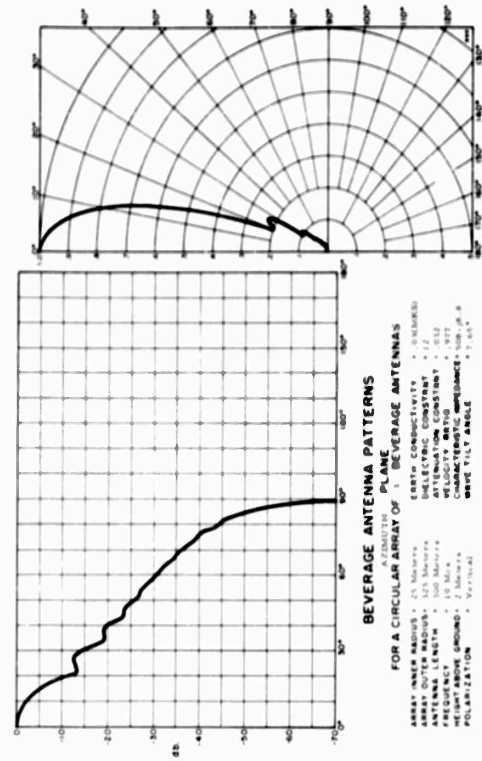


FIGURE B-39

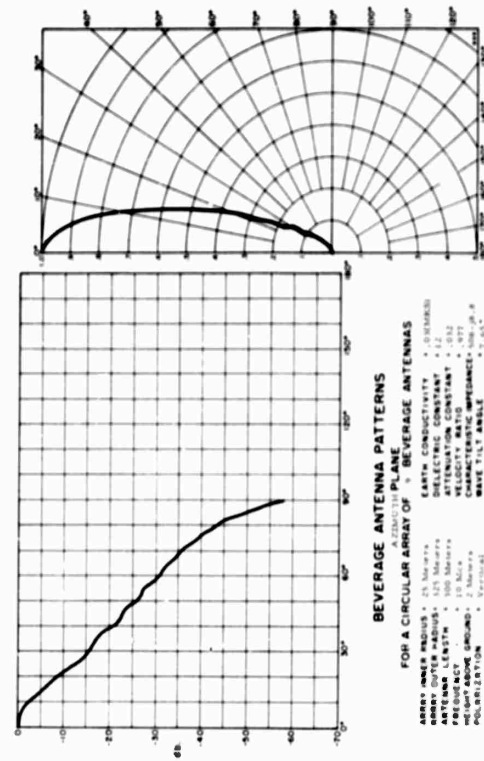


FIGURE B-40

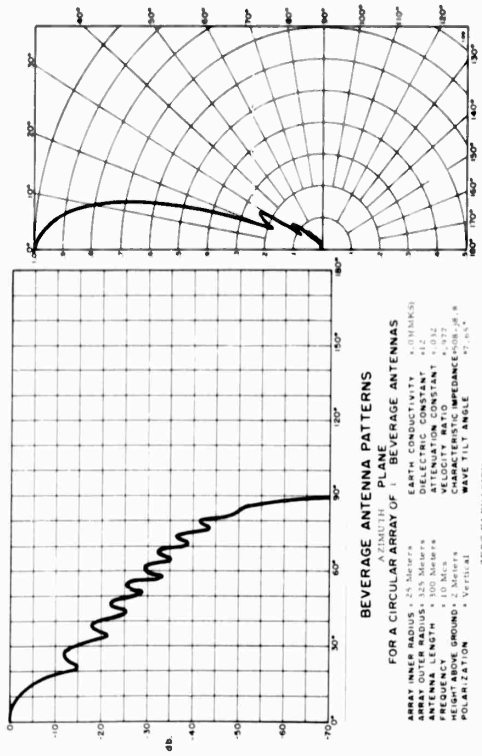


FIGURE B-37

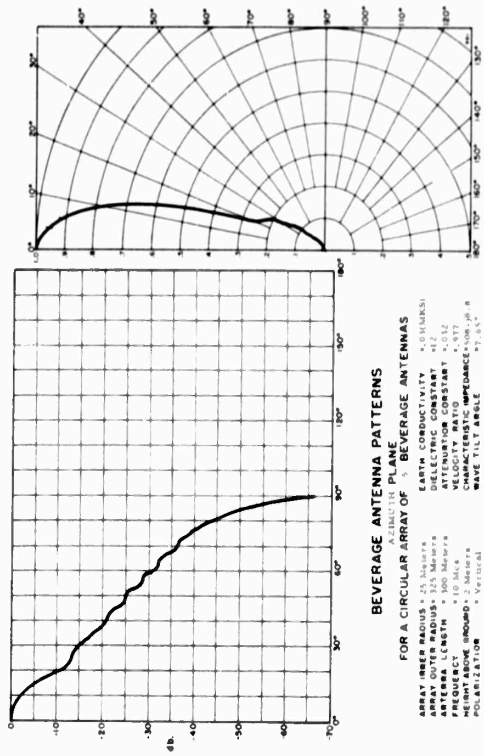


FIGURE B-38

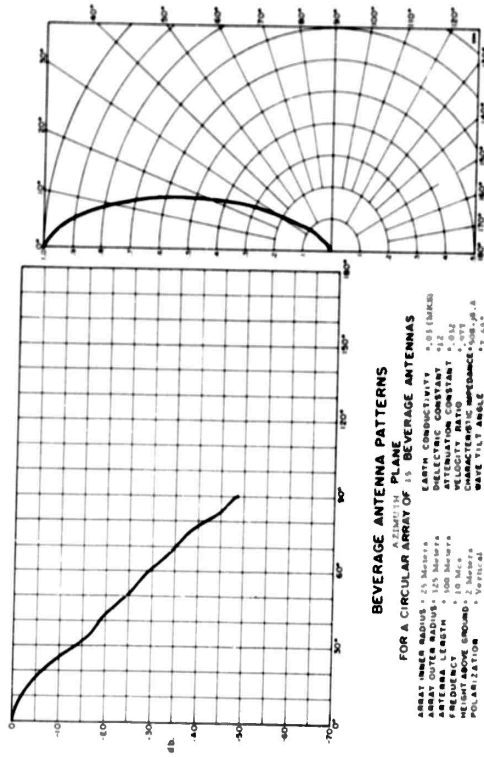


FIGURE 31-41

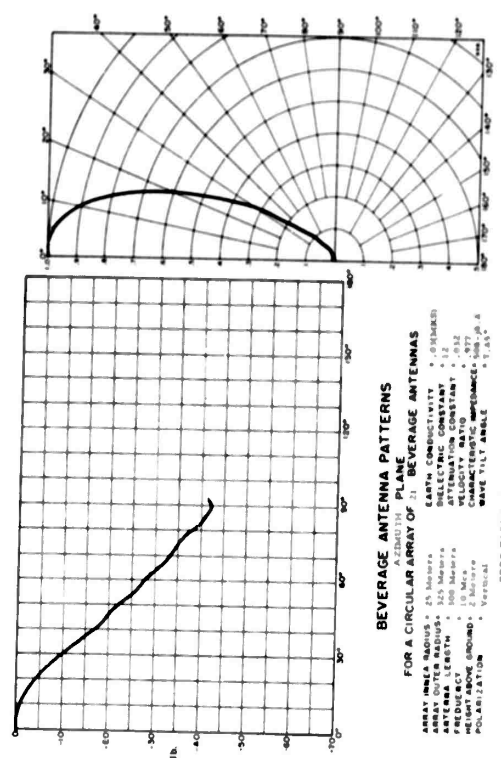


FIGURE 31-42

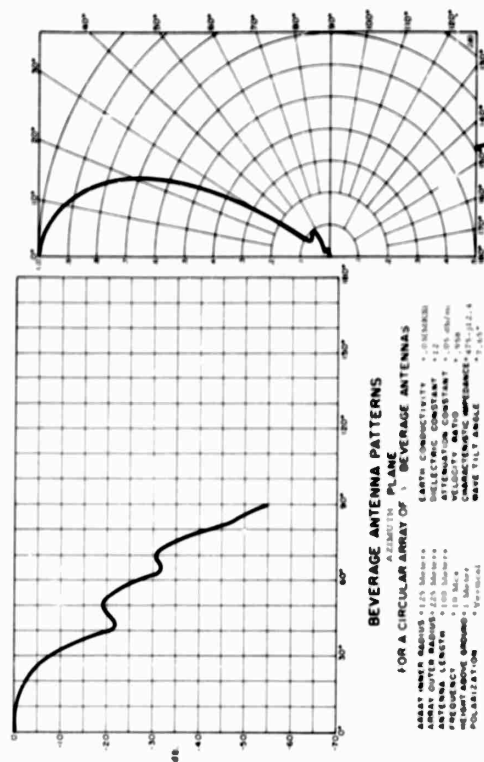


FIGURE B-40

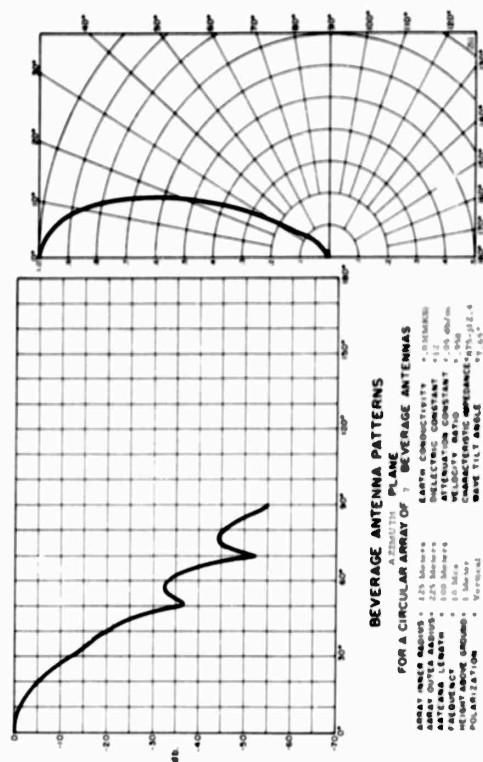


FIGURE B-41

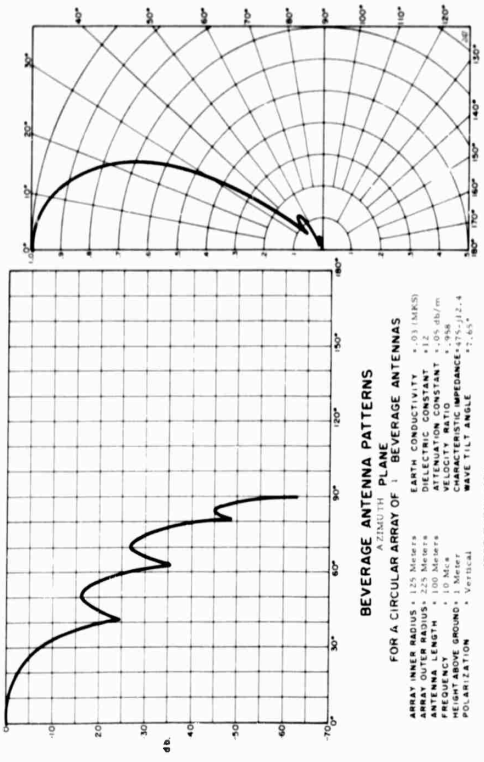


FIGURE B-42

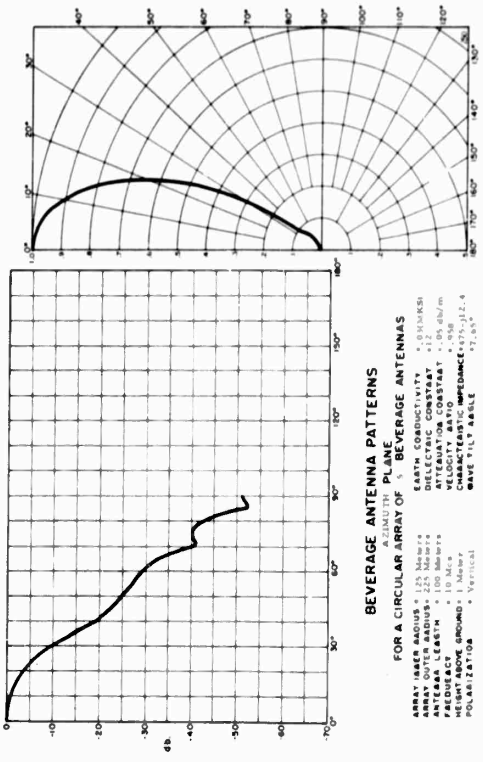


FIGURE B-43

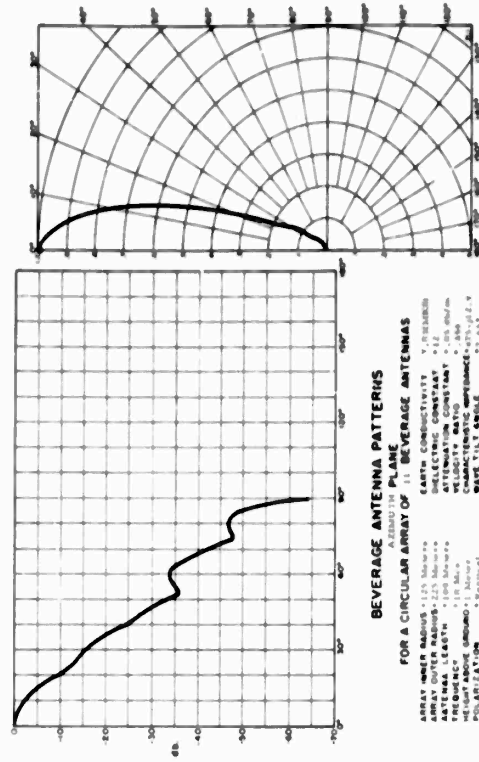


FIGURE II-47

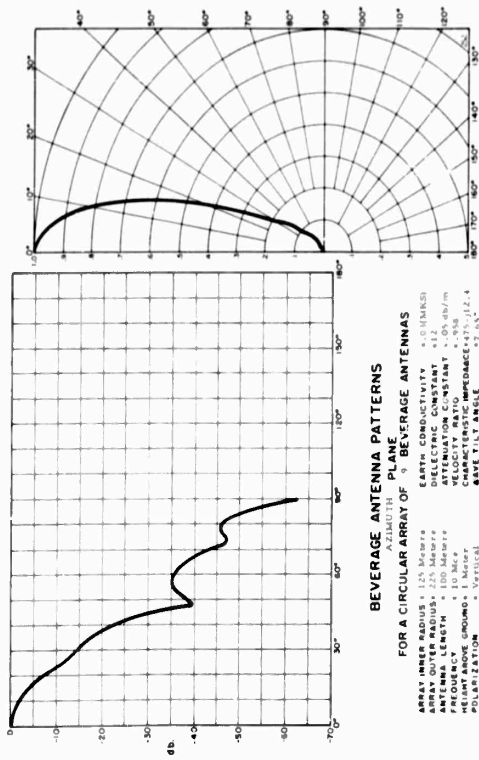


FIGURE II-48

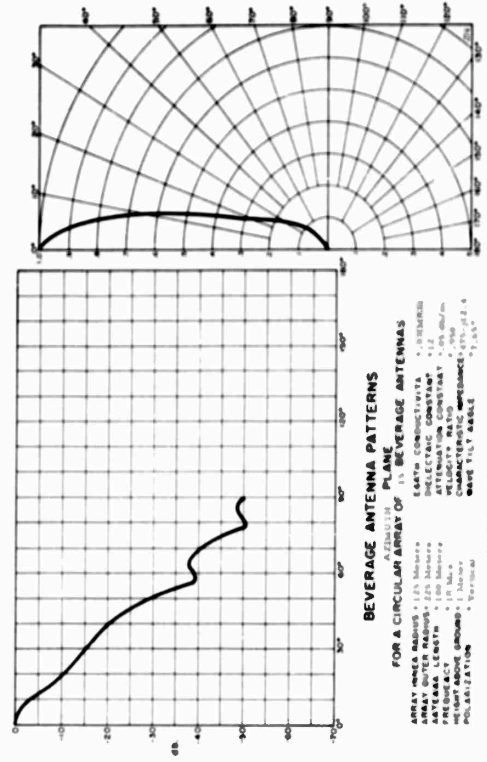


FIGURE II-49

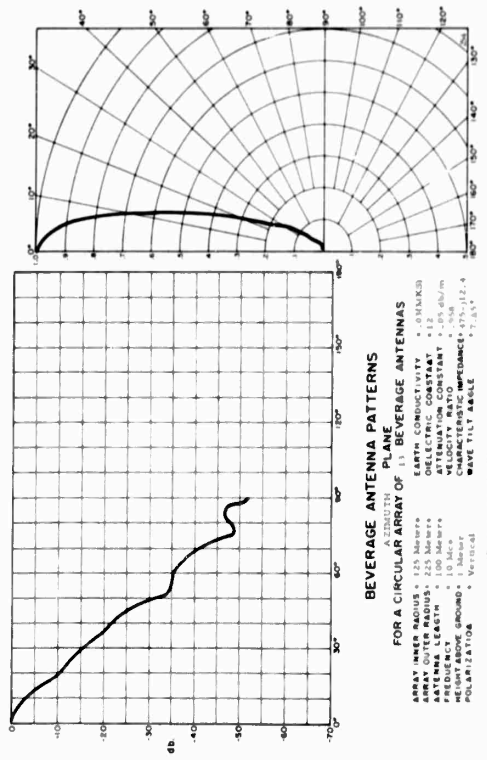


FIGURE II-50

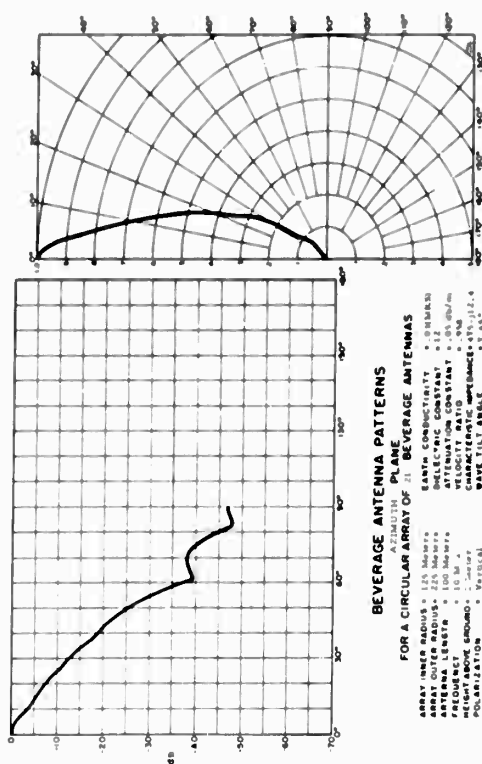


FIGURE B-41

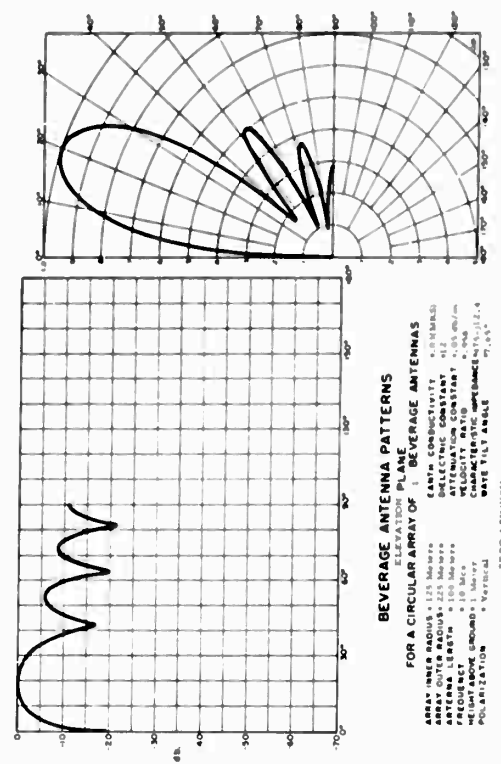


FIGURE B-42

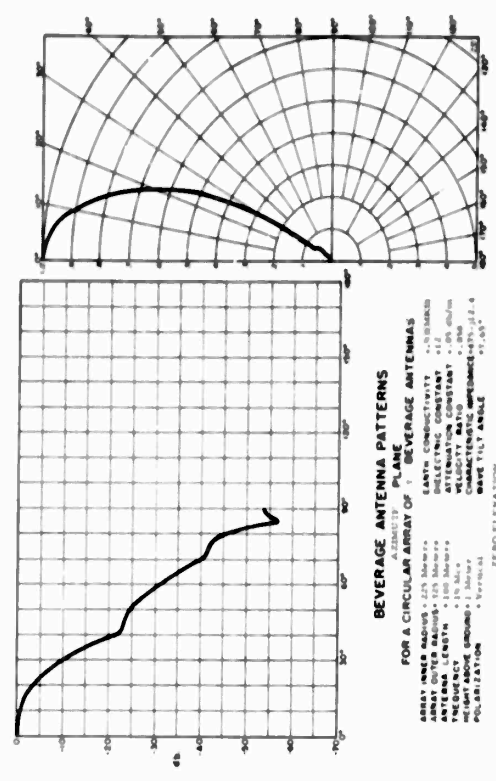


FIGURE II-44

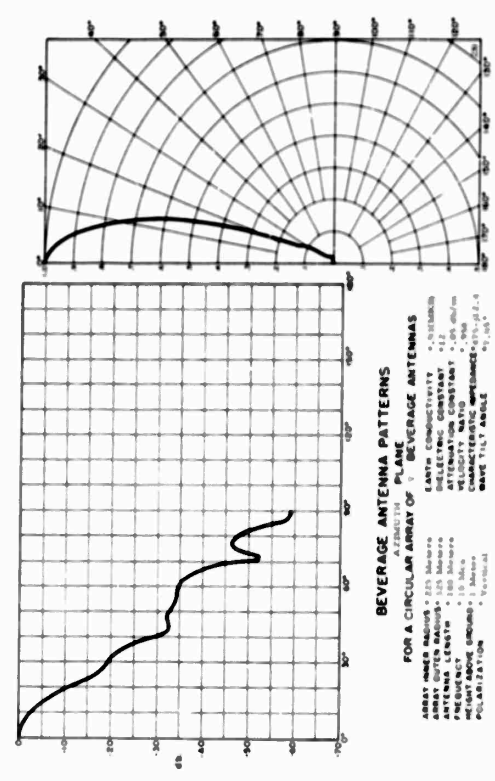


FIGURE II-45

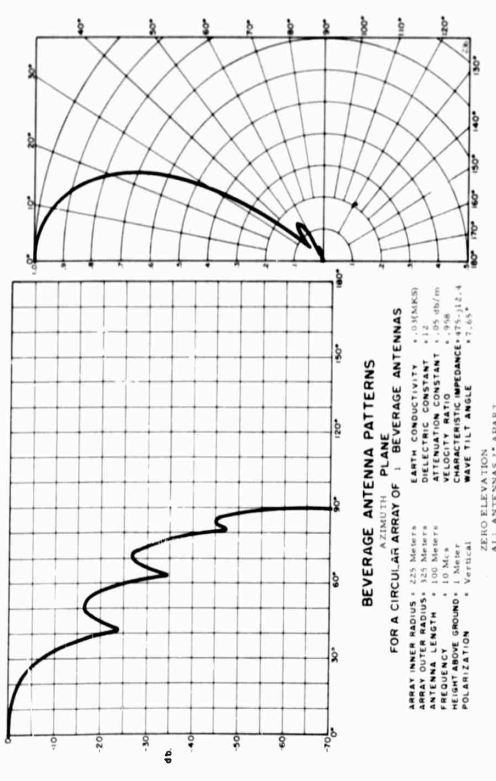


FIGURE II-51

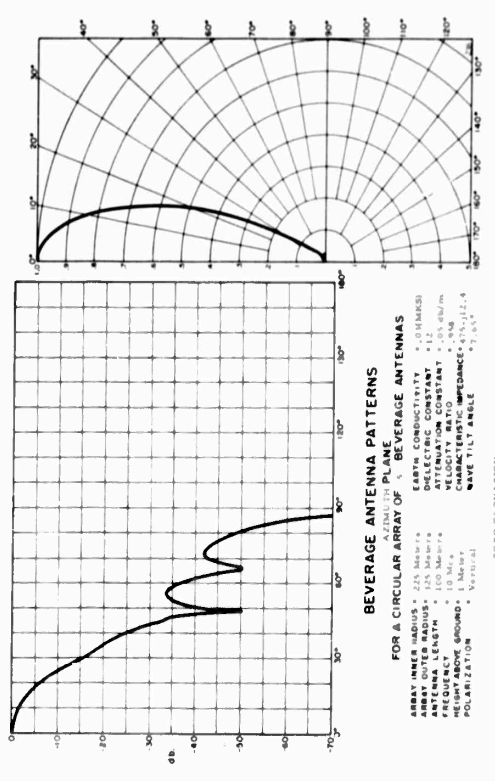


FIGURE II-53

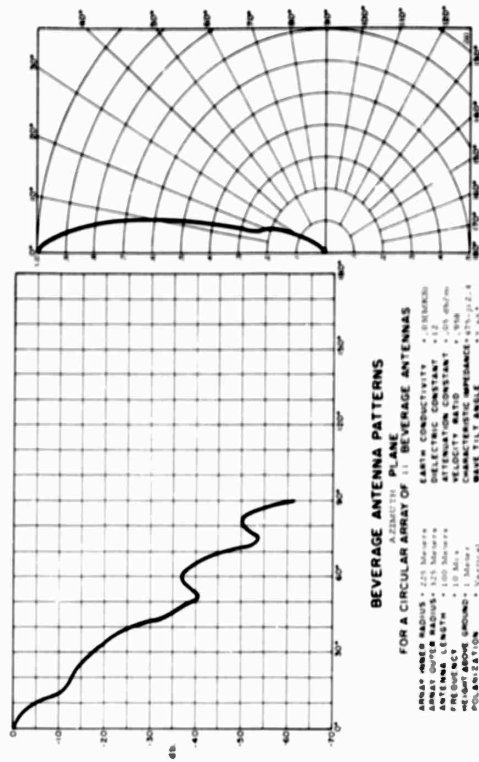


FIGURE D-57

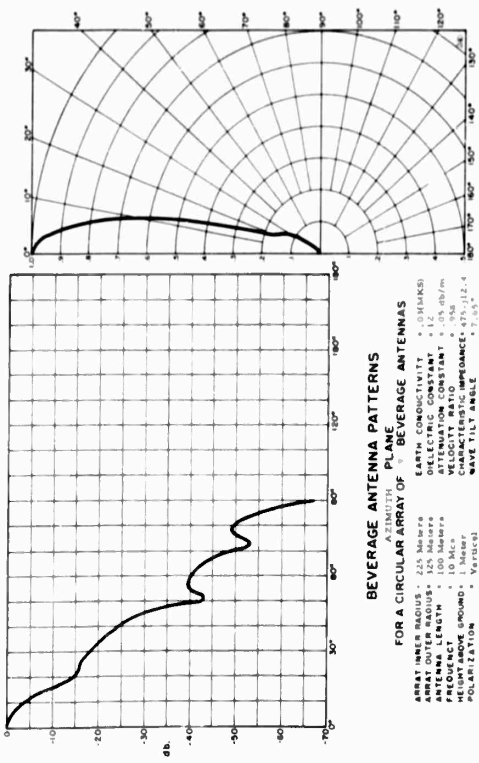


FIGURE D-58

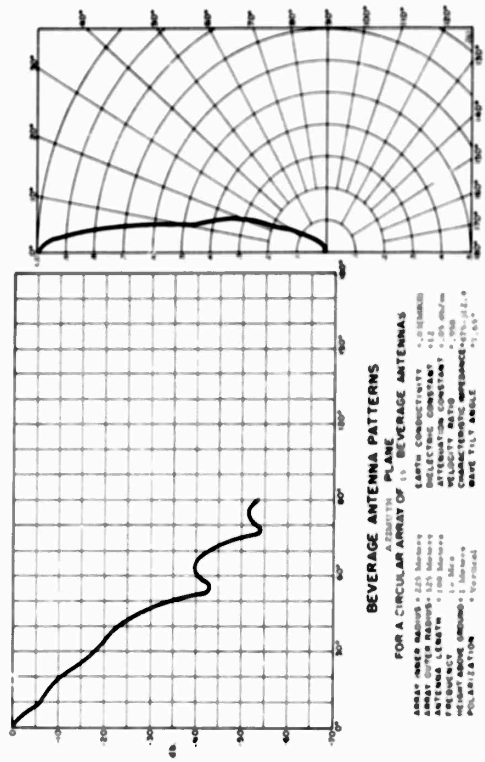


FIGURE D-59

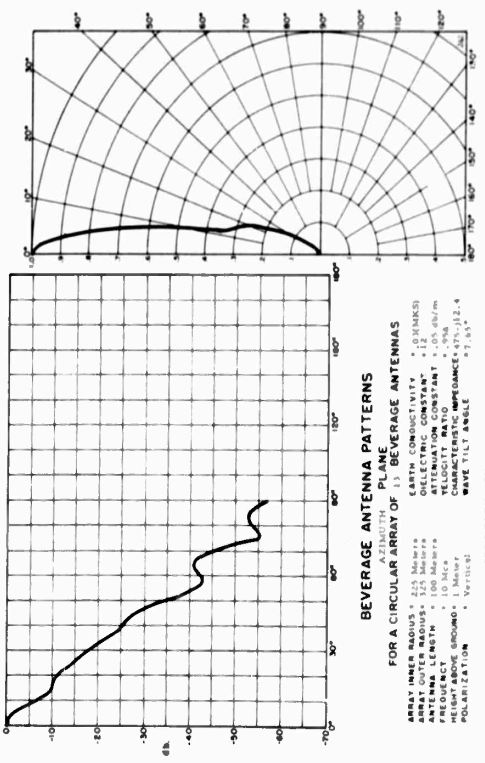
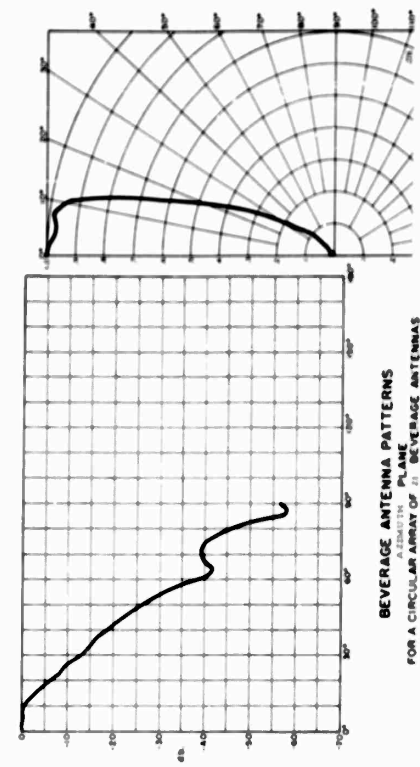
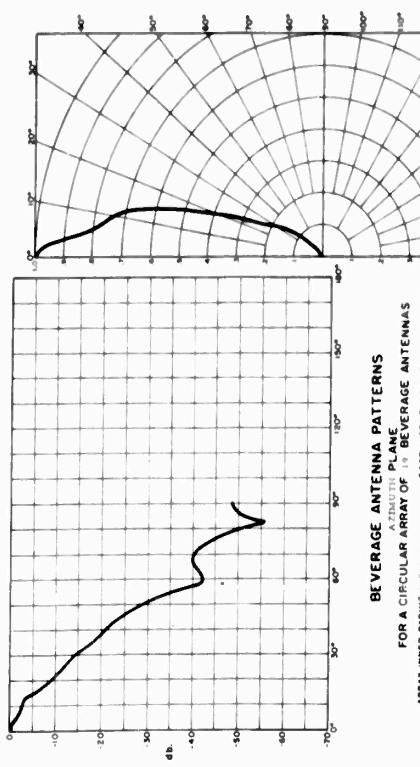


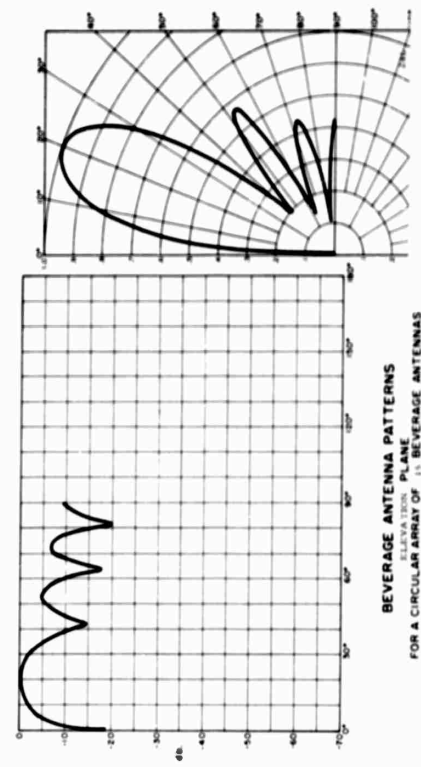
FIGURE D-60



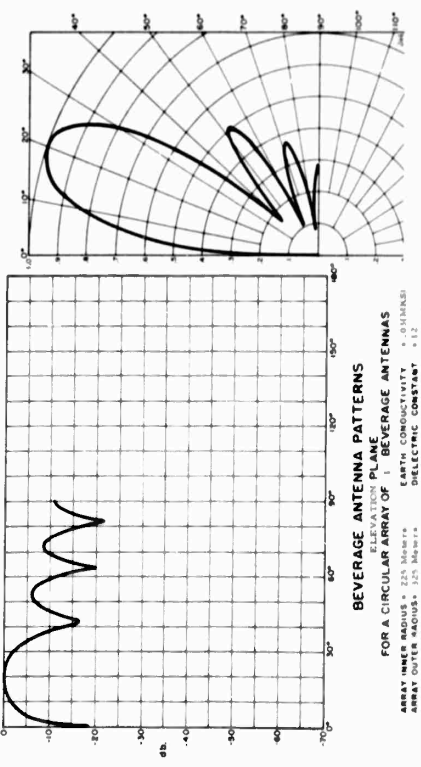
BEVERAGE ANTENNA PATTERNS
 AZIMUTH PLANE
FOR A CIRCULAR ARRAY OF 21 BEVERAGE ANTENNAS
 ARRAY INNER RADIUS * 225 Meters
 ARRAY OUTER RADIUS * 225 Meters
 ANTENNA LENGTH * 10 Meters
 FREQUENCY * 10 Mcz
 HEIGHT ABOVE GROUND * 1 Meter
 POLARIZATION * Vertical
 EARTH CONDUCTIVITY * 0.01 MKS
 DIELECTRIC CONSTANT * 1.2
 ATTENUATION CONSTANT * 0.5 db/m
 VELOCITY RATIO * 0.98
 CHARACTERISTIC IMPEDANCE * 475-j12.4
 WAVE TILT ANGLE * 7.55°
 ZERO ELEVATION
 ALL ANTENNAS 2° APART



BEVERAGE ANTENNA PATTERNS
 AZIMUTH PLANE
FOR A CIRCULAR ARRAY OF 19 BEVERAGE ANTENNAS
 ARRAY INNER RADIUS * 225 Meters
 ARRAY OUTER RADIUS * 225 Meters
 ANTENNA LENGTH * 10 Meters
 FREQUENCY * 10 Mcz
 HEIGHT ABOVE GROUND * 1 Meter
 POLARIZATION * Vertical
 EARTH CONDUCTIVITY * 0.01 MKS
 DIELECTRIC CONSTANT * 1.2
 ATTENUATION CONSTANT * 0.5 db/m
 VELOCITY RATIO * 0.98
 CHARACTERISTIC IMPEDANCE * 475-j12.4
 WAVE TILT ANGLE * 7.55°
 ZERO ELEVATION
 ALL ANTENNAS 2° APART



BEVERAGE ANTENNA PATTERNS
 AZIMUTH PLANE
FOR A CIRCULAR ARRAY OF 11 BEVERAGE ANTENNAS
 ARRAY INNER RADIUS * 225 Meters
 ARRAY OUTER RADIUS * 225 Meters
 ANTENNA LENGTH * 10 Meters
 FREQUENCY * 10 Mcz
 HEIGHT ABOVE GROUND * 1 Meter
 POLARIZATION * Vertical
 EARTH CONDUCTIVITY * 0.01 MKS
 DIELECTRIC CONSTANT * 1.2
 ATTENUATION CONSTANT * 0.5 db/m
 VELOCITY RATIO * 0.98
 CHARACTERISTIC IMPEDANCE * 475-j12.4
 WAVE TILT ANGLE * 7.55°
 ZERO AZIMUTH
 ALL ANTENNAS 2° APART



BEVERAGE ANTENNA PATTERNS
 AZIMUTH PLANE
FOR A CIRCULAR ARRAY OF 7 BEVERAGE ANTENNAS
 ARRAY INNER RADIUS * 225 Meters
 ARRAY OUTER RADIUS * 225 Meters
 ANTENNA LENGTH * 10 Meters
 FREQUENCY * 10 Mcz
 HEIGHT ABOVE GROUND * 1 Meter
 POLARIZATION * Vertical
 EARTH CONDUCTIVITY * 0.01 MKS
 DIELECTRIC CONSTANT * 1.2
 ATTENUATION CONSTANT * 0.5 db/m
 VELOCITY RATIO * 0.98
 CHARACTERISTIC IMPEDANCE * 475-j12.4
 WAVE TILT ANGLE * 7.55°
 ZERO AZIMUTH
 ALL ANTENNAS 2° APART

FIGURE II-41

FIGURE II-42

FIGURE II-43

FIGURE II-44

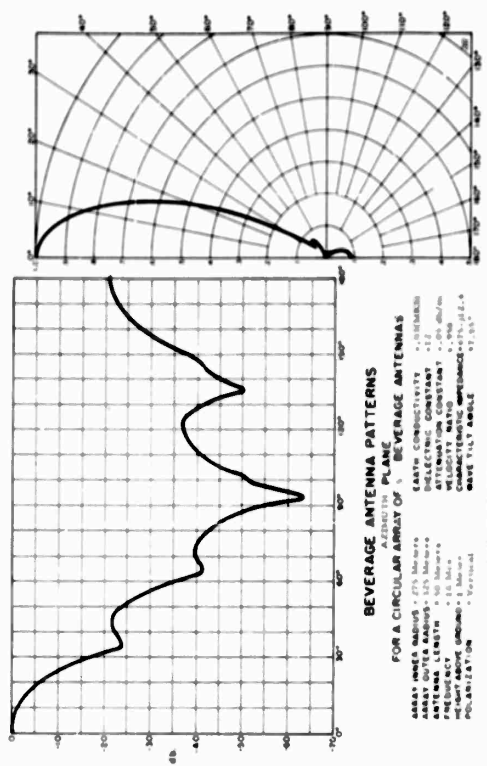


FIGURE II-44

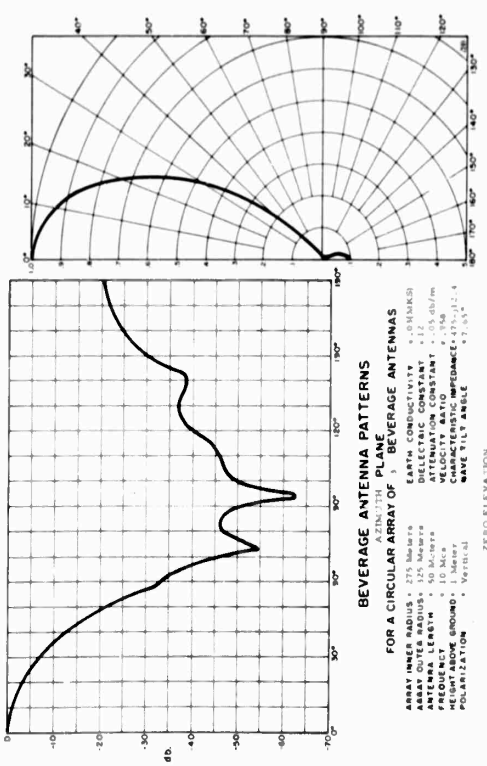


FIGURE II-45

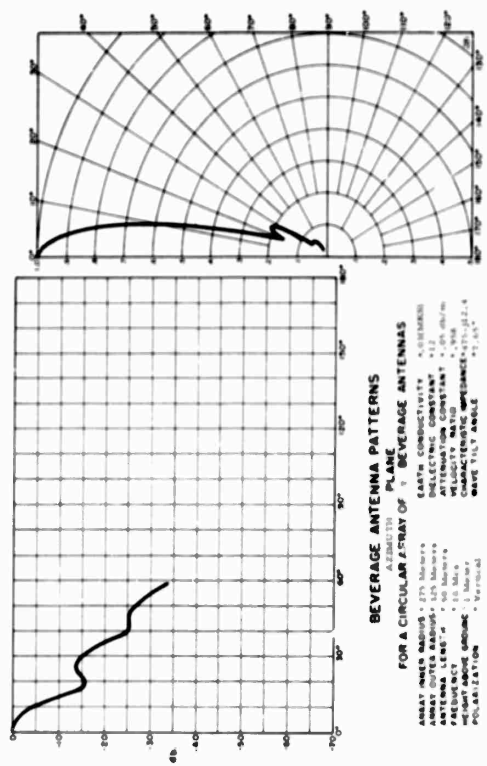


FIGURE II-46

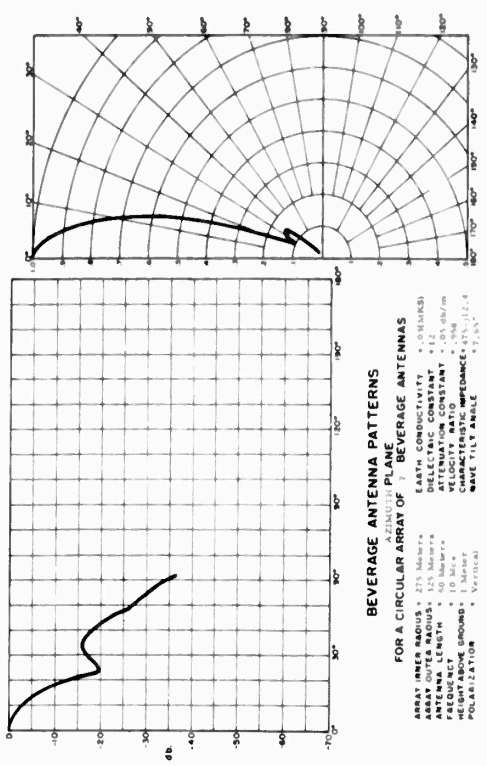
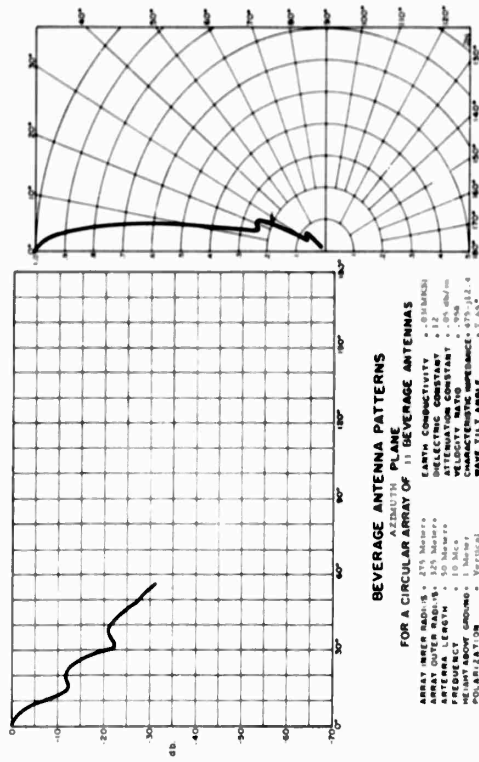


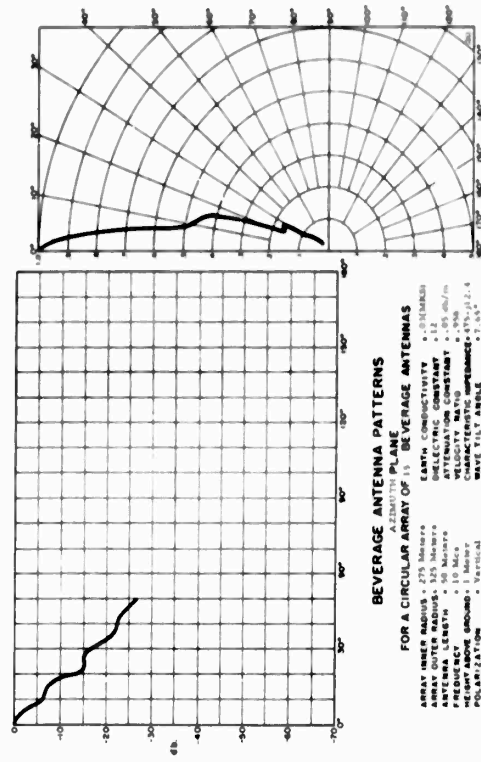
FIGURE II-47



BEVERAGE ANTENNA PATTERNS
FOR A CIRCULAR ARRAY OF 31 BEVERAGE ANTENNAS

ALL ANTENNAS 2° APART
 ZERO ELEVATION
 POLARIZATION = Vertical
 HEIGHT ABOVE GROUND = 1 Meter
 FREQUENCY = 10 Mc
 WAVELENGTH = 30 Meters
 ATTENUATION CONSTANT = 0.05 db/m
 DIELECTRIC CONSTANT = 1.2
 EARTH CONDUCTIVITY = 0.001 MUMHO
 ARRAY OUTER RADIUS = 375 Meters
 ARRAY INNER RADIUS = 275 Meters
 CHARACTERISTIC IMPEDANCE = 675-j12.4
 WAVE TILT ANGLE = 7.55°

FIGURE D-49



BEVERAGE ANTENNA PATTERNS
FOR A CIRCULAR ARRAY OF 15 BEVERAGE ANTENNAS

ALL ANTENNAS 2° APART
 ZERO ELEVATION
 POLARIZATION = Vertical
 HEIGHT ABOVE GROUND = 1 Meter
 FREQUENCY = 10 Mc
 WAVELENGTH = 30 Meters
 ATTENUATION CONSTANT = 0.05 db/m
 DIELECTRIC CONSTANT = 1.2
 EARTH CONDUCTIVITY = 0.001 MUMHO
 ARRAY OUTER RADIUS = 375 Meters
 ARRAY INNER RADIUS = 275 Meters
 CHARACTERISTIC IMPEDANCE = 675-j12.4
 WAVE TILT ANGLE = 7.55°

FIGURE D-79

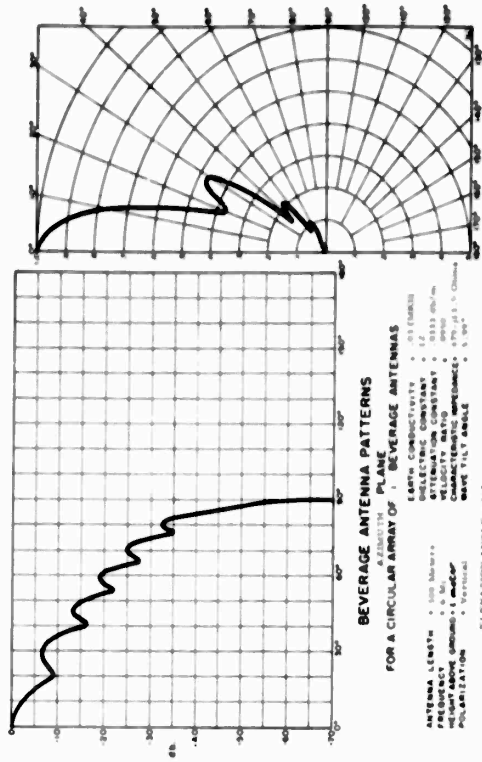


FIGURE II-71

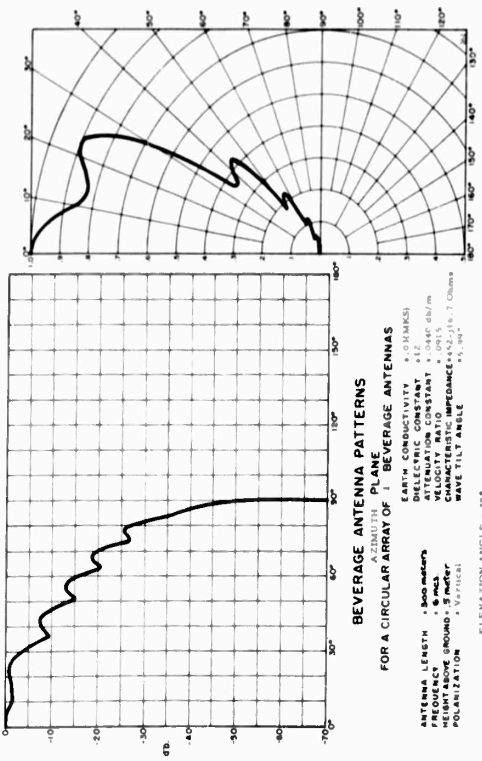


FIGURE II-72

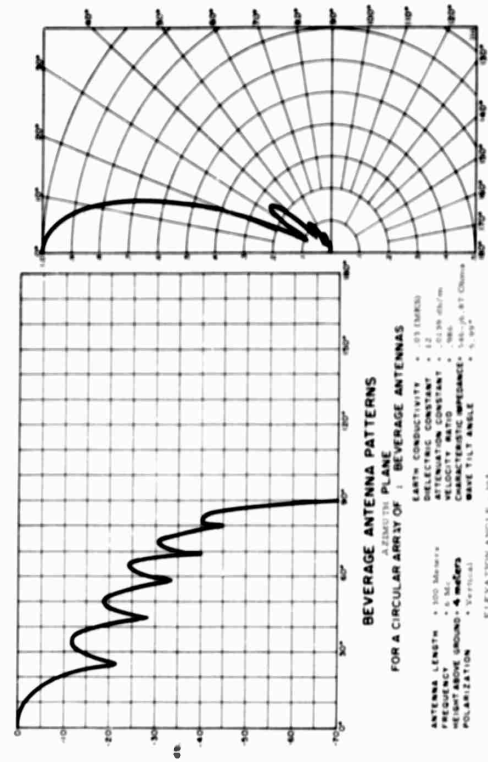


FIGURE II-73

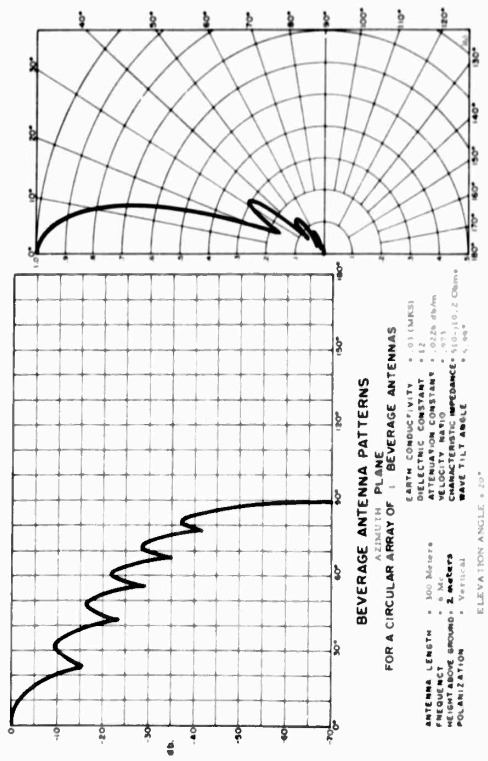


FIGURE II-74

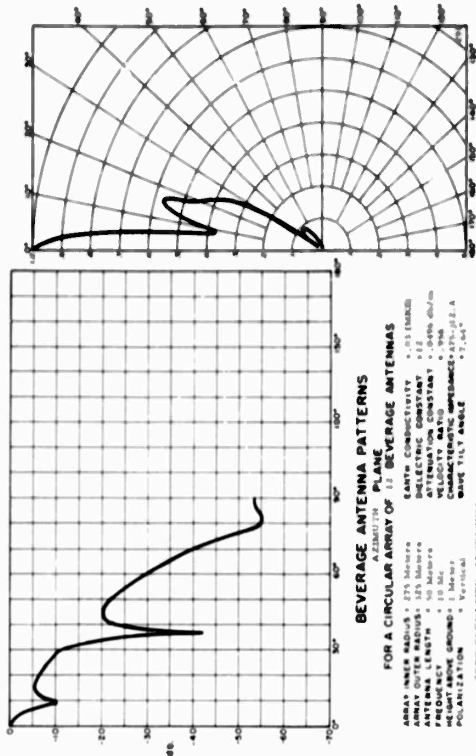


FIGURE II-75
 (See Text for explanation of antenna placement)

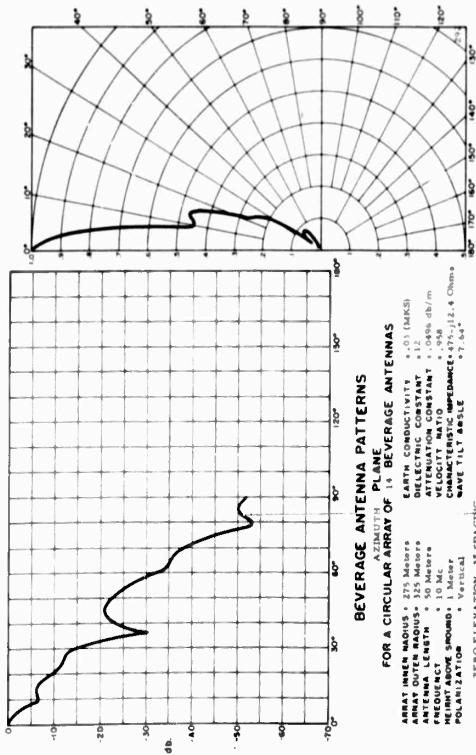


FIGURE II-76
 (See Text for explanation of antenna placement)

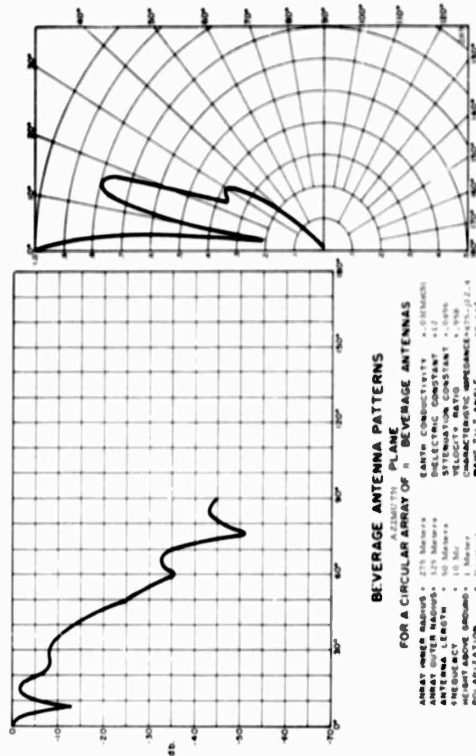


FIGURE II-77
 (See Text for explanation of antenna placement)

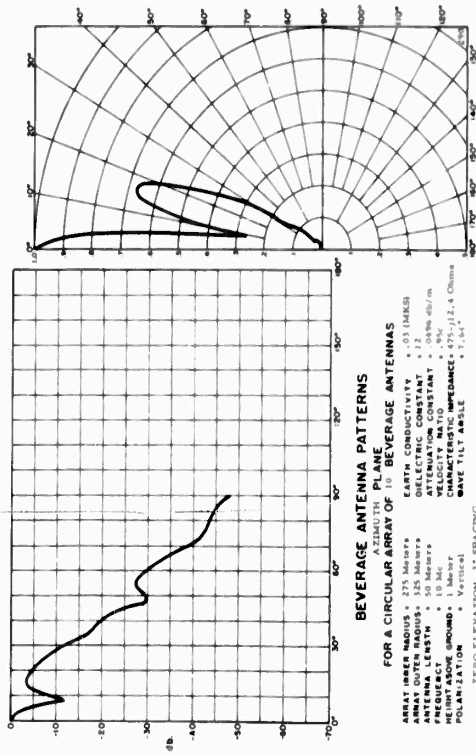


FIGURE II-78
 (See Text for explanation of antenna placement)

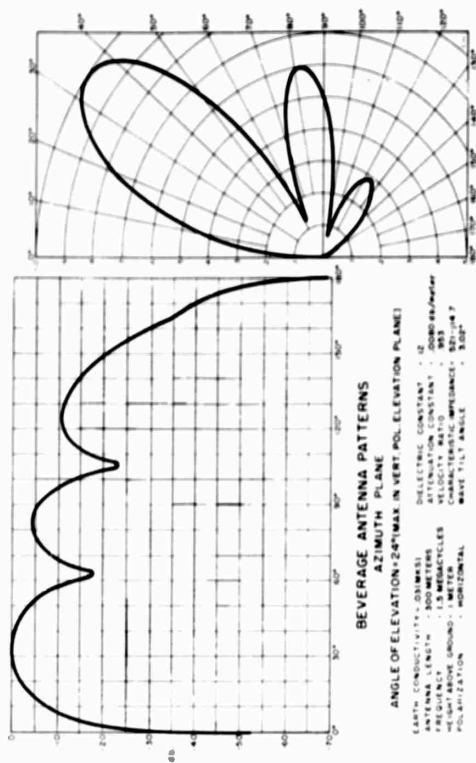


FIGURE III-2

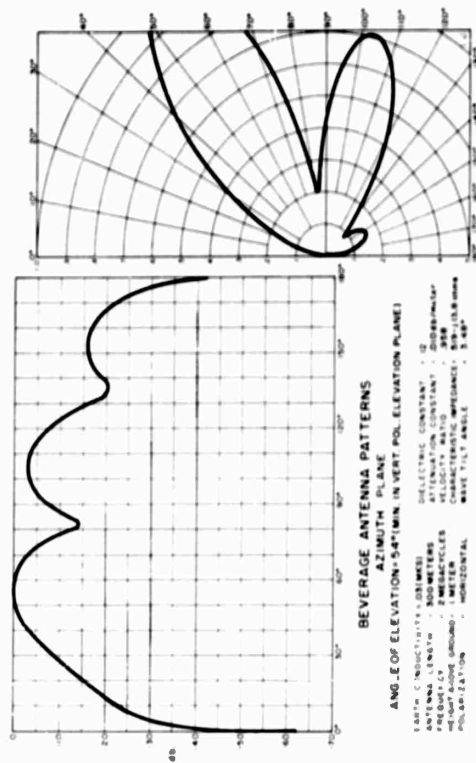


FIGURE III-4

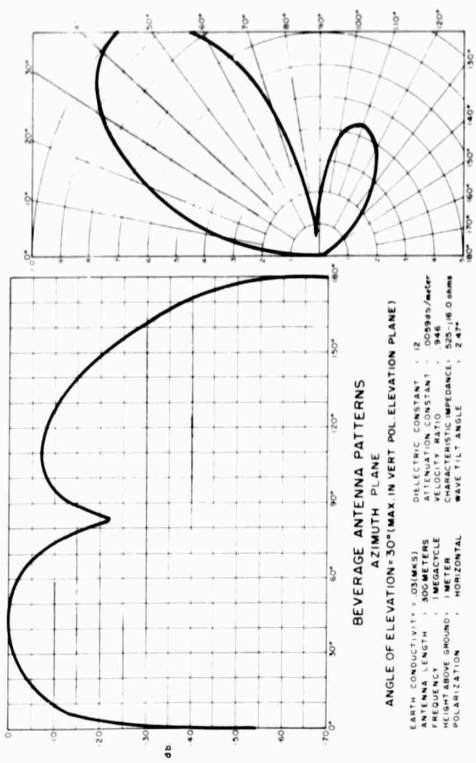


FIGURE III-1

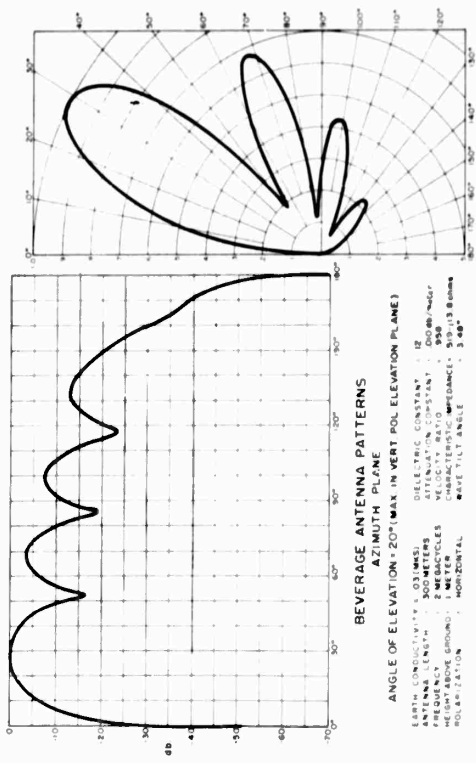


FIGURE III-3

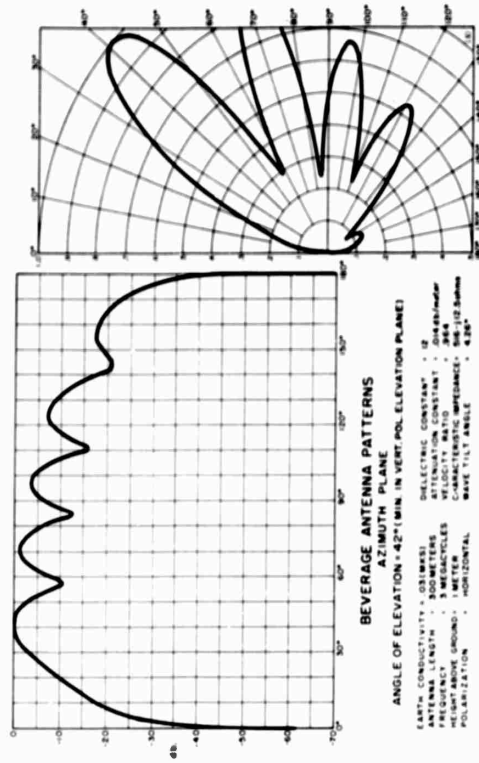


FIGURE III-4

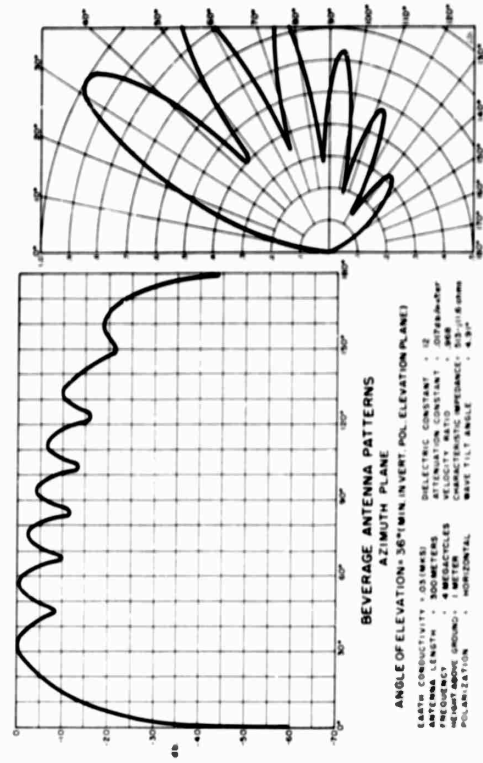


FIGURE III-6

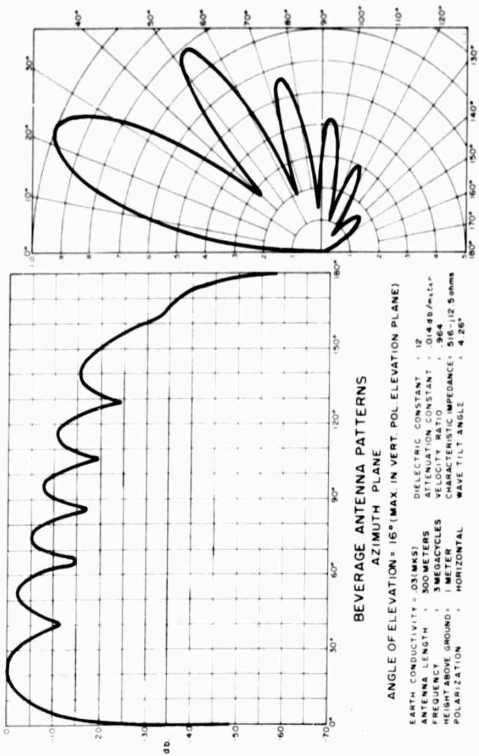


FIGURE III-5

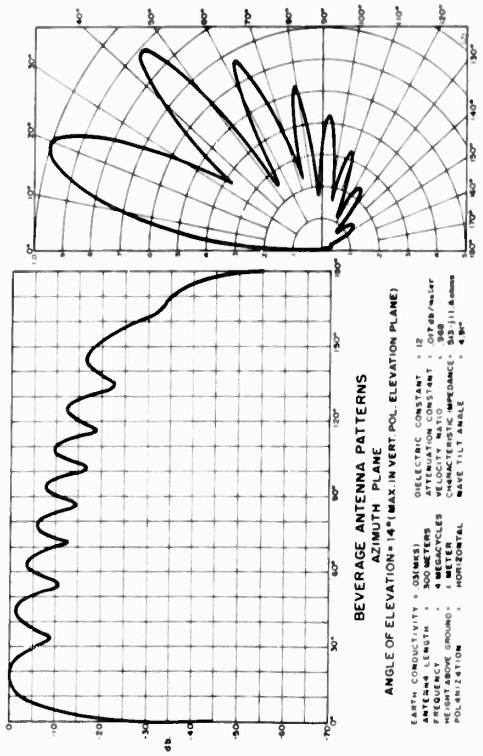


FIGURE III-7

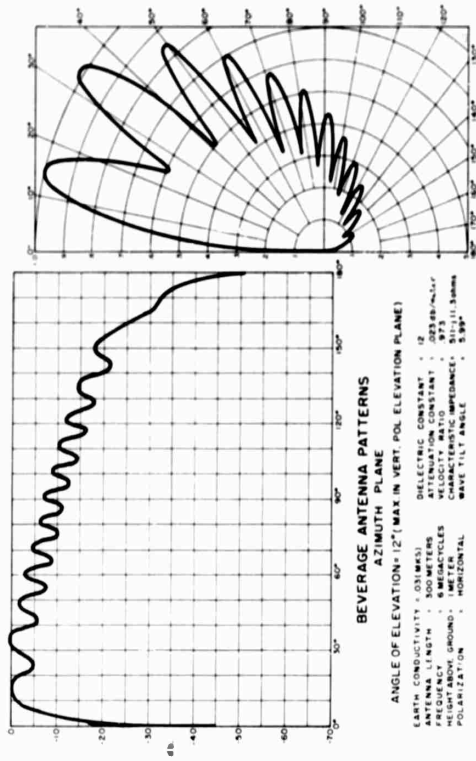


FIGURE III-9.

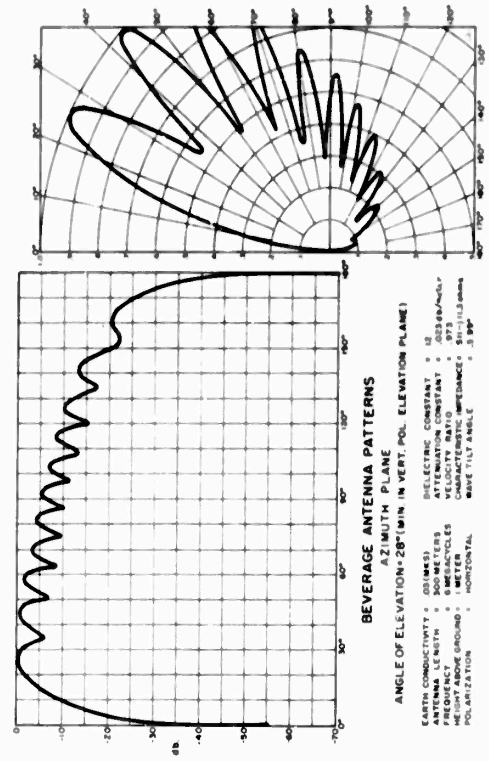


FIGURE III-10.

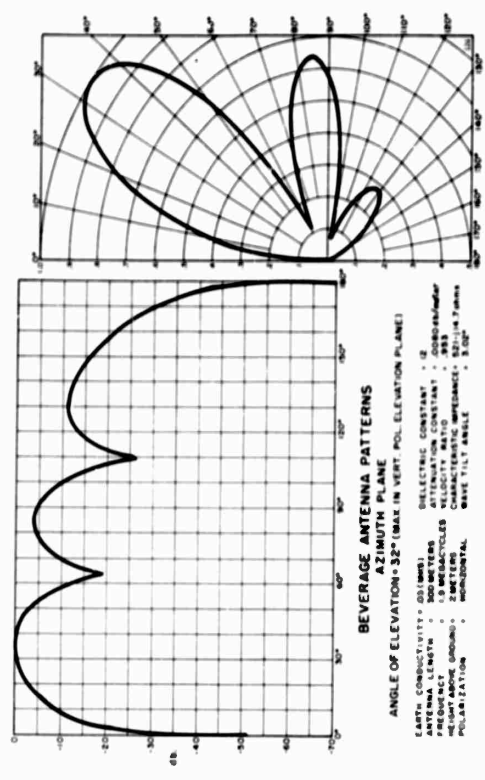


FIGURE 10-11

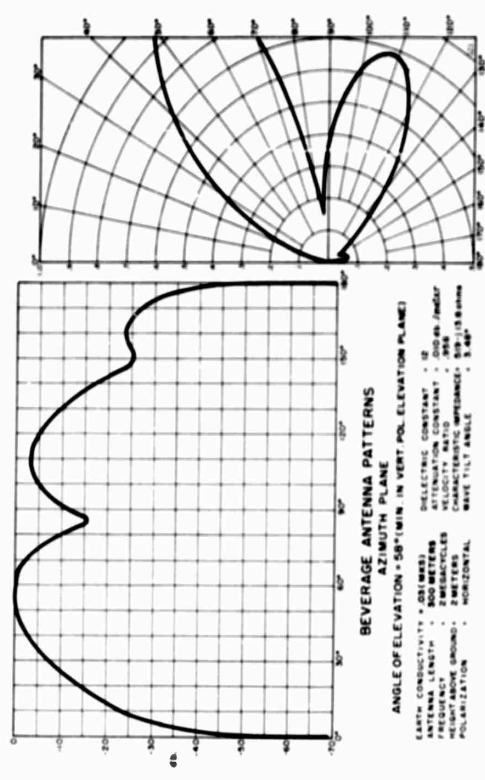


FIGURE 10-12

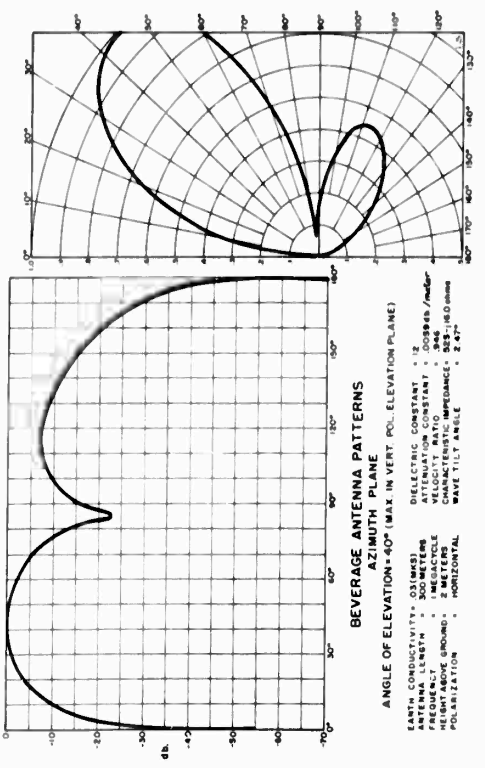


FIGURE 10-13

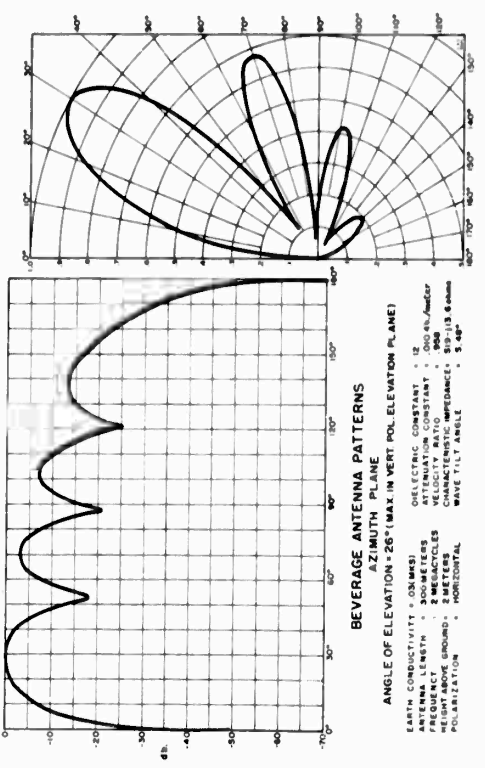


FIGURE 10-14

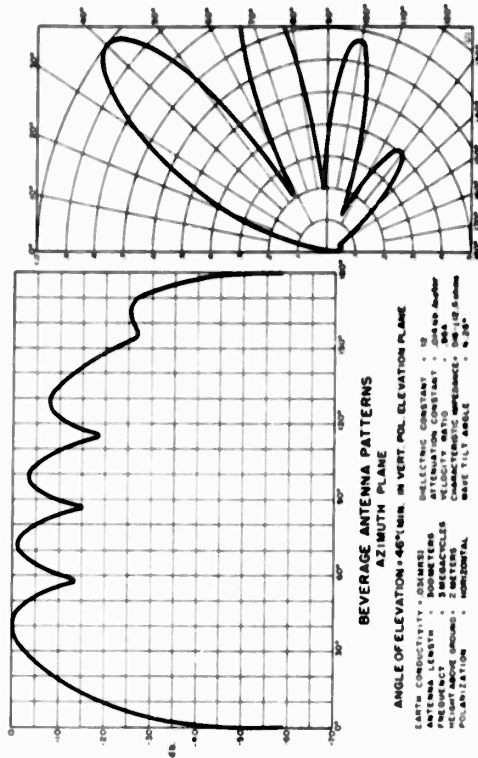


FIGURE III-14

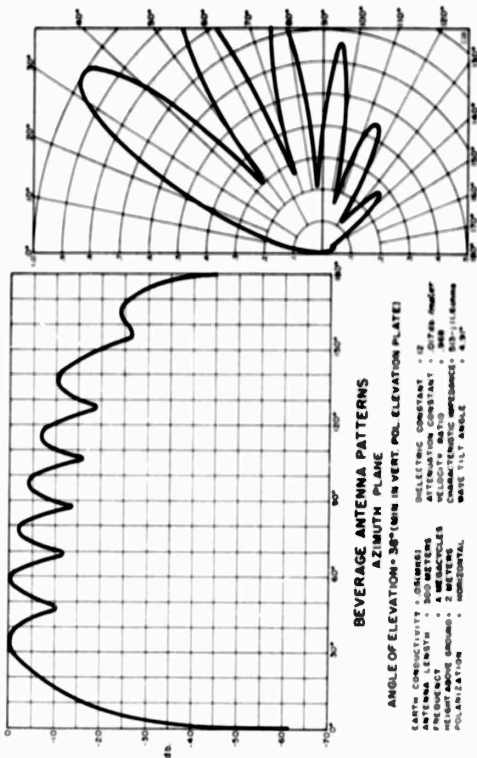


FIGURE III-15

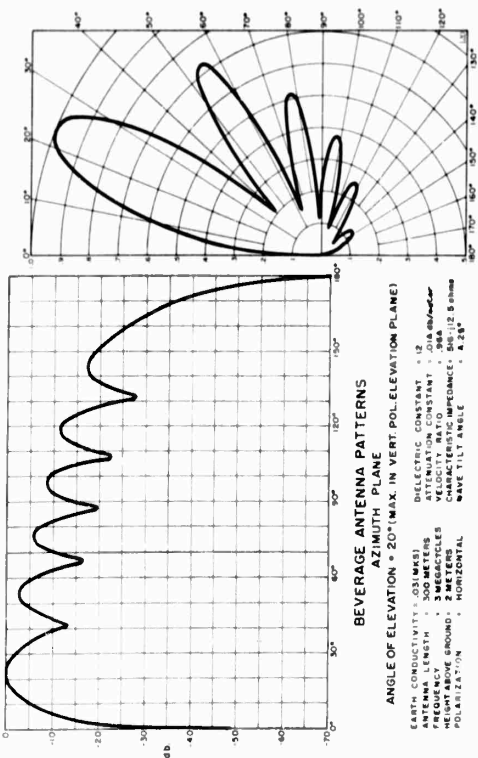


FIGURE III-16

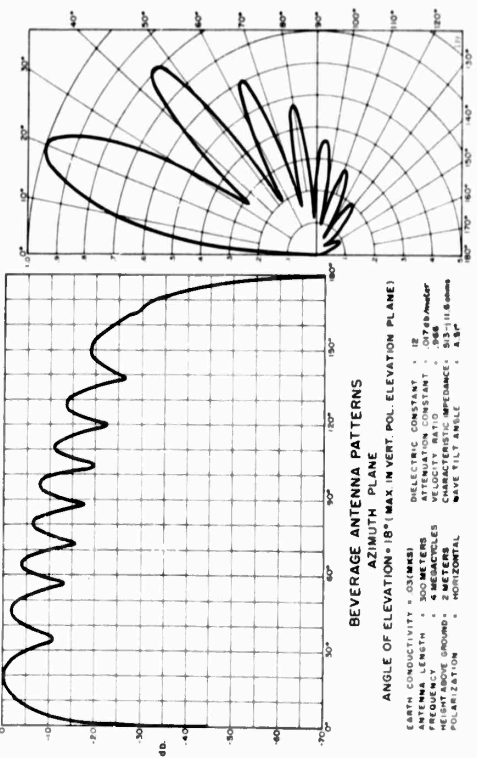


FIGURE III-17

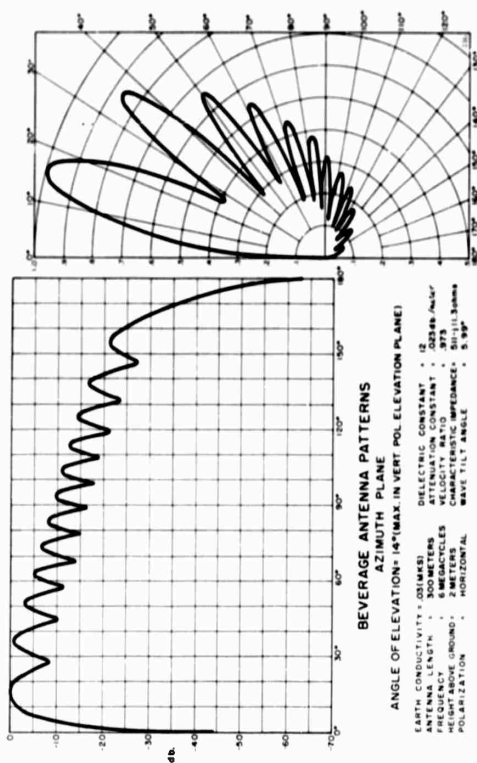


FIGURE 18-19

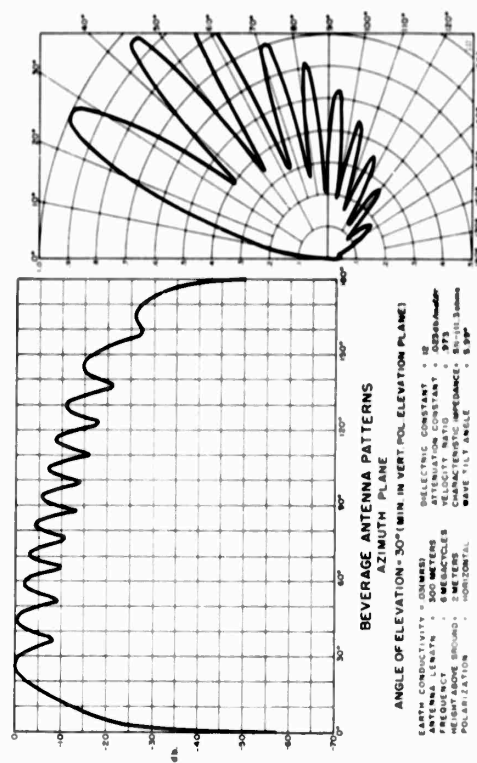


FIGURE 18-20

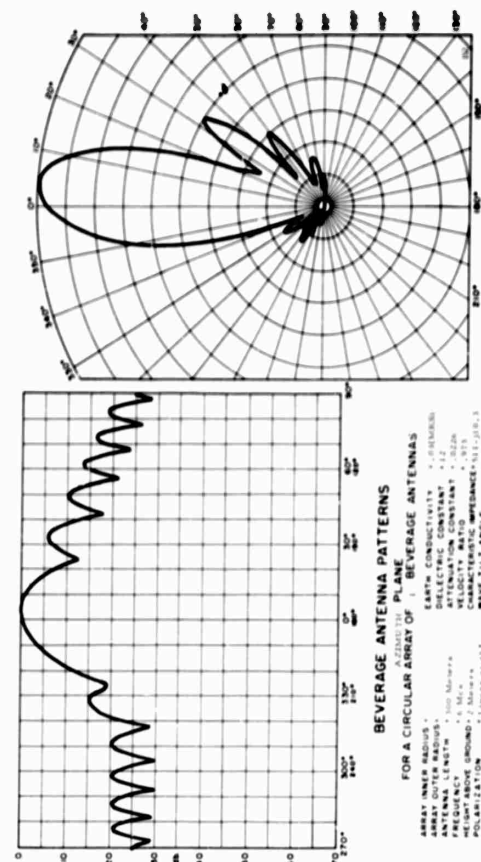


FIGURE III-21

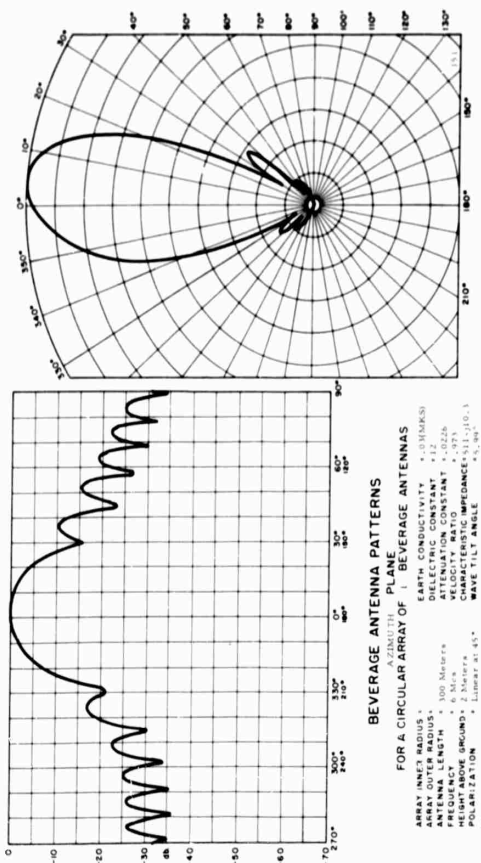


FIGURE III-22

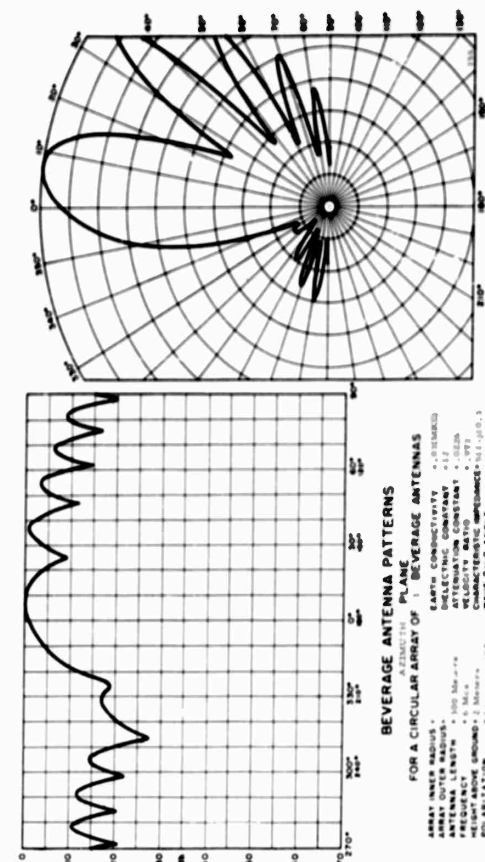


FIGURE III-23

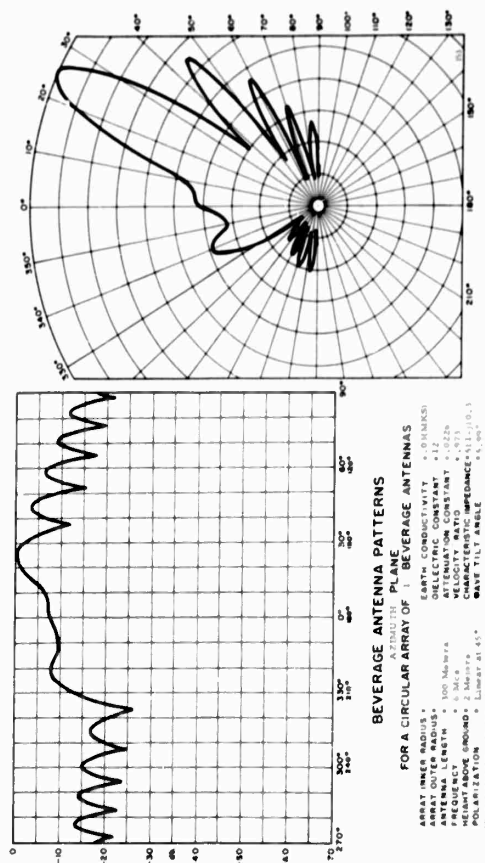


FIGURE III-24

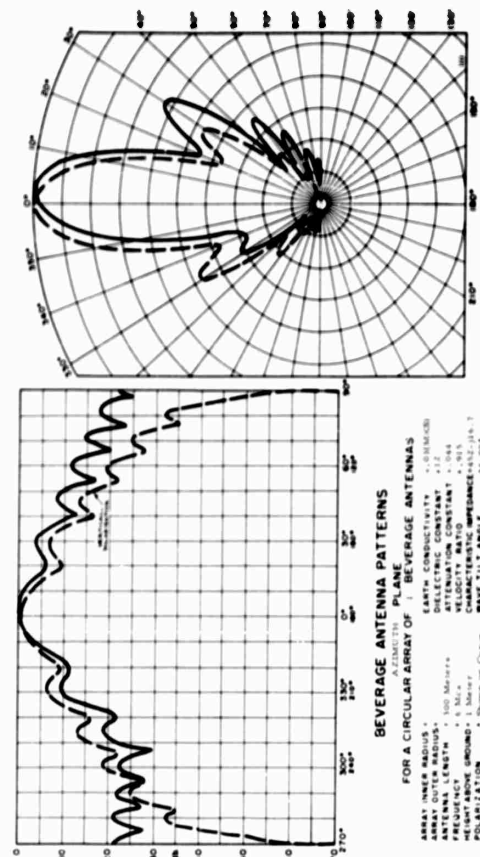


FIGURE III-25

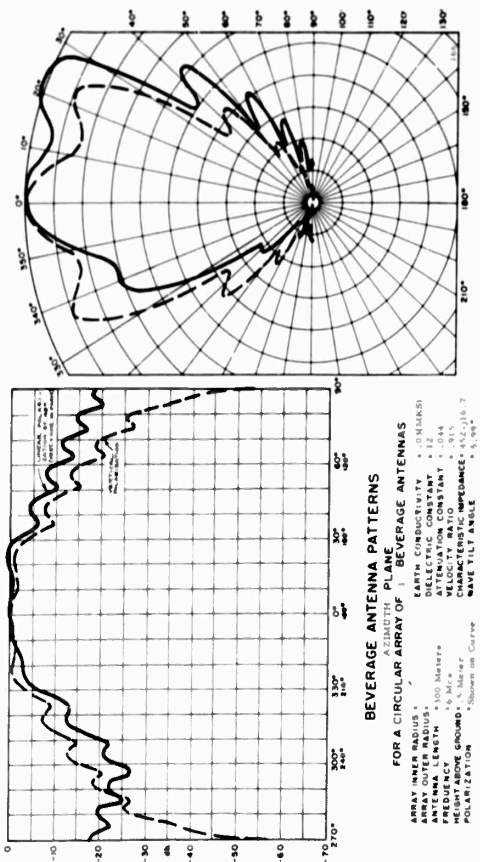


FIGURE III-26

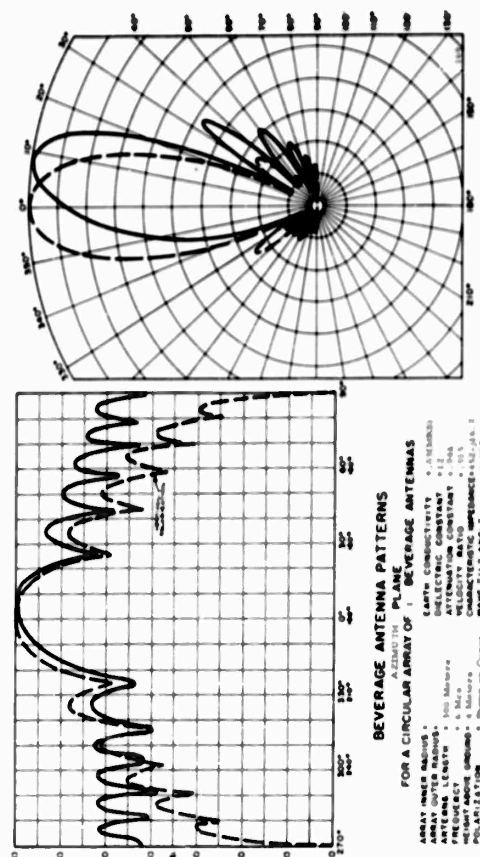


FIGURE III-27

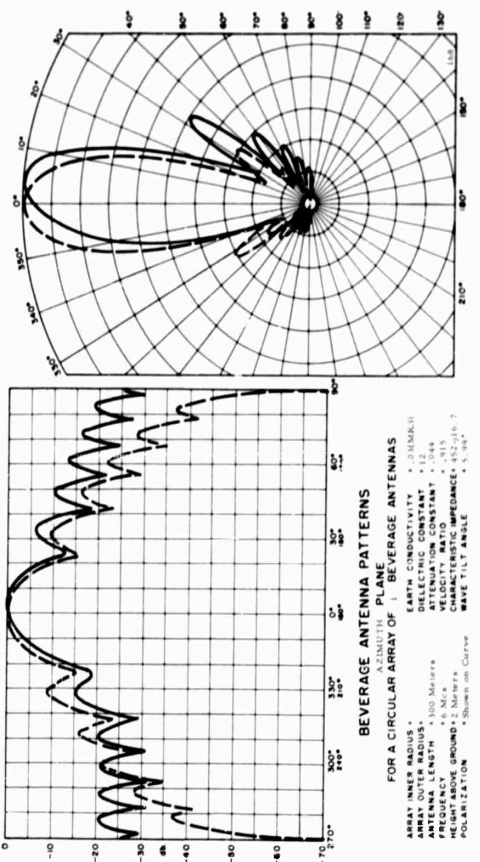


FIGURE III-28

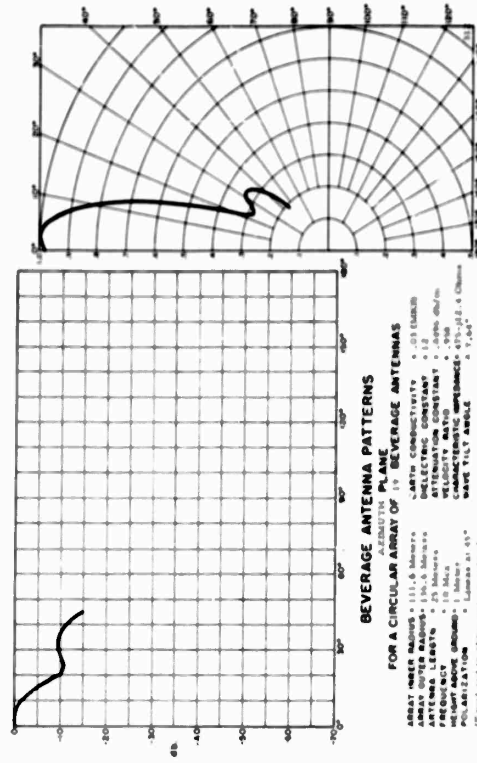


FIGURE III-29

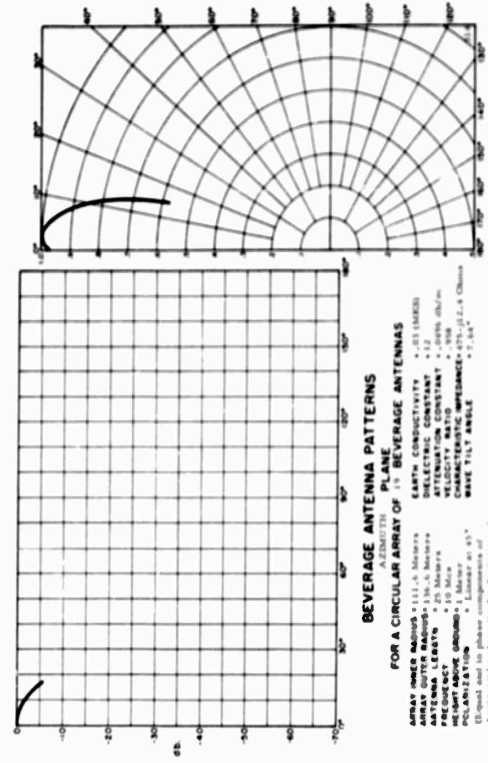


FIGURE III-30

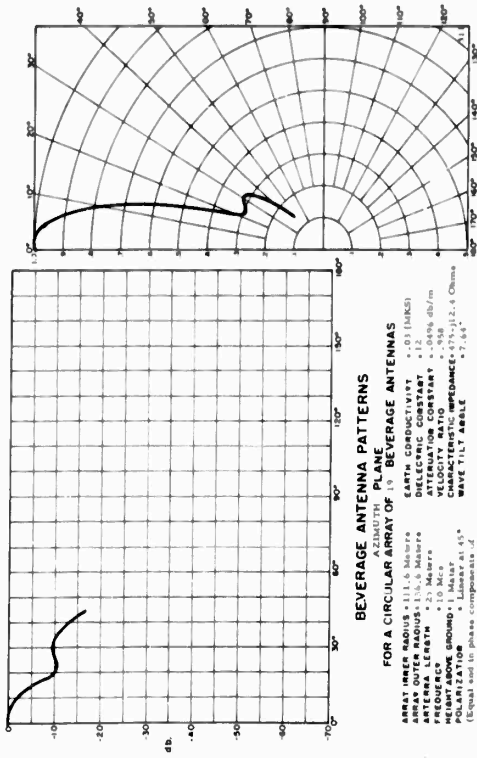


FIGURE III-31

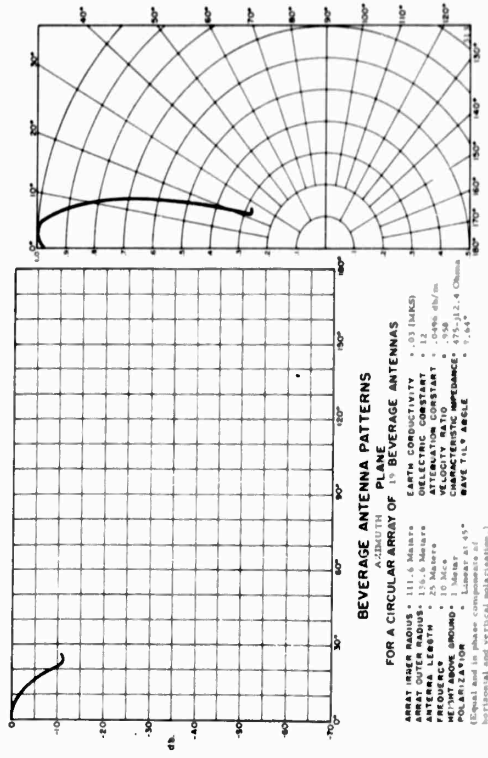


FIGURE III-32

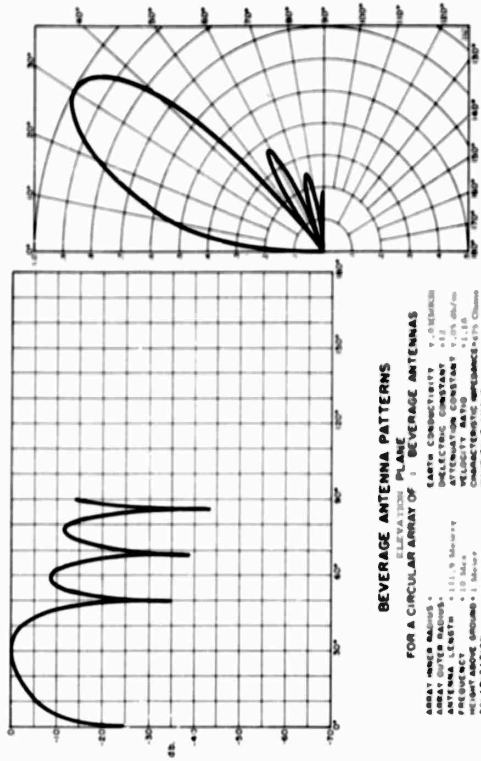


FIGURE IV-1

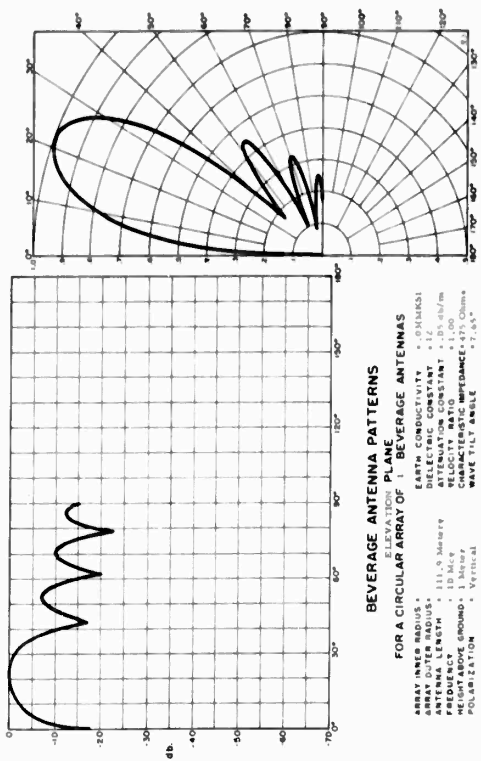


FIGURE IV-2

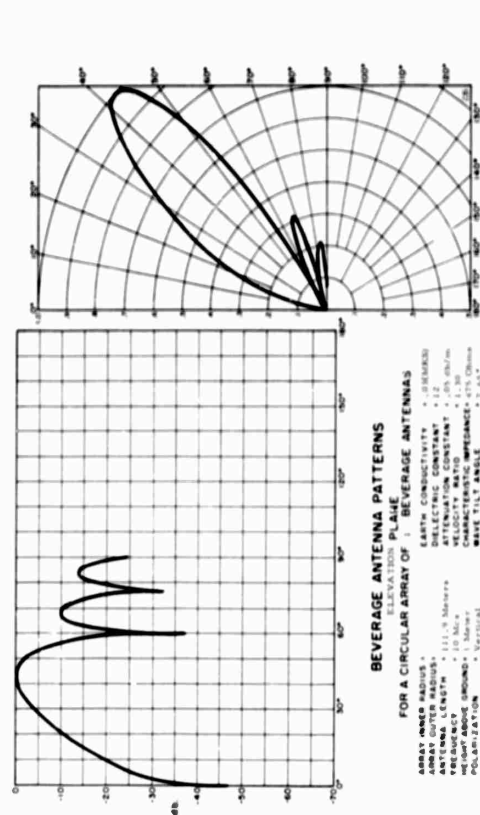


FIGURE IV-3

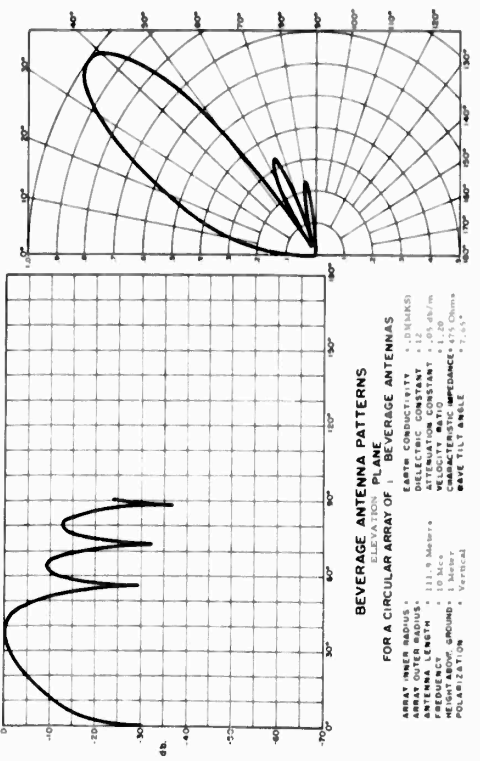
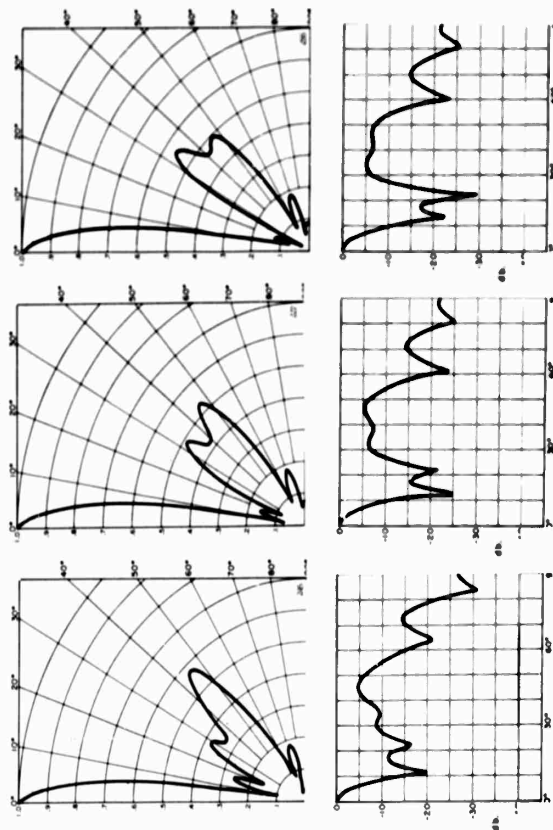


FIGURE IV-4



BEVERAGE ANTENNA PATTERNS
 IN THE AZIMUTH PLANE
 FOR A CIRCULAR ARRAY OF 4 BEVERAGE ANTENNAS

ARRAY RADIUS • 24.75 Meters
 EARTH CONDUCTIVITY • 0.01 MKS
 ANTENNA LENGTH • 111.9 Meters
 ATTENUATION CONSTANT • 25 dB/m
 FREQUENCY • 10 Mc/s
 VELOCITY RATIO • 2.98
 POLARIZATION • VERTICAL
 WAVE TILT ANGLE • 7.15°

TWO PAIRS 180° APART IN PHASE

FIGURE IV-5

F. Comments and Conclusions

Theoretical characteristics of a circular array of radially arranged Beverage antennas have been investigated with respect to direction finding applications in the medium, high frequency and very high frequency ranges. Results suggest that the Beverage antenna may be used as an effective antenna element in wide aperture circular direction finding arrays over wide frequency ranges normally associated with frequency independent antennas.

The Beverage antenna consists simply of a long horizontal wire, parallel to the surface of the earth and at a low height above ground. It is always arranged radially from the receiving point to the direction of desired reception since it is an end fire antenna operating in a traveling wave mode. A typical element for the 2 to 30 mc range may be constructed for less than \$50 (the cost of materials) and it is therefore possible to construct a circular array of 180 such antennas on a 900-ft diameter site for less than a total cost of \$20,000 exclusive of receiving and commutating equipment, and input cables. In view of such an unusually low cost for a wide aperture antenna system, covering more than the entire high frequency range, it is of interest to make a detailed theoretical and experimental examination of performance characteristics. Both investigations have been under way at this laboratory for about four years. A new and detailed theoretical investigation has been under way for the past two years, and a number of broad conclusions may now be stated. This report (Part IV) is almost entirely concerned with theory except where experimental work has provided confirmation or where directions of theoretical investigation have been indicated. Detailed conclusions are given in Part II and Part III of this report which concern theoretical results as compared with measured results on existing systems.

1. Accuracy Expected Based on Theory

It was reported in 1962 that low standard deviations could be obtained on long range randomly polarized sky wave signals in the frequency range of 3 to 30 mc. In 1961 a figure of 1° was measured for 36 antennas 300 meters long looking in a 72° sector toward the northeast quadrant. In 1961 a standard deviation of 4.28° was also obtained with 36 112-meter-long antennas covering 360° during the same testing period. Further accuracy experiments have been conducted since that time showing improved results (see Part III) and some accuracy calculations reported herein have been made for assumed incident fields of mixed polarization. Polarization error calculations reported herein indicate that long range horizontally polarized sky wave components may momentarily introduce

small errors, up to a few degrees, under the worst conditions. The appearance of the patterns when horizontally polarized components are present is slightly asymmetrical (or fully symmetrical when only vertical polarization is present). Thus even though the polarization error is low, a clear criterion exists for observing when polarization error is at its lowest. The polarization error does not appear to be significant, and the results of experiments reported in Section III bear this out.

2. Bandwidth

The antenna is essentially a matched transmission line and has an impedance which is approximately independent of frequency. Calculations indicate that very favorable impedances can be obtained for a 40 to 1 frequency range, say, from 1 to 40 mc. There is no theoretical reason why a constant impedance may not be obtained for a very wide frequency range, say, 1 to 100 mc or a range which is so wide as to be limited by other characteristics.

It is possible to obtain narrow beamwidths in the azimuth plane over a wide frequency range without phasing the antennas. Furthermore, it is possible to vary the beamwidth quickly at a given frequency. It is also possible to obtain very favorable elevation patterns so that narrow beam azimuth patterns are obtained up to angles of elevation of 70° over the entire HF frequency range. It is to be emphasized that these patterns are obtained without phasing the elements but are obtained by simple summation of a sector of antennas as they occur in the circular array (by commutating the summed sectors, the patterns are displayed on a CRT). Further details and exact beamwidths which can be obtained are reported in Part II.

3. Effective Height and Sensitivity

Analysis shows that the effective height of an ideal Beverage antenna is approximately $\delta l / 2$ where δ is the wave tilt in radians typically on the order of 10 or 15 degrees, and l is the antenna length in meters. This means that a single element 100 meters long may have an effective height on the order of five meters at a typical frequency. Summation of arrays of 10 to 20 elements may produce effective heights 5 to 10 times the element effective height. The antennas are, therefore, comparable in sensitivity to other wide aperture typical antenna arrays used for high frequency direction finding.

4. Computer Analysis

A digital computer program has been prepared to make exact calculations of azimuth and elevation patterns for circular arrays of Beverage antennas. Only a few hundred patterns have been computed at this time, and the detailed investigation of all the parameters which may be varied to produce optimum results has only been initiated. Nevertheless favorable patterns in both azimuth and elevation planes for both vertical and horizontal polarization have been obtained. Design suggestions for very narrow beam azimuth patterns with very broad elevation patterns are simple and promising. The most significant of these is to use shorter elements with a larger inner radius for a fixed overall array diameter.

5. Continued Investigation

On the basis of the theoretical investigations conducted so far, it is clearly apparent that the theoretical investigation should be continued to optimize azimuth and elevation patterns, and an extensive experimental program should be initiated to compare the performance of a low cost Beverage system with other wide aperture high frequency direction finders. It is suggested that the present existing antenna arrays at Southwest Research Institute be used for such tests.

G. Recommendations

It is recommended that investigation of the circular Beverage array for wide aperture high frequency direction finding be continued, utilizing the antennas in their simple low cost form. Comparison with other wide aperture high frequency direction finders should be made on a quantitative basis. Several types of high frequency direction finders are in use or have been suggested and should be compared. These include the Wullenweber, the Doppler array, the Beverage array, the interferometer array and others, and finally the recently suggested variation on the Luneberg Lens.* Each of these antenna systems may have an area of application where its performance is near a maximum. Since the Beverage system is unquestionably the lowest in cost of these four, and there is every indication that its accuracy performance is comparable, its performance should be measured in considerable detail.

*Tanner, R. L., et. al., "An Investigation of the HF Wire-Grid Lens Antenna for Direction Finding," RADC-TDR-63-211, December, 1963, Contract No. AF30(602)-2742, TRG-West, A Division of TRG, Incorporated, Menlo Park, California.

H. Bibliography

1. Bailey, A. D., Dyson, J. D., and Hayden, E. C., "Studies and Investigations Leading to the Design of a Radio Direction Finder System for the MF-HF-VHF Range," Fourth Quarterly Report, 30 June 1962, Contract No. DA 36-093-SC-87264, EERL, University of Illinois, Urbana, Illinois.
2. Beverage, Harold H., Rice, Chester W., and Kellogg, Edward W., "The Wave Antenna, a New Type of Highly Directive Antenna," Transactions of the American Institute of Electrical Engineers, Volume 42, February 1923, pp. 215-266.
3. Burgess, R. E., "Noise in Receiving Aerial Systems," Proceedings of Physical Society, Vol. 53, May 1941, p. 293.
4. Carson, John R., "Wave Propagation in Overhead Wires with Ground Return," The Bell System Technical Journal, Volume V, 1926, pp. 539-554.
5. Feldman, C. B., "The Optical Behavior of the Ground for Short Radio Waves," Proceedings of the I.R.E., Vol. 21, No. 6, June 1933, pp. 764-801.
6. Gill, E. W. B., "A Simple Method of Measuring Earth Constants," Proc. of the Inst. of Electrical Engineers (London), Vol. 96, March 1949, pp. 141-145.
7. Herlitz, Ivar, "Appendix B, Analysis of Action of Wave Antenna," (An Appendix to the paper by Beverage, Rice and Kellogg, "The Wave Antenna, a New Type of Highly Directive Antenna"), Transactions of the American Institute of Electrical Engineers, Volume 42, February 1923, pp. 260-266.
8. Jordan, Edward C., Electromagnetic Waves and Radiating Systems, New York, Prentice-Hall, Inc., 1950.
9. Nyquist, H., "Thermal Agitation of Electric Charge in Conductors," Physical Review, Vol. 32, July 1928, p. 110.
10. Piggott, W. R., "A Method of Determining the Polar Diagrams of Long Wire and Horizontal Rhombic Aerials," Dept. of Scientific and Industrial Research, Radio Research Special Report No. 16, London, H.M. Stationery Office, 1948.

11. Schelkunoff, Sergei A., and Friis, Harald T., Antennas Theory and Practice, New York, John Wiley & Sons, Inc., 1952, p. 301, problem 9.13.
12. Skilling, Hugh Hildreth, Transient Electric Currents, McGraw-Hill Book Company, Inc., New York, 1952.
13. Skilling, Hugh H., Electric Transmission Lines, McGraw-Hill Book Company, Inc., New York, 1951.
14. Storer, James E., and King, Ronold, "Radiation Resistance of Two-Wire Line," Proceedings of the IRE, Vol. 39, No. 6, 1951, pp. 1408-1412.
15. Terman, F., Radio Engineers Handbook, McGraw-Hill Book Co., Inc., New York, 1943, p. 476.
16. Wait, James R., "Radiation from a Ground Antenna," Canadian Journal of Technology, Vol. 32, No. 1, January 1954, pp. 1-9.
17. Wait, James R., "Propagation of Radio Waves over a Stratified Ground," Geophysics, Vol. 18, 1953, pp. 416-422.
18. Wise, W. H., "Capacity of a Pair of Insulated Wires," Quarterly of Applied Mathematics, Vol. 7, January 1950, pp. 432-436.
19. Wise, W. H., "Potential Coefficients for Ground Return Circuits," The Bell System Technical Journal, Vol. 27, April 1948, pp. 365-371.
20. Wise, W. Howard, "The Physical Reality of Zenneck's Surface Wave," The Bell System Technical Journal, Vol. XVI, January 1937, pp. 35-44.
21. Wise, W. H., "Some Bessel Function Expansions," The Bell System Technical Journal, Vol. XLI, October 1935, pp. 700-706.
22. Wise, W. H., "Propagation of High-Frequency Currents in Ground Return Circuits," Proceedings of the IRE, Vol. 22, No. 4, April 1934, pp. 522-527.

23. Wise, W. Howard, "Note on Dipole Radiation Theory," Physics, Vol. 4, October 1933, pp. 354-358.
24. Wise, W. Howard, "Effect of Ground Permeability on Ground Return Circuits," The Bell System Technical Journal, Vol. X, July 1931, pp. 472-484.
25. Zenneck, J., "The Propagation of Plane Electromagnetic Waves over a Flat Earth and Its Application to Wireless Telegraphy," Annalen der Physik, Vol. 23, 1907, p. 846.


APPENDIX I

REPRINT OF "WAVE PROPAGATION IN OVERHEAD WIRES
WITH GROUND RETURN" BY JOHN R. CARSON

SOUTHERN

LIBRARY

~~FEB 1926~~

<p>BELL TELEPHONE LABORATORIES INCORPORATED</p>	<p>NOVEMBER 1926</p>  <p>REPRINT B-219</p>
<p>WAVE PROPAGATION IN OVERHEAD WIRES WITH GROUND RETURN</p>	
<p>BY</p>	
<p>JOHN R. CARSON</p>	
<p>American Telephone and Telegraph Company</p>	
<p>A MATHEMATICAL ANALYSIS OF WAVE PROPAGATION IN GROUND-RETURN CIRCUITS WITH FORMULAS FOR CALCULATING INDUCTIVE DISTURBANCES IN NEIGHBORING LINES</p>	

BELL TELEPHONE LABORATORIES
INCORPORATED
463 WEST STREET, NEW YORK

REPRINT OF PAPER

Published in

THIS BELL SYSTEM TECHNICAL JOURNAL
VOL. V, PP. 339-344
OCTOBER, 1926

Copyright, 1926, by
AMERICAN TELEPHONE AND TELEGRAPH COMPANY

Printed in the United States of America

Wave Propagation in Overhead Wires with Ground Return

By JOHN R. CARSON
American Telephone and Telegraph Company

I

THE problem of wave propagation along a transmission system composed of an overhead wire parallel to the (plane) surface of the earth, in spite of its great technical importance, does not appear to have been satisfactorily solved.¹ While a complete solution of the actual problem is impossible, on account of the inequalities in the earth's surface and its lack of conductive homogeneity, the solution of the problem, where the actual earth is replaced by a plane homogeneous semi-infinite solid, is of considerable theoretical and practical interest. The solution of this problem is given in the present paper, together with formulas for calculating inductive disturbances in neighboring transmission systems.

The axis of the wire is taken parallel to the z -axis at height h above the xz -plane and passes through the y -axis at point O' as shown in Fig. 1 herewith. The "image" of the wire is designated by O'' .

For $y > 0$ (in the dielectric) the medium is supposed to have zero conductivity, while for $y < 0$ (in the ground) the conductivity of the medium is designated by λ . The xz -plane represents the surface of separation between dielectric and ground.

We consider a wave propagated along the z -axis and the current, charge and field are supposed to contain the common factor $\exp(-\Gamma z + i\omega t)$, which, however, will be omitted for convenience in the formulas. The propagation constant, Γ , is to be determined. It is assumed, *ab initio*, as a very small quantity in c.g.s. units.²

In the ground ($y \leq 0$) the axial electric force is formulated as the

¹ See Rudenberg, *Zt. f. Angewandte Math. u. Mechanik*, Band 5, 1925. In that paper the current density in the ground is assumed to be distributed with radial symmetry. The resulting formulas are not in agreement with those of the present paper. Since this paper was set up in type I have learned that formulas equivalent to equations (26), (28), (31) for the mutual impedance of two parallel wires were obtained by my colleague, Dr. G. A. Campbell, in 1917. It is to be hoped that his solution will be published shortly.

² The simplifying assumptions introduced in this analysis are essentially the same as those employed and discussed in "Wave Propagation Over Parallel Wires: The Proximity Effect," *Phil. Mag.*, Vol. xli, April, 1921.

general solution, symmetrical with respect to x , of the wave equation; thus

$$E_z = - \int_0^\infty F(\mu) \cos x\mu e^{i\sqrt{\mu^2 + \alpha} y} d\mu, \quad y \leq 0 \quad (1)$$

where

$$\alpha = 4\pi\lambda\omega,$$

$$\lambda = \text{conductivity of ground in c.m. c.g.s. units,}$$

$$i = \sqrt{-1},$$

$\omega/2\pi = \text{frequency in cycles per second.}$

(In the following analysis and formulas, c.m. c.g.s. units are employed throughout).

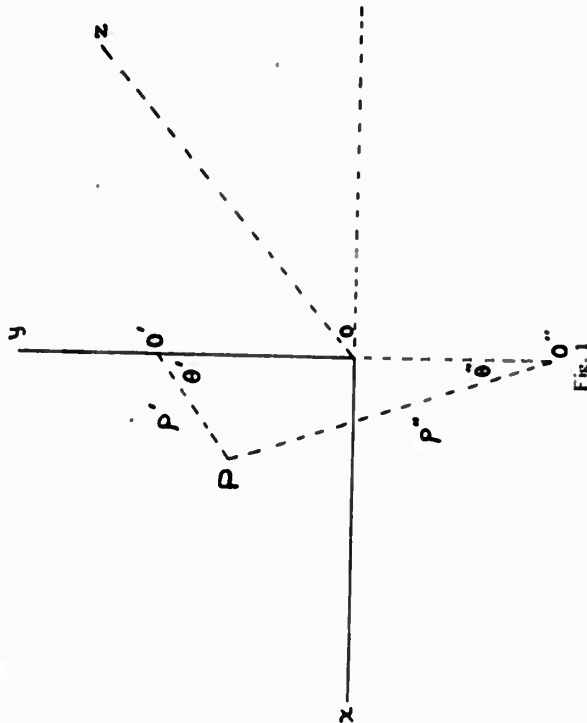


Fig. 1

Assuming that in the ground E_x and E_y are negligible compared with E_z , we have from the formula, $\text{curl } E = -\frac{\partial H}{\partial t}$,

$$i\omega H_x = -\frac{\partial E_z}{\partial y}$$

$$i\omega H_y = \frac{\partial E_z}{\partial x}$$

Whence, in the ground

$$H_x = \frac{1}{i\omega} \int_0^\infty \sqrt{\mu^2 + i\alpha} F(\mu) \cos x\mu e^{\sqrt{\mu^2 + i\alpha} y} d\mu \quad (2)$$

$$H_y = \frac{1}{i\omega} \int_0^\infty \mu F(\mu) \sin x\mu e^{\sqrt{\mu^2 + i\alpha} y} d\mu \quad (3)$$

it being understood that $y \leq 0$. The function $F(\mu)$ in the preceding formulas is to be determined by the boundary conditions.

In the dielectric, H_x and H_y may be regarded as composed of two components; thus

$$\begin{aligned} H_x &= H_x^0 + H_x' \\ H_y &= H_y^0 + H_y' \end{aligned}$$

where H_x^0, H_y^0 designate the field due to the current I in the wire, and H_x', H_y' the field of the ground current.

Neglecting axial displacement currents in the dielectric, and assuming that the wire is of sufficiently small radius so that the distribution of current over its cross section is symmetrical, we have

$$H_x^0 = \frac{\cos \Theta'}{\rho'} \cdot 2I, \quad (4)$$

$$H_y^0 = \sin \Theta' \cdot 2I, \quad (5)$$

$$\begin{aligned} \rho' &= \sqrt{x^2 + (y-h)^2}, \\ \cos \Theta' &= \frac{h-y}{\rho'}, \end{aligned} \quad (6)$$

$$\sin \Theta' = x/\rho'.$$

The secondary magnetic field H_x', H_y' is taken as

$$H_x' = \int_0^\infty \phi(\mu) \cos x\mu e^{-\sqrt{\mu^2 + i\alpha} y} d\mu, \quad (7)$$

$$H_y' = - \int_0^\infty \phi(\mu) \sin x\mu e^{-\sqrt{\mu^2 + i\alpha} y} d\mu. \quad (8)$$

At the surface of separation $y=0$, H_x^0, H_y^0 are expressible as the Fourier integrals

$$H_x^0 = 2I \int_0^\infty \cos x\mu e^{-h\mu} d\mu, \quad (9)$$

$$H_y^0 = 2I \int_0^\infty \sin x\mu e^{-h\mu} d\mu. \quad (10)$$

Also at the surface of separation of the two media ($y=0$), H_x and H_y must be continuous. Equating the values of H_x and H_y at $y=0$, as given by (2), (3) and by (7), (8) and (9), (10), we have

$$\frac{1}{i\omega} \sqrt{\mu^2 + i\alpha} F(\mu) = 2I e^{-h\mu} + \phi(\mu),$$

$$\frac{1}{i\omega} \mu F(\mu) = 2I e^{-h\mu} - \phi(\mu),$$

whence

$$F(\mu) = \frac{i\omega e^{-h\mu}}{\sqrt{\mu^2 + i\alpha} + \mu} 4I, \quad (11)$$

$$\phi(\mu) = \frac{(\sqrt{\mu^2 + i\alpha} - \mu) e^{-h\mu}}{\sqrt{\mu^2 + i\alpha} + \mu} 2I, \quad (12)$$

which determines the functions $F(\mu)$ and $\phi(\mu)$.

Inserting the value of $F(\mu)$, as given by (11) in (1), the axial electric force E_z in the ground ($y \leq 0$) and therefore the distribution of current density in the ground is expressed as a Fourier integral in terms of the frequency $\omega/2\pi$, the current I in the wire, the height h of the wire above ground, and the conductivity λ of the ground. Similarly the insertion of $\phi(\mu)$, as given by (12) in formulas (7) and (8) gives the magnetic field H_x, H_y in the dielectric. Thus

$$E_z(x, y) = E_z = -i4\omega I \int_0^\infty \frac{e^{-\mu y}}{\sqrt{\mu^2 + i\alpha} + \mu} e^{\sqrt{\mu^2 + i\alpha} x} \cos x\mu d\mu \quad y \leq 0. \quad (13)$$

This can be further simplified if we write

$$x' = x\sqrt{\alpha}$$

$$y' = y\sqrt{\alpha}$$

$$h' = h\sqrt{\alpha},$$

whence

$$E_z = -4\omega I \int_0^\infty (\sqrt{\mu^2 + i\alpha} - \mu) e^{-h'\mu} e^{\sqrt{\mu^2 + i\alpha} x'} \cos x'\mu d\mu \quad y' \leq 0. \quad (14)$$

The axial electric force in the dielectric is now to be formulated. This is always derivable from a vector and a scalar potential; thus

$$E_z = -i\omega A_z - \frac{\partial V}{\partial z} \quad (15)$$

where A_z is the vector potential of the axial currents, and V the scalar potential. Consequently,

6

unit length. (With small error this may usually be taken as the resistance per unit length of the wire.) The axial electric intensity at the surface of the wire is then zI . Equating this to the axial electric intensity at the surface of the wire as given by (18) and replacing ∂z by $-I$, we have

$$zI = -4\omega I \int_0^\infty (\sqrt{\mu^2 + i - \mu}) e^{-2\mu z} d\mu - i 2\omega I \log(\rho''/a) + \Gamma I \tag{19}$$

Writing $V = Q/C$ and

$$i\omega Q = \Gamma V - G I = \Gamma V - \frac{G}{C} Q,$$

where G is the leakage conductance to ground per unit length, we have, solving for Γ ,

$$\Gamma^2 = (G + i\omega C) [z + i2\omega \log(\rho''/a)] + 4\omega \int_0^\infty (\sqrt{\mu^2 + i - \mu}) e^{-2\mu z} d\mu. \tag{20}$$

Writing this in the usual form

$$\Gamma^2 = (R + iX)(G + i\omega C), \tag{21}$$

the characteristic impedance is given by

$$K^2 = \frac{R + iX}{G + i\omega C} \tag{22}$$

and the series impedance per unit length of the circuit is

$$R + iX = Z = z + i2\omega \log(\rho''/a) + 4\omega \int_0^\infty (\sqrt{\mu^2 + i - \mu}) e^{-2\mu z} d\mu. \tag{23}$$

It will be observed that the first two terms on the right hand side of (23) represent the series impedance of the circuit if the ground is a perfect conductor; the infinite integral formulates the effect of the finite conductivity of the ground.

The mutual impedance³ Z_{12} between two parallel ground return circuits with wires at heights h_1 and h_2 above ground and a separation x between their vertical planes is given by

$$Z_{12} = i2\omega \log(\rho''/\rho') + 4\omega \int_0^\infty (\sqrt{\mu^2 + i - \mu}) e^{-\mu(h_1 + h_2 + x)} \cos x' \mu d\mu. \tag{24}$$

³ It will be noted that the mutual impedance is equal to the axial electric intensity at the axis of the second wire due to the varying magnetic field of unit current in the first wire and the corresponding distribution of ground's current.

5

$$E_z(x,y) - E_z(x,0) = -i\omega(A_z(x,y) - A_z(x,0)) - \frac{\partial}{\partial z}(V(x,y) - V_0). \tag{16}$$

Here $E_z(x,0)$ is the axial electric intensity at the surface of the ground plane ($y=0$), and

$$A_z(x,y) - A_z(x,0) = \int_0^y H_x(x,y) dy. \tag{17}$$

$V(x,y) - V_0$ is the difference in the scalar potential between the point x,y and the ground, which is due to the charges on the wire and on the surface of the ground. For convenience, it will be designated by V .

By means of (16) and the preceding formulas we get⁴

$$E_z = -4\omega I \int_0^\infty (\sqrt{\mu^2 + i - \mu}) e^{-(h+y)\mu} \cos x' \mu d\mu - i 2\omega I \log(\rho''/\rho') - \frac{\partial}{\partial z} V, \tag{18}$$

where

$$\rho' = \sqrt{(h-y)^2 + x^2} = \text{distance of point } x,y \text{ from wire,}$$

$$\rho'' = \sqrt{(h+y)^2 + x^2} = \text{distance of point } x,y \text{ from image of wire.}$$

The first two terms on the right hand side of (18) represent the electric force due to the varying magnetic field; the term $-\frac{\partial}{\partial z} V$ represents the axial electric intensity due to the charges on the surface of the wire and the ground. If Q be the charge per unit length, V is calculable by usual electrostatic methods on the assumption that the surface of the wire and the surface of the ground are equipotential surfaces, and their difference of potential is Q/C where C is the electrostatic capacity between wire and ground.⁵

II

By aid of the preceding analysis and formulas, we are now in a position to derive the propagation constant, Γ , and characteristic impedance, K , which characterize wave propagation along the system. Let z denote the "internal" or "intrinsic" impedance of the wire per

⁴ As a check on this formula note that together with (14) it satisfies the condition of continuity of E_z at $y=0$.

⁵ See "Wave Propagation Over Parallel Wires: The Proximity Effect," *Phil. Mag.*, Vol. 31, Apr., 1921.

which has been worked out and communicated to me by R. M. Foster. It is

$$\frac{\alpha}{\beta} \left\{ K_1(\alpha\beta) + G(\alpha\beta) \right\}$$

where $K_1(x)$ is the Bessel function of the second kind and first order as defined by Jahne und Fimde, Funktionentafeln, pg. 93, and $G(x)$ is the absolutely convergent series

$$G(x) = \frac{x^2}{3} - \frac{x^4}{3^2 \cdot 5} + \frac{x^6}{3^2 \cdot 5^2 \cdot 7} - \dots$$

On the basis of this solution, it is a straightforward though intricate and tedious process to derive the following solution for $J(p, q)$ of equation (29).

Writing $r = \sqrt{p^2 + q^2}$ and $\theta = \tan^{-1}(q/p)$, it is $J = P + iQ$ in which

$$P = \frac{\pi}{8} (1 - s_1) + \frac{1}{2} \left(\log \frac{2}{\gamma r} \right) s_2 + \frac{1}{2} 0.5 s_2' - \frac{1}{\sqrt{2}} \sigma_1 + \frac{1}{2} \sigma_2 + \frac{1}{\sqrt{2}} \sigma_2 \tag{32}$$

$$Q = \frac{1}{4} + \frac{1}{2} \left(\log \frac{2}{\gamma r} \right) (1 - s_1) - \frac{1}{2} 0.5 s_1' + \frac{1}{\sqrt{2}} \sigma_1 - \frac{\pi}{8} s_2 + \frac{1}{\sqrt{2}} \sigma_2 - \frac{1}{2} \sigma_2 \tag{33}$$

In these equations $\log \gamma$ is Euler's constant: $\gamma = 1.7811$, $\log \frac{2}{\gamma} = 0.11593$, $\log \gamma = 0.57722$ and $\sigma_1, \sigma_2, \sigma_3, \sigma_4, s_1, s_2, s_1', s_2'$ are infinite series defined as follows:

$$s_2 = \frac{1}{1 \cdot 2!} \left(\frac{r}{2} \right)^2 \cos 2\theta - \frac{1}{3 \cdot 4!} \left(\frac{r}{2} \right)^4 \cos 4\theta + \dots$$

$$s_2' = \frac{1}{1 \cdot 2!} \left(\frac{r}{2} \right)^2 \sin 2\theta - \frac{1}{3 \cdot 4!} \left(\frac{r}{2} \right)^4 \sin 4\theta + \dots$$

$$s_1 = \frac{1}{2 \cdot 3!} \left(\frac{r}{2} \right)^3 \cos 3\theta - \frac{1}{4 \cdot 5!} \left(\frac{r}{2} \right)^5 \cos 5\theta + \dots$$

where

$$\rho'' = \sqrt{(h_1 + h_2)^2 + x^2}$$

$$\rho' = \sqrt{(h_1 - h_2)^2 + x^2}$$

$$h_1' = h_1 \sqrt{\alpha}$$

$$h_2' = h_2 \sqrt{\alpha}$$

$$x' = x \sqrt{\alpha}$$

From the preceding the series self impedance of the ground return circuit may be conveniently written as

$$Z = Z^0 + Z' \tag{25}$$

and the mutual impedance as

$$Z_{12} = Z_{12}^0 + Z_{12}' \tag{26}$$

where Z^0, Z_{12}^0 are the self and mutual impedances respectively, on the assumption of a perfectly conducting ground, and

$$Z' = 4\omega \int_0^\infty (\sqrt{\mu^2 + i - \mu}) e^{-2h_1 \mu} d\mu, \tag{27}$$

$$Z_{12}' = 4\omega \int_0^\infty (\sqrt{\mu^2 + i - \mu}) e^{-(h_1 + h_2)\mu} \cos x' \mu d\mu. \tag{28}$$

The calculation of the circuit constants and the electromagnetic field in the dielectric depends, therefore, on the evaluation of an infinite integral of the form

$$J(p, q) = J = \int_0^\infty (\sqrt{\mu^2 + i - \mu}) e^{-\mu x} \cos q\mu d\mu. \tag{29}$$

In terms of this integral

$$Z' = 4\omega J(2h_1, 0) \tag{30}$$

$$Z_{12}' = 4\omega J(h_1' + h_2', x'). \tag{31}$$

To the solution of the infinite integral $J(p, q)$ we now proceed.

III

The solution of equation (29), that is, the evaluation of $J(p, q)$ can be made to depend on the solution of the infinite integral

$$\int_0^\infty \sqrt{\mu^2 + \alpha^2} e^{-\beta \mu} d\mu$$

10

For large values of r ($r > 10$), these reduce to

$$J = \frac{1+i \cos \theta}{\sqrt{2}} r - \cos 2\theta \quad (38)$$

In view of the somewhat complicated character of the function in the range $1/4 \leq r \leq 5$ the curves shown below have been computed. These show $J = P+iQ$ as a function of r for $\theta = 0, \frac{\pi}{8}, \frac{\pi}{4}, \frac{3\pi}{8}, \frac{\pi}{2}$. By interpolation it is possible to estimate with fair accuracy the value of the functions for intermediate values of θ .

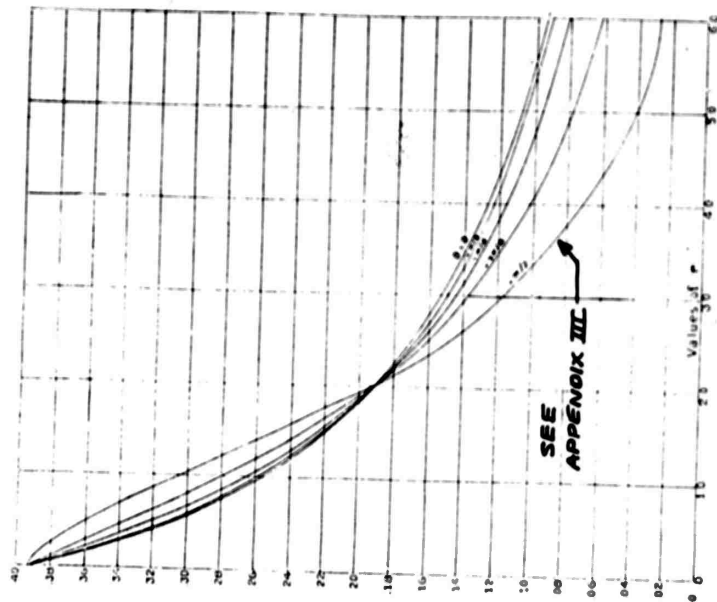


Fig. 2 $P = \text{real part of } J$

9

$$s_1' = \frac{1}{2!} \left(\frac{r}{2}\right)^4 \sin 4\theta - \frac{1}{4!} \left(\frac{r}{2}\right)^8 \sin 8\theta + \dots,$$

$$\sigma_1 = \frac{r \cos \theta}{3} - \frac{r^3 \cos 5\theta}{3^2 \cdot 5^2 \cdot 7} + \frac{r^5 \cos 9\theta}{3^2 \cdot 5^2 \cdot 7^2 \cdot 9^2 \cdot 11} - \dots,$$

$$\sigma_2 = \frac{r^3 \cos 3\theta}{3^2 \cdot 5} - \frac{r^7 \cos 7\theta}{3^2 \cdot 5^2 \cdot 7^2 \cdot 9} + \frac{r^{11} \cos 11\theta}{3^2 \cdot 5^2 \cdot 7^2 \cdot 9^2 \cdot 11^2 \cdot 13} - \dots,$$

$$\sigma_3 = \left(1 + \frac{1}{2} - \frac{1}{4}\right) \frac{1}{1!} \left(\frac{r}{2}\right)^2 \cos 2\theta$$

$$- \left(1 + \frac{1}{2} + \frac{1}{3} + \frac{1}{4} - \frac{1}{8}\right) \frac{1}{3!} \left(\frac{r}{2}\right)^6 \cos 6\theta + \dots,$$

$= \frac{5}{4} s_2$ approximately,

$$\sigma_4 = \left(1 + \frac{1}{2} + \frac{1}{3} - \frac{1}{6}\right) \frac{1}{2!} \left(\frac{r}{2}\right)^4 \cos 4\theta$$

$$- \left(1 + \frac{1}{2} + \frac{1}{3} + \frac{1}{4} + \frac{1}{5} - \frac{1}{10}\right) \frac{1}{4!} \left(\frac{r}{2}\right)^8 \cos 8\theta + \dots$$

$= \frac{5}{3} s_4$ approximately.

It is to be regretted that the foregoing formulas appear so complicated. The series, however, are very rapidly convergent and for $r \leq 2$ only the two leading terms of each series need be retained. For $r \leq 1$, only the leading terms are of importance.

For the important range $r \leq 1/4$,

$$P = \frac{\pi}{8} - \frac{1}{3\sqrt{2}} r \cos \theta + \frac{r^2}{16} \cos 2\theta \left(0.6728 + \log \frac{2}{r}\right) + \frac{r^2}{16} \theta \sin 2\theta, \quad (34)$$

$$Q = -0.0386 + \frac{1}{2} \log \left(\frac{2}{r}\right) + \frac{1}{3\sqrt{2}} r \cos \theta. \quad (35)$$

For $r > 5$ the following asymptotic expansions, derivable from (29) by repeated partial integrations, are to be employed.

$$P = \frac{1}{\sqrt{2}} r - \frac{\cos \theta}{r^2} + \frac{\cos 2\theta}{\sqrt{2}} + \frac{1}{r^3} + \frac{3 \cos 3\theta}{\sqrt{2}} + \frac{\cos 5\theta}{r^5} + \dots, \quad (36)$$

$$Q = \frac{1}{\sqrt{2}} \cos \theta - \frac{1}{\sqrt{2}} \frac{\cos 3\theta}{r^2} + \frac{3 \cos 5\theta}{\sqrt{2}} + \frac{\cos 7\theta}{r^4} - \dots, \quad (37)$$

11

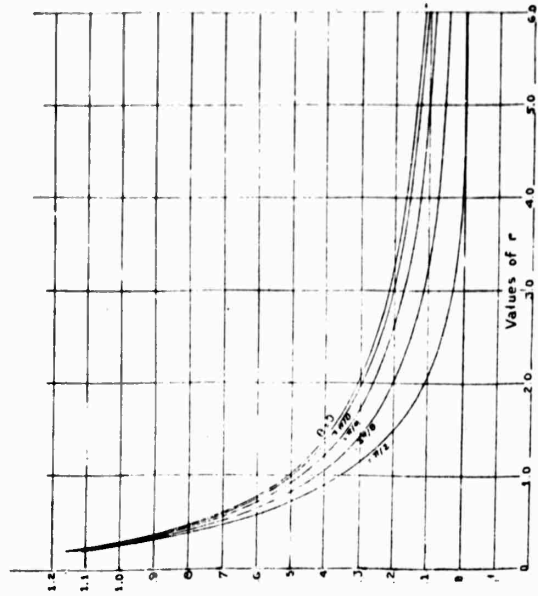


Fig. 3 Q = imaginary part of J .

IV

The theory and formulas of the preceding sections will now be reviewed and summarized as regards their principal applications to technical transmission problems where the ground forms, in whole or part, the "return" part of the circuit. In such problems we are interested in the electric intensity in the dielectric and in the ground, and in particular in the self impedance and mutual impedances of ground return circuits. The calculation of these quantities is provided for by the general analysis and the solution of the infinite integral J . Reference should be made to Fig. 1 shown in section I for the geometry of the system and coordinate system employed.

1. *The Axial Electric Intensity E_z in the Dielectric.* (See equations (15) and (18)).

$$E_z = -\frac{\partial}{\partial z} V - (i2\omega \log(\rho''/\rho) + 4\omega J)I$$

12

where

- $\rho' = \sqrt{(h-y)^2 + x^2}$
= distance of point in dielectric from axis of wire.
- $\rho'' = \sqrt{(h+y)^2 + x^2}$
= distance of point in dielectric from image of wire.
- $r = \rho'' \sqrt{\alpha}$
- $\theta = \sin^{-1}(x/\rho'')$
- $\alpha = 4\pi\lambda\omega$.

These values of r and θ are, of course, to be employed in calculating $J = P + iQ$ from the formulas and curves of the preceding section. As a special case the electric intensity at the surface of the earth is

$$E_s = -4\omega J$$

$$\rho'' = \sqrt{h^2 + x^2}$$

$$r = \rho'' \sqrt{\alpha}$$

$$\theta = \sin^{-1}(x/\rho'')$$

2. *Self Impedance of Ground Return Circuit.* (See equations (25), (27), (30)).

$$Z = Z^0 + 4\omega J$$

$$Z^0 = \text{self impedance with perfectly conducting ground.}$$

$$r = 2h \sqrt{\alpha}$$

$$\theta = 0.$$

3. *Mutual Impedance of Ground Return Circuits.* (See equations (26), (28), (31)).

$$Z_{12} = Z_{12}^0 + 4\omega J$$

$$Z_{12}^0 = \text{mutual impedance with perfectly conducting ground.}$$

$$r = \sqrt{\alpha} \sqrt{(h_1 + h_2)^2 + x^2} = \rho'' \sqrt{\alpha}$$

$$\theta = \sin^{-1}(x/\rho'')$$

The axial electric intensity E_z in the ground ($y < 0$) is given by equation (1), and the subsequent analysis, whence

$$E_z = -4\omega J \int_0^\infty (\sqrt{\mu^2 + 1} - \mu) \cos x' \mu e^{-\theta(\mu + \sqrt{\mu^2 + 1})} d\mu$$

13

where, as before

$$x' = x\sqrt{\alpha}$$

$$h' = h\sqrt{\alpha}$$

and

$$g' = \sqrt{\alpha} \text{ times the depth below the surface of the ground.} \\ = g\sqrt{\alpha}.$$

The integral can undoubtedly be evaluated in somewhat the same way as (29) and can in any case be numerically computed without much difficulty. Owing, however, to the secondary technical interest in the electric intensity below the surface of the earth, the detailed solution has not been undertaken, nor has the magnetic field been worked out.

V

The practical utility of the preceding theory and formulas will now be illustrated by a brief sketch of their application to two important transmission problems.

THE WAVE ANTENNA

When a transmission line with "ground return" is employed as a radio receiving antenna it is called a wave antenna. The theory and design of such an antenna requires a knowledge of the transmission characteristics of the ground return circuit, which are calculable, as shown above, from the geometry and constants of the overhead wire, together with $Z' = 4\omega J$, which may be termed the "ground return" impedance.

We assume that the wire is approximately 30 ft. above the ground ($h = 10^3$) and that the frequency is $5 \cdot 10^4$ c.p.s. corresponding to the frequency employed in Trans-Atlantic radio communication. The ground conductivity λ is exceedingly variable, depending on the locality and weather conditions. Calculations of Z' will therefore be made for two extreme cases, $\lambda = 10^{-12}$ and $\lambda = 10^{-14}$ which should cover the range of variation encountered in practice.

For $\lambda = 10^{-12}$,

$$\sqrt{\alpha} = \sqrt{4\pi\lambda\omega} = 2 \cdot 10^{-3}$$

and for $\lambda = 10^{-14}$,

$$\alpha = 2 \cdot 10^{-4}.$$

14

Correspondingly, $r = 2h\sqrt{\alpha}$ has the values 4.0 and 0.4, respectively. Reference to the preceding formulas and curves for J , for $r = 4.0$ and $r = 0.4$, give

$$J = 0.126 + i 0.168, \quad \lambda = 10^{-12}$$

$$J = 0.323 + i 0.871, \quad \lambda = 10^{-14}$$

whence the corresponding values of Z' are

$$Z' = 4\omega \cdot (0.126 + i 0.168),$$

$$Z' = 4\omega \cdot (0.323 + i 0.871).$$

These are the "ground return" impedances per unit length in elm. c.g.s. units; to convert to ohms per mile they are to be multiplied by the factor 1.61×10^{-4} . Consequently setting $\omega = \pi \cdot 10^8$, we get

$$Z' = 6.44\pi(1.3 + i 1.7), \quad \lambda = 10^{-12}$$

$$Z' = 6.44\pi(3.2 + i 8.7), \quad \lambda = 10^{-14}.$$

Comparison of these formulas shows that an hundred-fold increase in the resistivity of the ground increases the resistance component of the ground return impedance by the factor 2.5 and increases its reactance only five-fold. That is to say, the ground return impedance is not sensitive to wide variations in the resistivity of the earth, a fortunate circumstance in view of its wide variability and our lack of precise information regarding it.

INDUCTION FROM ELECTRIC RAILWAY SYSTEMS

A particularly important application of the preceding analysis is to the problems connected with the disturbances induced in parallel communication lines by alternating current electric railways. Assuming the frequency as 25 c.p.s., we have corresponding to $\lambda = 10^{-12}$ and $\lambda = 10^{-14}$,

$$\sqrt{\alpha} = 0.45 \times 10^{-4} \text{ and } 0.45 \times 10^{-3}.$$

Taking the height of the trolley wire as approximately 30 ft., $h = 10^3$ and assuming the parallel telephone as the same height above ground and separated by approximately 120 ft., $x = 4 \cdot 10^3$, and

$$r = \sqrt{\alpha} \sqrt{(2h)^2 - x^2} \\ = 4.47 \times 10^3 \sqrt{\alpha},$$

For the case of $\lambda = 10^{-12}$, the corresponding calculations give

$$Z'_{12} = 4\omega(0.391 + i 2.27)$$

with *no current in rail*, and

$$Z''_{12} = 4\omega(-0.001 - i 0.002)$$

with *equal and opposite current in rail*. It is evident from these figures that the reduction in mutual impedance, due to the current in the rail, is practically independent of the ground conductivity, at least at the separation specified.

and corresponding to the values of α taken above

$$r = 0.2 \text{ and } 0.02 \text{ in round numbers,}$$

while

$$\theta = \sin^{-1} \frac{4}{\sqrt{20}} = 63^\circ 30' \text{ approximately.}$$

For both cases, therefore, we can employ, in calculating $J = P + iQ$, the approximate formulas,

$$P = \frac{\pi}{8} - \frac{1}{3\sqrt{2}} r \cos \theta + \frac{r^2}{16} \cos 2\theta \left(.6728 + \log \frac{2}{r} \right) + \frac{r^2}{16} \theta \sin 2\theta,$$

$$Q = -0.0386 + \frac{1}{2} \log \left(\frac{2}{r} \right) + \frac{1}{3\sqrt{2}} r \cos \theta.$$

For $\lambda = 10^{-12}$ and $r = 0.2$, this gives

$$J = 0.369 + i 1.135$$

and

$$Z'_{12} = 4\omega(0.369 + i 1.135).$$

The foregoing assumes that the only return conductor is the ground. If, however, an equal and opposite current flows in the rail we must subtract from the foregoing mutual impedance, the mutual impedance between rail and telephone line; that is, the mutual impedance Z'_{12} between the telephone line and a conductor at the surface of the earth. For this case

$$\rho'' = \sqrt{h^2 + x^2} = 4.12 \times 10^3$$

$$\theta = \sin^{-1} \frac{4}{\sqrt{17}} = 76^\circ$$

$$\cos \theta = 0.242, \quad r = 0.184 \text{ for } \lambda = 10^{-12}.$$

The corresponding value of J is

$$J = 0.378 + i 1.165$$

and the *residual* mutual impedance between railway and parallel telephone line is,

$$Z'_{12} = 4\omega(0.369 - 0.378 + i (1.135 - 1.165)) \\ = 4\omega(0.009 - i 0.030).$$

The very large reduction in mutual impedance, due to the current in the rail, is striking.

APPENDIX II

REPRINT OF "PROPAGATION OF HIGH-FREQUENCY CURRENTS
IN GROUND RETURN CIRCUITS" BY W. H. WISE

BELL TELEPHONE SYSTEM
TECHNICAL PUBLICATIONS

MATHEMATICAL
PHYSICS



MONOGRAPH
B-791

**PROPAGATION OF
HIGH-FREQUENCY CURRENTS
IN GROUND RETURN CIRCUITS**

BY

W. H. WISE

American Telephone and Telegraph Company

A DERIVATION OF THE
MUTUAL IMPEDANCE FORMULA WITHOUT THE ASSUMPTION
THAT THE FREQUENCY IS SO LOW THAT POLARIZATION
CURRENTS MAY BE NEGLECTED

BELL TELEPHONE LABORATORIES
INCORPORATED
463 WEST STREET, NEW YORK

Published in
PROCEEDINGS OF THE INSTITUTE OF RADIO ENGINEERS
VOL. 22, PP. 922-937
APRIL, 1934

Copyright, 1934, by
THE INSTITUTE OF RADIO ENGINEERS

Printed in the United States of America

PROPAGATION OF HIGH-FREQUENCY CURRENTS IN GROUND RETURN CIRCUITS*

By
W. H. WISE

(American Telephone and Telegraph Company, New York City)

Summary—The electric field parallel to a ground return circuit is calculated without assuming that the frequency is so low that polarization currents in the ground may be neglected. It is found that the polarization currents may be included by replacing the r in Carson's well-known formulas by $r\sqrt{1+i(\epsilon-1)2c\omega}$.

INTRODUCTION

THE problem to be solved is that of calculating the electric field parallel to an alternating current flowing in a straight, infinitely long wire placed above and parallel to a plane homogeneous earth. Carson's derivation of this field¹ is based on three restricting assumptions: (1) The ground permeability is unity; (2) the wave is propagated with the velocity of light and without attenuation; (3) the frequency is so low that polarization currents may be neglected. The first of these restrictions is usually of no consequence and the formula would be quite complicated if the permeability were not made unity. As pointed out in a later paper by Carson² the second restriction amounts merely to assuming reasonably efficient transmission. The effect of the third restriction begins to be noticeable at about 60 kilocycles. The object of the present paper is the removal of the third restriction.

DERIVATION OF THE MUTUAL IMPEDANCE FORMULA

The electric and magnetic fields of any current may be obtained by differentiating the current's wave function. The wave function for a horizontal current-element dipole has been formulated as an infinite integral by H. von Hoerschelmann.³

* Decimal classification: R110. Original manuscript received by the Institute, October 16, 1933.

¹ John R. Carson, "Wave propagation in overhead wires with ground return," *Bell Sys. Tech. Jour.*, vol. 5, pp. 539-554, October, (1926). It is stated in this paper that the propagation constant is assumed to be a very small quantity in c.g.s. units. Since this follows from the second and third restrictions it cannot be classed as a separate restriction. The second restriction is not explicitly stated in this paper but is implicit in equations (4) and (5) and the preceding explanatory remark.

² W. Howard Wise, "Effect of ground permeability on ground return circuits," *Bell Sys. Tech. Jour.*, vol. 10, pages 472-484, July, (1931).

³ John R. Carson, "Rigorous and approximate theories of electrical transmission along wires," *Bell Sys. Tech. Jour.*, vol. 7, p. 11, January, (1928).
⁴ H. von Hoerschelmann, *Jahrb. der draht. Teleg.*, Bd. 5, pp. 14-188, (1912).

The wave-function of the current in the wire will be obtained by integrating the wave-functions of the current-element dipoles along the wire from minus infinity to plus infinity. It will be assumed at the start that the current in the wire is exponentially attenuated. The wave-function of the current is thus found to be

$$\begin{aligned} \Pi = & a \times e^{-\gamma z} \int_{-\infty}^{\infty} I e^{-\gamma y} \left(\frac{e^{-i\pi R_1}}{R_1} - \frac{e^{-i\pi R_2}}{R_2} \right. \\ & + \int_0^{\infty} \frac{2J_0(\rho r)}{l+m} e^{-\gamma \rho} d\rho \left. \right) dx + b \times 0 \\ & - c \times 2e^{-\gamma z} \int_{-\infty}^{\infty} I e^{-\gamma y} \frac{\partial}{\partial x} \int_0^{\infty} \frac{(1-x^2)J_0(\rho r)}{(l+m)(l+r^2m)} e^{-\gamma \rho} d\rho dx. \end{aligned}$$

a , b , and c are unit vectors pointing in the x , y , and z directions. The time factor is $e^{i\omega t}$.

$$R_1 = \sqrt{x^2 + y^2 + (h-z)^2}$$

$$R_2 = \sqrt{x^2 + y^2 + (h+z)^2}$$

$$\rho = \sqrt{z^2 + y^2}$$

$$k = 2\pi/\lambda; \quad k_1^2 = k_2^2(\epsilon - i2c\omega) = \epsilon\mu\omega^2 - i4\pi\sigma\omega, \quad \mu = 1$$

$$l = \sqrt{l^2 - k^2}; \quad m = \sqrt{l^2 - k_1^2}; \quad w = h + z; \quad r^2 = k^2/k_1^2$$

$$\gamma = \alpha + i\beta$$

$$\begin{aligned} -E_x = & i\omega \left[\Pi_x + \frac{1}{k^2} \frac{\partial}{\partial x} \left(\frac{\partial \Pi_x}{\partial x} + \frac{\partial \Pi_y}{\partial y} + \frac{\partial \Pi_z}{\partial z} \right) \right] = i\omega \pi_a + \frac{\partial V^0}{\partial x} \\ = & i\omega e^{-\gamma z} \int_{-\infty}^{\infty} I e^{-\gamma y} \left(\frac{e^{-i\pi R_1}}{R_1} - \frac{e^{-i\pi R_2}}{R_2} + \int_0^{\infty} \frac{2J_0(\rho r)}{l+m} e^{-\gamma \rho} d\rho \right) dx \\ & + \frac{\partial V^0}{\partial x} \end{aligned}$$

Carson's formula (24) for Z_{12} , the mutual impedance between two parallel lines, is readily obtained by writing $\gamma = k = 0$. This, in effect, is Polloczek's⁴ fundamental assumption. It results from the supposition

* The reader should note that $V = \int E_x dy$ and that this scalar potential is not quite the same as the potential to ground which Carson finally denotes by V .
⁴ F. Polloczek, "Über das Feld einer unendlich langen Wechselstromdurchflössenen Einfachleitung," *Z.N.F.*, vol. 3, p. 339, (1928). "Gegenseitige Induktion zwischen Wechselstromleitungen von endlicher Länge," *Annalen der Physik*, Folge IV, Bd. 87, (1928).

that $2\pi D/\lambda$, where D is the largest dimension of our physical system, is negligible in comparison with unity so that we can ignore all phase effects due to finite velocity of propagation. But we must be consistent in our approximations and blot out the dielectric constants of both ground and air at the same time that we throw away the phase effects; otherwise we end up with a formula which is neither like Carson's nor correct in the way it contains the dielectric constants.

The problem, then, is that of evaluating the integral

$$Z_{12} = i\omega \int_{-\infty}^{\infty} \left(\frac{e^{-ikr}}{R_1} - \frac{e^{-ikr}}{R_2} + \int_0^{\infty} \frac{2f_0(\rho v)}{l+m} e^{-\gamma d} e^{-\gamma' dx} \right) e^{-\gamma' dx}$$

without assuming that k and γ are extremely small. The dipole wavefunction used in getting this formula is only valid if $\mu = 1$.

We shall write $\gamma = ik$. This is an ideal value for γ but the following considerations make it an imperative choice; (1) to assume that the current is propagated down the line with a velocity less than that of



Fig. 1

light makes the integral very hard to evaluate, and (2) to assume that the attenuation is not zero on an infinite line amounts to assuming an infinite source of energy and makes Z_{12} infinite.

It should not be inferred from this that the resulting formulas are necessarily poor if the physical system does not closely approximate these ideal properties. The procedure being followed is analogous to the successive approximation method for solving differential equations. ik is a convenient first approximation to the propagation constant. The resulting expression for Z_{12} is used to compute a second approximation to the propagation constant. $\gamma^2 = (z + Z_{12})(G + i\omega C)$ where z is the impedance of the wire per unit length and Z_{12} is computed at the surface of the wire. Practical experience with the second approximation so obtained shows that ik is a satisfactory first approximation. Since Z_{12} is infinite if the attenuation is not zero and the second approximation to γ is not a pure imaginary it is not possible to get a third approximation by repeating the analysis with ik replaced by the second approximation. So, the use of an infinite line formula presupposes reasonably efficient transmission.

It should be remarked here that the capacity C is not entirely independent of the ground constants. The characteristic impedance of the line is

$$\sqrt{(z + Z_{12})/(G + i\omega C)} = - \int_0^{\infty} E_p dz / I e^{-\gamma z}$$

and, starting with the infinite integral formulation of II, it is easy enough to set up an infinite integral for $\int_0^{\infty} E_p dz$, but the evaluation of this integral is not a simple matter.

With $\gamma = ik$ the first two terms of Z_{12} reduce to $i\omega 2 \log \rho''/\rho'$. They are, omitting the factor $i\omega$,

$$\begin{aligned} & \int_{-\infty}^{\infty} \left(\frac{e^{-ik(\sqrt{x^2+z^2})}}{\sqrt{x^2+z^2}} - \frac{e^{-ik(\sqrt{x^2+y^2})}}{\sqrt{x^2+y^2}} \right) e^{-ikz} dz \\ &= \lim_{a,b \rightarrow \infty} \int_{-a}^a \left(\frac{e^{-ik(\sqrt{x^2+z^2+a^2})}}{\sqrt{x^2+z^2+a^2}} - \frac{e^{-ik(\sqrt{x^2+z^2+b^2})}}{\sqrt{x^2+z^2+b^2}} \right) e^{-ikz} dz \\ &= \lim_{a,b \rightarrow \infty} \int_a^b \frac{e^{-ik(\sqrt{x^2+z^2+a^2})}}{\sqrt{x^2+z^2+a^2}} d(\sqrt{x^2+z^2+a^2}) \\ &= \lim_{a,b \rightarrow \infty} \int_a^b \frac{e^{-it}}{t} dt - \int_a^b \frac{e^{-it}}{t} dt, \end{aligned}$$

where,

$$\begin{aligned} g_1 &= k(\sqrt{a^2+z^2} - a), & g_2 &= k(\sqrt{b^2+z^2} + b), \\ g_3 &= k(\sqrt{a^2+z^2} - a), & g_4 &= k(\sqrt{b^2+z^2} + b), \\ &= \lim_{a,b \rightarrow \infty} - (ig_1 + (ig_2 + (ig_3 - (ig_4) \\ &= -i(-Sig_1 + Sig_2 + Sig_3 - Sig_4) \\ &= \lim_{a,b \rightarrow \infty} - (ig_1 + (ig_2 + Sig_3 + Sig_4) \\ &= \lim_{a,b \rightarrow \infty} - (ig_1 + (ig_2 + Sig_3 + Sig_4) = 2 \log \rho''/\rho'. \end{aligned}$$

So, with $\gamma = ik$, we have

$$Z_{12} = i2\omega \log \frac{\rho''}{\rho'} + i2\omega \int_0^{\infty} \frac{e^{-\gamma' x}}{l+m} \left(\int_{-\infty}^{\infty} J_0(\sqrt{x^2+y^2}) e^{-ikz} dx \right) dz.$$

Since $J_0(\sqrt{x^2+y^2})$ and $\cos kx$ are even functions of x and $\sin kx$ is an odd function of x

$$\int_{-\infty}^{\infty} J_0(\sqrt{x^2+y^2}) e^{-ikz} dx = 2 \int_0^{\infty} J_0(\sqrt{x^2+y^2}) \cos kx dx$$

Carson's formula for $P+iQ$ differs from this one only in that he has β where we have $\alpha\beta$. It follows that, to get the new series expansions for P and Q we have only to replace the r in Carson's series by $r\sqrt{1+i(\epsilon-1)/2c\lambda\sigma}$.

THE HIGH-FREQUENCY SERIES FOR P AND Q

Writing $s = \sqrt{1+i(\epsilon-1)/2c\lambda\sigma} = \xi e^{i\eta}$, where ϵ is the dielectric constant of the ground referred to air as unity, c is the velocity of light in centimeters per second, λ is the wavelength in centimeters and σ is the conductivity of the ground in electromagnetic units, Carson's asymptotic series for P and Q are replaced by

$$P \sim \frac{\cos \theta}{\sqrt{2}r\xi} (\cos \eta + \sin \eta) - \frac{\cos 2\theta}{r^2\xi^2} \cos 2\eta + \frac{\cos 3\theta}{\sqrt{2}r^3\xi^3} (\cos 3\eta - \sin 3\eta) + \dots$$

$$Q \sim \frac{\cos \theta}{\sqrt{2}r\xi} (\cos \eta - \sin \eta) + \frac{\cos 2\theta}{r^2\xi^2} \sin 2\eta - \frac{\cos 3\theta}{\sqrt{2}r^3\xi^3} (\cos 3\eta + \sin 3\eta) + \dots$$

and Carson's series for use when $r < 1/4$ are replaced by

$$P = \frac{\pi}{8} - \frac{r\xi}{3\sqrt{2}} \cos \theta (\cos \eta + \sin \eta) + \frac{\pi r^2 \xi^2}{64} \cos 2\theta \sin 2\eta + \frac{r^2 \xi^2}{16} \cos 2\theta \left[\cos 2\eta \left(0.6728 + \log \frac{2}{r\xi} \right) + \eta \sin 2\eta \right] + \frac{\eta}{2} + \frac{r^2 \xi^2}{16} \theta \sin 2\theta \cos 2\eta + \dots$$

$$Q = -0.03861 + \frac{1}{2} \log \frac{2}{r\xi} + \frac{r\xi}{3\sqrt{2}} \cos \theta (\cos \eta - \sin \eta) + \frac{r^2 \xi^2}{16} \cos 2\theta \left[\sin 2\eta \left(0.6728 + \log \frac{2}{r\xi} \right) - \eta \cos 2\eta \right] + \frac{r^2 \xi^2}{16} \theta \sin 2\theta \sin 2\eta - \frac{\pi r^2 \xi^2}{64} \cos 2\theta \cos 2\eta + \dots$$

$$= 0 \text{ if } \nu < k$$

$$= 2 \frac{\cos y\sqrt{\nu^2 - k^2}}{\sqrt{\nu^2 - k^2}} \text{ if } k \leq \nu^*$$

$$\therefore Z_{12} = i2\omega \log \frac{\rho''}{\rho'} + i4\omega \int_k^\infty \frac{e^{-\nu l}}{l+m} \frac{\cos y l}{l} \nu d\nu$$

$$= i2\omega \log \frac{\rho''}{\rho'} + \frac{i4\omega}{-k^2 + k^2} \int_k^\infty (m-l)e^{-\nu l} \cos y l \frac{\nu d\nu}{l}$$

$$= i2\omega \log \frac{\rho''}{\rho'} + \frac{4\omega}{i(k^2 - k^2)} \int_0^\infty (\sqrt{l^2 + i(k^2 - k^2)} - l) e^{-\nu l} \cos y l \cdot dl$$

$$= i2\omega \log \frac{\rho''}{\rho'} + 4\omega (P + iQ).$$

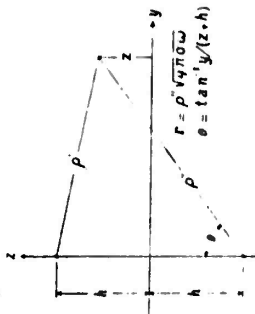


Fig. 2

Writing $i(k_2^2 - k^2) = 4\pi\sigma\omega + i(\epsilon-1)k^2 = 4\pi\sigma\omega(1+i(\epsilon-1)/2c\lambda\sigma) = \alpha\beta^2$, $w\sqrt{4\pi\sigma\omega} = w\sqrt{\alpha} = w'$, $y\sqrt{\alpha} = y'$ and making the change of variable $l = \nu\sqrt{\alpha}$ we have

$$P + iQ = \frac{1}{s^2} \int_0^\infty (\sqrt{\nu^2 + i\alpha^2} - \nu) e^{-\nu l} \cos y' \nu \cdot \nu d\nu$$

$$= \frac{1}{s^2} R_1 \left(\frac{\zeta s}{\beta} \{ K_1(\zeta s \beta) + G(\zeta s \beta) \} - \frac{1}{\beta^2} \right),$$

where $\zeta = \sqrt{i}$, $\beta = (w' + jy') = re^{i\theta}$, and R_1 indicates that the real part is to be taken with ζ and s regarded as real parameters and j the only imaginary.

* To get this put $\sigma = 0$ and $\nu = -1/2$ in formula (13) on page 255 in Nielsen's "Handbuch der Cylinderfunktionen."
 † $K_1(x)$ is the Bessel function of the second kind and first order as defined by Jahnke and Emde, "Funktionentafeln," p. 93, and

$$G(x) = \frac{x^2}{3} - \frac{x^4}{3^2 \cdot 5} + \frac{x^6}{3^2 \cdot 5^2 \cdot 7} - \dots$$

APPENDIX III
LETTER FROM W. H. WISE CORRECTING
PREVIOUS PAPERS

94 Paterson Road
 Fanwood, N. J.
 October 14, 1963

Mr. D. N. Travers
 8500 Culebra Road
 San Antonio 6, Texas

Dear Mr. Travers:

I have mailed some reprints to you. None of these monographs contains an alternative to calculating Carson's eight series, modified for high frequencies.

If you have been looking at Carson's BSTJ paper, or Monograph B-219, you may have noticed that his curve labeled $\pi/2$ is out of place in the neighborhood of $r = 2.5$ in Figure 2. The numerical information for this figure was correctly computed and was then given to a draughtsman who prepared the figure. Seeing that the other curves seemed to pass through a single point at $r = 2$ he leaped to the conclusion that the $\pi/2$ curve should pass through this point. So he passed the $\pi/2$ curve through this point, without mentioning what he had done. The crime was discovered after the paper was out. Later, when reprints had become a scarce item, IT&T asked for a copy from which they could make copies for their engineers. I was given the task of correcting Figure 2 by scratching out the displaced part of the curve and then inking it in where it belongs.

There are two misprints in Monograph B-1558. There are no misprints in the BSTJ article. The contractor for the reprints used a proof submitted for an estimate of cost to make the reprints, instead of waiting for the corrected page proof.

I find in my copy of Monograph B-791 a reference to a paper by Sidney Weinbaum in the Journal of Applied Physics, December 1944, Vol.

15, No. 12, page 840. He shows how to evaluate $\int_0^x \frac{e^{-ik\sqrt{x^2 + \rho^2}}}{\sqrt{x^2 + \rho^2}} dx$

by deriving a differential equation for it and then getting a series solution for the differential equation. The variable is $-jk\rho$. This series is said to be an improvement over the older one.

I do not know that anyone has attempted to improve on Carson's series.

Yours truly,

/s/ W. Howard Wise

APPENDIX IV

REPRINT OF "POTENTIAL COEFFICIENTS FOR GROUND
RETURN CIRCUITS" BY W. H. WISE

MONOGRAPH 3-1558



BELL TELEPHONE SYSTEM

TECHNICAL PUBLICATIONS

**Potential
coefficients
for ground return
circuits**



by
W. N. Wise

9-1558; W. N. WISE

BELL TELEPHONE LABORATORIES, Incorporated
463 West Street, New York 14, N. Y.

Potential Coefficients for Ground Return Circuits

By W. HOWARD WISE

This paper is concerned with the effect of the finite conductivity and dielectric constant of the earth on the potential coefficient for a 1-wire ground return circuit. It has been customary to say that the potential coefficient V/Q is

$$P_{11} = \epsilon^2 \log \epsilon^2 / \epsilon', \text{ cm units per cm.}$$

It is generally realized of course that this is just a good approximation to the true P_{11} . To see that it is just an approximation one has only to imagine the earth turning into air, in which case the distance ϵ^2 will eventually cease to have significance. The object of this paper is to derive the complete expression for P_{11} .

It turns out that

$$P_{11} = \epsilon^2 \log \epsilon^2 / \epsilon' + 4(M + iN) \tag{7}$$

where

$$M + iN = \int_0^{\infty} \frac{e^{-\beta z} \sqrt{1 + \epsilon^2} \cos \gamma \sqrt{\beta^2 + \epsilon^2} d\beta}{\sqrt{\beta^2 + \epsilon^2} + \epsilon^2 \beta + (\epsilon^2 - 1)2\beta} \tag{8}$$

$\epsilon = 4\pi\epsilon_0$, as in Carson's work on Z_{11} and is in ohms on Z_{11} at high frequencies^{1,2}

$$P_{11} = \sqrt{1 + i(\epsilon^2 - 1)/2\epsilon\epsilon'}$$

- ϵ = dielectric constant in electromagnetic units
- ϵ' = conductivity in electromagnetic units
- ϵ^2 = 10^9 in ordinary and
- λ = wavelength in centimeters
- c = velocity of light, in cm per sec.

$$M + iN \text{ vanishes as } f \rightarrow 0, f \rightarrow \infty, \epsilon \rightarrow \infty, \epsilon' \rightarrow \infty.$$

Ordinarily $4(M + iN)$ will not be an important correction to $2 \log \epsilon^2 / \epsilon'$; but if the frequency is high and λ or ϵ' is small it can be a worthwhile correction. For example, if $\lambda = .02545$ inch, $\epsilon = 15$ and $\epsilon' = 5$ cm, then, with ϵ for wire radius,

$$P_{11} = \epsilon^2 \log 2\lambda / \epsilon' + 4(M + iN)$$

$1/P_{11}$ is the capacity to ground. If there were two parallel wires the scalar potential at the first wire would be $V_1 = P_{11}Q_1 + P_{12}Q_2$.

DERIVATION OF THE FORMULA

WE BEGIN with the wave-function for an exponentially propagated current in a straight wire parallel to a flat earth. The wave-function for a horizontal current-element dipole has been formulated as an infinite

¹ John R. Carson: "Wave Propagation in Overhead Wires with Ground Return," *Bull. Sys. Tech. Jour.*, 5, pp. 539-564, 1926.
² W. Howard Wise: "Propagation of High-Frequency Currents in Ground Return Circuits," *Proc. I. R. E.*, 22, pp. 522-527, 1934.

integral by H. von Hoerschelmann³. The wave-function for the current in the wire is obtained by integrating the wave-functions of the current-element dipoles along the wire from minus infinity to plus infinity. It is

$$\begin{aligned} \Pi = & a \times e^{-\gamma z} \int_{-\infty}^{\infty} I_0 e^{-\gamma x} \left(\frac{e^{-ibx_1}}{R_1} - \frac{e^{-ibx_2}}{R_2} \right) \\ & + \int_{-\infty}^{\infty} \frac{2I_0(v\rho)}{l+m} e^{-mz} v \cdot dv \, dz + b \times 0 \quad (1) \\ - c \times & 2e^{-\gamma z} \int_{-\infty}^{\infty} I_0 e^{-\gamma x} \frac{\partial}{\partial x} \int_0^{\infty} \frac{(1-r^2)J_0(vp)}{(l+m)(l+r^2m)} e^{-mz} dv \, dz. \end{aligned}$$

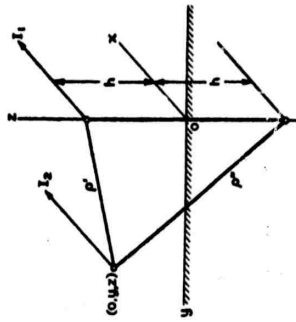


Fig. 1

The time factor is $e^{i\omega t}$. a , b and c are unit vectors pointing in the x , y and z directions.

$$\begin{aligned} R_1 &= (x^2 + y^2 + (h-s)^2)^{1/2} \\ R_2 &= (x^2 + y^2 + (h+s)^2)^{1/2} \\ \rho &= (x^2 + y^2)^{1/2} \\ h &= 2\pi/\lambda \\ h_2^2 &= 4\mu\omega^2 - i4\pi\sigma\mu\omega \text{ in electromagnetic units} \end{aligned}$$

By supposing ϵ to be measured in electrostatic units we can write

$$h_2^2 = h^2(e - i2\epsilon\sigma/\lambda)$$

³H. Von Hoerschelmann, Jahrb. der draht. Telegr. 5, pp. 14-188, 1912.

It is assumed that μ is everywhere unity in electromagnetic units.

$$\begin{aligned} l &= (x^2 - y^2)^{1/2}, & m &= (x^2 - h_2^2)^{1/2} \\ w &= h + z, & r^2 &= h^2/h_2^2 \\ \gamma &= \alpha + i\beta \text{ is the desired propagation constant} \end{aligned}$$

The electric field parallel to the wire is

$$\begin{aligned} E_z = & -i\omega \left[\Pi_z + h^{-2} \frac{\partial}{\partial z} \left(\frac{\partial}{\partial x} \Pi_x + \frac{\partial}{\partial y} \Pi_y + \frac{\partial}{\partial z} \Pi_z \right) \right] \\ & = -I_0 e^{-\gamma z} Z_{11} - \frac{\partial V}{\partial z} \quad (2) \end{aligned}$$

It has previously been shown that¹

$$Z_{11} = i\omega [2 \log e''/\rho' + 4(Q - iP)] \quad (3)$$

where

$$\begin{aligned} Q - iP &= \frac{1}{i\omega^2} \int_0^{\infty} (\sqrt{x^2 + h^2} - x) e^{-\gamma x} \cos \gamma y \cdot dx, \\ w' &= w \sqrt{\alpha} \text{ and } \gamma' = \gamma \sqrt{\alpha}. \end{aligned}$$

To get the potential coefficient for a ground return circuit it is necessary to compute the scalar potential.

$$\begin{aligned} V &= i\omega h^{-2} \left(\frac{\partial}{\partial x} \Pi_x + \frac{\partial}{\partial y} \Pi_y + \frac{\partial}{\partial z} \Pi_z \right) \\ &= Q \rho_{10} \quad (4) \end{aligned}$$

As in previous work the propagation constant γ is assigned the value $i\beta$ as a first approximation. This is an ideal value for γ but the following considerations make it an imperative choice: (1) to assume that the current is propagated down the line with a velocity less than that of light makes the integrals very hard to evaluate, (2) to assume that the attenuation is not zero on an infinite line amounts to assuming an infinite source of energy and makes the integrals diverge.

It should not be inferred that the resulting formulas are necessarily poor if the physical system does not closely approximate the ideal one in which γ is $i\beta$. $i\beta$ is employed as a convenient first approximation in evaluating the correction terms in Z_{11} and ρ_{10} . Eventually, if there were but one wire, one would compute $\gamma = \sqrt{i\epsilon + Z_{11}(G + i\omega C/\rho_{10})}$, wherein Z_{11} and ρ_{10} have been evaluated with $i\beta$ for γ , and this would be a second approximation to γ . Past experience with the second approximation so obtained has justified the expectation that it would be a satisfactory final result. Since

the integrals diverge if the attenuation is not zero the use of an infinite line formula p-supposes reasonably efficient transmission.

Since $\Pi \propto e^{-\gamma z}$ we have

$$i\omega k^{-1} \frac{\partial}{\partial z} \Pi_s = \frac{\omega}{k} \Pi_s = \frac{I}{ik} Z_{12} = \frac{cI}{i\omega} Z_{12}$$

Since $-\frac{\partial I}{\partial z} = \frac{\partial Q}{\partial t}$ or $i\omega I = i\omega Q$ or $I = cQ$ this is

$$i\omega k^{-1} \frac{\partial}{\partial z} \Pi_s = Qc^2 [2 \log \rho''/\rho' + 4(Q - iP)] \tag{5}$$

We have next to consider

$$\begin{aligned} \frac{\partial \omega}{\partial z} \Pi_s &= \frac{2\omega(1-\tau^2)}{ik^2} I \frac{\partial}{\partial z} \int_0^\infty e^{-\tau z} \frac{\partial}{\partial z} \int_0^\infty \frac{J_0(\rho p) e^{-\tau p}}{(l+m)(l+\tau^2 m)} \tau dp dz \\ \Pi_s &= Qc^2 \frac{2(1-\tau^2)}{ik} \frac{\partial}{\partial z} \int_0^\infty \frac{e^{-\tau z}}{(l+m)(l+\tau^2 m)} \int_0^\infty e^{-\tau p} \frac{\partial}{\partial z} J_0(\rho p) dz \end{aligned}$$

The infinite integral is

$$\int_0^\infty \frac{e^{-\tau p} \tau dp}{(l+m)(l+\tau^2 m)} \left[e^{-\tau z} J_0(\rho p) \right] + \gamma \int_0^\infty e^{-\tau p} J_0(\rho p) dz$$

Since $J_0(\rho \sqrt{p^2 + \gamma^2})$ and $\cos kz$ are even functions of z and $\sin kz$ is an odd function of z

$$\begin{aligned} \int_0^\infty J_0(\rho \sqrt{p^2 + \gamma^2}) e^{-\tau z} dz &= 2 \int_0^\infty J_0(\rho \sqrt{p^2 + \gamma^2}) \cos kz \cdot dz \\ &= 0 \text{ if } \tau < k \\ &= 2 \frac{\cos \gamma \sqrt{p^2 - k^2}}{\sqrt{p^2 - k^2}} \text{ if } k \leq \tau \end{aligned}$$

and so our integral is

$$2ik \int_0^\infty \frac{e^{-\tau z}}{(l+m)(l+\tau^2 m)} \cdot \frac{\cos \gamma p}{l} dp$$

or, since $P = \tau^2 - k^2$,

$$2ik \int_0^\infty \frac{e^{-\tau z} \cos \gamma p \cdot dl}{(l + \sqrt{P + \tau^2(k^2 - k^2)})(l + \tau^2 \sqrt{P + \tau^2(k^2 - k^2)})}$$

or, if we put $l = \tau \sqrt{\alpha}$

$$\text{and } i(k^2 - k^2) = 4 \text{area} \left(1 + i \frac{k^2 - 1}{2k\tau} \right) = \alpha \tau^2$$

$$\frac{2ik}{\sqrt{\alpha}} \int_0^\infty \frac{e^{-\tau z} \cos \gamma \tau \cdot d\tau}{(\tau + \sqrt{\tau^2 + \alpha})(\tau + \tau^2 \sqrt{\tau^2 + \alpha})}$$

where, as in Q - iP, $\tau' = \tau \sqrt{\alpha}$ and $\gamma' = \gamma \sqrt{\alpha}$.

Noting next that $\frac{\partial}{\partial z} e^{-\tau z} = -\sqrt{\alpha} e^{-\tau z}$, we have

$$\begin{aligned} i\omega \frac{\partial}{\partial z} \Pi_s &= -Qc^2 \frac{4}{k} \int_0^\infty \frac{(1-\tau^2) e^{-\tau z} \cos \gamma \tau \cdot d\tau}{(\tau + \sqrt{\tau^2 + \alpha})(\tau + \tau^2 \sqrt{\tau^2 + \alpha})} \\ &= -Qc^2 \frac{4}{k} \int_0^\infty \frac{\sqrt{\tau^2 + \alpha} - \tau}{\tau + \tau^2 \sqrt{\tau^2 + \alpha}} e^{-\tau z} \cos \gamma \tau \cdot (1-\tau^2) \tau \cdot d\tau \end{aligned}$$

Since $(1-\tau^2)\tau = \tau + \tau^2 \sqrt{\tau^2 + \alpha} - \tau^2(\sqrt{\tau^2 + \alpha} + \tau)$ this is

$$\begin{aligned} -Qc^2 \frac{4}{k} \int_0^\infty \left[\frac{\sqrt{\tau^2 + \alpha} - \tau}{\tau + \tau^2 \sqrt{\tau^2 + \alpha}} - \frac{\tau^2 \sqrt{\tau^2 + \alpha}}{\tau + \tau^2 \sqrt{\tau^2 + \alpha}} \right] e^{-\tau z} \cos \gamma \tau \cdot d\tau \\ = -Qc^2 \left[-4(Q - iP) + 4 \int_0^\infty \frac{e^{-\tau z} \cos \gamma \tau \cdot d\tau}{\sqrt{\tau^2 + \alpha} + \tau/\alpha} \right] \tag{6} \end{aligned}$$

On adding (6) to (5) we have

$$QP_{12} = Qc^2 \log \rho''/\rho' + 4(M + iP) \tag{7}$$

where

$$M + iP = \int_0^\infty \frac{e^{-\tau z} \cos \gamma \tau}{\sqrt{\tau^2 + \alpha} + \tau/\alpha} d\tau$$

$$= \int_0^\infty \frac{e^{-\tau z} \cos \gamma \sqrt{\alpha} \tau}{\sqrt{\tau^2 + \alpha} + \tau/\alpha} d\tau \tag{8}$$

$M + iP$ vanishes as $f \rightarrow 0, \tau \rightarrow \infty, \alpha \rightarrow \infty$ or $\tau \rightarrow \infty$.

When $k^2 - k^2$ is minute the leading terms in the approximation (9)

$$\text{for } M + iP \text{ are } \frac{C}{2} - \frac{1}{2} \log \left(\frac{\tau^2 \sqrt{(\alpha^2 - \beta^2)/2}}{\alpha} \right)$$

AN APPROXIMATION FOR $M + iP$

It is possible to get series expansions for $M + iP$ but these which have been obtained do not facilitate computation. A fairly good approximation to $M + iP$ is arrived at as follows.

quently it is important to observe that a coarser kind of approximation may often be good enough. Thus, taking y to be zero,

$$M + iN \approx \int_0^{\infty} \frac{e^{-at}}{s + at} dt = -\frac{1}{a} e^{as} \operatorname{li}(e^{-as}).$$

If ε is very small one might use

$$M + iN \approx \int_0^{\infty} \frac{dt}{s + at} + \int_1^{\infty} \frac{e^{-at}}{(1+a)t} dt - \frac{1}{a} \log\left(1 + \frac{a}{s}\right) - \frac{1}{1+a} \operatorname{li}(e^{-a}).$$

Ordinarily precision is not required in $M + iN$ because $\varepsilon(M + iN)$ is a small term in ρ_{12} .

Let $ie^{as} = s^2$, $s = e^{i(\pi+2k\pi)}$
 $e^{-i2k\pi} = a = 1/\rho^2$
 $e^{-i(2k+1)\pi} \cos \frac{1}{2}\pi = \frac{1}{2}(e^{-i\pi} + e^{-i3\pi})$
 $f' = (h+s-i)\sqrt{\frac{a}{\rho}}$
 $f'' = (h+s+i)\sqrt{\frac{a}{\rho}}$
 $g = (h+s)\sqrt{\frac{a}{\rho}}$
 Since $(f^2 + s^2)^{1/2} = (f^2 + 2hs + s^2 - 2hs)^{1/2}$
 $= f + s - hs/(f+s) + \dots$

we put
 $1/(\sqrt{f^2 + s^2} + at) = 1/(f+s - hs/(f+s) + at)$
 $= (f+s)/[(a+1)f^2 + (a+1)hs + s^2]$
 where $r_1 = s(1 + \sqrt{1-4/(a+1)})/2$
 and $r_2 = s(1 + \sqrt{1-4/(a+1)})/2$.
 Then

$$M + iN \approx \frac{1}{(a+1)(r_2 - r_1)} \int_0^{\infty} \left(\frac{r_2}{f+r_1} - \frac{r_1}{f+r_2} \right) \frac{e^{-at}}{2} dt$$

$$= \frac{1}{2(a+1)(r_2 - r_1)} [-r_2 e^{r_1 a} \operatorname{li}(e^{-r_1 a}) + r_1 e^{r_2 a} \operatorname{li}(e^{-r_2 a}) - r_2 e^{r_1 a} \operatorname{li}(e^{-r_1 a}) + r_1 e^{r_2 a} \operatorname{li}(e^{-r_2 a})] \quad (9)$$

When $y = 0$ this reduces to

$$M + iN \approx \frac{1}{(a+1)(r_2 - r_1)} [-r_2 e^{r_1 a} \operatorname{li}(e^{-r_1 a}) + r_1 e^{r_2 a} \operatorname{li}(e^{-r_2 a})]. \quad (10)$$

$$\operatorname{li}(e^{-\pi}) = -\int_1^{\infty} \frac{e^{-t}}{t} dt = C + \log s + \sum_{n=1}^{\infty} \frac{(-s)^n}{n!},$$

where $C = .577215665$ and, if $s = re^{i\theta}$, $-\pi \leq \theta \leq \pi$.

$$\operatorname{li}(e^{-\pi}) \sim \frac{e^{-\pi}}{-s} \sum_{n=1}^{\infty} \frac{(-s)^n}{(-s)^n} + R_n.$$

The accompanying charts give M and N for $y = 0$ and $\varepsilon = 15$. With $s = h$ they give M and N for ρ_{11} . The computed points are indicated by solid dots on the chart for M ; they were obtained by numerical integration.

The approximation (10) was checked against the values obtained by numerical integration at a number of points. The discrepancy in each case amounted to less than one per cent for both M and N . This approximation is a much easier way to evaluate the integral than is numerical integration but it is a tedious computation with many chances for error. Conse-

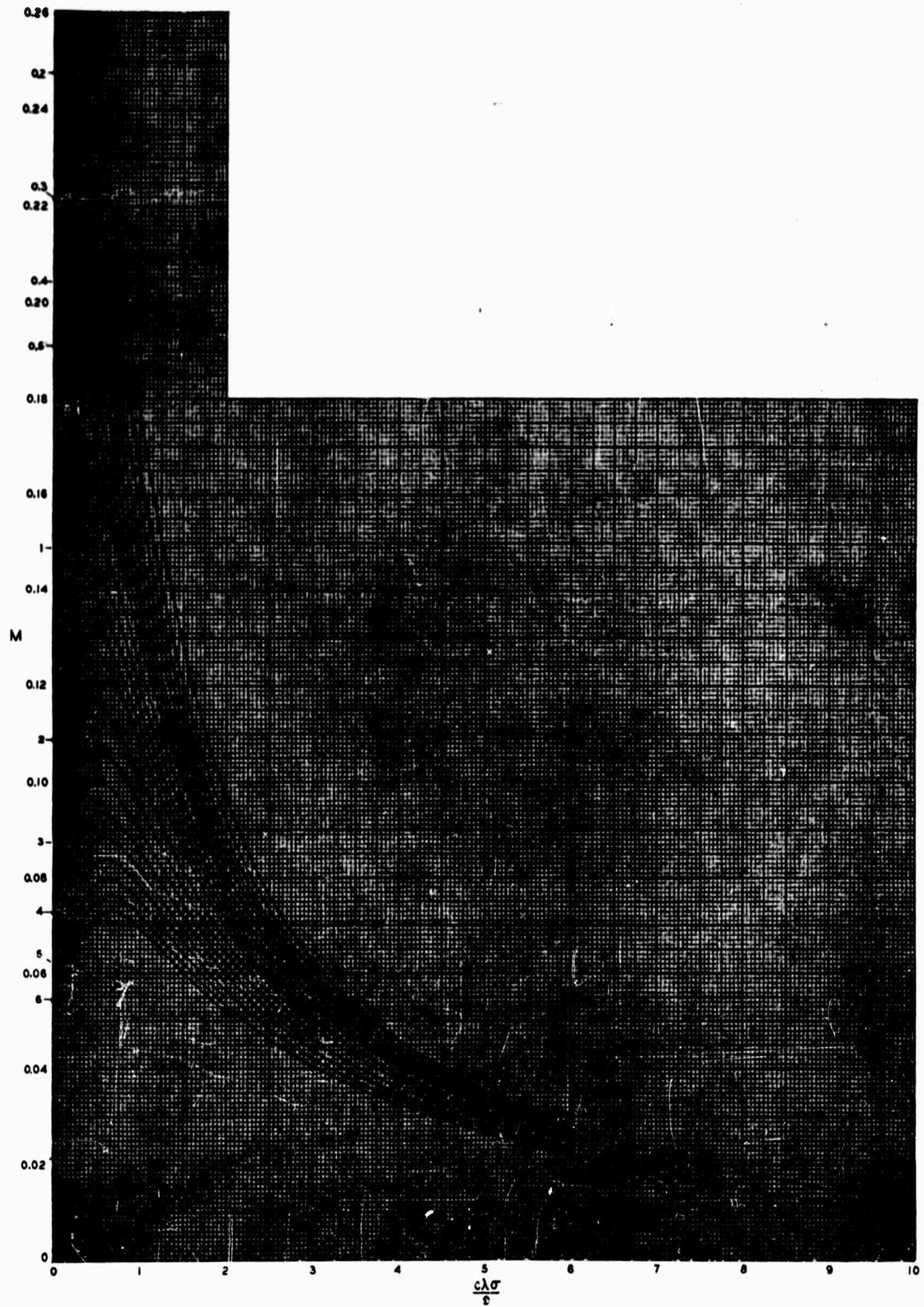


Fig. 2— M , computed with $\epsilon = 15$ and $\gamma = 0$. The number associated with a curve is the value of $(h + s)\sqrt{a}$.

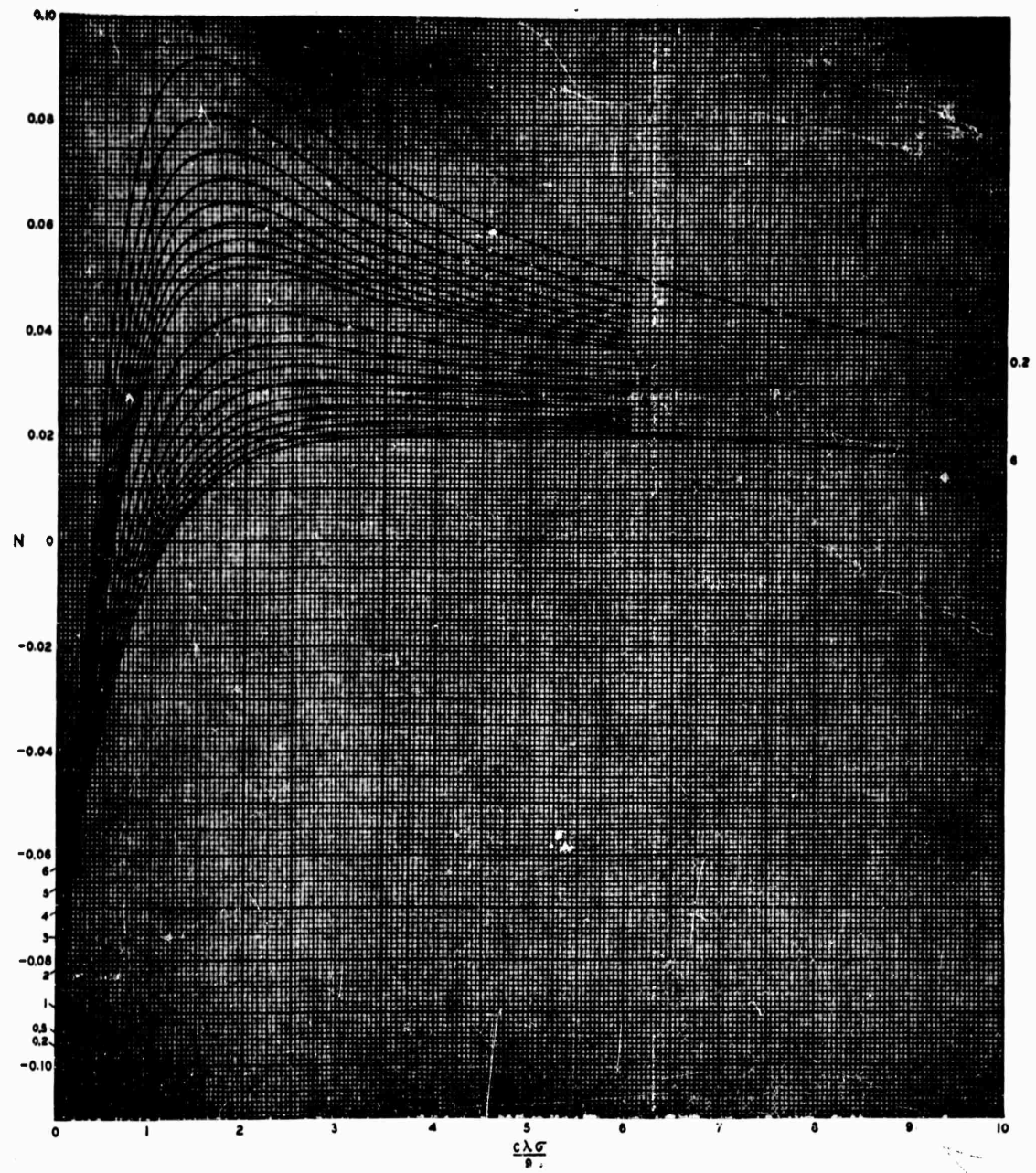


Fig. 3— N , computed with $\epsilon = 15$ and $\gamma = 0$. The number associated with a curve is the value of $(h + s)\sqrt{a}$.